Development and Characterization of Targeted Nanoparticulate System for Tumor Metastasis Inhibition

THESIS

SUBMITTED IN FULFILMENT FOR THE AWARD OF THE DEGREE OF

Doctor of Philosophy

IN

PHARMACEUTICAL SCIENCES

BABASAHEB BHIMRAO AMBEDKAR UNIVERSITY
LUCKNOW
प्रज्ञा शील करुणा
ESTABLISHED 1996

Submitted By

Chandra Bhushan Tripathi

Enrollment no. 564/13

Supervisor

Prof. (Dr.) Shubhini A. Saraf

DEPARTMENT OF PHARMACEUTICAL SCIENCES
SCHOOL FOR BIOSCIENCES AND BIOTECHNOLOGY
BABASAHEB BHIMRAO AMBEDKAR UNIVERSITY
(A CENTRAL UNIVERSITY)
VIDYA VIHAR, RAIBARELI ROAD, LUCKNOW-226025, U.P., INDIA

(2018)

DECLARATION

I hereby declare that the thesis entitled **"Development and Characterization of Targeted Nanoparticulate System for Tumor Metastasis Inhibition"** has been prepared by me under the supervision of **Prof. (Dr.) Shubhini A. Saraf** at Department of Pharmaceutical Sciences, School for Biosciences and Biotechnology, Babasaheb Bhimrao Ambedkar University, Lucknow (U.P.).

No part of this thesis has formed the basis for the award of my degree, diploma or fellowship previously. I further declare that the material embodied in the present work is based on original research work and indebtedness to others has been duly acknowledged at relevant places. I hereby also declare that the thesis is essentially free from all kind of plagiarism.

21/05/2018

Chandra Bhushan Tripathi

CERTIFICATE

This is to certify that the thesis titled **"Development and Characterization of Targeted Nanoparticulate System for Tumor Metastasis Inhibition"** submitted by **Mr. Chandra Bhushan Tripathi** is an original research work and has not been previously submitted in part or full for the award of any other degree or diploma to this or any other university.

The thesis submitted to Babasaheb Bhimrao Ambedkar University Lucknow satisfies all the requirements as stipulated in the *Doctor of Philosophy (Ph.D.) regulations-1999 as amended in 2008/2010/2013* and it is fit for submission and evaluation for the award of the degree of Doctor of Philosophy of the University.

Date: 21st May '2018

Supervisor

Dr Shubhini A. Saraf
Professor & Head (Deptt. of Pharm. Sciences)
Babasaheb Bhimrao Ambedkar University
(A Central University)
Lucknow

Head of the Department

Dr Shubhini A. Saraf
Professor & Head (Deptt. of Pharm. Sciences)
Babasaheb Bhimrao Ambedkar University
(A Central University)
Lucknow

Acknowledgements

This is perhaps the hardest part that I have to write. There are always moments when you look back in time, recall and reminisce things about the past. Writing this acknowledgment is one of those very few moments, when I fondly look back and feel gratitude towards this institution and the people whose unconditional help was mandatory for me to complete my thesis.

I am thankful to our Vice-chancellor ***Prof. R. C. Sobti****, Babasaheb Bhimrao Ambedkar University (A Central University), Lucknow, India for his encouraging wisdom words during research tenure.*

I would surely be short of words while expressing my sincere regards to my worthy guide, ***Prof Shubhini A Saraf,*** *Professor and Head and Department of Pharmaceutical Sciences, Babasaheb Bhimrao Ambedkar University (A Central University), Lucknow, India. Her uncompromising quest for excellence, integral view on research and her mission for providing only high-quality work and not less have made a deep impression on me. I was fortunate to receive her dexterous guidance right from the beginning to end, lavish help, conscientious efforts, continuous encouragement, freehearted attention, inspiration, constructive criticism, valued suggestions, tireless efforts without which it would not have been possible for me to execute this project successfully. I will never forget the spirit of sincerity, devotion, dedication, moral certitude and ethics, which she has inculcated within me during this period. I learned to believe in my future, my work, and myself. She inculcated the positive values in me to make me a better human being and I have learnt from her. Thank you Ma'am for all that I have got from you.*

I am incredibly grateful to my Departmental Research Committee (DRC) members of Department of Pharmaceutical Sciences, B.B.A.U, Lucknow, especially Prof Shubhini A. Saraf, Dr. R. Venkatesh Kumar, Dr. N.K.S. More, Dr. V. Elangovan, Dr. Gaurav Kaithwas, and Dr. Sudipta Saha for their invaluable suggestions and support throughout my sojourn in the department during my research work.

I accord my thanks to the Dr. V. Elangovan Dr. Sangeeta Saxena, and Mr. Mukesh, BBAU, Lucknow for providing me University Science Instrumentation Centre (USIC) facilities to carry out my project.

I am very thankful to Prof. K.P. Gupta, Prof. Shailendra Saraf, Dr. Sapna Kushwaha, Dr. Vikas Mishra and Dr. Rajnikant for their patronage in scrutinizing the observations and sharing their pearls of wisdom with me to realize my research work.

I also acknowledge with a sense of appreciation to DR. Sunil Goria (Librarian), Mr. O. P. Saini and Mr. Nilesh Verma (Assistant Librarian), BBAU, for their kind support.

My Sincere thanks to office staff and non-teaching staff Mr. Ramesh, Mr. Anand, Mr. Bhandari, Mr. Amar, for their respective technical capabilities who have always extended their full hearted support in carrying out my work in time.

I am also thankful to my seniors Mahendra Singh, Jovita Kanoujia and Pooja Singh for their friendly support, enlightening discussions, meetings, and having fun together. My gratitude also goes to my colleagues particularly Poonam Parashar, Malti Arya, Manjhari Singh and Swetlana Gautam,Jitendra, Amit Keshari, Amit, Vineet for their friendly support, enlightening discussions and meetings. I am also grateful to my juniors Ashok, Samipta, Priyanka, Raviraj, Raquiben, Rajneesh, Subhadeep, Lakhveer, Meena, Shurbhi and several others who were always with me whenever I needed them.

The chain of my gratitude would be definitely incomplete if I would forget to thank the first cause of this chain, i.e., my parents for their unconditional support and encouragement. I wish to special thanks for my loving wife Ms Deepti for her blessings, unconditional supports and encouragements for higher studies. I wish to extend my warmest and cordial thanks to other family members who motivated me and gave moral support in making every vital decisions of my life. To them, I owe my cherished yesterday, wonderful today and dream-filled tomorrow.

I would like to specially thank my Father-in-law, Mother-in-law for their blessings, and encouragements for higher studies. Also, I wish to extend my warm thanks and blessings to my younger family members with special mention of Arpita and Anand for their love, invaluable moral supports and inconsistent encouragement which always kept me energetic and full of enthusiasm while doing my research.

Finally I would like to express my whole hearted appreciation to all of those, whom I may not be able to name individually, for helping directly or indirectly and I also apologize for not mentioning personally one by one.

And last but not the least, thank you, "God" for bestowing every grace on me.

Date: ***Chandra Bhushan Tripathi***

CONTENTS

List of Tables

List of Figures

ABBREVIATIONS

AB/TEB : Alveolar buds/terminal end buds
ALA : α-Linolenic acid
BAX : bcl-2-associated X
BBD : Box-Behnken design
Bcl-2 : B-cell lymphoma-2
CCD : Central composite design
Cdks : Cyclin-dependent protein kinases.
CMAs : Critical material attributes
CQAs : Critical quality attributes
DCC : N,N'-Dicyclohexylcarbodiimide
DCF : 2',7'-dichlorodihydrofluorescein
DCFDA : 2, 7-dichlorofluorescin diacetate
DCT : Dense connective tissue
DMBA : 7,12-Dimethylbenz[a]anthracene
DoE : Design of experiments
Dox : Doxorubicin
EMEM : Eagle's Minimum Essential Medium
FACS : Fluorescence-activated cell sorting
FBS : Fetal Bovine Serum
FITC : Fluorescein isothiocyanate
FTIR : Fourier-transform infrared spectroscopy
GSH : Glutathione
HABA : 2-(4-hydroxyphenylazo)benzoic acid
HBSS : Hank's Balanced Salt Solution
HRP : Horse radish peroxidise
IC_{50} : Half maximal inhibitory concentration
LCT : Loose connective tissue
MDA : Malondialdehyde
MMP : Mitochondrial membrane potential
MMP-9 : Matrix metalloproteinase-9
MTT : 3-(4,5-Dimethylthiazol-2-yl)-2,5-diphenyl tetrazolium bromide
NE : Nanoemulsion
NHS : N-hydroxysuccinimide
NLCs : Nanostructured lipid carriers
PBS : Phosphate buffer saline
PEG-bis-amine: Poly(ethylene glycol)bis(amine)
RB : Retinoblastoma tumor suppressor protein
Rh-123 : Rhodamine-123
RIPA : Radio Immuno Precipitation Assay
ROS : Reactive oxygen species
SMVT : Sodium-dependent multivitamin transporter
SOD : Superoxide dismutase
TBARs : Thiobarbituric acid reactive substances
w.r.t. : with respect to
ω3-FA : ω3-fatty acids

1. Introduction

During the last couple of decades, science of formulation development has improved remarkably witnessing the development and successive implementation of diverse types of new drug delivery systems. The effectiveness of a drug in disease therapy depends on the capability of the dosage form in delivering the drug molecules to the site of action at a rate and extent sufficient to show the desired pharmacological response. Targeted delivery system has now become an established field in pharmaceutical research. By using a targeted system that assists in directing a drug to a specific site in the body where it needs to exert its effect, target tissue specificity of the therapeutic agent can be increased while the off target effects can be curtailed (Torchilin 2000, Tripathi et al. 2016, Tripodo et al. 2014, Zhang et al. 2011).

Various reasons why it is preferable to direct drugs to their site of action may be described by the pharmaceutical factors like drug instability and solubility, biopharmaceutical factor such as low absorption and high membrane binding, pharmacokinetic factors i.e., short half life, higher volume of distribution and low specificity, clinical factors like low therapeutic index, anatomical and cell barriers and finally commercial factors (Bertrand et al. 2014, Lammers et al. 2008).

Thus, a targeted drug delivery system can supply drug molecules selectively to site(s) of action(s) in such a manner that it provides maximum therapeutic efficacy through predetermined and controlled manner, preventing drug inactivation or degradation during transit in the systemic circulation and protects the body from adverse drug reactions owing to inappropriate disposition. For the drugs with narrow therapeutic index, targeted drug delivery may offer an effective treatment alternative at relatively lower drug concentration (Torchilin 2000).

Although a drug targeting strategy can potentially improve the clinical efficacy of therapeutic effectiveness in many diseases, most drug targeting research has been focused on tumor. Current chemotherapy of cancer still faces a major drawback of lack of selectivity and specificity of antineoplastic drugs toward tumor cells. The cells of the bone marrow and of the gastrointestinal tract that are rapidly proliferating are adversely affected by the cytotoxic action of antineoplastic drugs. This causes a

narrow therapeutic index for several anticancer chemotherapeutic agents (Jain and Stylianopoulos 2010, Lammers et al. 2008).

Because of their low molecular weight and high hydrophobicity, most of the routinely used antineoplastic agents are rapidly cleared from blood circulation and often show a large volume of distribution. Also, accumulation of drug nontarget tissue causes toxicity towards different healthy tissues. Additionally, several other obstacles are required to be overcome before an i.v. administered anticancer agent can show antitumor efficacy. These barriers might include enzymatic and hepatic drug degradation and inactivation, high interstitial fluid pressure that is typical characteristics of tumors, to cellular and nuclear membranes, and to the presence of drug efflux pumps (Allen and Cullis 2004, Lammers et al. 2008, Peer et al. 2007, Torchilin 2000).

Characteristics of an ideal tumor targeted nanomedicine may be outlined as follows:

(1) Increase in the drug localization in cancer tissue through passive as well as active targeting

(2) Decrease in drug concentrations in sensitive and non-target tissues

(3) Decreases leakage of drug during transit to the target tissue

(4) Protect drug degradation and premature clearance

(5) Maintains drug at target site for prolonged period of time

(6) Facilitate and improves cellular uptake and intracellular trafficking

(7) Should be biocompatible and biodegradable

1.1. Principles of drug targeting to tumor

1.1.1. Passive targeting

Passive targeting primarily aims to improve the blood circulation time of targeted drug delivery systems and by doing so it exploits the pathophysiology of solid tumors where convoluted and poorly defined vasculature differentiates them from healthy tissues. Prototypic examples of nanomedicine formulations are liposomes, micelles, polymers, emulsions, nanoparticles and antibodies. The nanomedicines are primarily aimed to improve the blood circulation time for entrapped or conjugated

chemotherapeutic drug and, by doing so, to enable it to exploit the fact that solid tumors possess a convoluted and undifferentiated vasculature system in comparison to the vasculature of healthy tissues. This allows extravasation or leakage of carrier materials loaded with drug molecules with sizes of upto several hundreds of nanometers (Allen and Cullis 2004, Lammers et al. 2008, Maeda et al. 2000, Matsumura and Maeda 1986, Peer et al. 2007).

Also, the solid tumors lack functional lymphatic system, therefore, they are unable to remove or eliminate extravasated nanocarrier systems. Due to the tendency of higher leaking tumors allows long-circulating nanocarriers to selectively accumulate in tumors with an increase in circulation time, through a mechanism known as the enhanced permeability and retention (EPR) effect. Despite some drawbacks, most of the currently marketed products like Myocet (nonPEGylated liposomal doxorubicin), Doxil (PEGylated liposomal doxorubicin), Daunoxome (nonPEGylated liposomal daunorubicin), Abraxane (albumin-based pacitaxel) and Genexol-PM (paclitaxel-containing polymeric micelles; pre-approved in Korea) rely on this phenomenon (Allen and Cullis 2004, Lammers et al. 2008, Maeda et al. 2000, Matsumura and Maeda 1986, Peer et al. 2007, Torchilin 2000).

1.1.2. Active Targeting to cancer cells

Active targeting depends on specific interactions between drug, drug conjugate or drug carriers and the target cells. These interactions are enabled via targeting ligands, like antibodies, proteins and peptides, which specifically bind to receptors over expressed on the target cells. Active drug targeting is generally implemented to improve cancer cells detection and higher cancer cell uptake (Lammers et al. 2008, Talekar et al. 2012, Torchilin 2000, Wu et al. 2016, Zempleni et al. 2009, Zhang et al. 2014). Examples of targeting ligands that are routinely employed for actively targeting nanocarrier formulation to tumor cells are biotin, folate, transferrin and galactosamine. However, regardless of significant advancements made at the preclinical level with regard to active targeting, only antibody-based nanomedicines, such as Zevalin, Mylotarg, Ontak and Bexxar have been approved for clinical use. However, there are a number of physiological and anatomical hurdles that are to be surpassed before an antibody- or peptide-targeted formulation can bind to cancer

cells. These may include the presence of pericyte, smooth muscle cell and fibroblast-based cell layers between endothelial and tumor cells, the high cellular density within solid malignancies, and the high interstitial fluid pressure that is characteristics of tumors. Therefore, because of the binding-site barriers that restricts the penetration of actively targeted drug carrier into the cancer interstitium, the actively targeted drug carriers tend to have issues in finding their target tissue or cells (Talekar et al. 2012, Torchilin 2000, Wu et al. 2016, Zempleni et al. 2009, Zhang et al. 2014).

1.1.3. Active targeting to endothelial cells

To overcome some of the above mentioned shortcomings with regard to active drug targeting, i.e., those related to the presence of several additional cell layers between endothelial and tumor cells, to the high tumor cellular density and to the high interstitial fluid pressure in tumors, a number of different endothelial cell-targeted nanocarrier formulations have been developed and evaluated over the years. Ligands that may be used to target drug delivery systems to tumor microvasculature include the antibody fragments L19 and oligopeptides like NGR and RGD (Lammers et al. 2008, Talekar et al. 2012, Torchilin 2000).

1.1.4. Triggered drug delivery

These are the systems that can be triggered to release their entrapped drug upon exposure to external stimulus like heat, light, ultrasound and magnetic fields. These stimuli-responsive nanomedicines (like Thermodox, a temperature-sensitive PEGylated liposomes containing doxorubicin) are designed to release the entrapped chemotherapeutic drug upon applying locally confined triggers thereby maximizing drug release at the pathological site, while preventing damage to potentially endangered healthy tissues. The demerit of such formulations includes difficult preparation methods, release of significant amounts of drug without applying actual trigger, or they appear so stable that the triggering conditions are so intense that they are hardly conformable and the stimuli themselves become harmful (Davis et al. 2008, Lammers et al. 2008, Peer et al. 2007, Talekar et al. 2012, Torchilin 2000).

1.2. Targeting ligands

Ligands employed for targeting drug/ drug delivery systems are antibodies, peptides, proteins, nucleic acid and small molecules have all been described in brief.

1.2.1. Antibodies and their fragments

Antibodies are extensively explored ligands used for targeting in the clinical studies and over thirty types of monoclonal antibodies have been already approved for clinical use like trastuzumab, rituximab, bevacizumab and cetuximab. The first reported example for targeted nano drug delivery systems are liposomes decorated with antibodies (PEGylated Doxorubicin liposomes (Doxil®/Caelyx®) incorporating a Fragment antigen-binding [F(ab′)] of cetuximab) (Kamaly et al. 2012, Mamot et al. 2012). [28, 29]

1.2.2. Proteins

Proteins are naturally occurring molecules that are used for targeting using endogenous targets and can be explored for therapeutic applications. For example, transferrin (Tf) affibodies (antibody mimetics), aptamers, or ankyrin repeat proteins have been designed to target the nanocarriers (Choi et al. 2010, Pandey et al. 2015, Winkler et al. 2009). [30, 31, 36]

1.2.3. Peptides

Peptides are different from their larger counterparts (i.e., proteins) by having amino acid sequences lower than 50 residues. The most widely explored peptide ligand is probably that of RGD (arginine–glycine–aspartic acid) peptide family. Other cell penetrating peptides for targeted nanocarriers include Cys-Arg-Glu-Lys-Ala, Asn-Gly-Arg, and Ile-Thr-Asp-Gly-Glu-Ala-Thr-Asp-Ser-Gly (LABL) (Allen and Cullis 2004, Lammers et al. 2008, Torchilin 2000, Winkler et al. 2009). [1, 8, 31, 32]

1.2.4. Nucleic acid based ligands

Nucleic acid-based aptamers are another class of ligands that are completely different in structures from protein and peptide-based aptamers. Nucleic acid aptamers (Apts) are single-stranded oligonucleotides, such as RNA, DNA, or modified nucleic acids. Owing to their distinctive conformational structures, aptamers possess high affinity and specificity for target site (Lammers et al. 2008, Xiao and Farokhzad 2012). [8, 33]

1.2.5. Small molecules

Small molecular weight compounds have different properties which are strongly recommended for a targeting ligand such as small size, improved stability and low production costs. Among various synthetic and natural small molecules reported, a common example is folic acid (i.e., folates or vitamin B9). Folate is required for the normal cellular metabolism and cell survival particularly during the period of rapid cell division which happen in cancerous cells. Folate receptors (FR) are therefore upregulated in different type of cancers such as lung, colon, mammary gland, kidney and brain. Normal cells have relatively lower FR levels on their cell surface, making them an attractive target to develop cancer specific drug therapy. Folate has high affinity ($Kd \sim 10^{-10} M$) for folate receptors (Bae et al. 2013, Lammers et al. 2008, Shinoda et al. 1998, Stella et al. 2000, Talekar et al. 2012, Zhang et al. 2014). Another example of small molecule targeting ligands is triphenylphosphonium. Carbohydrate moieties, including galactose, mannose, glucose, and their derivatives, have also been extensively utilized as targeting ligands (Allen and Cullis 2004, Kue et al. 2016, Lammers et al. 2008, Torchilin 2000). Carbohydrates are recognized by cellular membrane proteins called lectins. [1, 8, 27] Recent findings suggest that biotin and/or biotin-conjugated drug can be constructively targeted to the tumor cells with the help of overexpressed biotin-selective transporters (Ren et al., 2015). Biotin has a critical role in cell signaling, epigenetic gene regulation and chromatin structure at the cellular level (Zempleni et al., 2015). Mammalian cells lack biotin synthetic pathway, therefore, depend on sources like plants and bacterial systems for the same. The mammalian cells accomplish uptake through biotin transporter (high-affinity for biotin) and also through SMVT. The main transporters for biotin uptake is SMVT, which is overexpressed in several aggressive tumors such as leukemia, ovarian, colon, lung, renal and breast tumor (Tripodo et al. 2014, Wu et al. 2016, Zempleni et al. 2009).

1.3. Approaches for targeted drug delivery

Three strategies have been used to achieve drug targeting. These are

1) Site specific pharmacologically active molecules.

2) Preparation of inert agents that show its activity after activation by enzymes at the site of action, i.e., prodrug.

3) Use of a pharmacologically inert drug carrier system that can selectively direct the drug molecules to specific site for action: this may include particulate delivery systems like microparticles, nanoparticles, liposomes, niosomes, nanoemulsion, microemulsion solid lipid nanoparticles, nanostructured lipid complexes, lipoproteins, activated carbon; Cellular Carriers: erythrocyte, platelets, leucocytes. Soluble macromolecular systems i.e., protein drug conjugates (antibody, antibody fragment drug conjugates, albumin drug conjugates, lipoprotein, lectins) dextrans, synthetic polymers (PLGA, polyHPMA, Poly-L-aspartic acid, albumin)

1.4. Carrier systems for targeted drug delivery

Drug carriers utilize biologically inactive macromolecules to direct a drug to its target site in the body. These may be divided into two types- particulates and soluble macromolecular.

The concept of using particulates as targeted delivery originates from their use in radio diagnostic agents in investigation of RES system in liver, spleen and bone marrow and lymph nodes, gastrointestinal examinations etc. Because of small size, these particulate drug delivery systems can be directly introduced into systemic circulation via intra-articular, intra-venous route or to some other body compartment like lung, nose etc. The fate of particulate nanocarrier systems in the biological system depends on the morphological characteristics such as size, shape, charge and surface hydrophobicity of the particles (Allen and Cullis 2004, Bae et al. 2013, Bertrand et al. 2014, Davis et al. 2008, Jain and Stylianopoulos 2010, Lammers et al. 2008). [(1)]

Nanoparticles are colloidal particles of size ranging between 10-1000nm. Most commonly employed method to prepare nano/microparticles are emulsion, micelles, interfacial polymerization (emulsion/micellar) and coacervation. Smaller particle size is required for good tissue tolerance, uptake and transfer, and causes no foreign body reaction. Most product investigated till date are sterile, freeze dried, free flowing powder, usually containing 0.1% of non-ionic surfactant to assist redispersion in

saline. Nanospheres can carry a high dose with high entrapment efficiency (over 90%). Antibody or other ligand can be attached to nanoparticles core to guide the carrier to the target site(s) (Allen and Cullis 2004, Bertrand et al. 2014, Cho et al. 2008, Davis et al. 2008, Jain and Stylianopoulos 2010, Lammers et al. 2008).

Nanoparticles after intravenous administration can easily be recognized by the cells of immune systems, and are rapidly cleared from the systemic circulation by macrophases. The incorporation of drug molecules to conventional drug carriers leads to alteration in the drug disposition profile, as it is mostly uptaken by mononuclear phagocytes system like liver, lungs, spleen, and bone marrow. Therefore, for a successful targeted delivery system it is necessary to avoid or lower the opsonization of carrier system and prolong the circulation time of nanotherapeutics in blood. This can be achieved by (a) surface modification of nanocarriers with hydrophilic polymers; (b) development of nanocarrier with biodegradable copolymers such as polyethylene glycol (PEG), polyoxamer, polyethylene oxide, polysorbate 80, poloxamine etc (Allen and Cullis 2004, Cairns et al. 2006, Jain and Stylianopoulos 2010, Lammers et al. 2008, Maeda et al. 2000, Tomasina et al. 2013, Torchilin 2000).

There is increasing an interest amongst pharmaceutical scientist in the utilization of lipid based nano-carriers as drug delivery systems to encapsulate therapeutic agents. Lipidic nano-carriers system such as microemulsions, nanoemulsions, solid lipid nanoemulsion, nanostructured lipid carriers, etc. are of great interest as colloidal nano delivery systems. They can easily be made-up from food-grade ingredients by using simple processing methods such as mixing, homogenization and shearing etc. Lipophilic drugs can be delivered using nanoemulsion or microemulsion. The drug to be delivered is added to the lipid phase which upon dispersion into continuous aqueous phase forms nanoglobules (with isotropic lipid core) to give oil in water (o/w) nanoemulsions. Nanoemulsion has been used as a carrier for lipophilic anticancer drugs such as docetaxel, tamoxifen, chlormbucil and dacarbazine etc. (Ganta et al. 2010, Ganta et al. 2016, Kakumanu et al. 2011, Tagne et al. 2008). Formulation consideration for nanoemulsion includes the selection of emulgents and co-emulgents. Emulgents and co-emulgents are required in larger quantities to stabilize the nanoemulsion. Emulgents selection should be more cautious so as to minimize any potential toxicity induced by emulgents. Nanoemulsions are the part of

multiple phase colloidal dispersions, which exists as non-equilibrium colloidal systems, having distinctive physicochemical as well as functional properties such as higher encapsulation of drug, higher physical stability and are opaque to nearly transparent in appearance. These properties depend on composition as well as preparation method of nanoemulsions. Due to their incredibly small droplet size (10-100nm), nanoemulsions have the potential of harnessing the large surface area to volume ratio of these formulations to improve the targeting and bioavailability of the active ingredients (Allen and Cullis 2004, Anton and Vandamme 2011, Ganta et al. 2010, Ganta et al. 2014, Lollo et al. 2014, Mendes et al. 2009, Singh et al. 2018, Singh et al. 2016a, Singh et al. 2017, Tripathi et al. 2017, Zhang et al. 2011, Zhao et al. 2013).

Nanostructured lipid carriers (NLCs) have effectively been utilized as the new generation novel colloidal carrier systems for parenteral drug delivery. NLCs improve localization of drug inside a tumor and are known to have enhanced safety (Singh et al. 2016b, Singh et al. 2016c, Torchilin 2000). Composed of solid lipids and liquid lipids, NLCs are physiologically acceptable, biodegradable, nontoxic and non-irritant. Recent developments in targeted delivery have further improved the potency of such systems to deliver the drug molecules specifically to the tumor cells thereby avoiding dose related toxicity (Mussi et al. 2014, Singh et al. 2016d). NLCs as drug carriers, can be used to entrap lipophilic drug and unstable molecules to protect it from environment and make it less susceptible for degradation or deactivation. NLCs having longer systemic circulation times are found to accumulate in extravascular site of disease such as sites of inflammation, infection and tumors. This accumulation can result in 03 to 100-times more drug delivery to a target site compared to the injection of the same dose of free drug. The facilitation of the binding of the NLCs to target cells through the use of ligand to increase localization of drug and target cell killing is extensively studied. Specificity and selectivity of actively targeted NLCs depends on the ligand's affinity towards target cell marker/over expressed receptors (Allen and Cullis 2004, Fernandes et al. 2017, Joshi and Muller 2009, Lammers et al. 2008, Liu et al. 2011, Mizushima 1996).

Lipid based colloidal nano-carriers system such as nanoemulsions and nanostructured lipid carrier are of great interest as colloid based drug delivery systems.

1.4.1 Nanoemulsions

Nanoemulsions are oil-in-water (O/W), water-in-oil (W/O) dispersion of two immiscible phases stabilized using a suitable surface active agent with size usually less than 500 nm. Nanoemulsions have attracted much attention in pharmaceutical research areas for delivery of hydrophilic as well as lipophilic molecules, in recent times. Low viscosity, high kinetic stability, longer shelf life, ease of preparation, transparency, higher drug solubilization and the protection from adverse environment etc., make them suitable and attractive drug carrier systems for poorly water-soluble drugs. Nanoemulsions possess higher drug solubilization capacity for hydrophobic drugs than simple miceller dispersions and have greater kinetic stability in comparison to coarse emulsions. Nanoemulsions despite having the similar globule size range to microemulsion, they differ enormously in structural aspects and thermodynamic stability. In case of parenteral formulations, nanoemulsions have been effectively employed to solubilize and protect sensitive drug molecules against harsh environmental factors like, oxidation, pH, hydrolysis, to target specific organs by exploiting enhanced permeability and retention effect, and to escape RE S. NEs are optically isotropic and kinetically stable systems and usually the amalgamation of different components such as a lipophilic phase (oil or lipid), a hydrophilic phase (water or aqueous buffer), surfactant and co-surfactant and classified NEs as water-in-oil (w/o), oil-in-water (o/w) (Ganta et al. 2014, McClements 2012, Singh et al. 2017, Zhang et al. 2011, Zhang et al. 2012b).

1.4.1.1. Formulation aspects of nanoemulsion

The nanoemulsion formulation should form a clear dispersion and should remain stable on infinite dilution. Nanoemulsions have been successfully developed for several drugs for parenteral administration such as, docetaxel, paclitaxel, doxorubicin, camptothecin, tamoxifen etc. Nanoemulsions have also been considered as a means of topical (Pham et al. 2016), transdermal (Thevenin *et. al. 1996)*, nasal (Kumar et al. 2018) and oral drug delivery (Singh et al. 2018, Singh et al. 2016a, Tripathi et al. 2017). These systems offer several advantageous features, as enumerated in Fig. 1.

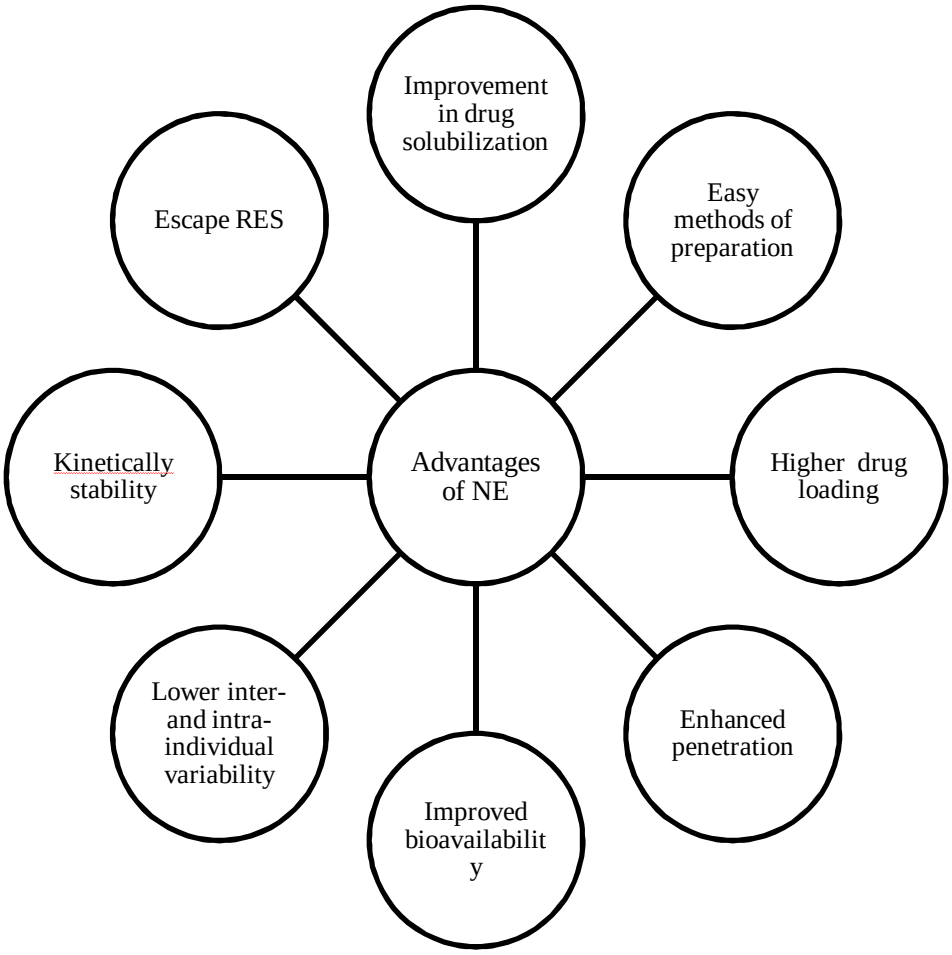

Fig. 1 Advantages of nanoemulsions

1.4.1.1.1. Excipient Characteristics

Historically, excipients were considered pharmaceutically inert substances that would be utilized mainly as fillers, diluents, lubricants, binders, coatings, solvents, and dyes, in the manufacturing of final drug products. Over the years, however, advances in pharmaceutical science and technology have facilitated the availability of a wide range of novel excipients. In some cases, known and/or unknown interactions can occur between an excipient and active ingredient, other inactive ingredient(s), biological surroundings, or even container closure system.

1.4.1.1.2. Lipidic Excipients

Since nanoemulsion is a lipid based drug delivery system, lipid is an essential constituent of the formulations. These formulations typically contain long/medium-chain triglyceride/di-glycerides, individual or mixed emulgents, and various hydrophilic emulgents (Tripathi et al. 2016). Lipid excipients can solubilize larger

amounts of lipophilic drugs within the dosage form. Amongst the vast list of these modified triglycerides, an account of some vegetable oils is enlisted as Table 1, along with their fatty acid composition (Delmas et al. 2011).

Table 1.1. Nomenclature of various fatty acids used in lipid based excipients.

Fatty acid chain length (number of atoms)	**Number and position(Δ) of unsaturated bonds**	**Common Name**	**Melting temperature (°C)**
08	0	Caprylic acid	16.5
10	0	Capric acid	31.6
12	0	Lauric acid	44.8
14	0	Myristic acid	54.4
16	0	Palmitic acid	62.9
18	0	Stearic acid	70.1
18	1 Δ 9	Oleic acid	16.0
18	3 Δ 9, 12, 15	α-linoleic acid	-16.5
18	2 Δ 9, 12	Linoleic acid	-5.0
18	3 Δ 6, 9, 12	γ-linoleic acid	-11.0
18	1 Δ 9 (-OH:12)	Ricinoleic acid	6.0
20	0	Arachidic acid	76.1
22	0	Behenic acid	80.0

1.4.1.1.3. Emulsifier/co-emulsifier

A suitable emulsifier is necessary to give the emulsifying characteristics to nanoemulsions. Emulgents are of amphiphilic nature and can invariably solubilize comparatively higher amounts of hydrophobic drug molecules. The factors that govern the selection of an emulsifier encompass its HLB value and safety. The HLB of a surfactant provides essential information on its potential use as emulgent in the formation and stability of nanoemulsion system (Delmas et al. 2011). The emulsifier employed in formulation of the nanoemulsion should have relatively higher HLB values and hydrophilicity to immediately form o/w globules. It would keep the drug in solubilized form for relatively longer period of time and avoid the precipitation of drug molecules within the g.i. lumen or after administration to systemic circulation. However, HLB of an emulsifier is not the only indicator of its surface active abilities, as many key surfactants differ considerably in their HLB values amongst each other, by as much as 8-10 units (Delmas et al. 2011, Singh et al. 2017).

An ideal emulsifier should show properties like, rapid arrangement at the oil/water interface, generation of lowered interfacial tension and ultimate stabilization of

nanoemulsion globule interface by steric hindrance and/or electrostatic repulsion. Any amphiphilic molecules can act as an emulsifier such as surfactants (sodium dodecyl sulfate, Tweens), amphiphilic proteins (caseinate), phospholipids (egg or soy lecithin), or polymer (PEG), polysaccharides (gum Arabic, starch) that can adsorb at the globule interface, thereby stabilizing nanoemulsion via steric stabilization (Ganta et al. 2014). The choice of emulsifier not only affects the stability of nanoemulsion system but can also offer the possibility of modulation of their size and functional properties. A PEG modification of nanoemulsion can be utilized for linking of targeting ligands exposed on the nanoemulsion surface. This results in higher cell specific targeting and selective drug delivery, as well as provides longer circulation properties after systemic administration for *in vivo* drug delivery (Jiang et al. 2013, Liu et al. 2017, Ohguchi et al. 2008).

1.4.1.2. Method and Theories of nanoemulsions formation

Nanoemulsion, like conventional emulsions (with sizes > μm), are in non-equalibrium state from a thermodynamic point of view. However, due to the small size of globules, the droplets are prevented from flocculation and coalescence, i.e., Ostwald ripening that governs the destabilization process. Hence, destabilization kinetics of nano-emulsions is quite slow (∼months) that they can be considered as kinetically stable systems (Ganta et al. 2014, McClements 2012, Singh et al. 2017).

Nanoemulsions are commonly produced via the so-called “high-energy” methods, utilizing specific devices (like high pressure homogenizers or ultrasonicators) that are able to provide sufficient energy required to increase water/oil interfacial area during the formation of submicronic droplets (McClements 2012). High pressure homogenization techniques involve the use of high pressure homogenizer or piston gap homogenizers to produce low particle size. During this process, several forces such as intense turbulence, hydraulic shear and cavitational forces work together to produce nanoemulsions with extremely small globule size. High energy ultrasonication technique is commonly employed in the preparation of nanoemulsion at laboratory scale. Energy of ultrasonication produces cavitational forces on the larger droplets resulting in disruption of oil phase that leads to droplet formation in submicron ranges (Delmas et al. 2011, McClements 2012, Singh et al. 2017). Low

energy methods are also used to form nanoemulsion formulations through spontaneous emulsification without utilizing any form of device or energy. Intrinsic physicochemical characteristics of the building components of nanoemulsion are responsible for formation of submicronic droplets in low energy methods (Delmas et al. 2011, McClements 2012, Singh et al. 2017). The process of nanoemulsion formation in low energy method involve only mixing of two liquid phases at normal temperatures, one consisting of lipidic phase into which a hydrophilic emulgent is mixed to form a homogeneous liquid phase and the other an aqueous phase, which may be pure water or buffer. Once these two phases are mixed together, the hydrophilic species (surfactant) present in the oily phase rapidly solubilize into the aqueous one, resulting into the demixing of the oil in the form of submicron droplets, immediately stabilized by the surfactant molecules spread on the interfaces of two liquids. The droplet size of nanoemulsions can be easily modulated through the oil/surfactant weight ratio. This low energy emulsification is in fact a competent method that enables the formation of kinetically stable emulsion droplets (Delmas et al. 2011, Ganta et al. 2014, McClements 2012, Singh et al. 2017).

1.4.2. Lipid Nanoparticles

Lipid nanoparticles are made up of solid matrix which is developed by substituting the liquid lipid of o/w emulsions by a solid lipid. The particles so formed are maintained at solid state at physiological temperature. The first generation of such particles i.e., solid lipid nanoparticles (SLN) was developed two decades earlier (Uner 2006). However, in case of second generation technology or SLNs, the particles are prepared by using blend of two lipids i.e., a solid lipid and a liquid lipid. The resulting blend is also solid at physiological temperature and is termed as nanostructured lipid carriers (NLCs) (Singh et al. 2016d, Uner 2006).

Solid lipid nanoparticles (SLN) are composed of a lipid phase which is present in crystallized form and has a highly-organized crystalline structure with the drug molecules being a part of the lipidic matrix **(Fig. 2 Left)**. SLN were originally designed to inculcate the benefits of polymeric nanoparticles, emulsions and liposomes and to avoid their disadvantages. The SLN are produced from one or more solid lipid/blend of solid lipids (Uner 2006).

Nanostructured lipid carriers (NLC) are produced using mixture of solid lipids and liquid lipids. To form the mixture for preparation of nanoparticles matrix, solid and liquid lipids are used in different ratio such as 60:40 up to a ratio of 99.9:0.1. Due to the presence of liquid phase, a depression in melting point in comparison to the pure solid lipid is observed **(Fig. 2 Right)**. The particles obtained are still solid at room and physiological temperatures (Fang et al. 2013). Development of NLCs overcomes some of the potential limitations of SLN. NLC, in comparison to SLN, disply a higher drug loading efficiency for a number of active compounds, have lower water content in the particle suspension and offer minimal expulsion of active drug during storage period(Beloqui et al. 2016).

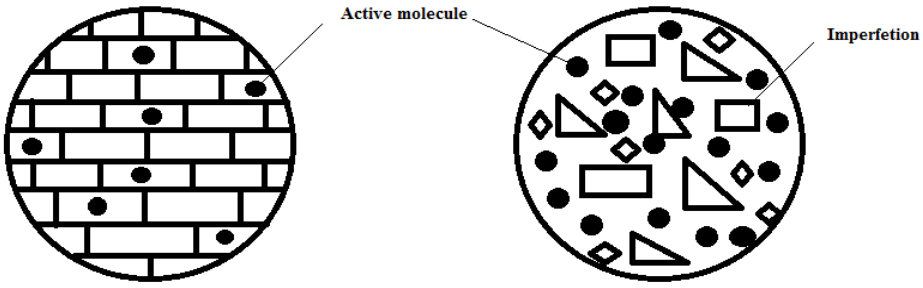

Fig.2. Left: Formation of a more or less perfect crystalline structure in SLN by identically shaped molecules similar to a brick wall made from identically shaped bricks with limited loading possibilities for actives. **Right:** Formation of a crystalline particle matrix with many imperfections comparable to building a wall from very differently shaped stones in NLC, which increased number of imperfections leads to an increased loading capacity.

1.4.2.1. Types of NLC

Depending upon the composition of NLCs and the production process, three types of structure have been proposed for NLC for the active molecule which can be incorporated into it. These are imperfect type, amorphous type and multiple types **(Fig. 3.)** (Beloqui et al. 2016, Uner 2006).

(1) Imperfect type NLC: These are defined as the imperfect crystal model, because in its matrix there are many imperfections which are capable to accommodate the higher quantities drug in molecular form and in amorphous clusters. Imperfect type of NLCs is thus obtained by mixture of spatially different lipidic components.

(2) Amorphous type NLC: These are composed of solid amorphous matrix without having a defined structure. These amorphous models are formed as a result of mixing of solid lipid with special liquid lipids which do not re-crystallize after homogenization and congealing.

(3) Multiple type NLC: The multiple type NLCs are produced by mixing of solid lipid with relatively higher amount of liquid lipid. In these matrixes the solubility of drug is higher; therefore the capacity of drug loading is increased.

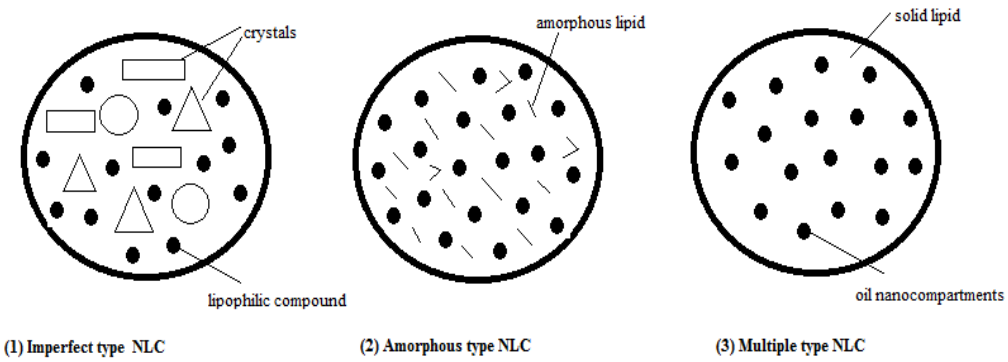

Fig.3. Basic types of Nanostructured Lipid Carriers

1.4.2.2. Advantages of Nanostructured Lipid Carrier:

The advantages of NLC over other colloidal carriers as discussed by (Muller et al. 2002a;b) are as followes:

1. Higher drug loading efficiency for a number of active molecules.
2. Lower water amount is required for the particle suspension.
3. Avoid/Minimize expulsion of active molecule during storage.
4. Better interaction with cellular membrane and hence higher cell internalization
5. Completely biodegradable and biocompatible due to lipidic excipients.
6. Prolonged release can be achieved
7. Higher encapsulation efficiency and stability

8. They may increase bioavailability, self-life and stability of bioactive compounds.
9. Can provide consumer acceptability, functionality and nutritional value

1.4.2.3. Method of preparation of lipid nanocarrier

Production techniques of NLC are similar to that of SLN. Several methods have been described in different reports for production of lipidic nanoparticles, especially SLN. Hot homogenization method is one the extensively utilized method for preparation of both NLCs and SLNs. This method offer several advantages (such as easy scalablility, lack of organic solvents and short production time) compared to the other methods (Uner 2006).

Some of the methods that are commonly used for the production of lipid nanocarrier are given below.

1. Hot homogenization
2. Cold Homogenization
3. Solvent evaporation method
4. Solvent emulsification diffusion technique
5. Solvent injection method
6. Microemulsion based method
7. Double emulsion method
8. High-speed homogenization followed by ultrasonication method
9. Ultrasonication method
10. Phase inversion temperature (PIT) method
11. Supercritical fluid method

1.4.2.3.1. Hot homogenization

Hot homogenization is performed at temperatures 5-10°C above the melting point of the solid lipid. Homogenization at elevated temperatures results in formation of smaller particle sizes due to the decrease in the viscosity of the inner lipid phase. However, raising the homogenization pressure or the number of cycles may lead to increase of the particle size owing to increase in the kinetic energy of the developed particles (**Scheme 1**) (Singh et al. 2016b).

1.4.2.3.2. Cold homogenization

Cold homogenization method was developed to overcome the shortcomings associated with hot homogenization procedure such as temperature induced drug degradation, distribution of drug into the aqueous phase during the process of homogenization. In case of cold homogenization the drug is mixed in melted lipid phase which is then cooled and homogenization is performed (**Scheme 2**) (Beloqui et al. 2016, Muller et al. 2002a;b).

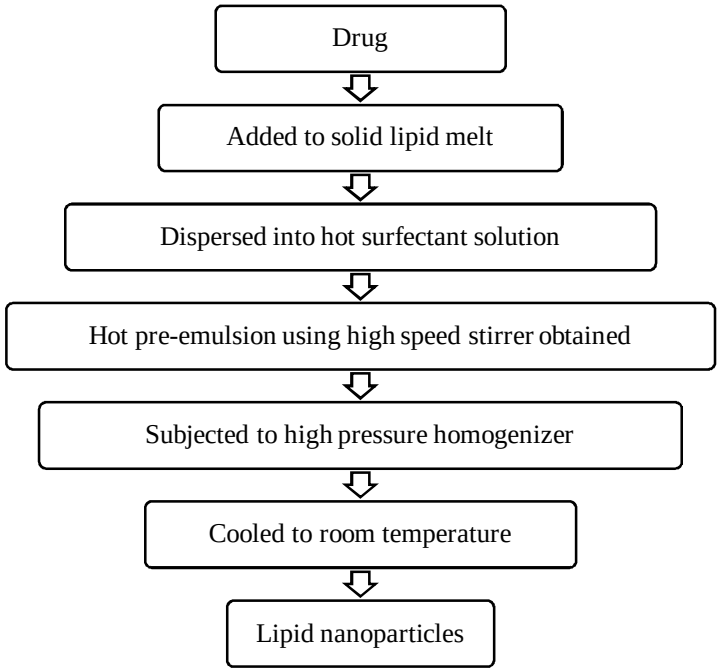

Scheme 1. Hot homogenization

1.4.2.3.3. Solvent evaporation method

In solvent evaporation method, the lipid is completely dissolved in a water-immisicible organic solvent (eg. Chloroform) which is then emulsified in an aqueous emulgent solution before evaporation of the solvent under reduced pressure. Once the solvent is evaporated, the lipid precipitates to form NLCs (**Scheme 3**) (Beloqui et al. 2016, Fang et al. 2013, Muller et al. 2002a;b).

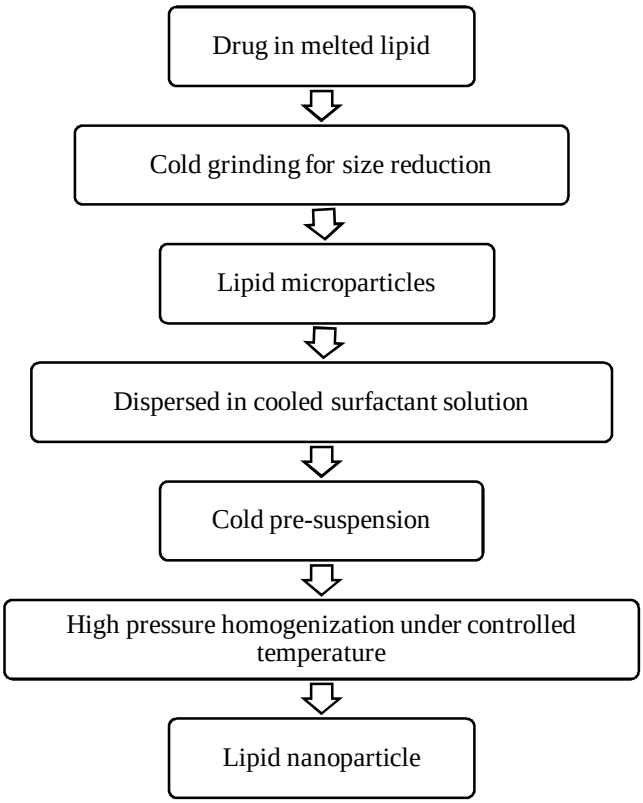

Scheme 2. Cold homogenization

1.4.2.3.4. Solvent emulsification and diffusion technique

This method involves partially water miscible solvents like benzyl alcohol and ethyl formate. Initially they are both saturated with water to make thermodynamic balance between both liquid. Later, the lipid is dissolved in the water saturated solvent and then emulsified with solvent saturated aqueous surfactant solution at raised temperature. After the addition of excess water, the lipid nanoparticles precipitate out due to diffusion of organic solvent from emulsion droplets to continuous aqueous phase (**Scheme 4**) (Beloqui et al. 2016, Fang et al. 2013, Muller et al. 2002a;b, Yuan et al. 2007).

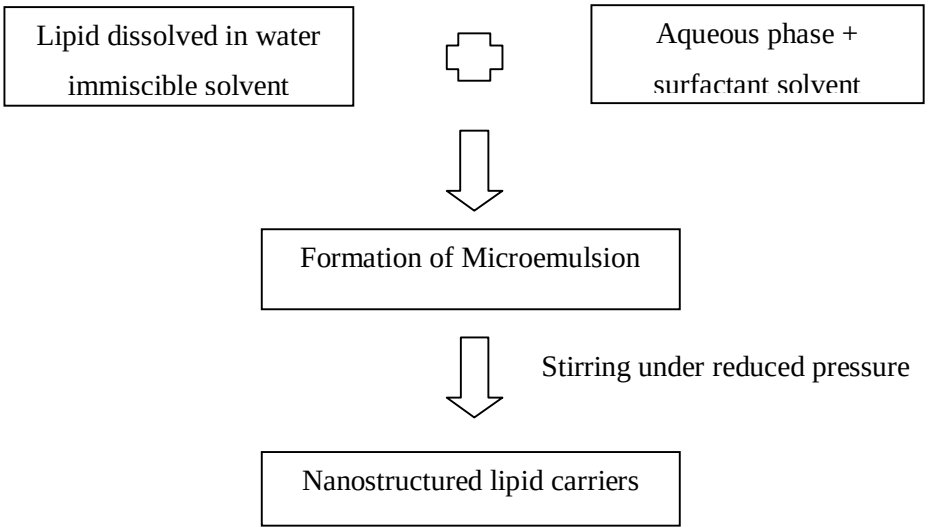

Scheme 3. Solvent evaporation method

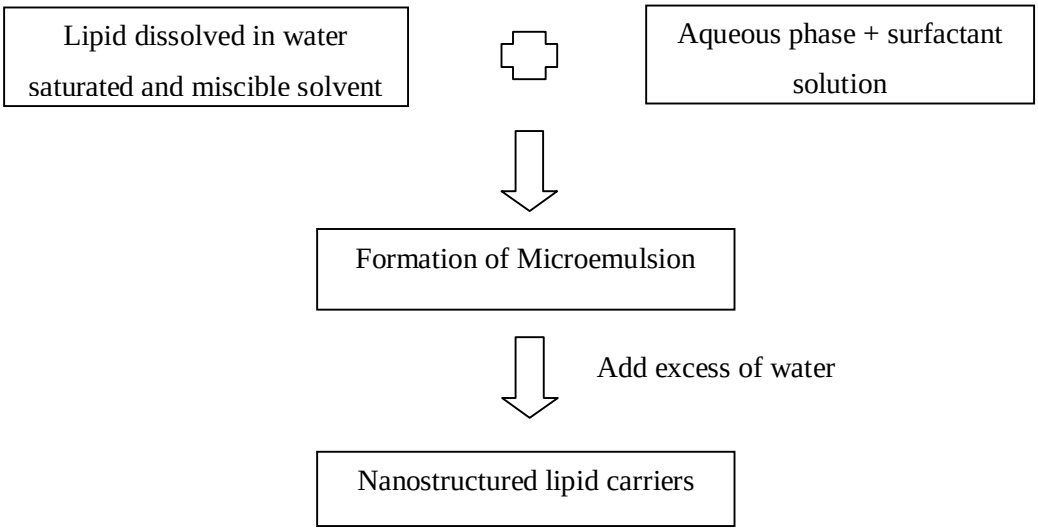

Scheme 4. Solvent emulsification and diffusion technique

1.4.2.3.5. Solvent injection method

This method is primarily based on the solvent diffusion method. The most commonly used solvents in this method are ethanol, acetone, isopropanol and methanol (**Scheme 5**) (Muller et al. 2002b).

1.4.2.3.6. Double emulsion method

In this method, the lipid melt is emulsified with an aqueous drug and surfactant solution at a high temperature by high shear homogenization. The obtained warm w/o nanoemulsion is the dispersed in the aqueous external phase of the w/o/w emulsion containing a stabilizer under mechanical stirring at 2-3°C. The resultant nano suspension is then concentrated and purified by diafilteration (**Scheme 6**) (Iqbal et al. 2012, Muller et al. 2002a;b).

1.4.2.3.7. Microemulsion based method

This method can be explained as the preparation of warm microemulsion by mixing around molten lipid phase, surfactant and co-surfactant into warm aqueous phase. This warm micro emulsion is then dispersed under continuous stirring in excess amount of cold water using a thermostated syringe. Finally, excess water is separated either by ultrafilteration or lyophilization (**Scheme 7)** (Yuan et al. 2007).

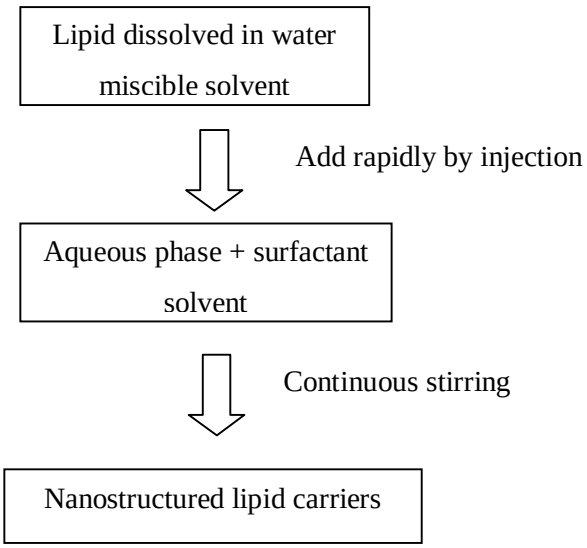

Scheme 5. Solvent injection method

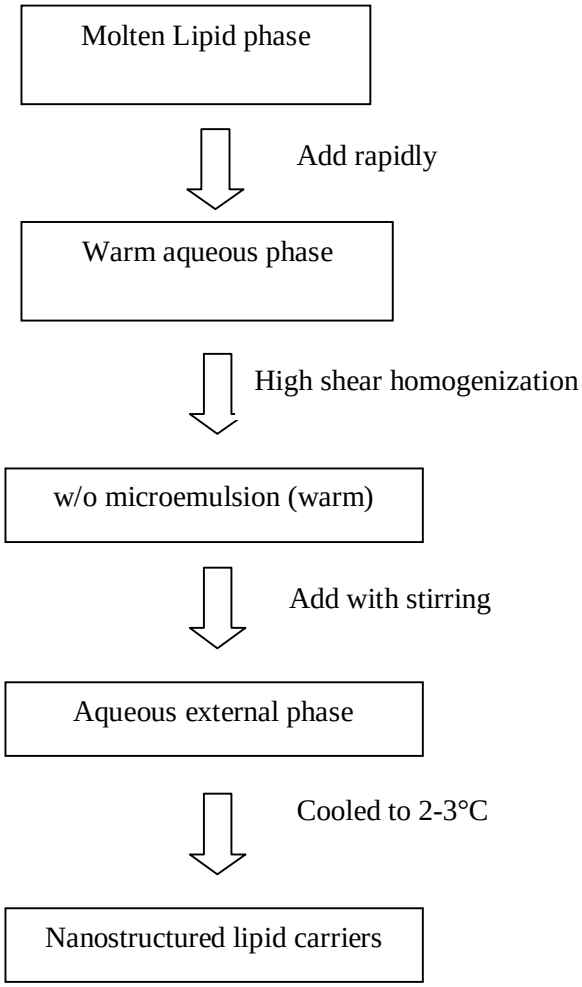

Scheme 6. Double emulsion method

1.4.2.3.8. High-speed homogenization followed by ultrasonication method

Lipid and aqueous phases are heated separately and the aqueous phase is added to lipid phase and high-shear homogenization is performed. The mixture is further subjected to sonication to produce NLCs (**Scheme 8**) (Iqbal et al. 2012, Singh et al. 2016b).

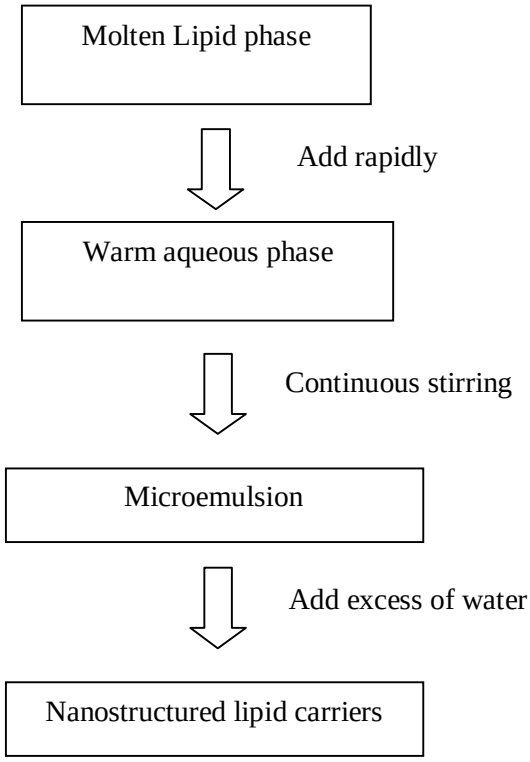

Scheme 7. Microemulsion based method

1.4.2.3.9. Ultrasonication method

This technique avoids the involvement of organic solvents or large amount of surfactants. Molted lipid is dispersed in an aqueous solution with the help of ultrasonication. The obtained emulsion is allowed to cool down to room temperature to produce NLCs (**Scheme 9**) (Fernandes et al. 2017, Singh et al. 2016d, Yuan et al. 2007).

1.4.2.3.10. Phase inversion temperature (PIT) method

Temperature induced inversion of phases is employed to produce the microemulsion and nanoparticles. The method is based on the facts that the nonionic surfactant reverses its properties depending upon temperature of the system. Increase in temperature result in dehydration of ethoxy groups resulting in increase in lipophilicity of surfactant and decrease in HLB value. The temperature at which the

affinity of surfactant is equal for lipid and aqueous phase is known as phase inversion temperature (**Scheme 10**) (Heurtault et al. 2002, Iqbal et al. 2012).

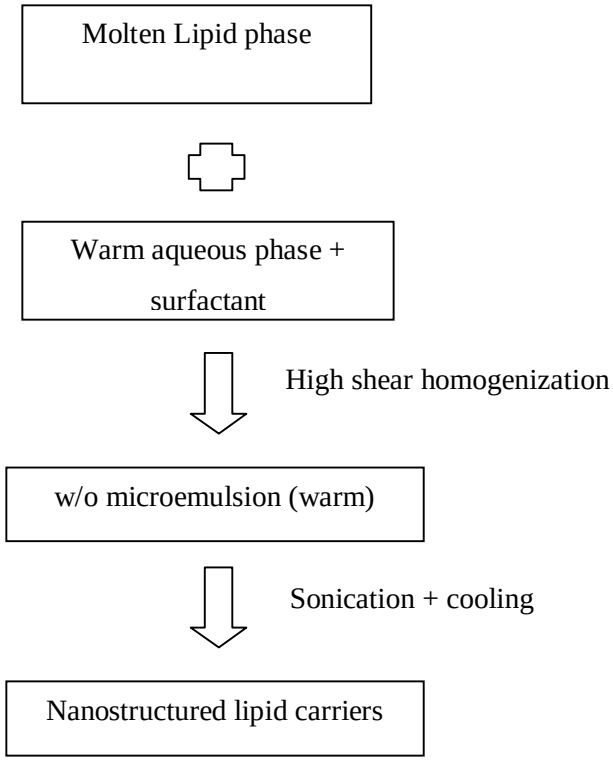

Scheme 8. High-speed homogenization followed by ultrasonication method

1.4.2.3.11. Supercritical fluid method

This is a newer technique and has advantageous characteristics of solvent-less processing. Supercritical fluids are obtained when a gas is kept above its critical pressure and temperature. Above the critical point of a fluid the solubility of any molecule can be easily modified by small changes of pressure of supercritical fluid. Carbon dioxide (99.99%) is a good choice as a critical fluid solvent as its critical point is low (31 °C and 74 bar), lower cost and nontoxic (Chen et al. 2009).

The four main Supercritical fluids processes used to produce nanoparticles are:

1. Rapid Expansion of Supercritical Solutions (RESS);
2. Gas Anti-Solvent (GAS) process;
3. Particles from Gas-saturated Solutions/Suspensions (PGSS);
4. Supercritical Fluid Extraction of Emulsions (SFEE).

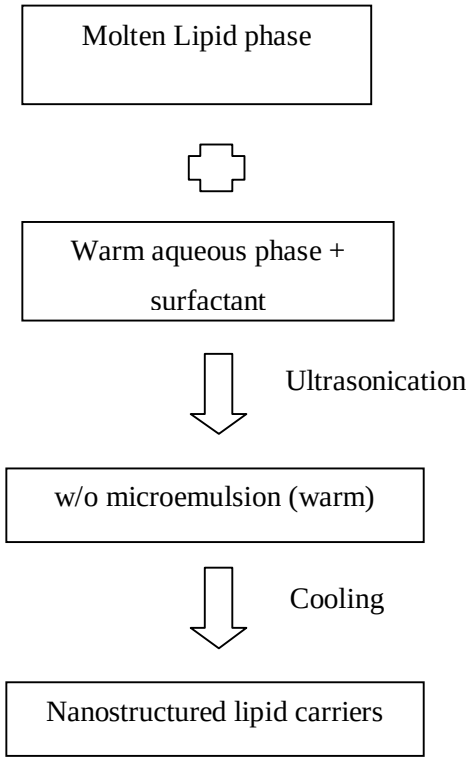

Scheme 9. Ultrasonication method

1.5. Breast Cancer

Cancer is one of the major public health issues worldwide. Cancer is considered as the second leading cause of mortality worldwide (Siegel et al. 2017). Breast cancer is one of the most common tumors diagnosed among US women and is the second leading cause for cancer related mortality among women after lung cancer. There are around 0.25 million and around 0.04 million cases of invasive breast cancer and breast cancer related deaths, respectively, are expected to take place among US women in 2017 (DeSantis et al. 2017, Siegel et al. 2017).

Cancer cases as well as cancer related mortality are markedly increasing among women in India. The reason behind this is low awareness and late stage detection. India is placed at the third place for cancer related cases among women, after China and US. Annual growth rate for number of cancer cases is growing at 4.5-5% according to the latest cancer reports. As per report “Call for Action: Expanding

cancer care for women in India, 2017", incidences of new breast cancer cases among women in India is expected to reach over 0.7 million. However, the actual incidence of cancer cases may be much more, i.e., 1.0 to 1.4 million per year as several cases remain unreported and undiagnosed. Also, India is among the top two countries worldwide on mortality related to women-specific cancers. Data from different surveys showed breast and cervical cancer mortality rates for India to be 1.6 to 1.7 times higher than the observed maternal mortality, signifying the adverse mortality rates for women specific cancers in the country. India is also spotted on the second place in case of incidence for ovarian cancer globally. India is facing a challenging scenario because of 11.54% rise in cases of newer incidence and 13.82% rise in cases of mortality due to breast cancer during 2008–2012. Furthermore, mortality has increased gradually from nearly 805 to 932 per 100000 deaths in duration of 2008 to 2012 (http://cancerindia.org.in/statistics) (Malvia et al. 2017, Ng et al. 2017).

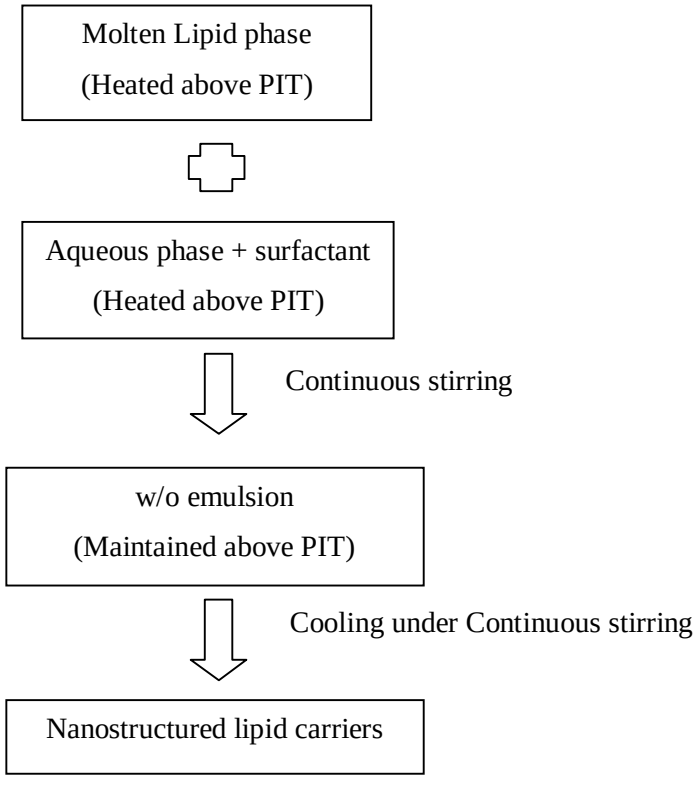

Scheme 10. Phase inversion temperature (PIT) method

Cancer is defined as a group of diseases that force the cells in the body to change in their normal characteristics and spread in an uncontrolled manner. Most types of cancer cells eventually form undifferentiated lump/mass of cells called a tumor, and are given names depending upon the part of the body where the tumor generates.Most breast cancers remain benigin in the breast tissues, i.e., in glands for milk production or in the ducts that connect lobules to the nipple.

1.5.1. Signs and symptoms

Breast cancer generally produces no specific symptoms particularly when tumor is small or on initial stages. The most common physical sign of a breast tumor is painless lump of cells felt under skin. Sometimes breast cancer spreads to lymph nodes of under arm and causes formation of a lump or a swelling. This phenomenon may occur even before the breast cancer is felt or detected. General symptoms include breast pain, heaviness along with persistent changes in tissue such as thickening, swelling, or redness of the skin and nipple related abnormalities such as spontaneous bloody discharge, erosion or retraction (Jones 2008, McPherson et al. 2000, Singletary 2003).

1.5.2. Diagnosis

Diagnosis of breast cancer is generally done either during a screening examination before symptoms appear, or after a woman notices a lump or nodule. Further, the masses can be observed on a mammogram. Generally most breast cancers turn out to be benign, do not grow uncontrollably or migrate, and are considered not to be life-threatening. Microscopic analysis of breast tissue is performed in most of cases where cancer is suspected. Further, to determine the extent of spread and stage of cancer and to characterize the type of the disease biopsy or surgical incision may be performed (Jones 2008, Malvia et al. 2017, McPherson et al. 2000).

1.5.3. In situ breast cancer

In situ breast cancers are identified as abnormal cells that have not penetrated to the nearby ducts or glands from which they originated. There are two main types of in situ breast cancer: ductal carcinoma in situ (DCIS) and lobular carcinoma in situ

(LCIS), also known as lobular neoplasia (Jones 2008, McPherson et al. 2000, Singletary 2003).

1.5.4. Invasive breast cancer

Most of the breast cancers diagnosed are invasive i.e., they have broken from the place of origin and migrated into surrounding breast tissue. Generally breast cancer has been considered as a single disease still there are up to 21 histological subtypes along with four molecular subtypes identified that differ in terms of presentation, risk factors, outcomes and response to treatment. Molecular subtypes have been characterized using biological markers such as presence or absence of hormone receptors (estrogen or progesterone, HR+/HR-) and expression levels of human epidermal growth factor receptor 2 (HER2) or extra copies of the HER2 gene (HER2+/HER2-). The four main molecular subtypes and their distribution in breast tissues are Luminal A (HR+/HER2-) (71%), Luminal B (HR+/HER2+) (12%),Triple negative (HR-/HER2-) (12%), HER2-enriched (HR-/HER2+) (5%) (McPherson et al. 2000, Singletary 2003).

1.5.5. Breast Cancer Treatment

Several risk factors like age, reproductive factors, personal and family history of cancer, exogenous and endogenous hormonal exposures, environmental factors, lifestyle factors such as diet and alcohol consumption have been shown to be involved in the development of breast cancer. Genetic and epigenetic changes such as BRCA1/2 mutations have also been shown to affect the risk breast cancer. The risks of cancer rises to 65–81% for cases with BRCA1 mutation carriers and 45–85% for BRCA2 mutation carriers (McPherson et al. 2000, Singletary 2003, Verma et al. 2012, Wu et al. 2013).

1.5.5.1. Treatment of Early-Stage Breast Cancer

Anthracycline based drug such as doxorubicin, epirubicin etc., and taxanes like docetaxel and paclitaxel based regimens form the foundation for primary stage breast cancer treatment. Most extensively utilized anthracycline based combinations are doxorubicin cyclophosphamide (AC) and 5-fluorouracil based combination, FAC (5-

FU, doxorubicin, and cyclophosphamide) or FEC (5-FU, epirubicin, and cyclophosphamide). Now-a-days, taxane based regimens like TAC (docetaxel, doxorubicin, and cyclophosphamide), ACT (AC followed by a taxane) and non-anthracycline TC (docetaxel+cyclophosphamide) have exhibited superior survival outcomes and a better safety profile than anthracycline based therapy regimens in several studies. There is always a concern of cumulative dose related cardiotoxicity associated with long term therapy of anthracyclines anticancers, nonanthracycline regimens are gaining more and more interest. However, the lack of cardiotoxicity with nonanthracycline regimens might be paralleled by efficacy benefits. The patients with breast cancer having HER2-positive tumors should benefit from treatment with trastuzumab as shown in several trials (Jones 2008, McPherson et al. 2000, Singletary 2003).

1.5.5.2. Treatment of Metastatic Breast Cancer (MBC)

Patients with Metastatic Breast Cancer are a heterogeneous group and therefore an individualized approach to treatment is now considered to be necessary. The oncologist consider some issues like treatments given for early-stage breast cancer, what drugs were used, what were the cumulative doses administered etc. Patients might have drug-resistant tumors, or they may have been administered with cumulative doses that could be responsible for unacceptable toxicity. Such factors can limit or prohibit the inclusion of these agents in future treatment strategies.

Five distinct patient categories should be considered (Jones 2008):

(1) No adjuvant treatment

(2) Adjuvant CMF (cyclophosphamide, methotrexate, and 5-FU) or an anthracycline-based regimen

(3) Adjuvant paclitaxel

(4) adjuvant docetaxel;

(5) Adjuvant therapy including trastuzumab.

1.5.5.3. Use of Targeted Agent

Even though significant advancements in tumor therapy, the treatment after cancer has metastasized remains an unmet challenge for clinicians (Goldman et al. 2017). Regardless of encouraging results from preliminary studies in most antitumor

therapies, the primary obstacle for clinical application of these drugs are their adverse effects on normal cells due to nonspecific distribution of delivery system to normal tissues along with tumor tissue. The lack of tumor specificity always remains an issue of debate for the modern pharmaceutical scientists (Cho et al. 2008, Oliveira et al. 2017). The future of therapy for MBC appears to involve combining effective single agent chemotherapeutic agents with novel and newer biological agents that can exploit specific targets in the cancer (Jones 2008). Designing target specific drug delivery systems, often regarded as the magic bullet approach, are able to overcome chemotherapy related side effects due to systemic therapy with improved efficacy and tolerability due to their local action. Amongst the various targeting approaches like antibodies, proteins, peptides, nucleic acid-based ligand and small molecules, most common targets for MBC are Human epidermal growth factor receptor 2, i.e., HER2-overexpressed receptor, vascular endothelial growth factor (VEGF), estrogen receptor (ER) and progesterone receptor (PR), folate receptor (FR), biotin receptor etc. The most widely investigated targeted therapy utilizing HER2 is trastuzumab. Bevacizumab is a VEGF targeted molecule that is currently under advanced clinical trials for MBC along with paclitaxel. Folate receptor is a membrane coupled glycoprotein receptor that is preferentially expressed in cancers of epithelial origin. It is barely expressed in normal human cells. Hence, these receptors support the possibility for targeting approaches in the management of breast carcinoma (Hartmann et al. 2007, Hu et al. 2014, Kue et al. 2016, Zhang et al. 2014). Recent findings advocated that biotin or biotin conjugated systems can constructively be targeted to the tumor cells with the help of overexpressed biotin-selective transporters. Biotin has a critical role in cell signaling, epigenetic gene regulation and chromatin structure at the cellular level. Mammalian cells lack biotin synthetic pathway, and therefore, depend on sources like plants and bacterial systems for the same. The mammalian cells accomplish uptake through biotin transporter (high-affinity for biotin) and also through SMVT. The main transporter for biotin uptake is SMVT, which is overexpressed in several aggressive tumors such as leukemia, ovarian, colon, lung, renal and breast tumor (Kue et al. 2016, Ren et al. 2015, Tripodo et al. 2014, Wu et al. 2013, Zempleni et al. 2009).

1.6. Reactive oxygen species and cancer

As a consequence of aerobic metabolism in cells, smaller amounts of reactive oxygen species (ROS) like hydroxyl free radicals ($^{\cdot}OH$), superoxide anions ($O_2^{\cdot-}$), singlet oxygen ($^1O_2$), hydrogen peroxide (H_2O_2) etc., are constantly generated in organisms (Borek 2017, Mates and Sanchez-Jimenez 2000, Padmavathi et al. 2006). Cellular antioxidants act as detoxifying agents for such species but in some cases the balance between free redical generation and its detoxification is disturbed. This imbalanced situation is referred to as oxidative stress (Iyengar et al. 2013, Roy et al. 2017). If such imbalance persists for a longer period, the oxidative damage to vital biomolecules, like oxidant caused damage to the genes or DNA, accumulates and subsequently causes several biological changes ranging from modulation of gene expression and signal transduction to transformation, mitogenesis, mutagenesis and cell death (Iyengar et al. 2013, Roy et al. 2017, Trivedi et al. 2011, Wiseman and Halliwell 1996).

Apoptosis and cancer are contrasting phenomena, but ROS have been demonstrated to play a vital role in both cases. There are reports that supports that ROS can induce apoptosis. In these evidences the mediators of cellular apoptosis that induces production of intracellular ROS are downregulated by antioxidants. Although, the exact chain of mechanisms involved is still controversial as redox status and/or hydrogen peroxide both has been suggested as vital factors for apoptosis(Mates and Sanchez-Jimenez 2000). [14, 15] Additionally, the linkage between the induction of carcinogenesis to oxidative DNA damage has been clearly established. Further, 8-oxo-2'-deoxyguanosine, a DNA oxidative product has been shown to be highly mutagenic. (Fan et al. 2013, Hinrichsen et al. 1990, Trivedi et al. 2011, Wiseman and Halliwell 1996)[16]

There are several studies that suggest that the dietary supplementation of antioxidants can alter the response to chemotherapeutic drugs. Also, antioxidants attenuate the development of adverse side effects that may develop as consequence of treatment with antineoplastic agents (Doroshow 1986, Figueroa et al. 2018, Mates and Sanchez-Jimenez 2000, Wiseman and Halliwell 1996).

Administration of antineoplastic agents results in oxidative stress, i.e., the production of free radicals and other ROS. Oxidative stress produced may reduce the rate of cellular proliferation. Reduction in cellular proliferation may interfere with the cytotoxic effects of chemotherapeutic drug those anticancer activity depends on rapid cellular proliferation. Antioxidants by detoxifying ROS may potentiate the anticancer effects of chemotherapeutic agents (Doroshow 1986, Figueroa et al. 2018, Mates and Sanchez-Jimenez 2000, Wiseman and Halliwell 1996) . ROS contribute to several side effects that are common to different anticancer drugs, such as gastrointestinal toxicity and mutagenesis. ROS is also involved in some side effects that occur with some specific drugs for example cisplatin-induced nephrotoxicity, doxorubicin-induced cardiotoxicity, and bleomycin-induced pulmonary fibrosis. Antioxidants can prevent or reduce such side effects. However, certain side myelosuppression and alopecia are not affected by antioxidants (Doroshow 1986, Figueroa et al. 2018, Mates and Sanchez-Jimenez 2000, Wiseman and Halliwell 1996).

2. Literature Review

Authors	Formulation/objective	Drug	Major Observations
(Sabzichi et al. 2017)	all-trans-retinoic acid loaded NLCs	Doxorubicin	two-fold increase in the % apoptosis in MDA-MB-231 breast cancer cells
(Yu et al. 2017)	Composition and effects of *Perilla frutescens* oil	*Perilla frutescens* oil	1. High percentage of ω-3 fatty acid 2. Anti-allergic, anti-inflammatory, anti-oxidant, anticancer, anti-microbial, anti-depressive and anti-cough effects.
(Tripathi et al. 2017)	ω-3 fatty acid content of *Perilla frutescens* oil	*Perilla frutescens* oil	50-70% of ω-3 fatty acids
(Yuan et al. 2016)	nanodelivery		1. Bypasses multispecific drug efflux transporters 2. Can be exploit to target cancer sites by bypassing these transporters 3. Reverses the drug resistance
(Iyengar et al. 2013)	Omega-3 fatty acids	Various	1. Prevention of breast cancer 2. explored the mechanisms by which ω-3 FA may show breast cancer protective activity
(D'Eliseo and Velotti 2016)	n-3 polyunsaturated fatty acids (PUFAs), eicosapentaenoic acid (EPA) and	Various	1. Exert anti-neoplastic activity by inducing apoptotic cell death in human cancer cells 2. Can be used alone or in

Authors	Formulation/objective	Drug	Major Observations
	docosahexaenoic acid (DHA)		combination with conventional therapies 3. Increases sensitivity of tumor cells to conventional drug therapies
(Wu et al. 2016)	Biotinylated carboxymethyl chitosan/CaCO3 hybrid nanoparticles	Doxorubicin	1. Targeted cancer cells 2. Overcome drug resistance 3. Strong anti-tumor activity against MCF-7 cell lines
(Tripodo et al. 2014)	Biotin conjugation	Various	Biotin can be utilized target to cancers like colon, breast, lung, renal
(Singh et al. 2016a)	Nanoemulsion	Simvastatin	1. Alpha linolenic acid based lipidic nanoemulsion 2. Bioavailability enhancement of simvastatin for hyperlipidemia
(Roy et al. 2017)	Efficacy of linolenic acid in breast cancer	Alpha linolenic acid	Significant effect upon the cellular proliferation through mitochondrial mediated apoptosis in MCF-7
(Huan et al. 2009)	α-linolenic acid conjugated drug	Doxorubicin	Improvement the cellular uptake, internalization and cytotoxicity in MCF-7 cells
(Hartmann et al. 2007)	Extent of expression of folate in various cancer	Folate receptors	1. High affinity folate receptor is preferentially expressed in cancers with epithelial origin 2. Supports the possibility of utilizing folate receptor for the

Authors	Formulation/objective	Drug	Major Observations
			management of breast carcinoma
(Elmore et al. 2002)	Expression of p53 family proteins in breast cancer	p16 expression	p53 family proteins like p16, p21 etc. are involved in breast tumor cell apoptosis and metastasis
(Park et al. 2004)	Expression of Caspase family proteins in breast cancer	Caspase-6, -7, -8, -9 and -10	Defects in Caspase-6, -7, -8, -9 and -10 activation was responsible for doxorubicin resistance in breast cancer cell lines MCF-7
(Um 2016)	Bcl-2 family proteins as key regulator of cancer	Bcl-2 family proteins	Key regulator of cancer cell apoptosis, invasion and metastasis through mitochondrial respiration and reactive oxygen species
(Zeng et al. 2014)	Nanoparticles based drug delivery systems	Nanoparticles	Able to overcome drug resistance in cancer cells mainly by avoiding the activation of efflux pumps in these cells.
(Zhang et al. 2012a)	Mechanism of doxorubicin-induced cardiotoxicity	Doxorubicin	Cardiomyocyte-specific Top2b gene (encoding topoisomerase-IIb) are involved in doxorubicin-induced cardiotoxicity
(Alkhatib and AlBishi 2013)	Doxorubicin based nanoemulsion	Doxorubicin	Selectively and significantly inhibited cell proliferation of MCF-7 cells and increased cellular apoptosis

Authors	Formulation/objective	Drug	Major Observations
(Bae et al. 2013)	Folate targeted nanoemulsion	Perfluorocarbon/rhodamine nanoemulsion	1. Phospholipid-anchored folate decorated perfluorocarbon/ rhodamine nanoemulsion 2. Targeted FR-expressing Nasopharyngeal Carcinoma
(Jiang et al. 2013)	Pegylated lipid nanoemulsion	Doxorubicin	1. Development of safe and effective PEGylated lipid nanoemulsion for doxorubicin delivery to A549 tumor cells. 2. LNEs were internalized into tumor cells *in vitro* and efficiently accumulate in tumor tissues *in vivo* by passive targeting
(Goldman et al. 2017)	Liposomes	multi-modal diagnostic agents-indocyanine green, rhodamine, gadolinium, europium	1. Developed 100 nm liposomes to target metastatic triple-negative murine breast-cancer metastases. 2. Liposomes were detected in the metastatic progression target breast cancer metastasis 3. Elevated levels of drug found in the pre-metastatic niche, several days before metastases are visualized by MRI or histologically in the tissue
(Pandey et al. 2015)	lactoferin (Lf) appended solid	Paclitaxel	1. Management of bronchogenic carcinoma

Authors	Formulation/objective	Drug	Major Observations
	lipid nanoparticles		2. Higher concentrations of PTX accumulated in lungs via Lf-coupled SLNs than plain SLNs and free PTX
(Bellezza et al. 2014)	resistance of PC3 prostate cancer cells to pro-oxidant damage	α-tocopheryl succinate	1. It inhibits oxidative phosphorylation of mitochondrial complexes I and II 2. Induces the expression of Nrf2-driven antioxidant/detoxifying genes
(Tomasina et al. 2013)	folate-functionalized nanoparticles for ovarian carcinoma	Tripentone	1. The system reaches SKOV3 cells rapidly 2. Internalized by a folate-receptor mediated endocytosis pathway 3. rapid delivery of the antitumor agent tripentone into cells
(Fan et al. 2013)	Selenocystine (SeC), acts as an effective enhancer of 5-FU	5-fluorouracil	1. Selenocystine (SeC), a naturally occurring selenoaminoacid 2. Effective enhancer of 5-FU-induced apoptosis in A375 human melanoma cells 3. involve of DNA damage-mediated p53 phosphorylation, and AKT and ERK inactivation 4. SeC significantly enhanced

Authors	Formulation/objective	Drug	Major Observations
			5-FU-induced loss of mitochondrial membrane potential through bcl-2 proteins
(Talekar et al. 2012)	EGFR and FR functionalized nanoemulsions	Phosphatidylinositol 3-kinase inhibitor	1. 57% decrease in IC(50) value of PIK75 following treatment with EGFR targeted nanoemulsion and 40% decrease following treatment with FR targeted nanoemulsion 2. Addition of ceramide enhanced the cytotoxicity of PIK75
(Lammers et al. 2008)	drug targeting to tumors	Various	Pitfalls and barriers for drug targeting was exhaustively reviwed along with clinical progress of targeted drug delivery
(Zhang et al. 2011)	lipid nanoemulsions loaded with doxorubicin-oleic acid ionic complex	Doxorubicin	1. high encapsulation efficiency 2. drug release pattern with rapid release at the initial stage 3. higher growth inhibitory effect
(Ganta et al. 2010)	long-circulating nanoemulsion (LNE) modified with poly(ethylene glycol)	Chlorambucil	1.4-fold higher area under the plasma concentration-time curve (AUC) 1.3-fold longer half-life compared non modified LNE

Authors	Formulation/objective	Drug	Major Observations
			2.7-fold higher AUC 7.6-fold longer half-life compared to chlorambucil solution
(Mendes et al. 2009)	nanoemulsion	Chemotherapeutic agents	decreases toxicity of the chemotherapeutic agents without decreasing the anticancer action by administering nanoemulsion concentrates of antineplastic agent in breast carcinoma tissue after locoregional injection
(Ohguchi et al. 2008)	folate-targeted nanoemulsion	aclacinomycin A	Selective FR-mediated uptake was achieved in a human nasopharyngeal tumor cell line
(Padmavathi et al. 2006)	paclitaxel and propolis as antioxidant	Paclitaxel and propolis	1. Effectively suppressed breast cancer, 2. Decrease in the extent of lipid peroxidation (LPO) increase in the activities of enzymic antioxidants SOD, catalase and glutathione peroxidase (GPx)) and non-enzymic antioxidants (reduced glutathione (GSH)
(Borek 2017)	high intake of anti-oxidant-rich foods	Antioxidants	1. Selenium and vitamin E reduced the risk prostate and colon cancer

Authors	**Formulation/objective**	**Drug**	**Major Observations**
			2. Carotenoids reduce breast cancer risk 3. Vitamins E and C have been shown to ameliorate adverse side effects associated with free radical damage
(Mates and Sanchez-Jimenez 2000)	Free radicals induce DNA sequence changes	Various	Free radicals induce changes in DNA sequence that cause mutations, deletions, gene amplification and rearrangements

3. Research Envisaged

The application potential of free radical scavengers such as antioxidants as cancer chemopreventive and chemotherapeutic agents has been supported by many epidemiological, preclinical, and clinical studies. Various experimental studies indicated that antioxidants and some phytochemicals selectively induce apoptosis in cancer cells but not in normal cells and prevent angiogenesis and metastatic spread, suggesting a potential role for antioxidants as adjuvants in cancer therapy.

Nanotechnology-based drug delivery has become one of the most extensively studied fields in nanomedicine in the recent decade. Various targeting mechanisms, including passive targeting via EPR effect, receptor mediated active targeted and environment-sensitive drug controlled release, have been applied widely in rationale design of targeting delivery systems.

The present study envisages preparing and characterizing a targeted nano-carrier for delivery of anticancer drug. Also, combination of naturally existing antioxidants can be utilized to combat oxidative stress present in several tumors. That may potentiate the chemotherapeutic effect of an anticancer drug and may alleviate the associated free radical toxic effects of anticancer drug(s), will be investigated in different cell lines. By using this approach we may avoid systemic toxicity, improve safety and efficacy of drug(s), reduce dosing, improve solubility of lipophilic drug(s), improve patient acceptability etc. of selected drug candidate(s). Advances in experimental and computational methodologies will be helpful in shortening the processing time from formulation design to clinical use.

4. Objectives of the work

The objective of this study is the development and characterization of targeted lipidic nanocarrier system for site specific delivery of anticancer drug (s). The targeted drug nanocarrier should preferentially deliver anticancer drug to the desired site utilizing some guiding molecule thereby reducing inappropriate disposition of drug to the normal cells. Further, the naturally occurring antioxidants can be associated with these nanocarriers which may potentiate the anticancer molecules and also provide an antioxidant shield to the normal cells thereby lowering drug related side effects.

The specific objectives were:

(1) To develop α-linolenic acid based targeted nanoemulsion and its evaluation for safety and efficacy cancer cell lines and cancer induced rat model.

(2) To develop *Perilla frutescence* oil based targeted nanostructured lipid carrier(s) and their evaluation in cancer cell lines and cancer induced rat model for safety and efficacy.

5. Hypothesis

It was hypothesized that the current study would result in development of a stable, safe and effective nanoemulsion and nanostructured lipid carrier of doxorubicin. The attachment of targeting ligand would selectively and effectively transport the encapsulated drug specifically to the target site owing to overexpressed receptors on cancer cell surface. Thus, a higher drug concentration of anticancer drug would be attained at the required site. The incorporation of naturally occurring antioxidants as well as anticancer agents (α-linolenic acid and *Perilla frutescence* oil in this case) in developed system would help in potentiating the effect of anticancer molecule. Also, the antioxidant characteristics of the incorporated lipids would act against the drug induced toxic effects. This approach would maximize therapeutic benefits of anticancer agents in comparison to conventional formulations and would be expected to facilitate the management of cancer with higher safety and efficacy.

6. Plan of Work

1. Literature Survey & Procurement of Materials
2. Preformulation study
    - Identification and Characterization of Drug
    - Selection of analytical method
3. Selection of excipients
4. Preparation of nanocarrier system
    - Pharmaceutical considerations
    - Physiological considerations
    - Pharmacological considerations
    - Optimization of drug delivery systems
5. *In vitro* Characterization of nanocarriers
    - Entrapment efficiency
    - Drug content and drug loading
    - *in vitro* release studies
    - Zeta potential and aggregation behavior
    - Size and size distribution studies
    - Shape (TEM)
    - Surface modification of nanocarrier
6. Cell lines study
    - MTT assay
    - Cell Cycle Analysis
    - Cell proliferation study
    - Reactive Oxygen Species estimation
    - Mitochondrial membrane potential
    - Cellular uptake study
7. Stability Studies
8. *In vivo* Studies
    - Tumor volume
    - Tumor incidence
    - Animal weight
    - Animal survival
    - Biochemical Estimation
    - Western blotting
    - Whole mounts mammary gland
9. Statistical analysis
10. Computation and Compilation of work

7. Reference

Alkhatib MH, AlBishi HM (2013) In vitro evaluation of antitumor activity of doxorubicin-loaded nanoemulsion in MCF-7 human breast cancer cells. J Nanopart Res. 15(1489

Allen TM, Cullis PR (2004) Drug delivery systems: entering the mainstream. Science. 303(5665):1818-22.

Anton N, Vandamme TF (2011) Nano-emulsions and micro-emulsions: clarifications of the critical differences. Pharmaceutical research. 28(5):978-85.

Bae PK, Jung J, Lim SJ, Kim D, Kim SK, Chung BH (2013) Bimodal perfluorocarbon nanoemulsions for nasopharyngeal carcinoma targeting. Mol Imaging Biol. 15(4):401-10.

Bellezza I, Grottelli S, Gatticchi L, Mierla AL, Minelli A (2014) alpha-Tocopheryl succinate pre-treatment attenuates quinone toxicity in prostate cancer PC3 cells. Gene. 539(1):1-7.

Beloqui A, Solinis MA, Rodriguez-Gascon A, Almeida AJ, Preat V (2016) Nanostructured lipid carriers: Promising drug delivery systems for future clinics. Nanomedicine. 12(1):143-61.

Bertrand N, Wu J, Xu X, Kamaly N, Farokhzad OC (2014) Cancer nanotechnology: the impact of passive and active targeting in the era of modern cancer biology. Adv Drug Deliv Rev. 66(0):2-25.

Borek C (2017) Dietary Antioxidants and Human Cancer. Journal of Restorative Medicine. 6(1):53-61.

Cairns R, Papandreou I, Denko N (2006) Overcoming physiologic barriers to cancer treatment by molecularly targeting the tumor microenvironment. Mol Cancer Res. 4(2):61-70.

Chen Y, Chen F, Wei W, Zhang X, Feng Q, Jin R (2009) [Preparation of nanostructured lipid carriers loaded with supercritical carbon dioxide fluid extraction of Xionggui powder]. Zhongguo Zhong Yao Za Zhi. 34(2):148-51.

Cho K, Wang X, Nie S, Chen ZG, Shin DM (2008) Therapeutic nanoparticles for drug delivery in cancer. Clin Cancer Res. 14(5):1310-16.

Choi CH, Alabi CA, Webster P, Davis ME (2010) Mechanism of active targeting in solid tumors with transferrin-containing gold nanoparticles. Proc Natl Acad Sci U S A. 107(3):1235-40.

D'Eliseo D, Velotti F (2016) Omega-3 Fatty Acids and Cancer Cell Cytotoxicity: Implications for Multi-Targeted Cancer Therapy. J Clin Med. 5(2):pii: E15.

Davis ME, Chen ZG, Shin DM (2008) Nanoparticle therapeutics: an emerging treatment modality for cancer. Nat Rev Drug Discov. 7(9):771-82.

Delmas T, Piraux H, Couffin AC, Texier I, Vinet F, Poulin P, Cates ME, Bibette J (2011) How to prepare and stabilize very small nanoemulsions. Langmuir. 27(5):1683-92.

DeSantis CE, Ma J, Goding Sauer A, Newman LA, Jemal A (2017) Breast cancer statistics, 2017, racial disparity in mortality by state. CA Cancer J Clin. 67(6):439-48.

Doroshow JH (1986) Prevention of doxorubicin-induced killing of MCF-7 human breast cancer cells by oxygen radical scavengers and iron chelating agents. Biochem Biophys Res Commun. 135(1):330-5.

Elmore LW, Rehder CW, Di X, McChesney PA, Jackson-Cook CK, Gewirtz DA, Holt SE (2002) Adriamycin-induced senescence in breast tumor cells involves functional p53 and telomere dysfunction. J Biol Chem. 277(38):35509-15.

Fan C, Chen J, Wang Y, Wong YS, Zhang Y, Zheng W, Cao W, Chen T (2013) Selenocystine potentiates cancer cell apoptosis induced by 5-fluorouracil by triggering reactive oxygen species-mediated DNA damage and inactivation of the ERK pathway. Free Radic Biol Med. 65(0):305-16.

Fang CL, Al-Suwayeh SA, Fang JY (2013) Nanostructured lipid carriers (NLCs) for drug delivery and targeting. Recent Pat Nanotechnol. 7(1):41-55.

Fernandes RS, Silva JO, Mussi SV, Lopes SCA, Leite EA, Cassali GD, Cardoso VN, Townsend DM, Colletti PM, Ferreira LAM, Rubello D, de Barros ALB (2017) Nanostructured Lipid Carrier Co-loaded with Doxorubicin and Docosahexaenoic Acid as a Theranostic Agent: Evaluation of Biodistribution and Antitumor Activity in Experimental Model. Mol Imaging Biol: doi: 10.1007/s11307-017-1133-3.

Figueroa D, Asaduzzaman M, Young F (2018) Real time monitoring and quantification of reactive oxygen species in breast cancer cell line MCF-7 by 2',7'-dichlorofluorescin diacetate (DCFDA) assay. J Pharmacol Toxicol Methods. 94(Pt 1):26-33.

Ganta S, Sharma P, Paxton JW, Baguley BC, Garg S (2010) Pharmacokinetics and pharmacodynamics of chlorambucil delivered in long-circulating nanoemulsion. J Drug Target. 18(2):125-33.

Ganta S, Singh A, Rawal Y, Cacaccio J, Patel NR, Kulkarni P, Ferris CF, Amiji MM, Coleman TP (2016) Formulation development of a novel targeted theranostic nanoemulsion of docetaxel to overcome multidrug resistance in ovarian cancer. Drug Deliv. 23(3):968-80.

Ganta S, Talekar M, Singh A, Coleman TP, Amiji MM (2014) Nanoemulsions in Translational Research-Opportunities and Challenges in Targeted Cancer Therapy. AAPS PharmSciTech. 15(3):694-708

Goldman E, Zinger A, da Silva D, Yaari Z, Kajal A, Vardi-Oknin D, Goldfeder M, Schroeder JE, Shainsky-Roitman J, Hershkovitz D, Schroeder A (2017) Nanoparticles target early-stage breast cancer metastasis in vivo. Nanotechnology. 28(43):43LT01.

Hartmann LC, Keeney GL, Lingle WL, Christianson TJ, Varghese B, Hillman D, Oberg AL, Low PS (2007) Folate receptor overexpression is associated with poor outcome in breast cancer. Int J Cancer. 121(5):938-42.

Heurtault B, Saulnier P, Pech B, Proust JE, Benoit JP (2002) A novel phase inversion-based process for the preparation of lipid nanocarriers. Pharm Res. 19(6):875-80.

Hinrichsen LI, Floyd RA, Sudilovsky O (1990) Is 8-hydroxydeoxyguanosine a mediator of carcinogenesis by a choline-devoid diet in the rat liver? Carcinogenesis. 11(10):1879-81.

Hu D, Sheng Z, Fang S, Wang Y, Gao D, Zhang P, Gong P, Ma Y, Cai L (2014) Folate receptor-targeting gold nanoclusters as fluorescence enzyme mimetic nanoprobes for tumor molecular colocalization diagnosis. Theranostics. 4(2):142-53.

Huan ML, Zhou SY, Teng ZH, Zhang BL, Liu XY, Wang JP, Mei QB (2009) Conjugation with alpha-linolenic acid improves cancer cell uptake and cytotoxicity of doxorubicin. Bioorg Med Chem Lett. 19(9):2579-84

Iqbal MA, Md S, Sahni JK, Baboota S, Dang S, Ali J (2012) Nanostructured lipid carriers system: recent advances in drug delivery. J Drug Target. 20(10):813-30.

Iyengar NM, Hudis CA, Gucalp A (2013) Omega-3 fatty acids for the prevention of breast cancer: an update and state of the science. Curr Breast Cancer Rep. 5(3):247-54.

Jain RK, Stylianopoulos T (2010) Delivering nanomedicine to solid tumors. Nat Rev Clin Oncol. 7(11):653-64.

Jiang SP, He SN, Li YL, Feng DL, Lu XY, Du YZ, Yu HY, Hu FQ, Yuan H (2013) Preparation and characteristics of lipid nanoemulsion formulations loaded with doxorubicin. Int J Nanomedicine. 8(0):3141-50.

Jones SE (2008) Metastatic breast cancer: the treatment challenge. Clin Breast Cancer. 8(3):224-33.

Joshi MD, Muller RH (2009) Lipid nanoparticles for parenteral delivery of actives. Eur J Pharm Biopharm. 71(2):161-72.

Kakumanu S, Tagne JB, Wilson TA, Nicolosi RJ (2011) A nanoemulsion formulation of dacarbazine reduces tumor size in a xenograft mouse epidermoid carcinoma model compared to dacarbazine suspension. Nanomedicine. 7(3):277-83.

Kamaly N, Xiao Z, Valencia PM, Radovic-Moreno AF, Farokhzad OC (2012) Targeted polymeric therapeutic nanoparticles: design, development and clinical translation. Chem Soc Rev. 41(7):2971-3010.

Kue CS, Kamkaew A, Burgess K, Kiew LV, Chung LY, Lee HB (2016) Small Molecules for Active Targeting in Cancer. Med Res Rev. 36(3):494-575.

Kumar S, Dang S, Nigam K, Ali J, Baboota S (2018) Selegiline nanoformulation in attenuation of oxidative stress and upregulation of dopamine in the brain for the treatment of Parkinson's disease. Rejuvenation Res. 2(10)

Lammers T, Hennink WE, Storm G (2008) Tumour-targeted nanomedicines: principles and practice. Br J Cancer. 99(3):392-7.

Liu D, Liu F, Liu Z, Wang L, Zhang N (2011) Tumor specific delivery and therapy by double-targeted nanostructured lipid carriers with anti-VEGFR-2 antibody. Mol Pharm. 8(6):2291-301.

Liu Y, Yu XM, Sun RJ, Pan XL (2017) Folate-Functionalized Lipid Nanoemulsion to Deliver Chemo-Radiotherapeutics Together for the Effective Treatment of Nasopharyngeal Carcinoma. AAPS PharmSciTech. 18(4):1374-81.

Lollo G, Rivera-Rodriguez GR, Bejaud J, Montier T, Passirani C, Benoit JP, Garcia-Fuentes M, Alonso MJ, Torres D (2014) Polyglutamic acid-PEG nanocapsules as long circulating carriers for the delivery of docetaxel. Eur J Pharm Biopharm. 87(1):47-54.

Maeda H, Wu J, Sawa T, Matsumura Y, Hori K (2000) Tumor vascular permeability and the EPR effect in macromolecular therapeutics: a review. J Control Release. 65(1-2):271-84.

Malvia S, Bagadi SA, Dubey US, Saxena S (2017) Epidemiology of breast cancer in Indian women. Asia Pac J Clin Oncol. 13(4):289-95.

Mamot C, Ritschard R, Wicki A, Stehle G, Dieterle T, Bubendorf L, Hilker C, Deuster S, Herrmann R, Rochlitz C (2012) Tolerability, safety, pharmacokinetics, and efficacy of doxorubicin-loaded anti-EGFR immunoliposomes in advanced solid tumours: a phase 1 dose-escalation study. Lancet Oncol. 13(12):1234-41. doi: 10.016/S470-2045(12)70476-X. Epub 2012 Nov 13.

Mates JM, Sanchez-Jimenez FM (2000) Role of reactive oxygen species in apoptosis: implications for cancer therapy. Int J Biochem Cell Biol. 32(2):157-70.

Matsumura Y, Maeda H (1986) A new concept for macromolecular therapeutics in cancer chemotherapy: mechanism of tumoritropic accumulation of proteins and the antitumor agent smancs. Cancer Res. 46(12 Pt 1):6387-92.

McClements DJ (2012) Nanoemulsions versus microemulsions: terminology, differences, and similarities. Soft matter. 8(6):1719-29

McPherson K, Steel CM, Dixon JM (2000) ABC of breast diseases. Breast cancer-epidemiology, risk factors, and genetics. BMJ. 321(7261):624-8.

Mendes S, Graziani SR, Vitorio TS, Padoveze AF, Hegg R, Bydlowski SP, Maranhao RC (2009) Uptake by breast carcinoma of a lipidic nanoemulsion after intralesional

injection into the patients: a new strategy for neoadjuvant chemotherapy. Gynecol Oncol. 112(2):400-4.

Mizushima Y (1996) Lipid microspheres (lipid emulsions) as a drug carrier — An overview. Adv Drug Deliv Rev. 20(2–3):113-15.

Muller RH, Radtke M, Wissing SA (2002a) Nanostructured lipid matrices for improved microencapsulation of drugs. Int J Pharm. 242(1-2):121-8.

Muller RH, Radtke M, Wissing SA (2002b) Solid lipid nanoparticles (SLN) and nanostructured lipid carriers (NLC) in cosmetic and dermatological preparations. Adv Drug Deliv Rev. 54(Suppl 1):S131-55.

Mussi SV, Sawant R, Perche F, Oliveira MC, Azevedo RB, Ferreira LA, Torchilin VP (2014) Novel nanostructured lipid carrier co-loaded with doxorubicin and docosahexaenoic acid demonstrates enhanced in vitro activity and overcomes drug resistance in MCF-7/Adr cells. Pharm Res. 31(8):1882-92.

Ng ZX, Ong MS, Jegadeesan T, Deng S, Yap CT (2017) Breast Cancer: Exploring the Facts and Holistic Needs during and beyond Treatment. Healthcare (Basel). 5(2):pii: e26.

Ohguchi Y, Kawano K, Hattori Y, Maitani Y (2008) Selective delivery of folate-PEG-linked, nanoemulsion-loaded aclacinomycin A to KB nasopharyngeal cells and xenograft: effect of chain length and amount of folate-PEG linker. J Drug Target. 16(9):660-7.

Oliveira MS, Goulart GCA, Ferreira LAM, Carneiro G (2017) Hydrophobic ion pairing as a strategy to improve drug encapsulation into lipid nanocarriers for the cancer treatment. Expert Opin Drug Deliv. 14(8):983-95.

Padmavathi R, Senthilnathan P, Chodon D, Sakthisekaran D (2006) Therapeutic effect of paclitaxel and propolis on lipid peroxidation and antioxidant system in 7,12 dimethyl benz(a)anthracene-induced breast cancer in female Sprague Dawley rats. Life Sci. 78(24):2820-5.

Pandey V, Gajbhiye KR, Soni V (2015) Lactoferrin-appended solid lipid nanoparticles of paclitaxel for effective management of bronchogenic carcinoma. Drug Deliv. 22(2):199-205.

Park SJ, Wu CH, Safa AR (2004) A P-glycoprotein- and MRP1-independent doxorubicin-resistant variant of the MCF-7 breast cancer cell line with defects in caspase-6, -7, -8, -9 and -10 activation pathways. Anticancer Res. 24(1):123-31.

Peer D, Karp JM, Hong S, Farokhzad OC, Margalit R, Langer R (2007) Nanocarriers as an emerging platform for cancer therapy. Nat Nanotechnol. 2(12):751-60.

Pham J, Nayel A, Hoang C, Elbayoumi T (2016) Enhanced effectiveness of tocotrienol-based nano-emulsified system for topical delivery against skin carcinomas. Drug Deliv. 23(5):1514-24.

Ren WX, Han J, Uhm S, Jang YJ, Kang C, Kim JH, Kim JS (2015) Recent development of biotin conjugation in biological imaging, sensing, and target delivery. Chem Commun (Camb). 51(52):10403-18.

Roy S, Rawat AK, Sammi SR, Devi U, Singh M, Gautam S, Yadav RK, Rawat JK, Singh L, Ansari MN, Saeedan AS, Pandey R, Kumar D, Kaithwas G (2017) Alpha-linolenic acid stabilizes HIF-1 alpha and downregulates FASN to promote mitochondrial apoptosis for mammary gland chemoprevention. Oncotarget. 8(41):70049-71.

Sabzichi M, Mohammadian J, Ghorbani M, Saghaei S, Chavoshi H, Ramezani F, Hamishehkar H (2017) Fabrication of all-trans-retinoic acid-loaded biocompatible precirol: A strategy for escaping dose-dependent side effects of doxorubicin. Colloids Surf B Biointerfaces. 159(620-28.

Shinoda T, Takagi A, Maeda A, Kagatani S, Konno Y, Hashida M (1998) In vivo fate of folate-BSA in non-tumor- and tumor-bearing mice. J Pharm Sci. 87(12):1521-6.

Siegel RL, Miller KD, Jemal A (2017) Cancer Statistics, 2017. CA Cancer J Clin. 67(1):7-30.

Singh M, Kanoujia J, Parashar P, Arya M, Tripathi CB, Sinha VR, Saraf SK, Saraf SA (2018) Augmented bioavailability of felodipine through an alpha-linolenic acid-based microemulsion. Drug Deliv Transl Res. 8(1):204-25.

Singh M, Kanoujia J, Singh P, Tripathi CB, Arya M, Parashar P, Sinha VR, Saraf SA (2016a) Development of an α-linolenic acid containing soft nanocarrier for oral delivery: in vitro and in vivo evaluation. RSC Adv. 6(81):77590-602.

Singh P, Arya M, Kanoujia J, Singh M, Gupta KP, Saraf SA (2016b) Design of topical nanostructured lipid carrier of silymarin and its effect on 7, 12-dimethylbenz [a] anthracene (DMBA) induced cellular differentiation in mouse skin. RSC Adv. 6(88):84965-77.

Singh P, Singh M, Kanoujia J, Arya M, Saraf SK, Saraf SA (2016c) Process optimization and photostability of silymarin nanostructured lipid carriers: effect on UV-irradiated rat skin and SK-MEL 2 cell line. Drug Deliv Transl Res. 6(5):597-609.

Singh S, Singh M, Tripathi CB, Arya M, Saraf SA (2016d) Development and evaluation of ultra-small nanostructured lipid carriers: novel topical delivery system for athlete's foot. Drug Deliv Transl Res. 6(1):38-47.

Singh Y, Meher JG, Raval K, Khan FA, Chaurasia M, Jain NK, Chourasia MK (2017) Nanoemulsion: Concepts, development and applications in drug delivery. J Control Release. 252(0):28-49.

Singletary SE (2003) Rating the risk factors for breast cancer. Ann Surg. 237(4):474-82.

Stella B, Arpicco S, Peracchia MT, Desmaele D, Hoebeke J, Renoir M, D'Angelo J, Cattel L, Couvreur P (2000) Design of folic acid-conjugated nanoparticles for drug targeting. J Pharm Sci. 89(11):1452-64.

Tagne JB, Kakumanu S, Ortiz D, Shea T, Nicolosi RJ (2008) A nanoemulsion formulation of tamoxifen increases its efficacy in a breast cancer cell line. Mol Pharm. 5(2):280-6.

Talekar M, Ganta S, Singh A, Amiji M, Kendall J, Denny WA, Garg S (2012) Phosphatidylinositol 3-kinase inhibitor (PIK75) containing surface functionalized nanoemulsion for enhanced drug delivery, cytotoxicity and pro-apoptotic activity in ovarian cancer cells. Pharm Res. 29(10):2874-86.

Tomasina J, Poulain L, Abeilard E, Giffard F, Brotin E, Carduner L, Carreiras F, Gauduchon P, Rault S, Malzert-Freon A (2013) Rapid and soft formulation of folate-functionalized nanoparticles for the targeted delivery of tripentone in ovarian carcinoma. Int J Pharm. 458(1):197-207.

Torchilin VP (2000) Drug targeting. Eur J Pharm Sci. 11(2):S81-91.

Tripathi CB, Beg S, Kaur R, Shukla G, Bandopadhyay S, Singh B (2016) Systematic development of optimized SNEDDS of artemether with improved biopharmaceutical and antimalarial potential. Drug Deliv. 23(9):3209-23.

Tripathi CB, Gupta N, Kumar P, Singh AK, Raj V, Parashar P, Singh M, Kanoujia J, Arya M, Saraf SA, Saha S (2017) Omega-3 Fatty Acid Synergized Novel Nanoemulsifying System for Rosuvastatin Delivery: In Vitro and In Vivo Evaluation. AAPS PharmSciTech: doi: 10.1208/s12249-017-0933-8.

Tripodo G, Mandracchia D, Collina S, Rui M, Rossi D (2014) New Perspectives in Cancer Therapy: The Biotin-Antitumor Molecule Conjugates. Med chem. S1:004(

Trivedi PP, Kushwaha S, Tripathi DN, Jena GB (2011) Cardioprotective effects of hesperetin against doxorubicin-induced oxidative stress and DNA damage in rat. Cardiovasc Toxicol. 11(3):215-25.

Um HD (2016) Bcl-2 family proteins as regulators of cancer cell invasion and metastasis: a review focusing on mitochondrial respiration and reactive oxygen species. Oncotarget. 7(5):5193-203.

Uner M (2006) Preparation, characterization and physico-chemical properties of solid lipid nanoparticles (SLN) and nanostructured lipid carriers (NLC): their benefits as colloidal drug carrier systems. Pharmazie. 61(5):375-86.

Verma R, Bowen RL, Slater SE, Mihaimeed F, Jones JL (2012) Pathological and epidemiological factors associated with advanced stage at diagnosis of breast cancer. Br Med Bull. 103(1):129-45.

Winkler J, Martin-Killias P, Pluckthun A, Zangemeister-Wittke U (2009) EpCAM-targeted delivery of nanocomplexed siRNA to tumor cells with designed ankyrin repeat proteins. Mol Cancer Ther. 8(9):2674-83.

Wiseman H, Halliwell B (1996) Damage to DNA by reactive oxygen and nitrogen species: role in inflammatory disease and progression to cancer. Biochem J. 313(Pt 1):17-29.

Wu J-L, He X-Y, Jiang P-Y, Gong M-Q, Zhuo R-X, Cheng S-X (2016) Biotinylated carboxymethyl chitosan/CaCO3 hybrid nanoparticles for targeted drug delivery to overcome tumor drug resistance. RSC Adv. 6(69083–93

Wu L, Wang F, Xu R, Zhang S, Peng X, Feng Y, Wang J, Lu C (2013) Promoter methylation of BRCA1 in the prognosis of breast cancer: a meta-analysis. Breast Cancer Res Treat. 142(3):619-27.

Xiao Z, Farokhzad OC (2012) Aptamer-functionalized nanoparticles for medical applications: challenges and opportunities. ACS Nano. 6(5):3670-6.

Yu H, Qiu JF, Ma LJ, Hu YJ, Li P, Wan JB (2017) Phytochemical and phytopharmacological review of Perilla frutescens L. (Labiatae), a traditional edible-medicinal herb in China. Food Chem Toxicol. 108(Pt B):375-91.

Yuan H, Wang LL, Du YZ, You J, Hu FQ, Zeng S (2007) Preparation and characteristics of nanostructured lipid carriers for control-releasing progesterone by melt-emulsification. Colloids Surf B Biointerfaces. 60(2):174-9.

Yuan Y, Cai T, Xia X, Zhang R, Chiba P, Cai Y (2016) Nanoparticle delivery of anticancer drugs overcomes multidrug resistance in breast cancer. Drug Deliv. 23(9):3350-57.

Zempleni J, Wijeratne SS, Hassan YI (2009) Biotin. Biofactors. 35(1):36-46.

Zeng X, Morgenstern R, Nystrom AM (2014) Nanoparticle-directed sub-cellular localization of doxorubicin and the sensitization breast cancer cells by circumventing GST-mediated drug resistance. Biomaterials. 35(4):1227-39.

Zhang S, Liu X, Bawa-Khalfe T, Lu LS, Lyu YL, Liu LF, Yeh ET (2012a) Identification of the molecular basis of doxorubicin-induced cardiotoxicity. Nat Med. 18(11):1639-42.

Zhang X, Sun X, Li J, Zhang X, Gong T, Zhang Z (2011) Lipid nanoemulsions loaded with doxorubicin-oleic acid ionic complex: characterization, in vitro and in vivo studies. Pharmazie. 66(7):496-505.

Zhang YT, Huang ZB, Zhang SJ, Zhao JH, Wang Z, Liu Y, Feng NP (2012b) In vitro cellular uptake of evodiamine and rutaecarpine using a microemulsion. Int J Nanomedicine. 7(0):2465-72.

Zhang Z, Wang J, Tacha DE, Li P, Bremer RE, Chen H, Wei B, Xiao X, Da J, Skinner K, Hicks DG, Bu H, Tang P (2014) Folate receptor alpha associated with triple-negative breast cancer and poor prognosis. Arch Pathol Lab Med. 138(7):890-5.

Zhao H, Lu H, Gong T, Zhang Z (2013) Nanoemulsion loaded with lycobetaine-oleic acid ionic complex: physicochemical characteristics, in vitro, in vivo evaluation, and antitumor activity. Int J Nanomedicine. 8(0):1959-73.

1. Drug profile

The drug selected for this study was Doxorubicin Hydrochloride which is an anticancer drug extensively used in chemotherapy of breast cancer, bladder cancer, Kaposi's sarcoma, lymphoma, and acute lymphocytic leukemia.

1.2 The drug: Doxorubicin (Dox)

Antineoplastic antibiotic obtained from *Streptomyces peucetius*. Doxorubicin is a hydroxy derivative of Daunorubicin.

1.3. Chemical structure

The structural formula of Dox is

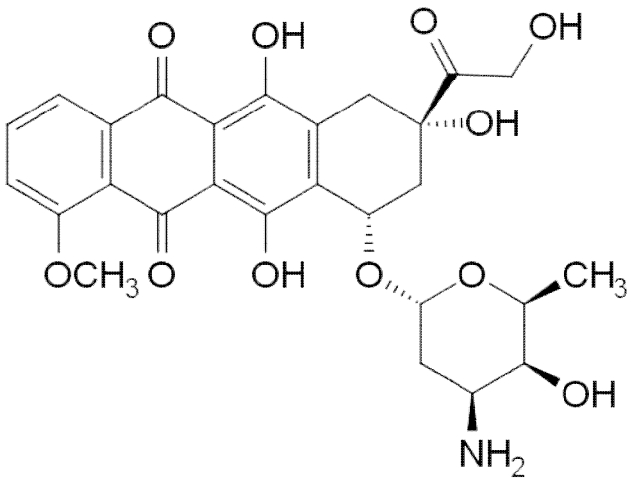

(7S,9S)-7-[(2R,4S,5S,6S)-4-amino-5-hydroxy-6-methyloxan-2-yl]oxy-6,9,11-trihydroxy-9-(2-hydroxyacetyl)-4-methoxy-8,10-dihydro-7H-tetracene-5,12-dione

1.4. Molecular formula: $C_{27}H_{29}NO_{11}$

1.5. Molecular weight: 543.53 g/mol

1.6. Category: Antineoplastic, anticancer, anthracycline antibiotic

1.7. Chemistry and Structure

Doxorubicin is a glycoside antibiotic. It consists of the tetracyclic quinoid aglycone adriamycinone (l4-hydroxydaunomycinone) linked to the aminosugar daunosamine (Arcamone et al. 1972).

1.7. Mechanism of action

The mechanism of action of doxorubicin is related to its capability to intercalate and bind to DNA and inhibit nucleic acid synthesis. Mechanism of activity of doxorubicin in various cell lines demonstrated rapid cell internalization, inhibition of cellular mitosis and chromatin binding and nucleic acid synthesis. Doxorubicin can induce mutations and chromosomal abnormality. It interferes with DNA replication by intercalation into it. Also, it hampers the topoisomerase II activity, enzyme that relaxes the negative supercoils for transcription process of DNA. It stabilizes the topoisomerase II complex that opens the DNA chain for replication thereby inhibiting the resealing of DNA double helix. Dox may also increase the generation of quinone type free radical which can cause cellular cytotoxicity (Frederick et al. 1990).

1.8. Pharmacokinetics

1.8.1. Absorption & Distribution: Half-life for distribution of doxorubicin is 5 minutes. Volume of distribution is found to be 809 to 1214 L/m.

1.8.2. Metabolism & Excretion: There are three major metabolic routes for doxorubicin, i.e., deglycosidation, one-electron reduction and two-electron reduction. However, approximately 50% of the total doxorubicin administered is eliminated unchanged. Two electron reductions are considered the primary metabolic pathway that yields a secondary alcohol, doxorubicinol. One electron reduction is mediated by various oxidoreductases to produce doxorubicin semiquinone radical. Deglycosidation is a minor metabolic pathway for doxorubicin metabolism. Doxorubicin and its metabolites are excreted through bile and urine.

1.8.3. Protein binding: 74-76%

1.9. Physicochemical properties: According to official monographs (USP) it is an orange-Red, crystalline solid, hygroscopic, 2% w/w soluble in water; soluble in aqueous alcohols; moderately soluble in anhydrous methanol; insoluble in non-polar organic solvents.

1.10. Sotrage: According to monographs, it should be stored in well-closed containers and between 15^{o} and 30^{o}C.

1.11 Adverse Effects:

Doxorubicin HCl can result in myocardial damage, including acute left ventricular failure. The risk of cardiomyopathy with doxorubicin is generally proportional to the cumulative exposure. Based on animal data, Dox can cause fetal harm when administered to a pregnant woman. Some common side effects (incidence rate 1-10%) are oral moniliasis, mouth ulceration, esophagitis, dysphagia, rectal bleeding, dehydration, weight loss, hyperbilirubinemia, hypokalemia, hypercalcemia, hyponatremia dizziness, depression, pruritus, skin discoloration, urinary tract infection, hematuria, vaginal moniliasis etc.

1.12. Identification of drug

1.12.1. Percentage purity

Percentage purity assay was done according to official pharmacopoeia.

1.12.2. Physical Appearance

Drug sample is an orange coloured, crystalline powder.

1.12.3. Melting point

Melting point of doxorubicin was estimated using melting point apparatus. The drug sample was filled in three separate capillaries and melting temperature range was recorded to be 228-232^{o}C.

1.12.4. Fourier transforms infrared spectrum (FTIR)

FTIR analysis of drug was done according to the official pharmacopoeia to check the purity of the drug. Scanning of the spectrum was performed from 4000 to 500 cm^{-1} using Nicolet 6700, Thermoscientific, spectrophotometer **(Fig. 1)**. The FTIR spectrum of sample showed three characteristic peaks at 3334.31 cm^{-1} –NH2, 2919.32 cm^{-1} –OH carboxylic acid, broad peak around 3500 $cm^{-1}$of –OH group attached to benzene ring, 2977.36 cm^{-1} –CH stretching and 1729.84 cm^{-1} for –CH bending of benzene ring, 1463.86 cm^{-1} C-H bending vibration of methyl group which were similar to the spectra in official monograph. Purity of the drug sample was thus confirmed.

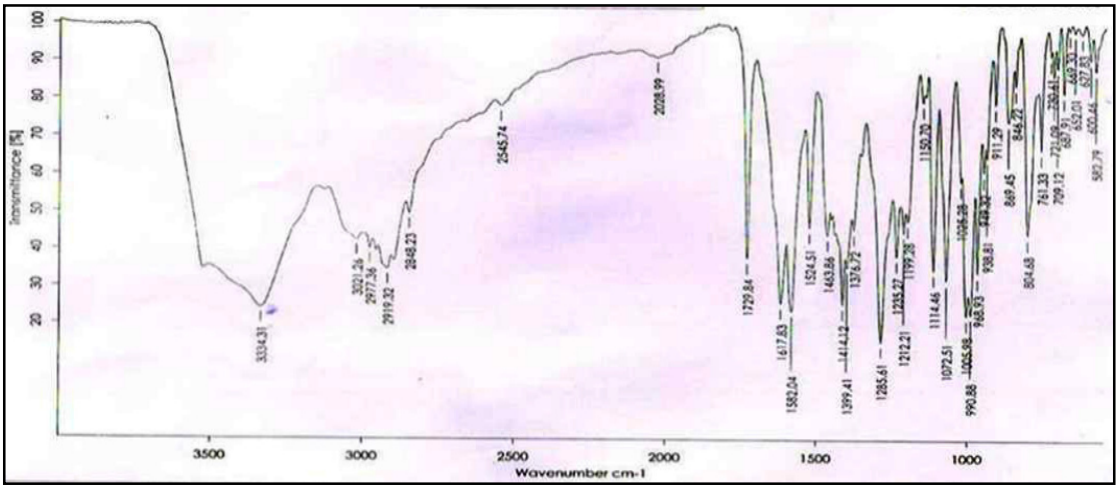

Fig. 1. FTIR spectrum of doxorubicin

1.12.5. NMR spectrum

1^{H} NMR spectrum was taken on Bruker II 400 NMR spectrometer at 400 mHz using DMSO-D6 as solvent **(Fig.2)**.

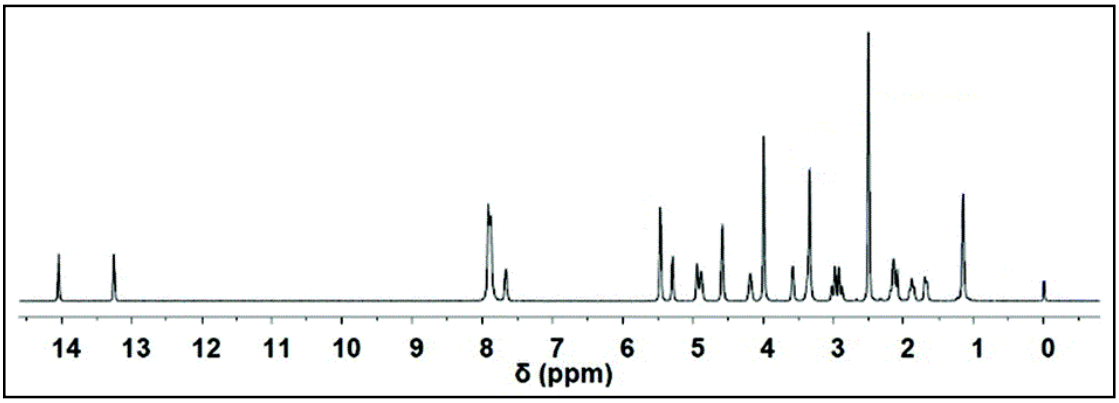

Fig. 2. ^{1H}NMR spectrum of doxorubicin**2. Excipient Profile**

2.1. α-Linolenic Acid (ALA)

ALA is a polyunsaturated fatty acid. ALA is an ω3-fatty acid, essential for health as it cannot be produced inside human body.

Physical appearance: Clear light yellow to yellow liquid

Molecular Formula: $C_{18}H_{30}O_2$

Molecular Weight: 278.436 g/mol

Molecular Structure:

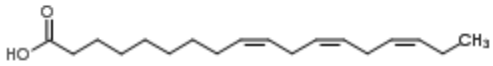

(9Z,12Z,15Z)-octadeca-9,12,15-trienoic acid

***FTIR* Characterization**

FTIR analysis of oil was performed to identify and characterized for purity.

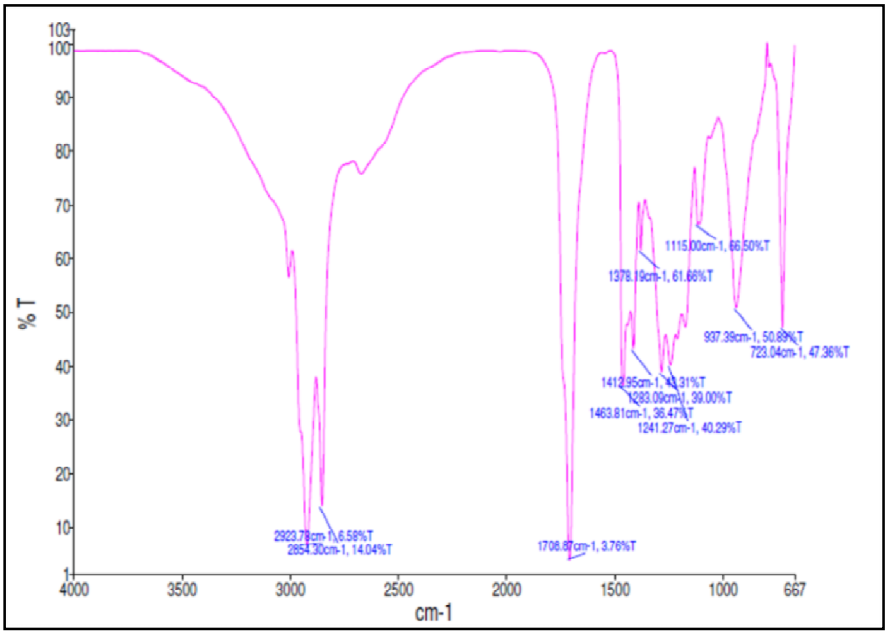

Fig. 3. FTIR spectrum of ALA

Therapeutic effects

Antioxidant, cardioprotective, cardiovascular diseases, atherosclerosis, lower risk of hypertension, anti-inflammatory, anticancer, antiproliferative, tumor inhibitory etc.

2.2. *Perilla frutescence* seed oil

Source: Seeds of *Perilla frutescens*, contains 54-69% ω-3 fatty acids

Physical appearance: Yellow oily liquid, specific gravity 0.92, Refractive index 1.49 and ester value 28.6

Composition:

Consisted of 91.2-93.9% neutral lipids, 3.9-5.8% glycolipids and 2.0-4.0% phospholipids; fatty acids like omega-3 fatty acids, omega-6 fatty acids and omega-9 fatty acids; Rosmarinic acid, furan compounds such as vinylfuran, 5-methylfurfuraldehyde, 3-methylfuran, palmitic acid, stearic acid, Vitamin E etc.

Characterization of oil (FAME analysis)

Fatty acid methyl ester (FAME) was performed of oil samples after suitable derivation of fatty acids to methyl esters **(Fig. 4)**. Methyl esters for the oil samples were prepared by solubilising 750 mg of oil in hexane (2 ml) and methanolic KOH (2N) (0.2 ml). The resultant mixture was then vortexed for 15 min. Both the phases were allowed to settle down and upper layer containing FAME was collected. The above samples were filtered (0.2 µm syringe filters) and injected to gas chromatographic analysis (Perkin Elmer GC- clarus 480; Column : Elite-5 Length-30 mt, Internal diameter- 0.25 mm). The detector employed was Flame ionization detector (250 ºC; carrier gas: nitrogen (10 psi); volume of injection 1µl; oven temperature: 150 (1 min), ramp 1-5 ºC/min to 230 ºC (5min), ramp 2-150 ºC/min to 245 for 12 min). Cetyl alcohol was utilized as internal-standard. A validated GC method was employed for analysis validated (Tripathi et al. 2017).

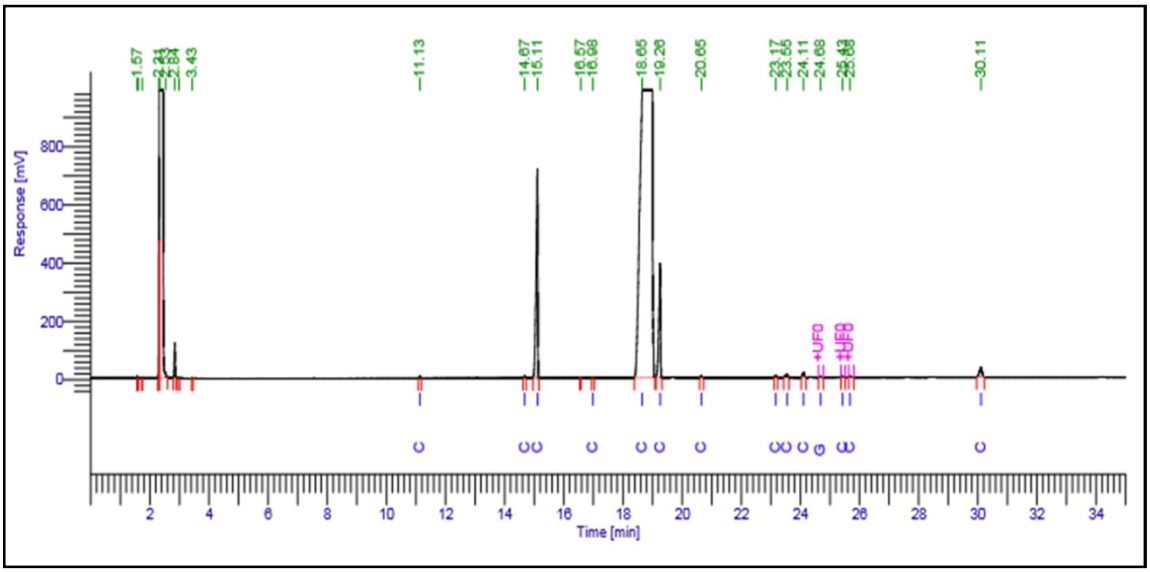

Fig. 4. Gas chromatogram of *Perilla frutescens* seed oil

The composition of fatty acids present in oil showed that saturated, monounsaturated (MUFA) and polyunsaturated fatty acids (PUFA) accounted for 13.4%, 15.5% and

70.3%, respectively, **(Fig. 4)** of the total fatty acid profile which was in corroboration with previous published literature (Tripathi et al. 2017, Yu et al. 2017).

Therapeutic effects

Perilla oil has been reported to have activities like cardiovascular preventive, cancer preventive, neurological benefits, anti-inflammatory, Antibacterial, Antiseptic etc.

2.3. Folic Acid

Folic acid is known as folate, folacin, and vitamin B9. Folate is required for the normal cellular metabolism and cell survival particularly during the period of rapid cell division which happen in cancerous cells. Folate receptors (FR) are therefore upregulated in different type of cancers such as lung, colon, mammary gland, kidney and brain.

Molecular Weight :441.404 g/mol

Molecular Formula : $C_{19}H_{19}N_7O_6$

Physical form: Yellowish-orange crystalline solid, odorless

Melting Point: 248-252 ℃

FTIR Spectra:

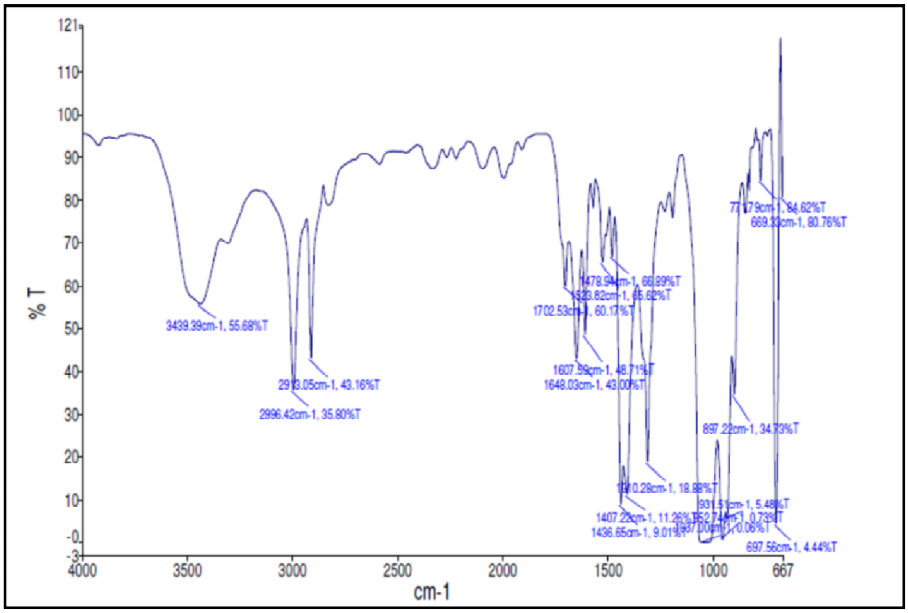

Fig. 5. FTIR spectrum of folic acid

2.4. Biotin

Biotin or vitamin B7 is composed of an ureido (tetrahydroimidizalone) ring fused with a tetrahydrothiophene ring. Mammalian cells lack biotin synthetic pathway, therefore, depend on sources like plants and bacterial systems for the same. The mammalian cells accomplish uptake through biotin transporter (high-affinity for biotin) and also through SMVT. The main transporter for biotin uptake is SMVT, which is overexpressed in several aggressive tumors such as leukemia, ovarian, colon, lung, renal and breast tumor.

Molecular Weight :244.309 g/mol

Molecular Formula :$C_{10}H_{16}N_2O_3S$

Physical form: Colorless, crystalline Solid

Melting Point: 230-234 °C

FTIR Spectra:

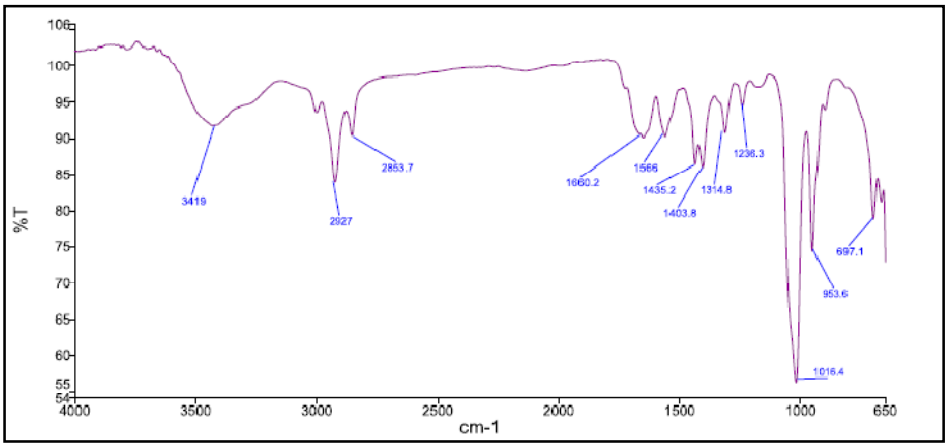

Fig. 6. FTIR spectrum of biotin

2.5. Lecithin

Lecithin complex mixture of acetone-insoluble phosphatides that consists chiefly of phosphatidylcholine, phosphatidylethanolamine, phosphatidylserine, and phosphatidylinositol, combined with various amounts of other substances such as triglycerides, fatty acids. Lecithin is taken as a medicine and is also used in the manufacturing of medicines. It is amphiphilic in nature and has been used as dispersing, emulsifying, and stabilizing agents.

Physical form: Vary greatly in their physical form, from semisolids to powders, depending upon the free fatty acid content, brown to light yellow.

Saponification value: 196

Iodine number: 95–100 for liquid; 82–88 for powder

Stearic acid

Stearic acid is also widely used in cosmetics, medicinal and food products. Stearic acid is extensively utilized in oral, parenteral and topical lipidic formulations.

Molecular Weight : 284.47 g/mol

Molecular Formula: $C_{18}H_{36}O_2$

Melting Point: 69-70 °C

Physical form: hard, white or faintly yellow-colored, glossy, crystalline solid or a white or yellowish white powder with a slight odor.

FTIR Spectra:

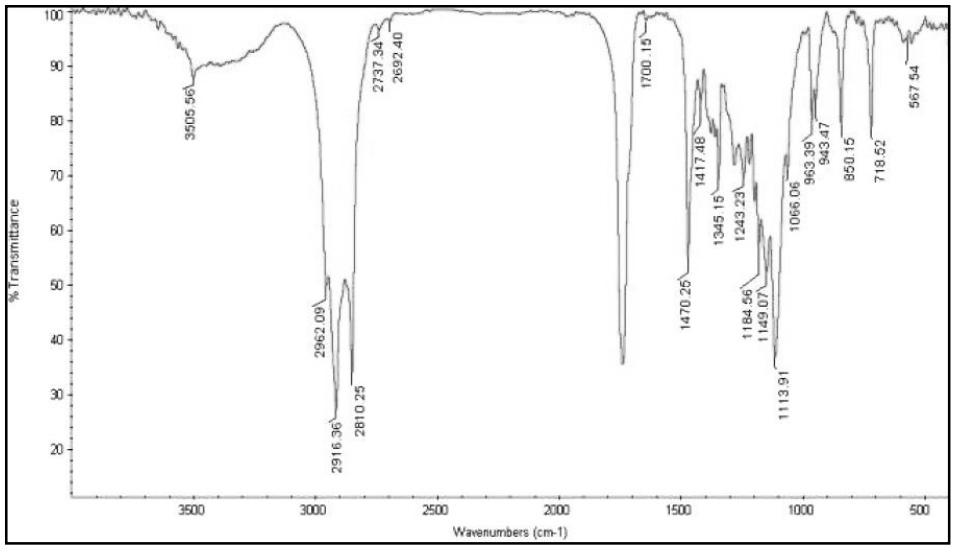

Fig. 7. FTIR spectrum of stearic acid

2.6. Tween 80

Tween 80 is a nonionic surfactant and emulsifier derived from polyethoxylated sorbitan and oleic acid, and is often used in foods. It is a viscous, water-soluble yellow liquid. It is safe and well-tolerated emulsifier with HLB of 15.

Molecular Weight : 604.822 g/mol

Molecular Formula : $C_{32}H_{60}O_{10}$

Physical form: Yellow to orange colored, oily liquid

Viscosity: 300-500 cP at 25°C

FTIR Spectra:

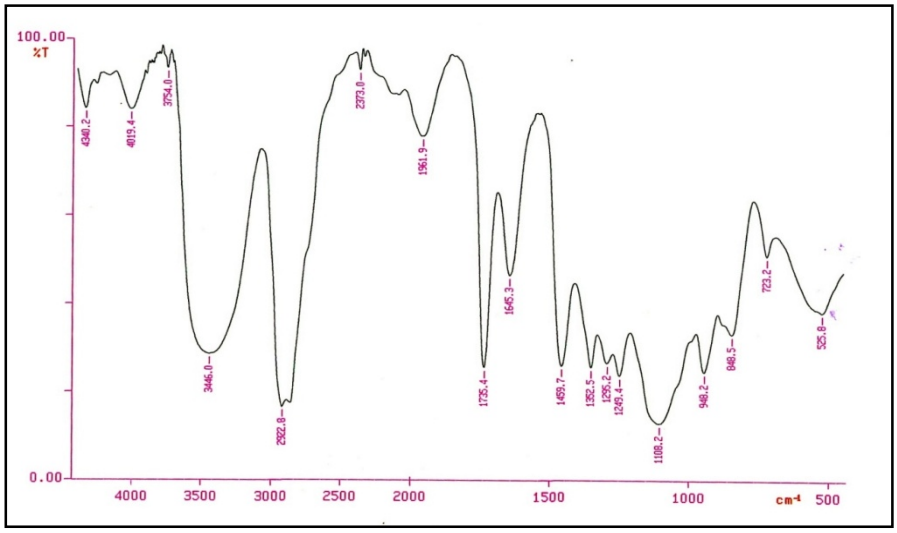

Fig. 8. FTIR spectrum of Tween 80

2.7. Cholesterol

Cholesterol is the principal sterol (a combination steroid and alcohol) found in the body tissues of all higher animals. Cholesterol is used in cosmetics and topical pharmaceutical formulations at concentrations of 0.3–5.0% w/w as an emulsifying agent. It imparts water-absorbing power to an ointment and has emollient activity.

Molecular Weight :386.67 g/mol

Molecular Formula :$C_{27}H_{46}O$

Physical form: white or faintly yellow, almost odorless, powder, or granules

Melting Point: 147-150 °C

FTIR Spectra:

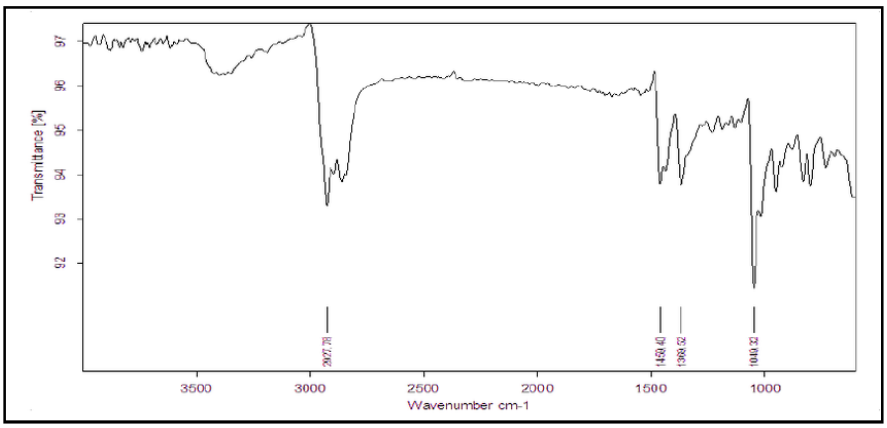

Fig. 9. FTIR spectrum of cholesterol

3. ANALYTICAL METHODS

3.1. Establishment of calibration plot of Dox using UV-spectrophotometer

Standard plots (n=3) for the pure drug were constructed in methanol and phosphate buffer (pH 7.4) to conduct *in vitro* drug release studies and solubility analysis of the drug in various oils and surfactants. Stock solution of the drug (100µg/ml) was prepared in methanol and phosphate buffer pH 6.8 individually. The drug solutions in different media were scanned in range of 200 to 400 nm on UV/VIS spectrophotometer for wavelength of maximum absorption (λ_{max} 485) **(Fig.10; Table 1 & 2)**. The regression of the observed data was performed and regression equation along with r^2 values derived for further use **(Fig. 11 & 12)**.

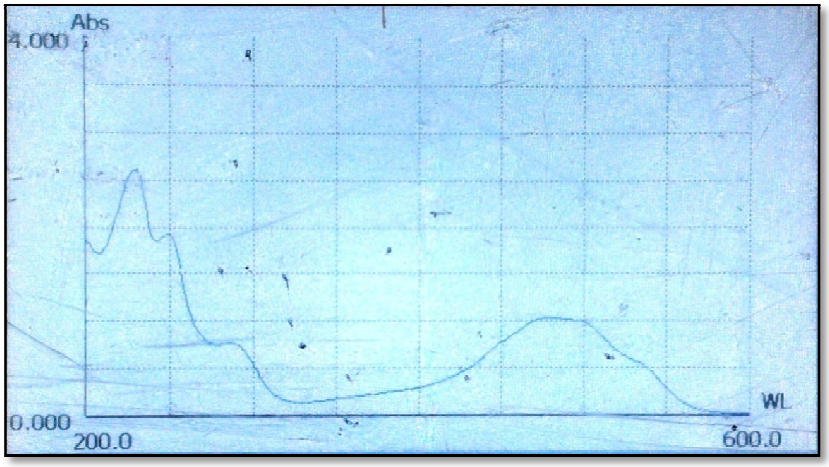

Fig. 10. UV spectra of Dox in methanol

Table 1. Concentration and average absorbance of doxorubicin in methanol

S. No.	Concentration (µg/ml)	Absorbance (mean±SD)
1.	0	0.000±0.000
2.	1	0.028±0.006
3.	5	0.105±0.008
4.	10	0.179±0.010
5.	20	0.376±0.007
6.	30	0.551±0.007
7.	40	0.718±0.009
8.	50	0.859±0.016
9.	60	1.025±0.011

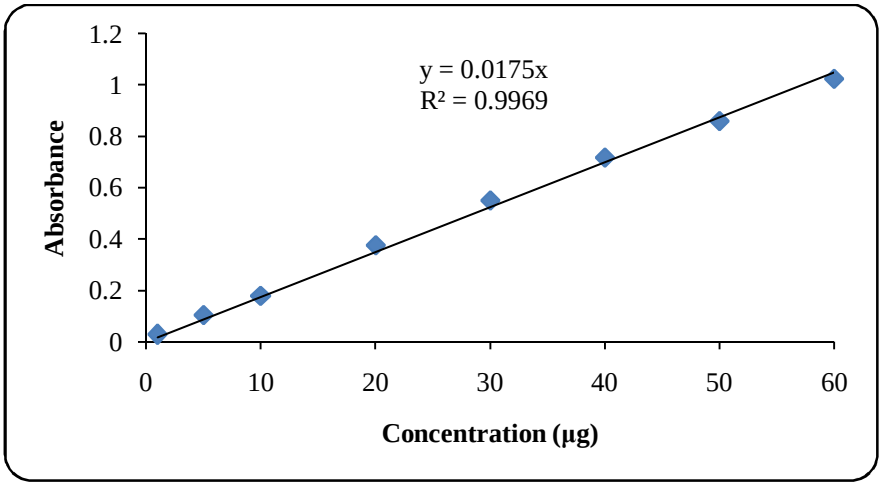

Fig. 11. Standard curve of Dox in methanol

Table 2. Concentration and average absorbance of Dox in phosphate buffer pH 7.4.

S. No.	Concentration (µg/ml)	Average Absorbance (mean±SD)
1.	0	0.000±0.000
2.	1	0.030±0.007
3.	5	0.115±0.005
4.	10	0.189±0.009
5.	20	0.401±0.008
6.	30	0.591±0.005
7.	40	0.743±0.007
8.	50	0.898±0.011
9.	60	1.105±0.009

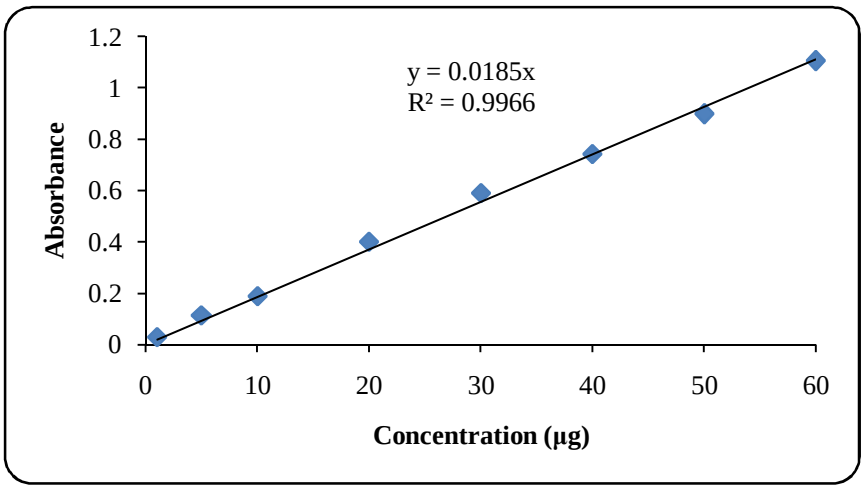

Fig. 12. Standard curve of Dox in phosphate buffer pH 7.4

The UV-Vis spectrophotometer method employed for doxorubicin analysis showed linearity in the concentration ranges of 1.0-60.0 µg/mL in phosphate buffer and methanol with r^2 = 0.9969 and 0.9966, respectively.

3.2. Standard curve of Dox in plasma

3.2.1. Method

1 mg/mL stock solution of doxorubicin was prepared in acetonitrile. Working solutions of 0.02, 0.05, 0.2, 1.0, 2, 10, 20, 50, 100, 200, 400, and 500 µg/mL were prepared using stock solution. Blank plasma and working solutions were kept in separate tubes and vortexed for 30 min. The tubes were centrifuged at 10,000 rpm for 10 min. The supernatant was isolated into different tubes and dried to for 8 h to get residue at 40°C. Later, the contents of respective tubes were reconstituted with 50 µL of acetonitrile, vortexed for 15 min and 20 µL of the resultant solution injected for HPLC analysis. The final concentration of working solutions were 0.01, 0.025, 0.1, 0.5, 1, 5, 10, 25, 50, 100, 200, and 250 µg/mL, respectively **(Table 3)**. Quality control (QC) samples were also prepared at concentrations of 0.1, 30.0 and 200.0 µg/mL, representing low QC, medium QC and high QC samples (LQC, MQC and HQC), respectively. Each of the caliberant and QC samples were prepared in triplicate for each concentration of the range. For test samples, 100 µL of test plasma and 100 µL blank acetonitrile were taken and processed through a method similar to the previously stated method.

Short and long term stability studies of QC samples were carried out in the same experiment. Short term stability studies were performed after 8, 12, and 24 h intervals. The same samples were stored at 4°C and long term stability studies were also examined at 2, 4, 8, 15, 30, and 60 days intervals. AUC of each peak was determined for comparing the stability of the compound through HPLC. Intra and inter day variations were measured at various time points.

HPLC with UV-detectors were selected as analytical tools for analysis of drug. Chromatography was performed with Waters HPLC system (model Water2489). The validated HPLC method was utilized (M/s Waters 2489, Milford, Massachusetts, USA). The system was equipped with Spherowsorb C18, 3.5 µm, 4.6×250 mm column, having flow rate 1.0 mL/min and ambient temperature. The mobile phase consisted of water at pH 3 adjusted with 85% w/v phosphoric acid and acetonitrile

(30:70) and the total run time was 10 min. The HPLC was run through Empower software ver.2 and absorbance was measured at 233 nm wavelength using Waters 2489 UV-Vis detector. For analysis of plasma samples, plasma was mixed with mobile phase, vortexed and centrifuged (5000 rpm, 10 min). The supernatant was extracted and collected in 2 ml centrifuge tube. The extracted supernatant was dried and reconstituted with the mobile phase, filtered through a 0.22µm membrane filter and then analyzed via HPLC **(Fig. 13)**.

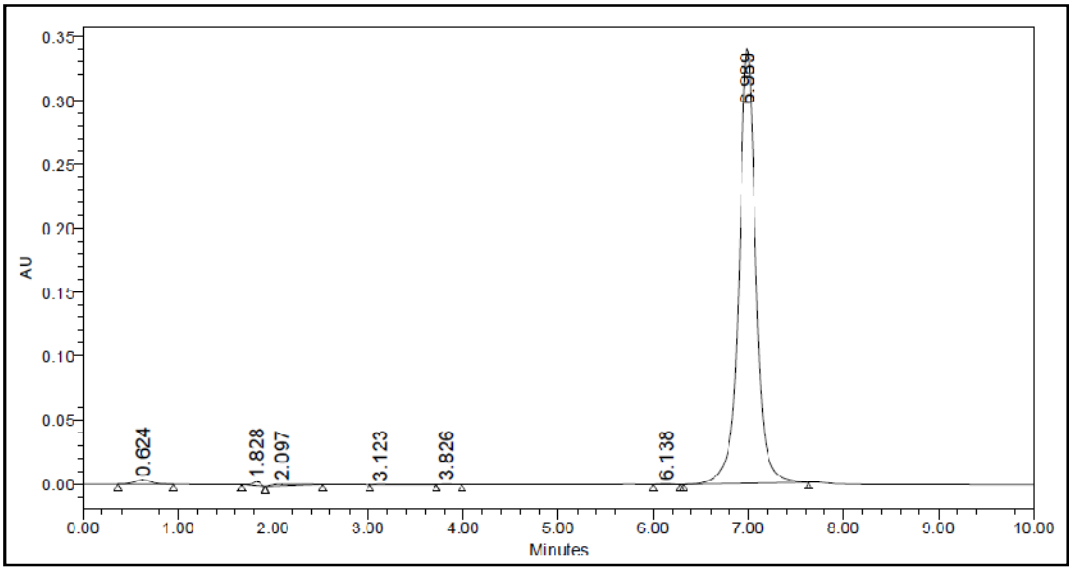

Fig. 13

Table 3. Standard curve data of Dox in plasma

S. No.	Conc. (µg/ml)	Average AUC (mean±SD)
1.	0.01	4136
2.	0.025	8894
3.	0.1	25122
4.	0.2	49150
5.	0.5	116787
6.	1	231976

Table 4. Short-term and Long-term Stability of optimized formulation in rat plasma

Concentration (ng/mL)	Short-term stability		Long-term stability	
	Mean ± SD (ng/mL)	RSD (%)	Mean ± SD (ng/mL)	RSD (%)
10	9.88±0.86	8.704453	9.78±0.97	9.9182
50	49.77±1.42	2.853124	49.81±1.09	2.18
500	499.63±1.36	0.272534	499.02±11.11	2.22

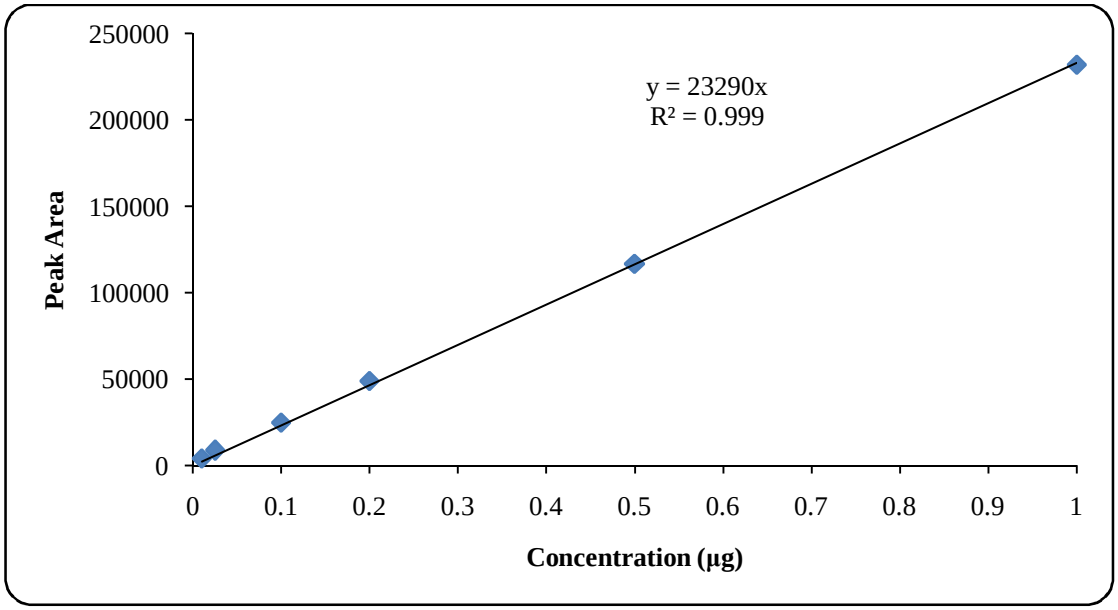

Fig. 14. Standard curve of Dox in plasma

The HPLC method employed for doxorubicin analysis in plasma showed linearity in the concentration ranges of 0.01-1.0 µg/mL in rat plasma with R^2 value of 0.999 **(Fig. 14)**.

Table 5. The Intra-day and Inter-day Precision of RSV-SNES in rat plasma

Concentration (ng/mL)	Intra-day precision (n=3)		Inter-day precision (n=3)	
	Mean ± SD (ng/mL)	RSD (%)	Mean ± SD (ng/mL)	RSD (%)
10	10.02±0.51	5.09	10.19±0.48	4.71
40	40.01±1.22	3.05	39.89±1.12	2.81
100	99.89±1.38	1.38	100.09±1.73	1.73
200	200.03±3.41	1.70	200.07±2.88	1.44
500	498.99±2.52	0.51	498.17±2.52	0.51
1000	999.93±1.49	0.15	1000.07±2.91	0.29

3.2.2. Discussion

Results observed from stability studies of plasma samples suggested that the formulations were stable after both short and long term storage **(Table 4)**. The percentage relative standard deviation (%RSD) was up to ~10% which indicated that the optimized formulations were stable in plasma after long term storage. Intraday and

interday precision data was found within range of 5% **(Table 5)**, demonstrated that the optimized method was accurate and precise for determination of doxorubicin concentration in rat plasma.

4. References

Monographs of doxorubicin. http://www.uspbpep.com/usp31/doxorubicin (Accessed on 05.01.2017)

Arcamone F, Cassinelli G, Franceschi G, Penco S, Pol C, Redaelli S, Selva A (1972). Structure and Physicochemical Properties of Adriamycin (Doxorubicin). International Symposium on Adriamycin. M. A. D. Carter S.K., Ghione M., Krakoff I.H., Mathé G. Berlin, Heidelberg, Springer Berlin**:** 9-22.

Frederick CA, Williams LD, Ughetto G, van der Marel GA, van Boom JH, Rich A, Wang AH (1990) Structural comparison of anticancer drug-DNA complexes: adriamycin and daunomycin. Biochemistry. 29(10):2538-49.

Tripathi CB, Gupta N, Kumar P, Singh AK, Raj V, Parashar P, Singh M, Kanoujia J, Arya M, Saraf SA, Saha S (2017) Omega-3 Fatty Acid Synergized Novel Nanoemulsifying System for Rosuvastatin Delivery: In Vitro and In Vivo Evaluation. AAPS PharmSciTech: doi: 10.1208/s12249-017-0933-8.

Yu H, Qiu JF, Ma LJ, Hu YJ, Li P, Wan JB (2017) Phytochemical and phytopharmacological review of Perilla frutescens L. (Labiatae), a traditional edible-medicinal herb in China. Food Chem Toxicol. 108(Pt B):375-91.

1. Introduction

Nowadays, tumor is one of the most prominent causes of death in developing as well as developed countries. Of various cancers, mammary gland carcinoma is one of the most detected cancers in females. Lung cancer has surpassed the incidences of breast cancer; however, mammary gland carcinoma still remains a leading factor for cancer deaths in females (Siegel et al. 2017, Wang et al. 2014).

Doxorubicin (Dox) is an anthracycline anticancer drug obtained from the fungus *Streptococcoccus peuceticus var*. *caesius*. It is one of the most potent chemotherapeutic agents in modern day breast anticancer therapies. It is one of the most potent chemotherapeutic agent amongst modern day breast anticancer therapies. Anticancer activity of Dox is due to its activity against topoisomerase II which plays a vital role in the negative supercoiling of DNA. Dox intercalates into the DNA causing the alteration in stereochemical conformation of the double-helical structure. Therefore, Dox inhibits DNA and RNA polymerases and obstructs the DNA replication and transcription (Trivedi et al. 2011, Wang et al. 2014). There are evidences that the treatment with Dox initiates cell signalling pathways through regulation of different proteins like bcl2, bax, BAD, MMP-9, caspase-9 etc., that lead to programmed cell death known as apoptosis (Karroum et al. 2012, Ogretmen and Safa 1996, Park et al. 2004, Vimala et al. 2014).

A-Linolenic acid (ALA) is a ω-3 fatty acid which is an essential polyunsaturated fatty acid (PUFA). It cannot be produced by the body and must be supplemented through dietary resources. It has been established that ALA reduces the progression of mammary gland carcinoma, curtails histological changes and improves the survival rate in animal models (Calder 2012, Iyengar et al. 2013, Roy et al. 2017).

Of late, lipidic drug delivery systems have extensively proved their worth as one of the highly promising systems for delivering the drug to the designated locations. Among the lipidic systems, lipid based nanoemulsions are effectively utilized to improve efficacy of the anticancer drugs and subsequently reduced side effects (Tripathi et al. 2016, Tripathi et al. 2017). Development in the targeted delivery approaches has further improved the potency of such systems to deliver the drug molecules specifically to the cancer cells thereby avoiding dose related toxicity (Jiang et al. 2013, Kandadi et al. 2012, Kouchakzadeh et al. 2017, Mizushima 1996).

In the present study, ALA based nanoemulsion (NE) was envisaged and systematically developed using Quality by Design (QbD) concept for the targeted delivery of Dox to the DMBA induced mammary gland carcinoma. Further, the drug induced cardiotoxicity is a major limiting feature for clinical use of Dox which may be attenuated by the concomitant administration of ALA. Therefore, it has been envisaged to use ALA as the oil phase along with lecithin and Tween 80 as emulgents and cholesterol as a co-emulgent to develop a NE. The NE shall be prepared by emulsification followed by sonication process. NE shall be surface decorated with folate as a targeting ligand with help of the N-hydroxysuccinimide (NHS). The surface decorated NE would be characterized for physicochemical properties like globule size, zeta potential, drug entrapment, drug loading, drug release profile and TEM. Subsequently, *in vitro* evaluations like cellular cytotoxicity, cellular proliferation, reactive oxygen species (ROS) generation, mitochondrial membrane potential (MMP) changes and cell cycle analysis would be performed. Thereafter, the *in vivo* efficacy of the surface decorated NE would be evaluated in DMBA induced mammary gland carcinoma in female rats by monitoring the tumor progression through animal survival, animal weight variations, biochemical parameters *i.e.*, thiobarbituric acid reactive substances (TBARS), protein carbonyl, superoxide dismutase (SOD), catalase and glutathione GSH levels as well as carmine staining of the mammary glands, upregulation/downregulation of various apoptotic regulators like B-cell lymphoma 2 (bcl2), bcl2-associated X (bax), caspase-9 and matrix metalloproteinase-9 (MMP-9), cardiotoxicity and biodistribution studies.

2. Materials

S. No.	Materials	Source
1.	Doxorubicin	Miracalus Pharma, India
2.	Methanol	ThermoFischer Scientific
3.	Hydrochloric acid	S.D. Fine chemicals Ltd., Mumbai,
4.	Ethanol	S.D. Fine chemicals Ltd., Mumbai,
5.	Methanol	ThermoFischer Scientific
6.	Acetone	ThermoFischer Scientific
7.	Isopropyl alcohol	ThermoFischer Scientific
8.	Acetonitrile HPLC grade	ThermoFischer Scientific
9.	Methanol HPLC grade	ThermoFisher Scientific
10.	Linolenic acid (omega 3 fatty acids)	Rolex Chemicals Mumbai, India
11.	Seasame oil	Sugandhco Pvt. Ltd, India
12.	Soya bean oil	Sugandhco Pvt. Ltd, India
13.	Perilla oil	Sugandhco Pvt. Ltd, India
14.	Oleic acid	Fisher Scientific Pvt. Ltd.,
15.	Tween 20	HiMedia Laboratories (Mumbai)
16.	Span 20	HiMedia Laboratories (Mumbai)
17.	Tween 80	HiMedia Laboratories (Mumbai)
18.	Span 80	HiMedia Laboratories (Mumbai)
19.	Kolliphor EL 40	HiMedia Laboratories (Mumbai)
20.	Lecithin	HiMedia Laboratories (Mumbai)
21.	Cholesterol	HiMedia Laboratories (Mumbai)
22.	Isopropyl myristate	HiMedia Laboratories (Mumbai)
23.	PEG 200	HiMedia Laboratories (Mumbai)
24.	PEG 400	HiMedia Laboratories (Mumbai)
25.	PEG 600	HiMedia Laboratories (Mumbai)

26.	Sodium hydroxide	SDFCL Pvt. Ltd., Mumbai, India
27.	N-hydroxysuccinimide (NHS)	Sigma Aldrich, USA
28.	N,N'-Dicyclohexylcarbodiimide (DCC)	Sigma Aldrich, USA
29.	Poly(ethylene glycol) bis(amine) (PEG-bis-amine	Sigma Aldrich, USA
30.	2-mercaptoethanol	Sigma Aldrich, USA
31.	Propidium Iodide	Sigma Aldrich, USA
32.	RNase A	Sigma Aldrich, USA
33.	Eagle's Minimum Essential Medium (EMEM)	Sigma Aldrich, USA
34.	Fetal Bovine Serum	Sigma Aldrich, USA
35.	Hank's Balanced Salt Solution (HBSS)	Sigma Aldrich, USA
36.	MTT (3-(4,5-Dimethylthiazol-2-yl)-2,5-diphenyl tetrazolium bromide)	Sigma Aldrich, USA
37.	2, 7-dichlorofluorescin diacetate	Thermo Fisher Scientific, USA
38.	Alamar blue® reagent	Thermo Fisher Scientific, USA
39.	Rhodamine 123 (Rh-123)	Thermo Fisher Scientific, USA
40.	Radio Immuno Precipitation Assay (RIPA) lysis buffer	Thermo Fisher Scientific, USA
41.	Antibodies	Santa Cruz, USA

3. Methods

3.1. Preformulation study

3.1.1. Solubility studies

Excess of drug was added to 2 mL of excipient taken in 30 mL culture tubes, in triplicate and shaken for 40 h at 120 oscillations per minute at 37 ± 1 °C using a wrist action shaker. The equilibrated samples were centrifuged at 10,000 rpm for 10 minutes to separate the undissolved drug. An aliquot of 500 µL of the supernatant was taken and diluted suitably with methanol and analyzed using UV–visible spectrophotometer (M/s Labtronics-LT 2910) at 485 nm. The concentration of Dox in the methanolic phase was calculated using the following equation 1 (Tripathi et al. 2016).

$$Conc.(\mu g.mL^{-1}) = \frac{\text{Observed Absorbance} \times \text{Dilution factor}}{0.0175} \quad \text{... (1)}$$

3.1.2. Lipids

Selection of lipid was based on drug solubilizing capacity of lipid in nanoemulsion system. Lipid phases studied were oleic acid, isopropyl myristate, sesame oil, soyabean oil, perilla oil, and linolenic acid.

3.1.3. Surfactants

The surfactant was selected on the basis of its ability to form stable microemulsion region with the selected oil and drug solubilizing capacity. The surfactants selected for the current study were Tween 80, Tween 20, lecithin, cholesterol, span80, PEG-200 were chosen amongst various commercially available excipients.

3.1.4. Pseudo-Ternary Phase Diagram

Pseudo-ternary phase diagrams were constructed for oil and mixture of emulgent and co-emulgent using 18 ratios for each combination ranging from 1:9 to 9:1 (Singh et al. 2016a, Tripathi et al. 2016). This was done so that the boundaries of microemulsion zone and different phases can be properly delineated. Slow titration with distilled water was conducted for each combination of oil, Surfactant and cosolvent. The amount of water

was varied between 5 and 95% of total volume at 5% intervals. After every addition of water, visual observation was made on the basis of following **(Fig. 1)**

- If transparent mixture was obtained on addition, it was taken as an o/w or w/o microemulsion on the basis of percentage of oil or water in the total mixture. If the percent oil was relatively more, it was recorded as w/o microemulsion, and if percent water was more, then it was recorded as o/w microemulsion.
- If a transparent gel was obtained, it was classified as microemulsion gel.
- If milky or cloudy appearance was observed then it was classified as an emulsion.
- If a milky gel was obtained then it was classified as an emulgel.

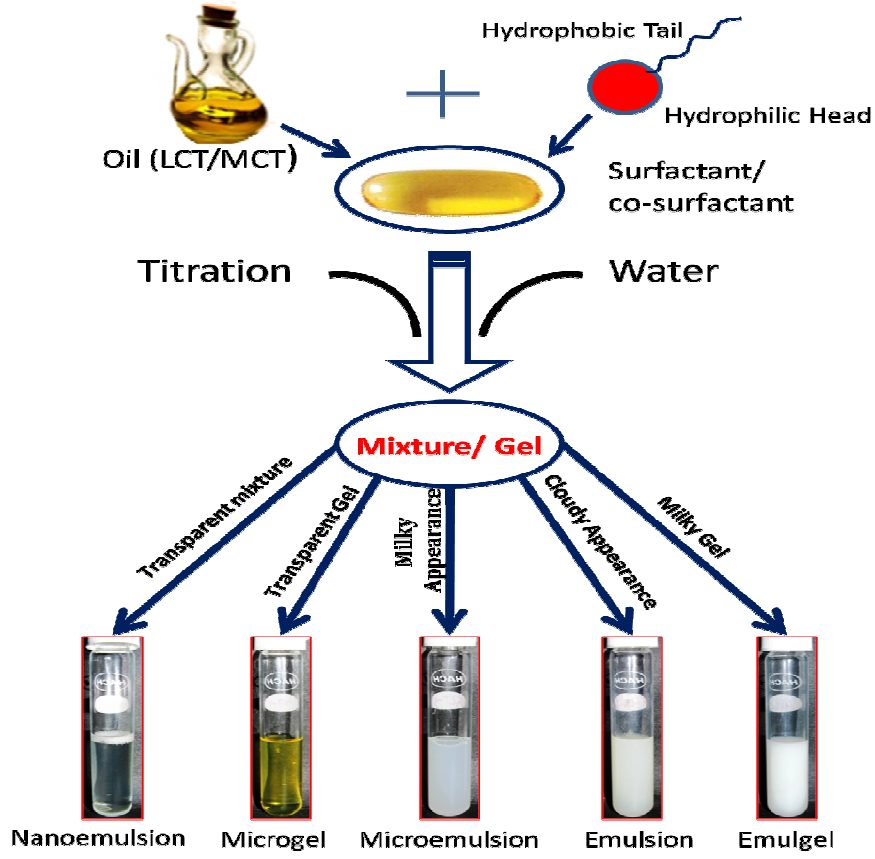

Fig. 1. Formation of different phases (i.e., nanoemulsion, microemulsion, microgel, emulsion and emulgel) as observed during pseudo-ternary phase diagrams

Pseudo-ternary phase diagrams were constructed for the regions of microemulsion, microemulsion gel, emulsion and emulgel using PCP-Disso software ver 3.0 (developed by Paradkar, Poona College of Pharmacy, Pune, India).

3.1.5. Selection of co-emulgent

Co-emulgent was selected on the basis of water absorption capacity for different combinations of lipids, emulgents and co-emulgents (Singh et al. 2016a). Combinations of ALA with cholesterol, span 80, and PEG 200 were mixed with S_{mix} in equal weight ratios and titrated via drop by drop addition of aqueous phase. The amount of aqueous phase at which the system became turbid was considered as the end point. Further, NE formulations of each of the combinations, as described above, were kept at elevated temperature (40±2 °C) for a month to access the stability of the system.

3.2. Experimental design

On the basis of above data, the most suitable range of critical material attributes (CMAs), *viz*., lipid (200-600 mg), emulgent (500-900 mg), cholesterol (100-200 mg) was selected. The aqueous phase was added to maintain total weight upto 2000 mg. The design of experiments (DoE) *i.e*., 3-factor 3-level Box–Behnken design (BBD) was selected for scientific and systematic optimization of NE (Singh et al. 2011, Tripathi et al. 2016, Tripathi et al. 2017). A total of 15 experimental trials loaded with drug in each were formulated which were characterized for critical quality attributes (CQAs), *viz*., globule size, drug loading, entrapment efficiency and drug release in 72 h. The different permutation combinations advised as per experimental design were formulated and evaluated for different CQAs and data for each CQA obtained are portrayed in **Table 1**.

3.4. Preparation of Nanoemulsion

Lipid nanoemulsion of Dox (Dox-NE) was prepared by emulsification followed by ultrasonication technique. Dox (10 mg), S_{mix} (lecithin, Tween 80 in ratio 1:1) and cholesterol added in ALA maintained at 60°C and mixed with continuous stirring at 1000 rpm. The aqueous phase was added to the oil phase with continuous stirring to get a coarse emulsion. Furthermore, the mixture was sonicated at 20 kHz, 750 Watt, 40% amplitude using probe sonicator, (M/s Labsonic®M, Sartorius, Germany) for 10 min.

Table 1. DoE layout plan for Dox loaded nanoemulsions as per the BBD

Factor	**Critical Material Attributes (CMAs)**	**Unit**	**Levels**		
			low	**intermediate**	**high**
X_1	Total lipid	mg	200	400	600
X_2	S_{mix}	mg	500	700	900
X_3	Cholesterol	mg	100	150	200
Response	**Critical Quality Attributes (CQAs)**		**Goal**		
Y_1	Particle Size	nm	Minimize		
Y_2	Entrapment Efficiency (EE)	%	Maximize		
Y_3	Drug Release	%	Maximize		
Y_4	Drug loading	%	Maximize		

Code	**Drug (mg)**	**Lipid (mg) (X_1)**	**S_{mix} (mg) (X_2)**	**Cholesterol (mg) (X_2)**
NE1	5	200	500	150
NE2	5	600	500	150
NE3	5	200	900	150
NE4	5	600	900	150
NE5	5	200	700	100
NE6	5	600	700	100
NE7	5	200	700	200
NE8	5	600	700	200
NE9	5	400	500	100
NE10	5	400	900	100
NE11	5	400	500	200
NE12	5	400	900	200
NE13	5	400	700	150
NE14	5	400	700	150
NE15	5	400	700	150

3.5. Globule size determination

The emulsion globule size of nanoemulsion (approximately 100-fold dilution with distilled water) was analyzed employing NanoPlus zeta/nano particle analyzer (M/s Micromeritics Instrument Corporation, USA). The instrument contains a 4mW He-Ne laser light source operating at a wavelength of 633 nm and work on the principle of non-invasive backscatter optics (NIBS) (Singh et al. 2011, Tripathi et al. 2016, Tripathi et al. 2017).

The measurements were made at detection angle of 90° and the measurement position within the cuvette was automatically determined by the software. The instrument recorded the intensity of fluctuation of laser beam and correlated it with the particle size distribution of emulsion droplet.

3.6. Entrapment efficiency and Drug loading

The drug loading and entrapment efficiency were determined using reported procedure with some modifications (Kandadi et al. 2012). Briefly, the entrapment was measured by keeping 1 mL of drug loaded NEs in dialysis membrane (12-14 kDa MWCO) for 2 h, and the dialyzed drug (free drug) was estimated using UV-Vis spectrophotometer at 485 nm **(Eq. 2)**. The amount of Dox in the aqueous phase was calculated. Further, drug loading in NEs was determined after dissolving 1 mL of NE (from donor compartment) in 10-mL chloroform/methanol 1:1 mixture. After suitable dilution, absorbance was taken using UV-Vis spectrophotometer at 485 nm, and percent drug loaded was calculated **(Eq. 3)**.

$$Entarpment\ Efficiency = \frac{Total\ weight\ of\ DOX\ dialyzed}{Total\ amount\ of\ DOX} x100 \qquad \textbf{...Eq. (2)}$$

$$Drug\ Loading = \frac{Total\ weight\ of\ DOX\ in\ donar\ compartment}{Total\ amount\ of\ drug+total\ amount\ of\ excipients} x100 \qquad \textbf{...Eq. (3)}$$

3.7. Drug diffusion study from nanoemulsion

The drug diffusion was performed by loading NE formulations into dialysis bag (3.5 kDa MWCO). The dialysis bag was placed in 100 mL diffusion media (PBS, pH 7.4) maintained at 37±0.5 °C with stirring rate of 400 rpm. Sample aliquots (1 mL) were withdrawn at different time intervals up to 72 h and replaced with equal amount of fresh

media. The drug concentration in the samples was analyzed using UV-visible spectrophotometer at 485 nm after suitable dilutions.

3.8. Mathematical model development and optimization of NE

The observed data obtained from the above studies was applied to fit the second-order polynomial equations, the multiple linear regression analysis (MLRA) with added interaction terms to establish the correlation between the CMAs with the CQAs through Design Expert 8.0 software (Trail version, M/s Stat-Ease, Minneapolis, USA). The coefficients which were found to be highly significant using the Student's t-test, were considered in developing the polynomial equations **(Eq. 4)**.

$$Y = \beta_0 + \beta_1 X_1 + \beta_2 X_2 + \beta_3 X_3 + \beta_4 X_1 X_2 + \beta_5 X_2 X_3 + \beta_6 X_1 X_3 + \beta_7 X_1^2 + \beta_8 X_2^2 + \beta_9 X_3^2 + \beta_{10} X_1^2 X_2 + \beta_{11} X_2^2 X_3$$

…Eq. (4)

where, Y represents the CQAs; β_0 the intercept; β_1 to β_{11} are the coefficients of various model terms. The response surface analysis was carried out for understanding the factor-response relationship and possible interaction(s) among them. Search for the optimum formulations was carried out by "trading-off" various CQAs by numerical optimization using overlay plots with suitable application of constraints on CQAs (Singh et al. 2011, Tripathi et al. 2016, Tripathi et al. 2017).

3.9. Surface modification of nanoemulsion

3.9.1. Preparation of Folate NHS ester

Activation of folic acid was performed as per previously reported method (Bae et al. 2013, Lee and Low 1994, Liu et al. 2011). Folic acid (300 mg, 0.68 mmol) and triethylamine (0.15 mL, 1.0 mmol) were dissolved in 10 mL dry dimethyl sulfoxide (DMSO), to which DCC (140 mg, 0.68 mmol) was added. The mixture was stirred for 1 h at room temperature in the dark, and NHS (115 mg, 1.0 mmol) was added. The reaction was stirred overnight at room temperature in the dark. The dicyclohexylurea precipitate (a side product of the reaction) was filtered via glass wool and folate-NHS ester was precipitated using diethylether. The yellow precipitate (active ester of folic acid) was filtered, washed several times with dry tetrahydrofuran, dried under vacuum, and stored as a yellow powder (**Scheme 1)**.

Scheme- 1

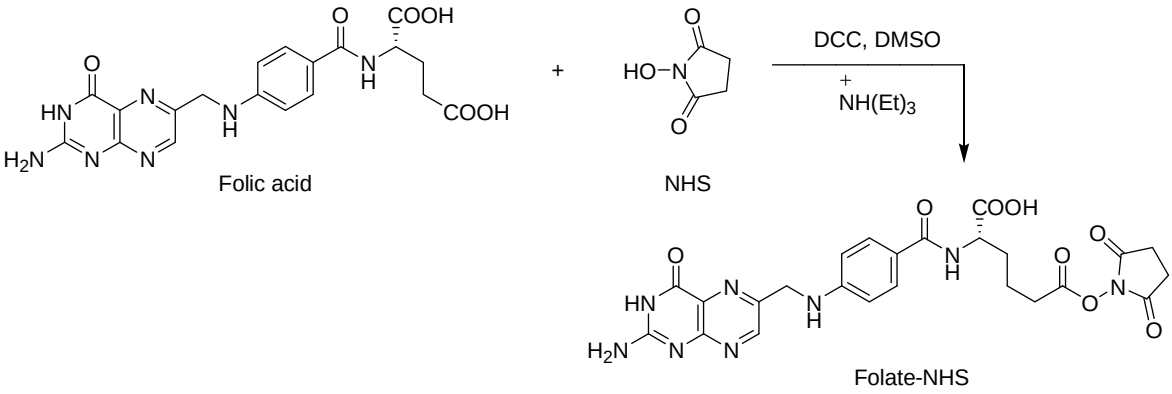

Scheme- 2

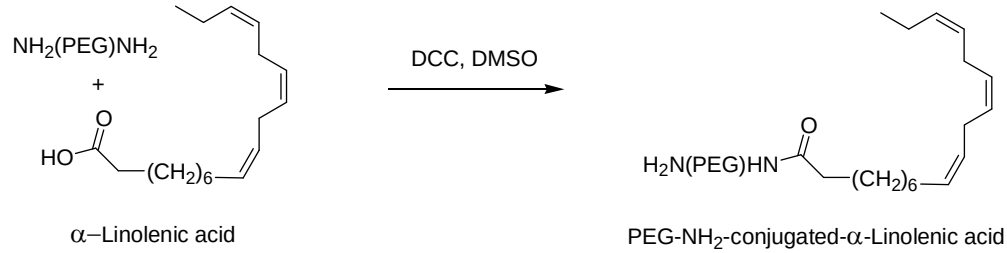

Scheme- 3

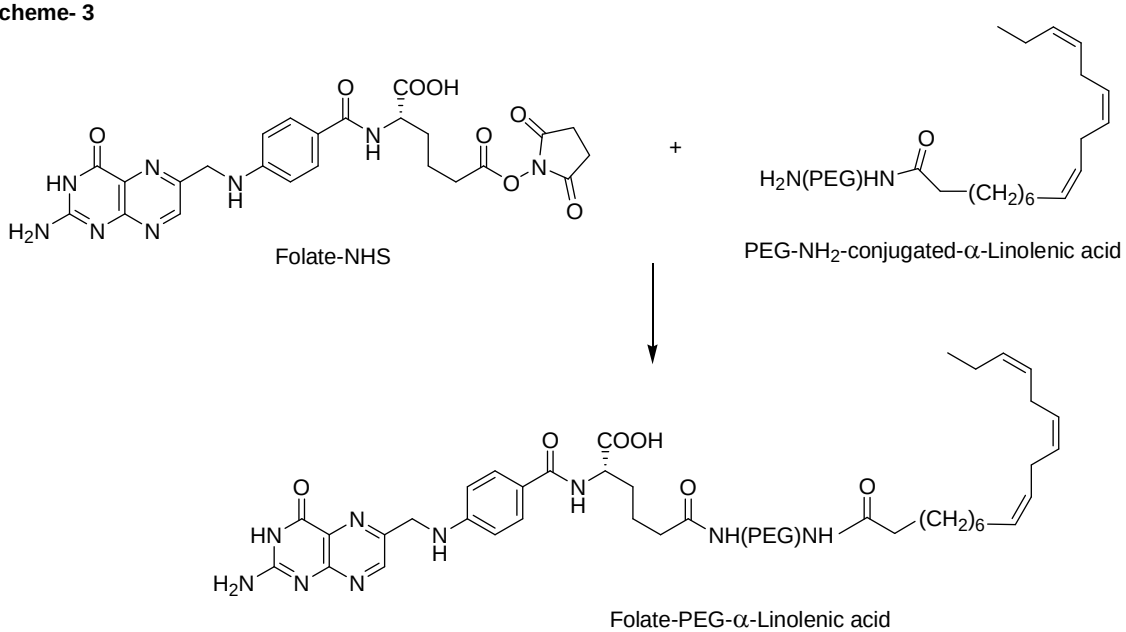

Scheme 1: Synthesis of Folate NHS ester; **Scheme 2:** Synthesis of PEG-NH_2 conjugated α-linolenic acid (ALA-PEG-NH_2); **Scheme 3:** Synthesis of folate attached α-linolenic acid (f-PEG-ALA).

3.9.2. Activation of fatty acid

The ALA (100 mg, 0.36 mmol) was dissolved in DMSO and then DCC (74.11 mg, 0.36 mmol) (ALA: DCC, 1:1 molar ratio) was added to the above solution. Subsequently, the mixture was stirred in dark for 12 h to complete the reaction. Thereafter, PEG-bis-amine (1257 mg, 0.36 mmol) (ALA:DCC:PEG-bis-amine, 1:1:1 molar ratio) was added to the above mixture and the reaction was stirred for 3 h to obtain PEG-amino derivative of fatty acid with primary amine at terminals *i.e.*, ALA-PEG-NH_2 (**Scheme 2**). The dicyclohexylurea precipitate, by product of reaction, was filtered via glass wool and the filtrate was precipitated using diethylether and dried under vacuum to collect ALA-PEG-NH_2 (Bae et al. 2013, Lee and Low 1994, Liu et al. 2011).

3.9.3. Folate modified nanoemulsion

Folate-NHS ester (20 mg/mL) suspended in phosphate buffer saline (PBS pH 7.4) was poured in equimolar ratio into NE prepared with mixture of activated ALA (ALA-PEG-NH_2) and ALA (1:20 w/w; 19 mg, 381 mg, respectively) for surface conjugation as per **Scheme 3**. This mixture was stirred gently overnight at room temperature. To complete the reaction 2-mercaptoethanol (10 mmol) was added in to the above mixture. Subsequently, folate decorated doxorubicin loaded NE (f-Dox-NE) was dialyzed (12–14 kDa MWCO) to remove unreacted 2-mercaptoethanol and folate-NHS ester (Bae et al. 2013, Lee and Low 1994, Liu et al. 2011).

3.10. Characterization of surface modification nanoemulsion

3.10.1. FTIR characterization

Synthesis of folate-NHS, ALA-PEG-NH2 and f-Dox-NE was confirmed by FTIR spectra recorded by adsorbing the samples on KBr disk using PerkinElmer FT-IR Spectrometer. Conjugation of folate to fatty acid (f-PEG-ALA) was characterized after freeze drying of f-Dox-NE by FTIR analysis.

3.10.2. ^{1}H-NMR characterization

The conjugation of folate to ALA through PEG was further characterized through ^{1}H-NMR spectroscopy (Bruker Avance 400, FT-NMR) using DMSO-D6 as solvent. Chemical shifts (δ) were expressed as parts per million (ppm) relative to the NMR solvent signal (d6-DMSO) using tetramethylsilane as internal standard.

3.10.3. Estimation of Folate Content attached to the surface

The amount of folate attached onto the surface of nanoparticles prepared by SESE, DESE or dialysis methods was determined by UV spectrophotometer. Analysis was carried out in CH2Cl2/DMSO (1:4) solvent. The nanoparticles were evaluated by measuring the absorbance of the sample at 358 nm (folic acid $\varepsilon = 15{,}760\ M^{-1}.cm^{-1}$) (Stella et al. 2000).

3.10.4. Physicochemical characterization of Folate modified nanoemulsion

Particle size, drug loading, entrapment efficiency, zeta potential and drug release comparisons of folate modified nanoemulsion were carried out as per methods previously described.

3.10.5. Robustness to dilution

Robustness to dilution for the optimized nanoemulsion was determined by suitably diluting (100, 500, 1000 folds) the optimized formulation with phosphate buffer pH 7.4 and observed for precipitation and cloudiness, if any, after 24 h.

3.10.6. Thermodynamic stability studies

To assess the stability of the optimized nanoemulsion, the formulation was subjected to various thermodynamic studies (Singh et al. 2018, Tripathi et al. 2017).

3.10.6.1. Centrifugation study

The optimized nanoemulsion (1 g) was diluted to 100 mL and centrifuged at 5000 rpm for 15 min and analysed for any instability manifested through phase separation, creaming or cracking, if any.

3.10.6.2. Freeze thaw cycle

Three freeze-thaw cycles were performed for the optimized nanoemulsion maintaining the temperatures between –21 and +25 °C, and observed for instability, if any.

3.10.7. Transmission electron microscopy studies of f-Dox-NE

The TEM analysis (TEM Fei Tecnai 200 Kv, Electron Optics) of f-Dox-NE was performed for morphological characterization of emulsion droplets. The sample was diluted with deionized water (1:25). A drop of above solution was placed on copper grids,

stained with phosphotungstic acid (1%) for 30 sec, and finally observed under electron microscope.

3.10.8. Stability of formulations in plasma and intravenous infusion solutions

Stability of NEs were measured in various media *viz*., rat plasma, phosphate buffer pH 7.4, normal saline (0.9% w/w NaCl). Each NE was diluted with above stated media and incubated for 24 h at 37 ℃. No change in particle size taken as confirmation of stability on storage. Aliquots of 1 mL of samples were taken at different time intervals i.e., 1, 4, 12 and 24 h and analyzed using NanoPlus analyzer. Aliquots of 10 ml of each sample were withdrawn for analysis at 1, 2, 4, 6, 8 and 24 h respectively, and observed visually for globule aggregation. Further, the aliquots were diluted 1000-fold with distilled water and evaluated for any significant change in globule size using Nanoplus particle size analyzer. No particle aggregation and no change in globule size distribution towards higher size range was observed, which was taken as an indicator for stability on storage (Ganta et al. 2016).

3.10.9. *Stability studies*

The stability studies on the f-dox-NE formulations were performed by filling the same in amber coloured glass vials and storing them at 5±3 °C (Refrigerator), 25±2 °C/60±5% RH, 40±2 °C/75%±5% RH, as per the ICH Q1A(R2) guidelines(stability chamber -M/s Thermolab, India). The formulations, kept in air-tight amber colored glass vials, were assayed periodically at 0, 1, 3 and 6 months respectively, for globule size, similarity factor (F2 values, for dissolution comparison) and drug content (Singh et al. 2018, Singh et al. 2016b, Tripathi et al. 2016).

3.11. *In vitro* studies

3.11.1. Cell culture conditions

MCF-7 cells were purchased from the American Type Culture Collection (ATCC, Manassas, VA, USA) and cultured in EMEM (Eagle's Minimum Essential Medium) with 10% v/v fetal bovine serum (FBS) and 1% v/v antibiotic (Penicillin/streptomycin), maintained in a humidified 95% O_2/5% CO_2 atmosphere at 37 °C. Cells were grown until 60- 70% confluency was obtained in the flasks and trypsinized with a solution 0.25% v/v

Trypsin with 2.25 mmol EDTA in HBSS. Trypan blue exclusion method was employed to determine the viable cells (Alkhatib and AlBishi 2013, Doroshow 1986).

3.11.2. Cell cytotoxicity study (MTT assay)

Cell cytotoxicity of Dox, Dox-NE, f-Dox-NE and ALA-NEs was performed using the MTT assay. In this assay, the conversion of this salt by mitochondrial enzymes reflects the number of viable cells. The MCF-7 cells were seeded into 96-well plates (density 1.0×10^3 cells per well) and incubated for 24 h, maintained at 95% O_2/5% CO_2 humidified atmosphere conditions at 37 °C to allow adhesion of cell to surface. Freshly prepared samples of formulations were used to treat cells adhered to the wells at the concentration ranging from 0 to 50µg/mL equivalent Dox (n=3). Plain PBS was taken as an untreated control. The culture cells were further incubated for 48 h. 20 µL of MTT solution (5 mg/mL MTT in PBS) was added to each well and cells were further incubated for 4 h, at 37 °C, leading to formation of blue MTT-formazan crystals. Viable cells internalize MTT into their mitochondria and metabolize it into blue formazan crystals. Following incubation, the MTT reagent was dissolved in 200 µL of DMSO. The optical density was assessed at 540 nm by ELISA plate reader (M/s Biotek, USA) (Lee et al. 2005, Singh et al. 2016a, Vimala et al. 2014, Wang et al. 2014).

3.11.3. Cell Cycle Analysis through Fluorescence-activated cell sorting (FACS) Analysis

MCF-7 cells ($1x10^6$ cells mL^{-1}) were suspended in 1 mL of PBS in centrifuge tube. The cells were centrifuged at 200g for 5 min at room temperature. PBS was removed and cell pellet was resuspended in 500 µL of PBS. Cells were fixed by adding 4 mL of 70% (v/v) cold ethanol to the cell suspension and kept overnight at 4 °C. Cell suspension was centrifuged at 400 g for 5 min and the supernatant (ethanol solution) was removed. Again the cells were washed in 5 mL of PBS and centrifuged at 400g for 5 min. Supernatant was removed and cells were resuspended in 1 mL of DNA staining solution (500 µL/ 10^6 cells; 200 mg of PI in 10 mL of PBS + 2 mg of DNase free RNase A) and incubated for at least 30 min at room temperature in the dark. The samples were analyzed by flow cytometer (488-nm laser line for excitation, FACS Calibur, M/s BD Biosciences, Franklin Lakes, NJ) in PI/RNase A solution without washing the cells at a low flow rate under 500 events/second. The percentage of cells in different phases of cell cycle was

analyzed by ModFit LT 3.0 software (Verity Software House). The cells without treatment were considered as control (Musa et al. 2015, Riccardi and Nicoletti 2006, Roy et al. 2017).

3.11.4. Cell proliferation studies

The cell proliferation assay was performed by Alamar blue® method. The MCF-7 cells were plated in 96 well culture plate (approximately 3000 cell/well) and incubated at 37 °C in EMEM with 10% FBS and 1% antibiotic with 5% CO2 for 24 h. The cells were treated with different samples at concentration 3.31µg/mL equivalent of Dox for 24 h. After incubation Alamar blue® was added at a final concentration of 5% v/v and plates were allowed to stand at 37 °C for 4 h. The plated were read at 570/600 nm in a plate reader (M/s Biotek, USA) and cell proliferation was calculated using colorimetric measurements. The cells without treatment were considered as control (O'Brien et al. 2000).

3.11.5. Reactive Oxygen Species estimation

MCF-7 cells were plated in 96 well culture plates (approximately 3000 cell/well) and incubated at 37 °C with 5% CO_2 for about 24 h. The cells were treated at different concentration (0-200 µg/mL) of samples for 24 h. After incubation DCFDA was added (final concentration 10 µmol) and the plate was incubated for 30 min in dark. DCFDA was removed and wells were washed once with PBS and finally cells were suspended in 100µl of PBS. The plate was read at 485/528 nm (Excitation/ Emission) at 100% sensitivity in a multimode reader (Synergy H1, M/s Biotech Inc, USA) and readings were presented as relative fluorescence unit for ROS generation. The cells without treatment were considered as control (Figueroa et al. 2018, Ottonello et al. 2001, Roy et al. 2017).

3.11.6. Mitochondrial membrane potential (MMP)

The MCF-7 cells were plated in 96 well culture plate (approximately 3000 cell/well) and incubated at 37 °C in EMEM (Eagle's Minimum Essential Medium with 10% FBS and 1% antibiotic) with 5% CO_2 for about 24 h. The cells were treated at different concentration (0- 200 µg/mL) of samples for 24 h. After incubation Rhodamine 123 (Rh 123) was added (final concentration 10 µM) and the plate was incubated for 30 min in dark. Subsequently, the medium was removed and wells were washed once with PBS and

finally 100µL of PBS was added to each well. The plate was read at 507/529 nm (Excitation/ Emission) at 100% sensitivity in multimode reader (Synergy H1, Biotech Inc, USA) and readings were presented as relative fluorescence unit for mitochondrial membrane potential (MMP). The cells without treatment were considered as control (Al-Qubaisi et al. 2013, Musa et al. 2015, Roy et al. 2017).

3.12. *In vivo* study

Female albino wistar rats, weighing 120-150 g were used for the experiment. Animals were housed in standard condition (25°C, 12h light/dark cycle) in polypropylene cages. The animals were fed with standard pellet diet and water *ad libitum*. The experiment was performed according to the CPCSEA guidelines for laboratory animals and ethics, Department of animal welfare, Government of India (SDCOPVS/AH/CPCSEA/01/0028).

3.12.1. Treatment Schedule for anticancer study

Animals were randomized and divided into seven groups of 10 animals each **(Table 2)**. Mammary gland carcinoma in each group (except Group I) was induced by single tail vein injection of DMBA (8 mg/kg i.v.) on day 1. The drug/formulations were administered (10 mg/kg e.q. Dox) thrice/weeks in last six weeks of total 16 weeks of *in vivo* studies. A gap of 10 weeks was provided to develop the cancer in animals. Tumor incidence and size were monitored by measuring the diameter of mammary glands of rats by using Vernier calliper. Tumor progression was further monitored by weight and survival of animals during the study. The blood samples were collected under mild chloroform anaesthesia through retro orbital puncture for further analysis. The blood samples were incubated at 37 ºC for 1 hr and centrifuged at 10,000 rpm for 20 min to collect serum and the serum samples were stored at -20 °C till further use. Animals were sacrificed on the 112th day after treatment and mammary tissues were removed and stored at -80 °C till further evaluation (Roy et al. 2017).

3.12.2. Biochemical Estimation

The mammary gland tissue (10 % w/v) was homogenized in 0.15 mol. KCl and centrifuged at 10,000 rpm. The supernatants were scrutinized for biochemical parameters including TBARS, superoxide dismutase SOD, catalase, GSH and protein carbonyl. All the experiments were performed in triplicate and were subjected to statistical analysis

using Graph Pad Prism (ver. 5.01, San Diego, California) (Alshabanah et al. 2010, Kaithwas and Majumdar 2012, Roy et al. 2017).

Table 2. Treatment groups selected for *in vivo* anticancer activity

Sr. No.	Groups	Treatment
1.	Group I (negative control)	received normal saline
2.	Group II (toxic control)	received normal saline and DMBA
3.	Group III (plaebo formulation)	NE with ALA + DMBA
4.	Group IV (standard drug)	Dox solution + DMBA
5.	Group V (marketed formulation)	Marketed formulation + DMBA
6.	Group VI (test 1)	Dox-NE+DMBA
7.	Group VII (test 2)	f-Dox-NE + DMBA

3.12.3. Western blot analysis

The mammary gland tissues were lysed in RIPA lysis buffer and total protein lysates were obtained and the protein content was quantified with the help of Bradford reagent. Equal amount of protein was separated by SDS-PAGE from each sample and transferred to nitrocellulose membranes. Subsequently, the membranes were blocked and immunoblotting was performed with appropriate antibodies *viz.*, bcl2 (mouse monoclonal, SC-7382), bax (mouse monoclonal, SC-23959), Caspase-9 (mouse monoclonal, SC-56073) and MMP-9 (goat polyclonal, sc-6840). β-actin (MA5-15739-HRP) was used as a standard reference in this study. Nitrocellulose membranes were incubated with an appropriate secondary antibody conjugated to horseradish peroxidise (HRP) followed by detection of protein using enhanced chemiluminescence (Western Bright ECL HRP substrate, Advansta, US). Quantitative analysis of protein expression was performed by scanning densitometry (ImageJ, NIH) (Arya et al. 2017, Roy et al. 2017, Trivedi et al. 2011, Vimala et al. 2014).

3.12.4. Microscopy of whole mounts of mammary glands through carmine staining

The mammary glands obtained from rats were stretched onto a glass slide and kept in a fixative solution composed of 60:30:10 ratio of ethanol: chloroform: acetic acid. Then, slides were stained with a carmine solution for 2 days, washed with 90%, 70%, 35% and 15% v/v ethyl alcohol for 1 h, respectively, and finally washed with distilled water three

times at 5 min interval. The tissue samples were dehydrated in alcohol with ascending concentrations and then dipped in xylene for two days and stained with a carmine alum solution to prepare whole mounts. The whole mounts were examined under the 4X microscope and evaluated for the number of alveolar buds/terminal end buds (AB/TEB) (Moraes et al. 2009, Moraes et al. 2007, Roy et al. 2017).

3.12.5. Cardiotoxicity

Doxorubicin is an effective antitumor agent. However, its clinical use is limited because of its toxicity in the heart (Cai et al. 2010). Dox has been reported to induce cardiotoxicity at cumulative dose of 15 mg/kg over a period of 6 weeks in rats. The study was designed according to the previously published report (Trivedi et al. 2011). Briefly, the animals were divided into four groups of 6 animals each. Group I served as control and received normal saline, Group II received Dox 4 mg/kg solution, Group III received ALA-NE as vehicle control, and Group IV received f-Dox-NE (4 mg/kg eq. Dox). All treatments were given once a week via intraperitonial injection route for 5 weeks. Animals were sacrificed after 1 week of receiving the last injection of Dox and heart tissues were removed. Biochemical estimation for lipid peroxidation (MDA levels) and GSH content was measured from tissue homogenates.

3.12.6. Biodistribution of Doxorubicin

Biodistribution of Dox was examined by injecting f-Dox-NE, Dox-NE, standard drug solution and marketed formulation at 10 mg/kg Dox equivalent dose through tail vein of DMBA induced rats. Different organs, *viz.*, mammary glands, liver, heart, kidney, spleen were removed post injection (at time intervals 4, 12, 24 and 48 h) and washed to remove the blood, weighed and homogenized and the Dox concentration was measured through the validated HPLC method (M/s Waters 2489, Milford, Massachusetts, USA). The system was equipped with Spherowsorb C18, 3.5 µm, 4.6×250 mm column, having flow rate 1.0 mL/min and ambient temperature. The mobile phase consisted of water at pH 3 adjusted with 85% w/v phosphoric acid and acetonitrile (30:70) and the total run time was 10 min. The HPLC was run through Empower software ver.2 and absorbance was measured at 233 nm wavelength using Waters 2489 UV-Vis detector (Dharmalingam et al. 2014, Lee et al. 2005).

3.13. Statistical analysis

One-way ANOVA with Bonferroni multiple comparison tests were used to find out significant statistical differences between the groups. Values of *$p<0.05$, **$p<0.01$, ***$p<0.001$ were considered as statistically significant. Statistical analysis was performed using Graph Pad Prism software (*ver.* 5.02).

4. Results

4.1. Preformulation studies

4.1.1. Solubility studies

The drug solubility plays an important role for the development of effective and stable NE formulations using various lipids. Dox displayed maximum solubility in isopropyl myristate (30.55±3.25 mg/mL) followed by the ALA (25.33±3.78 mg/mL) amongst various lipids. Isopropyl myristate being synthetic in nature was not included in further development studies. Dox also showed highest solubility in lecithin (55.49±4.76 mg/mL) followed by Tween-80 and cholesterol among various emulgents and co-emulgents studied **(Fig. 2, Table 3)**. Cholesterol was used as co-emulgent as well stabilizer for the nanoemulsion globules.

Table 3: Solubility of doxorubicin in different oils and emulgents

S. No.	Name of Excepient	Solubility (mg/ml)	S. No.	Name of Excepient	Solubility (mg/ml)
1.	Sesame oil	12±3	2.	Lecithin	54±4
3.	Oleic acid	20±3	4.	IPM	31±3
5.	Soybean oil	15±3	6.	Cholesterol	45±4
7.	Perilla oil	22±2	8.	Tween-20	35±4
9.	Linolenic Acid	25±3	10.	Span-80	21±3
11.	Tween-80	51±5	12.	PEG-200	29±4

4.1.2. Construction of pseudo-ternary phase diagrams

Pseudo-ternary phase diagram (TPD) is a prerequisite to demarcate the region of NE and to comprehend a stable nanoemulsion formed using various lipids and emulgents. The TPD enables us the selection of best possible combinations for best stable NE. Most of the diagrams constructed using the natural lipids like perilla oil, sesame oil, oleic acid and soybean oil showed very narrow range of the nanoemulsion region and gel formation which was undesirable for a nanoemulsion formulation **(Fig. 3 [A-E])**, hence excluded from further studies. The TPD of ALA with S_{mix} (lecithin and Tween 80; 1:1) displayed maximum nanoemulsion region **(Fig. 4 [B])**.

The smaller nanoemulsion region with the natural oils contributes to their poor emulsion formation capacities. However, this problem can be mitigated by adding some synthetic lipids like IPM. However, these may be undesirable for the parenteral route. Taking into consideration the delivery system, route of administration, safety, nature of excipients, solubility of the drug and TBD, ALA was selected as lipid phase and lecithin and Tween-80 as S_{mix} in equal weight ratio (1:1). The lipid and emulgents were considered as critical material attributes (CMAs) for nanoemulsion.

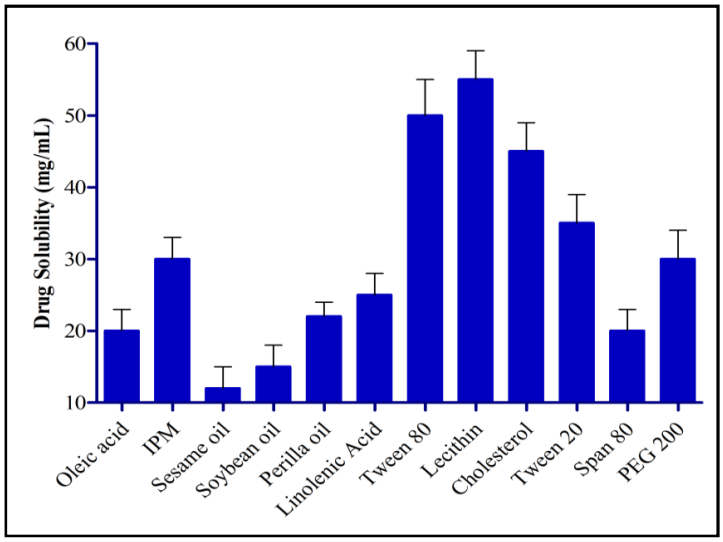

Fig. 2. Plot representing solubility of Dox in various excipients of the nanoemulsion. [Data presented as mean±SD, n=3]

4.1.3. Selection of co-emulgent

The stability and solubility and water absorption capacity suggested that cholesterol was the best co-emulgent among different studied emulsifiers. The nanoemulsion system formulated by cholesterol depicted highest water absorption capacity and highest stability even after storage of one month. Hence, cholesterol was taken as the co-emulgent (CMA) for formulation optimization studies **(Table 4)**.

4.2. Mathematical model development

A mathematical model was developed by using second-order quadratic model through multiple linear regression analysis (MLRA) to fit the observed data **(Table 5)**. An excellent goodness of fit of the observed data was monitored for the generated

coefficients of model equations for each of the CQAs of the product *i.e.*, drug release, globule size, entrapment efficiency (EE) and drug loading. High values of various coefficients i.e., R^2 ($p < 0.05$ in all the cases), insignificant lack of fit, and low values of the predicted sum of squares indicated that the model was best fitted (Singh et al. 2011, Tripathi et al. 2016).

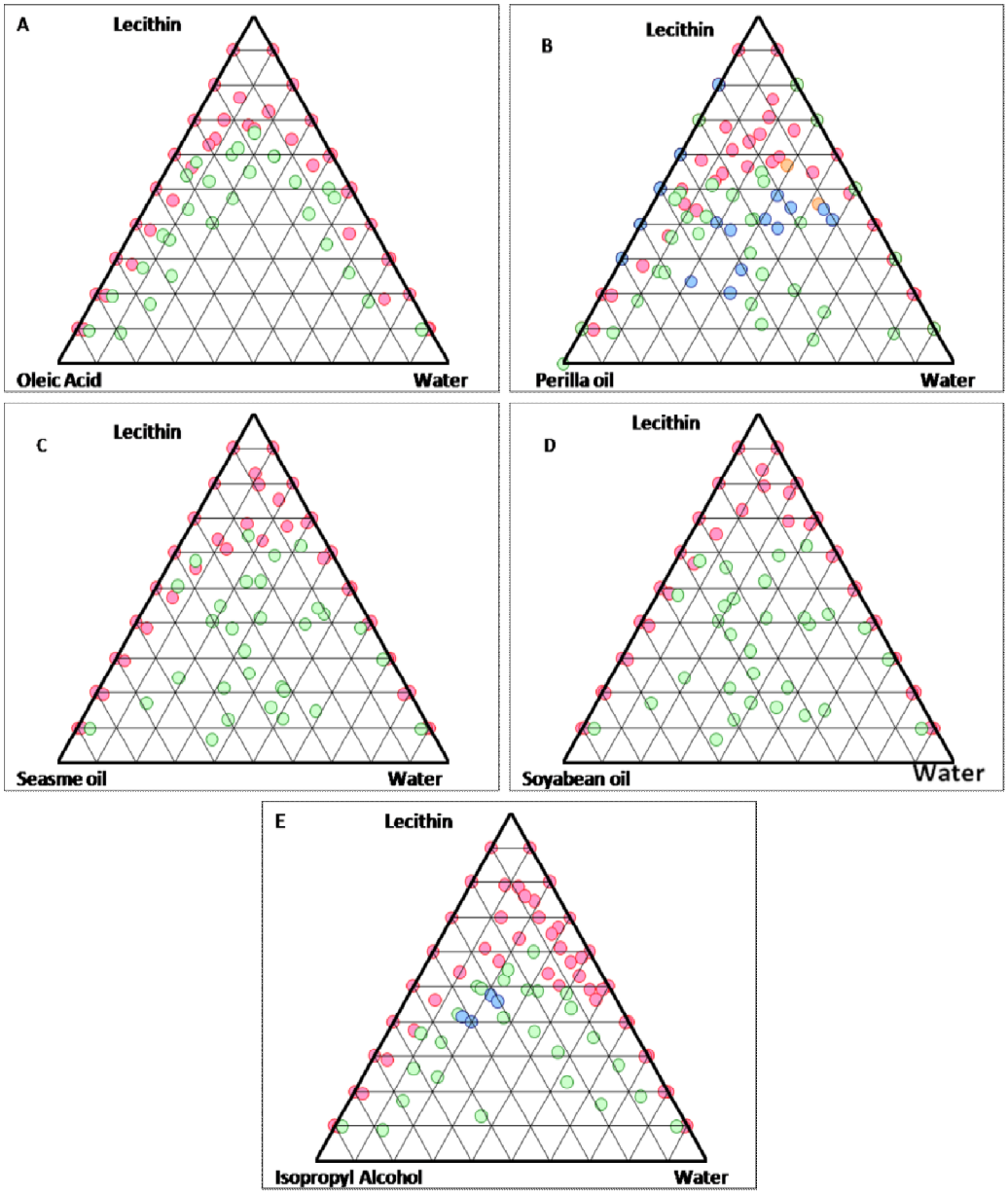

Fig. 3. Pseudoternary phase diagrams of different lipids viz., oleic acid, perilla oil, sesame oil, soyabean oil and isopropyl alcohol with lecithin.

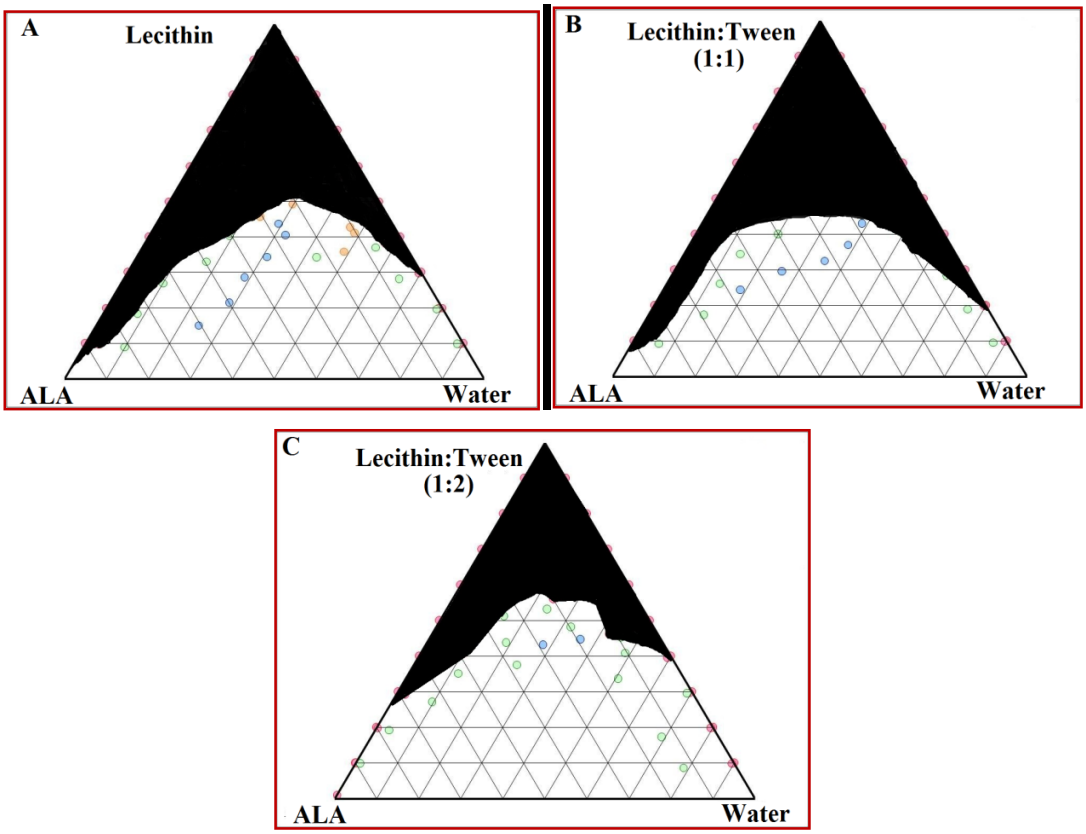

Fig. 4. Pseudoternary phase diagrams of the lipid (α-linolenic acid-ALA) with different emulgents (A) lecithin only, (B) lecithin: Tween 80 (1:1) and (C) lecithin: Tween 80 (1:2)

Table 4: Different co-emulgent with their water absorption capacity and stability

S. No.	Co-emulgent Name	Water absorption	Stability
1.	Cholesterol	26.55%	Stable
2.	PEG 200	12.35%	Stable
3.	Span 80	19.67%	Unstable

The effects of various selected excipients (CMAs) on the various CQAs of NE were presented through response surface analysis (RSM). The response surface plots **(Fig. 5 A-D**) explicitly describe the effects of lipid, emulgent and co-emulgent on various CQAs of the nanoemulsion.

The lipid, emulgent and co-emulgent conferred significant ($p<0.001$) effect on globule size of the nanoemulsion **(Fig. 5A)**. The lowest value for globule size was observed at middle levels of the lipid emulgent and co-emulgents. Further, significant interaction

among different excipients (except emulgent and cholesterol) was observed when data were fitted with modified quadratic model **Table 6A**.

Table 5. Physicochemical parameters for Dox loaded nanoemulsions prepared as per the BBD.

Code	Drug (mg/g of formulation)	Lipid (mg) (X_1)	S_{mix} (mg) (X_2)	Cholesterol (mg) (X_2)	Globule Size (nm) (Y_1)	Drug Release (%) (Y_2)	Drug loading (%) (Y_3)	Entrapment efficiency (%) (Y_4)
NE1	5	200	500	150	250.4±3.5	80.12±5.13	0.37±0.02	86.77±3.21
NE2	5	600	500	150	380.5±2.8	70.36±3.94	0.49±0.02	72.12±4.36
NE3	5	200	900	150	70.6±4.5	95.52±2.63	0.32±0.08	95.22±4.84
NE4	5	600	900	150	300.5±4.2	75.44±3.54	0.47±0.01	82.99±3.16
NE5	5	200	700	100	139.7±6.1	89.21±4.11	0.29±0.03	85.47±4.93
NE6	5	600	700	100	312.6±5.9	70.33±3.33	0.38±0.04	67.44±4.67
NE7	5	200	700	200	68.2±4.1	92.21±2.74	0.45±0.03	99.29±2.16
NE8	5	600	700	200	230.3±3.4	78.71±5.52	0.48±0.02	89.52±3.55
NE9	5	400	500	100	280.5±5.1	75.23±6.15	0.38±0.04	72.44±3.63
NE10	5	400	900	100	120.6±3.9	90.32±4.35	0.41±0.02	78.63±2.12
NE11	5	400	500	200	210.9±2.2	82.33±3.63	0.46±0.03	80.61±3.74
NE12	5	400	900	200	80.2±3.1	93.61±4.21	0.39±0.03	86.71±4.51
NE13	5	400	700	150	57.4±2.4	92.77±4.74	0.44±0.02	96.12±3.36
NE14	5	400	700	150	55.1±3.2	94.33±3.93	0.47±0.01	94.33±2.49
NE15	5	400	700	150	59.4±3.1	91.43±4.51	0.45±0.03	97.21±3.65

[Data presented as mean±SD, n=3]

As revealed in **Fig. 5B**, at the middle level of excipients, the drug release was found to be maximum when analyzed through the quadratic model, indicating significant effect ($p<0.05$) of the selected excipients on drug release. Here, ALA, cholesterol and emulgents played a vital role in regulating the drug release behavior of NE **(Table 6B)**. In case of drug loading (**Fig. 5C and Table 6C**) ALA and cholesterol showed a significant effect ($p<0.05$). As the concentration of ALA and cholesterol were increased the drug loading increased linearly, with the effect being more prominent for ALA. However, S_{mix} showed no significant effect on drug loading efficiency of NE ($p>0.05$). ALA, S_{mix} and cholesterol each demonstrated a significant role in the drug entrapment in various NE

($p<0.01$). Significant positive interaction between lipid and emulgent was observed ($p<0.05$) which is recorded in **Fig. 5D and Table 6D**. Data was appropriately fitted using modified quadratic equations as revealed by non-significant lack of fit ($p>0.05$) from the ANOVA data of each CQAs.

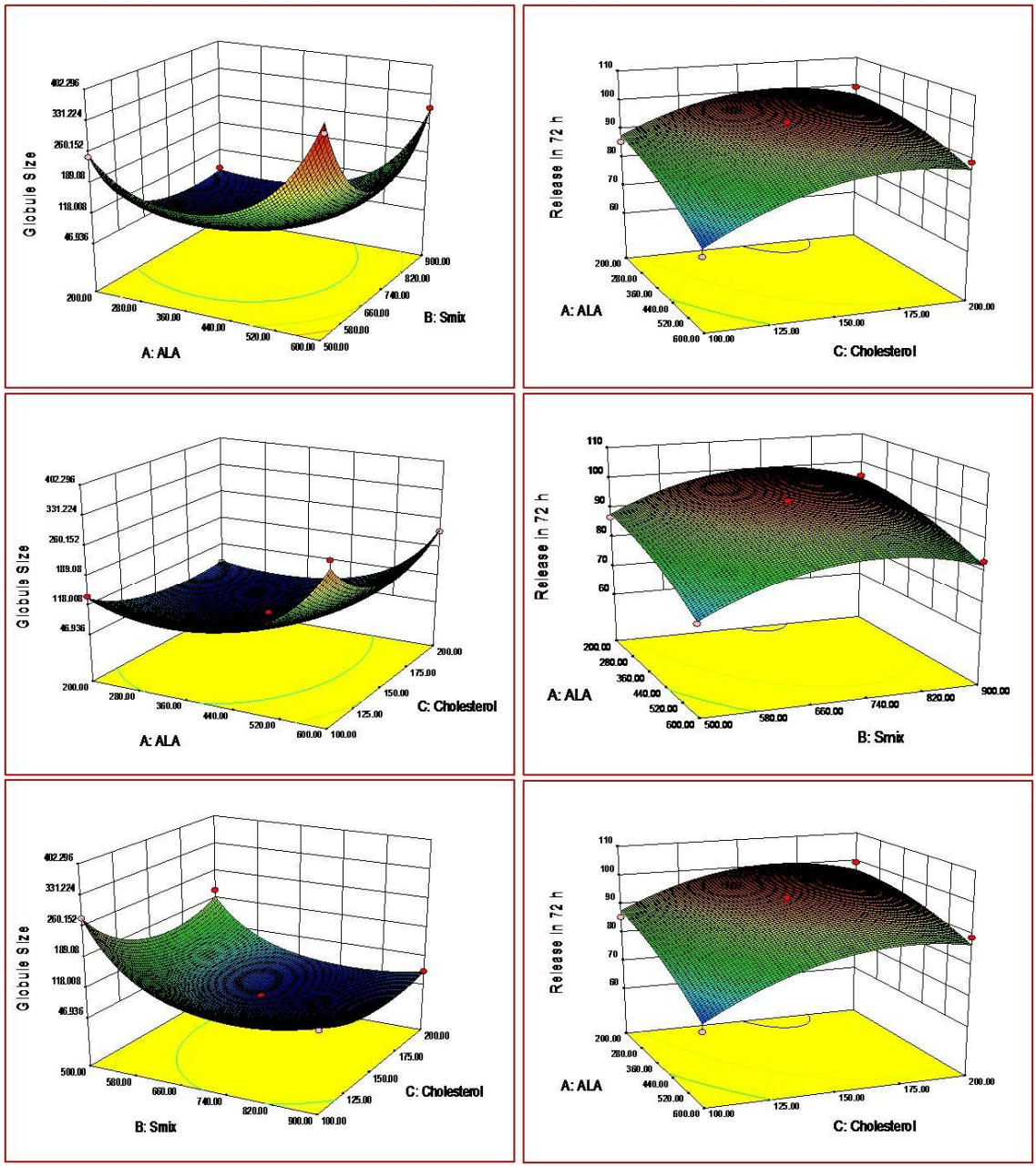

Fig. 5. Response surface plots showing the influence of lipid, emulgents mixture (S_{mix}) and co-emulgent on (A) globule size and (B) drug release of the nanoemulsion.

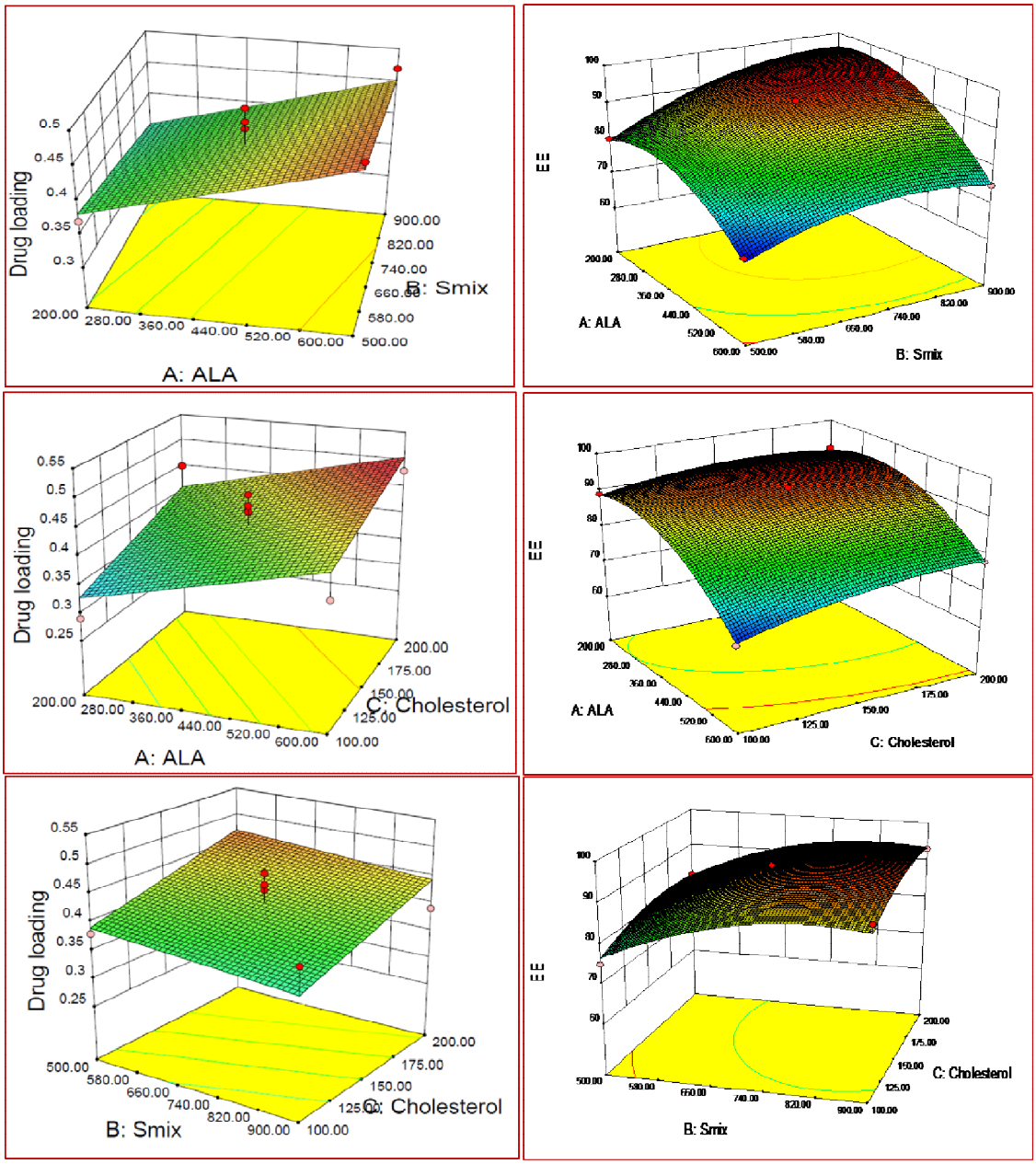

Fig. 5. Response surface plots showing the influence of lipid, emulgents mixture (S_{mix}) and co-emulgent on (C) drug loading and (D) entrapment efficiency (EE) of the nanoemulsion

Table 6A. ANOVA table for modified quadratic model fitting of particle size of nanoemulsions

Source	Sum of Squares	df	Mean Square	F Value	p-value Prob > F	
Model	1.35475	9	0.150528	132.0554	< 0.0001	Significant
A-ALA	0.3588	1	0.3588	314.769	< 0.0001	Significant
B-Smix	0.260141	1	0.260141	228.2168	< 0.0001	Significant
C-Cholesterol	0.069185	1	0.069185	60.69484	0.0006	Significant
AB	0.050665	1	0.050665	44.44789	0.0011	Significant
AC	0.007928	1	0.007928	6.955135	0.0461	Significant
BC	0.000654	1	0.000654	0.57387	0.4829	Not significant
A^2	0.320483	1	0.320483	281.1545	< 0.0001	Significant
B^2	0.278571	1	0.278571	244.3855	< 0.0001	Significant
C^2	0.09164	1	0.09164	80.39389	0.0003	Significant
Residual	0.005699	5	0.00114			
Lack of Fit	0.005235	3	0.001745	7.50723	0.1198	Not significant
Pure Error	0.000465	2	0.000232			
Cor. Total	1.360449	14				

P<0.05 was considered as significant

Table 6B. ANOVA table for modified quadratic model fitting of Drug release from nanoemulsions

Source	Sum of Squares	df	Mean Square	F Value	p-value Prob > F	
Model	1335.08	8	166.88	17.10	0.0013	Significant
A-ALA	380.88	1	380.88	39.02	0.0008	Significant
B-Smix	122.62	1	122.62	12.56	0.0122	Significant
C-Cholesterol	329.99	1	329.99	33.80	0.0011	Significant
AB	1.46	1	1.46	0.15	0.7119	Not significant
AC	14.98	1	14.98	1.53	0.2617	Not significant
A^2	23.93	1	23.93	2.45	0.1685	Not significant
B^2	288.92	1	288.92	29.60	0.0016	Significant
C^2	225.84	1	225.84	23.13	0.0030	Significant
Residual	58.57	6	9.76			
Lack of Fit	53.91	4	13.48	5.78	0.1530	Not significant
Pure Error	4.67	2	2.33			
Cor Total	1393.65	14				

P<0.05 was considered as significant

Table 6C. ANOVA table for modified quadratic model fitting of drug loading of nanoemulsions

Source	Sum of Squares	df	Mean Square	F Value	p-value Prob > F	
Model	0.033	3	0.011	7.019	0.0066	Significant
A-ALA	0.019	1	0.019	12.014	0.0053	Significant
B-Smix	0.002	1	0.002	0.956	0.3493	Not significant
C-Cholesterol	0.013	1	0.013	8.088	0.0160	Significant
Residual	0.017	11	0.002			
Lack of Fit	0.017	9	0.002	8.067	0.1151	Not significant
Pure Error	0.000	2	0.000			
Cor Total	0.051	14				

P<0.05 was considered as significant

Table 6D. ANOVA table for modified quadratic model fitting of entrapment efficiency of nanoemulsions

Source	Sum of Squares	df	Mean Square	F Value	p-value Prob > F	
Model	1133.18	8	141.65	58.95	< 0.0001	Significant
A-ALA	496.13	1	496.13	206.48	< 0.0001	Significant
B-Smix	264.50	1	264.50	110.08	< 0.0001	Significant
C-Cholesterol	55.13	1	55.13	22.94	0.0030	Significant
AB	25.00	1	25.00	10.40	0.0180	Significant
AC	6.25	1	6.25	2.60	0.1579	Not significant
A^2	210.01	1	210.01	87.40	< 0.0001	Significant
B^2	84.78	1	84.78	35.28	0.0010	Significant
C^2	23.85	1	23.85	9.93	0.0198	Significant
Residual	14.42	6	2.40			
Lack of Fit	9.75	4	2.44	1.04	0.5426	Not significant
Pure Error	4.67	2	2.33			
Cor. Total	1147.60	14				

P<0.05 was considered as significant

4.3. Optimization of formulation and validation studies

Search for the optimized formulation was performed by "trading-off" among various CQAs for the nanoemulsion. The goals like minimization of the globule size which is necessary for faster solubilization of drug, maximization of the entrapment efficiency, maximization of drug release, and drug loading was attempted. The optimized

formulation was chosen by graphical optimization methodology using overlay plot **(Fig. 3)**. The constraints were applied for the graphical optimization method using overlay plot. The constrains applied for the nanoemulsion optimization were globule size less than 100 nm, entrapment efficiency more than 90%, drug release more than 80%, and drug loading more than 10% fixed. The optimized formulation was selected based upon the afore-listed criteria. The composition of optimized NE (Dox-NE) was ALA-400 mg, lecithin-350 mg, Tween 80-350 mg and cholesterol-150 mg, exhibiting observed values of the CQAs as globule size of 52.7 nm, entrapment efficiency 92.51±3.62%, drug release of 94.86±1.87% in 72 h and drug loading 0.42±.08% **(Fig. 6)**.

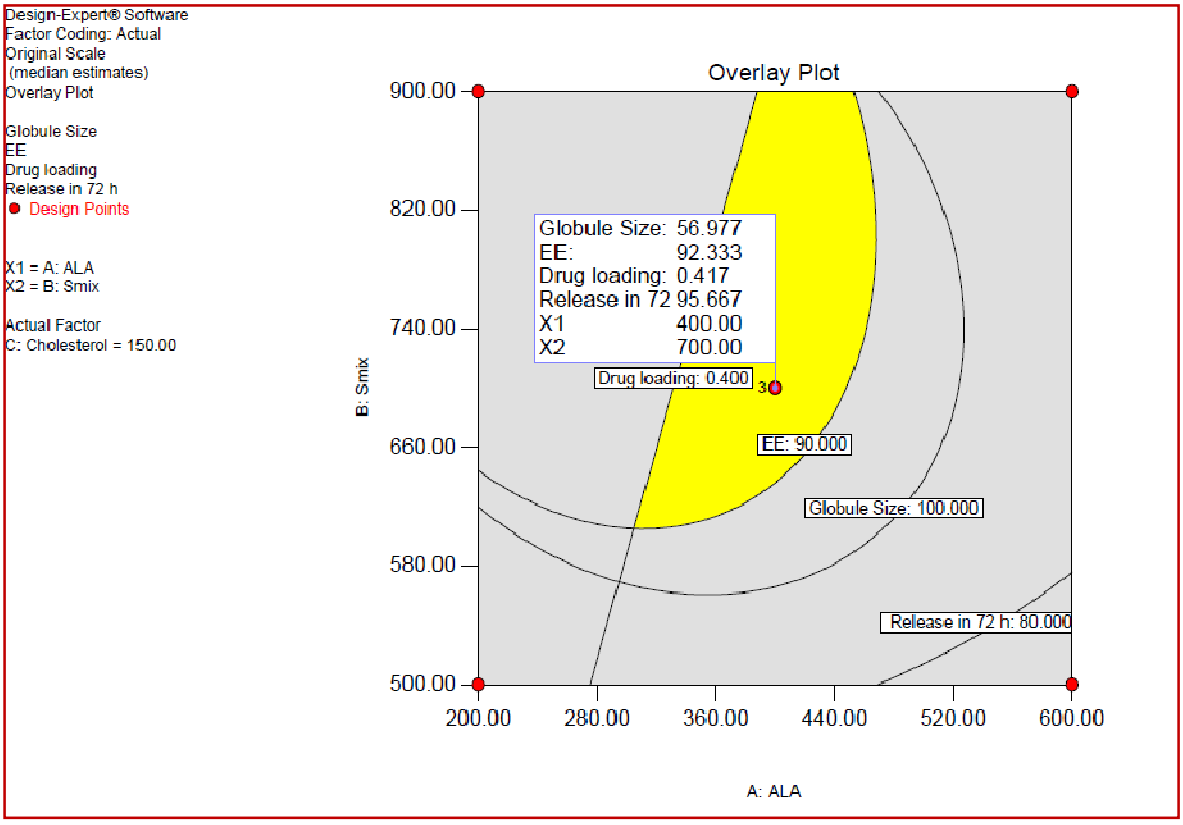

Fig. 6. Overlay plot depicting the desirable region (design space) as highlighted area for the nanoemulsion. Inset flag presents the composition of optimized nanoemulsion (X_1-400 mg, X_2 700 mg, X_3- 150 mg) and predicted values of CQAs.

Validation of the optimization methodology by comparing the observed responses with those of the predicted ones revealed the percent prediction error ranging between -0.18% and 10.63% for the Dox-NE, thus demonstrating high degree of the predictive ability of the design methodology **(Table 7)**.

Table 7. The observed and predicted values of CQAs for optimized formulation (Dox-NE)

Parameter	Observed values	Predicted values	Percent variation
Globule size	52.7 nm	56.95 nm	7.46
Entrapment efficiency	92.51±3.62%	92.34 nm	-0.18
Drug release	94.86±1.87%	95.66%	0.84
Drug loading	0.42±.08%	0.47%	10.63

4.4. Characterization of surface modification nanoemulsion

4.4.1. FTIR characterization

Conjugation of the folic acid to ALA involved the formation of two amide bonds first between ALA and NH2-PEG-NH2 while other another was between ALA-PEG-NH2 and Folate-NHS. These conjugations were characterized through IR spectroscopy to confirm the linkages. Important peaks obtained for the folic acid were at 897.2 cm^{-1} (aromatic C–H bending and benzene 1,4-disubstitution), 1478.9 cm^{-1} (CH–NH–CO amides bending), 2996.4 cm^{-1} (alkyl C–H and O-H stretch) 1702.5 cm^{-1} (aromatic C-C bending and stretching), , 3439.3 cm^{-1} (N–H stretch of primary amine and amide, C-H stretch) and 1310.11 cm^{-1} (C-O stretch ester) **(Fig. 7A)**. For ALA characteristic peaks was observed at 2923.7 cm^{-1} (carboxylic acid COOH and O–H unconjugated stretching), 2854.3 cm^{-1} (alkyl C-H stretching), 1,708.8 cm^{-1} (C=C Alkenyl stretch), 1463.8 cm^{-1} (CH_2, CH_3 deformation) **(Fig. 7B)**. For the Folate-NHS ester, the peaks were observed at 3491.8 cm^{-1} (amide N–H and C=O stretching), 2913.7 and 2996.1 cm^{-1} (carboxylic acid COOH and O–H unconjugated stretching), 1551.37 cm^{-1} (CH–NH–CO amides bending), 1663.8 cm^{-1} (ketone C=O stretch), 697.4, 896.9, 931.29 cm^{-1} (aromatic C-H bending and stretching) that confirmed the formation of folic acid NHS ester **(Fig. 7C)**. For the Folate-PEG-ALA, the peaks were observed at 3441.5 cm^{-1} (amide N–H and C=O stretching), 2913.8 and 2997.08 cm^{-1} (carboxylic acid COO-H, alkane C-H stretching and O–H unconjugated stretching), 1712.5 cm^{-1} (aromatic C-C bending and stretching), 1,649.7.8 cm^{-1} (ALA C=C Alkene stretch), 1,436.9 cm^{-1} (CH–NH–CO amides bending), 1212.2 cm^{-1} (PEG C-O-C stretching), 932.2, 897.8, 698.2 cm^{-1} (aromatic C-H bending and stretching), confirmed the attachment of the folic acid to ALA through PEG **(Fig. 7D).**

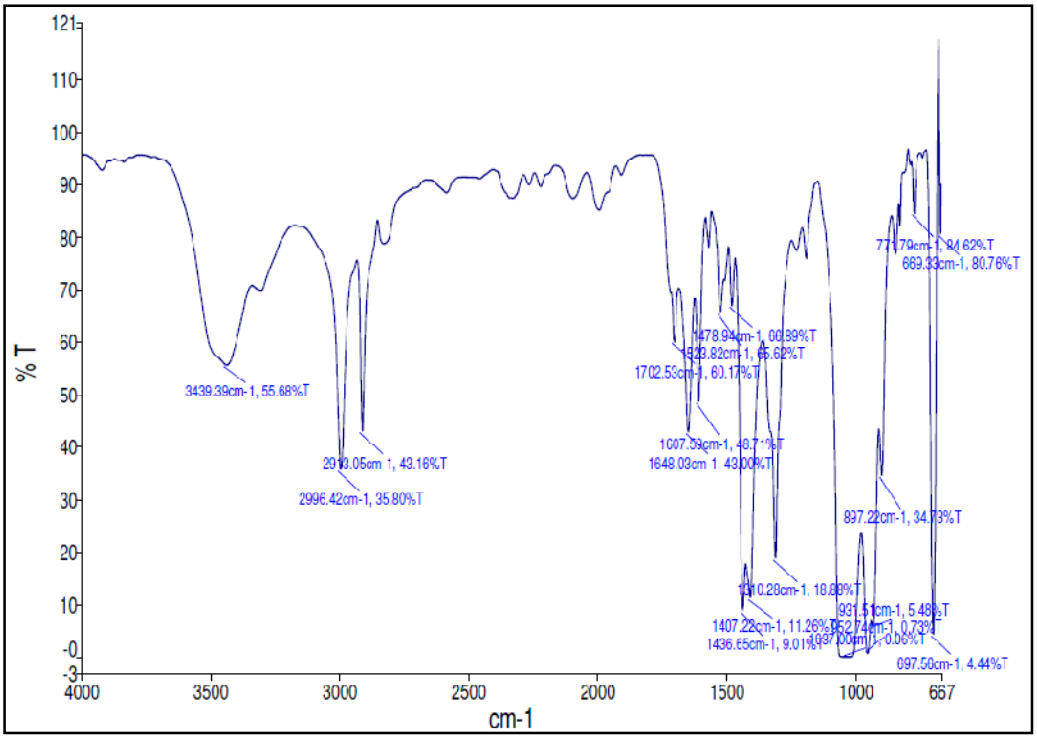

Fig. 7A. FTIR spectra of Folic Acid

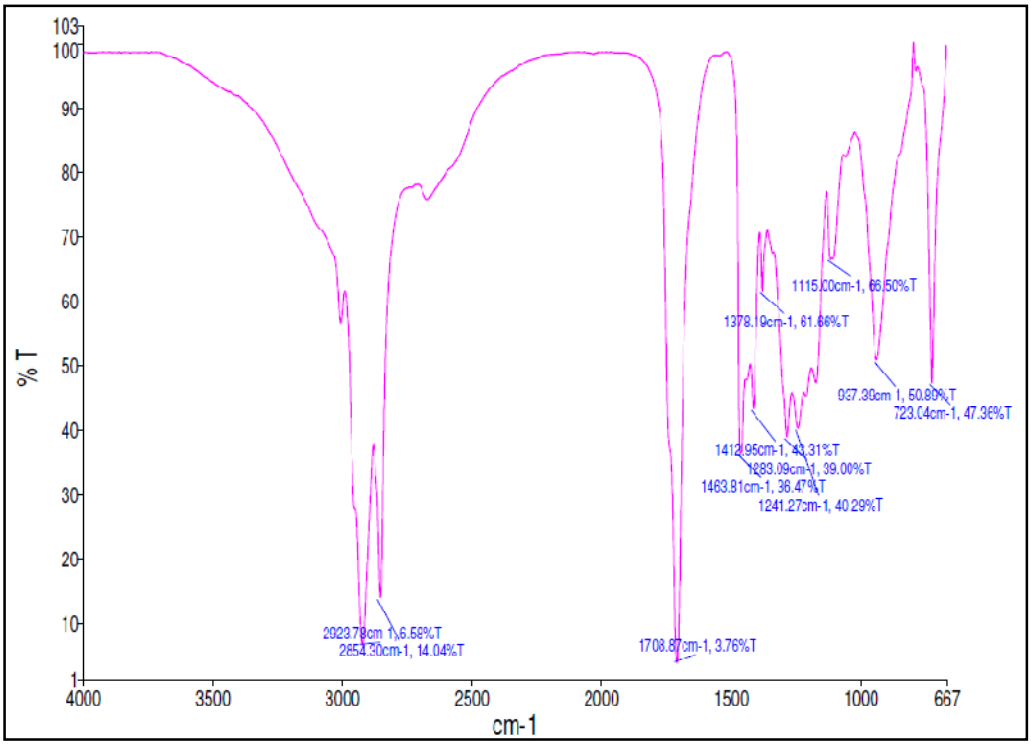

Fig. 7B. FTIR spectra of Fatty Acid (ALA)

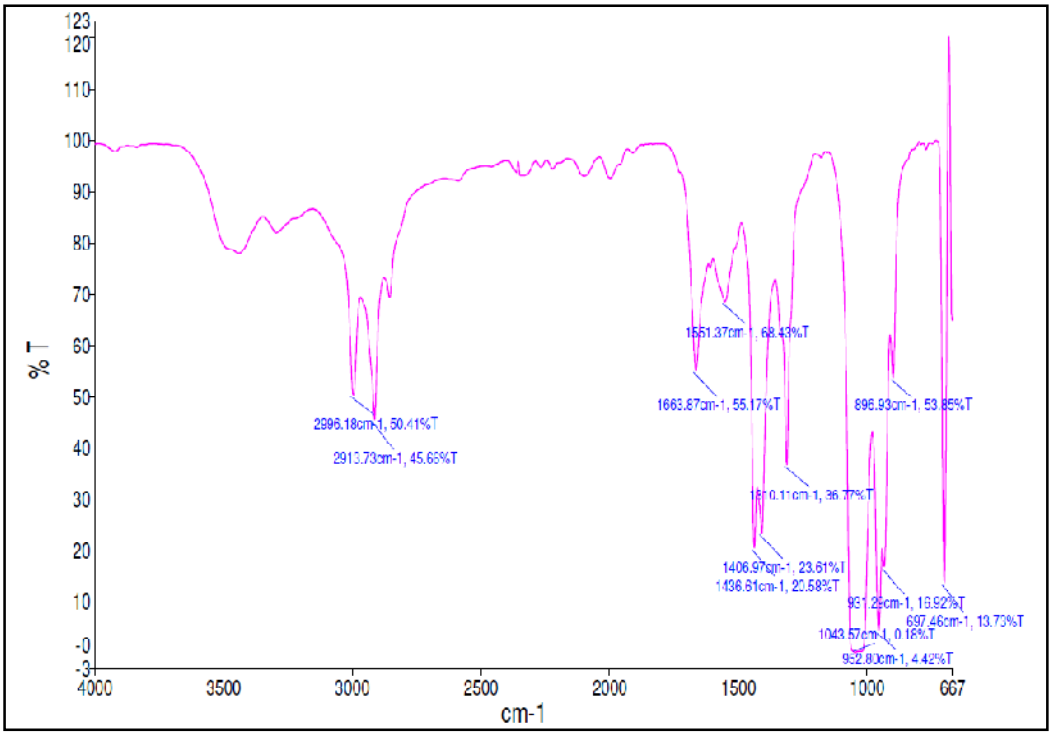

Fig. 7C. FTIR spectra of folate conjugated NHS (F-NHS)

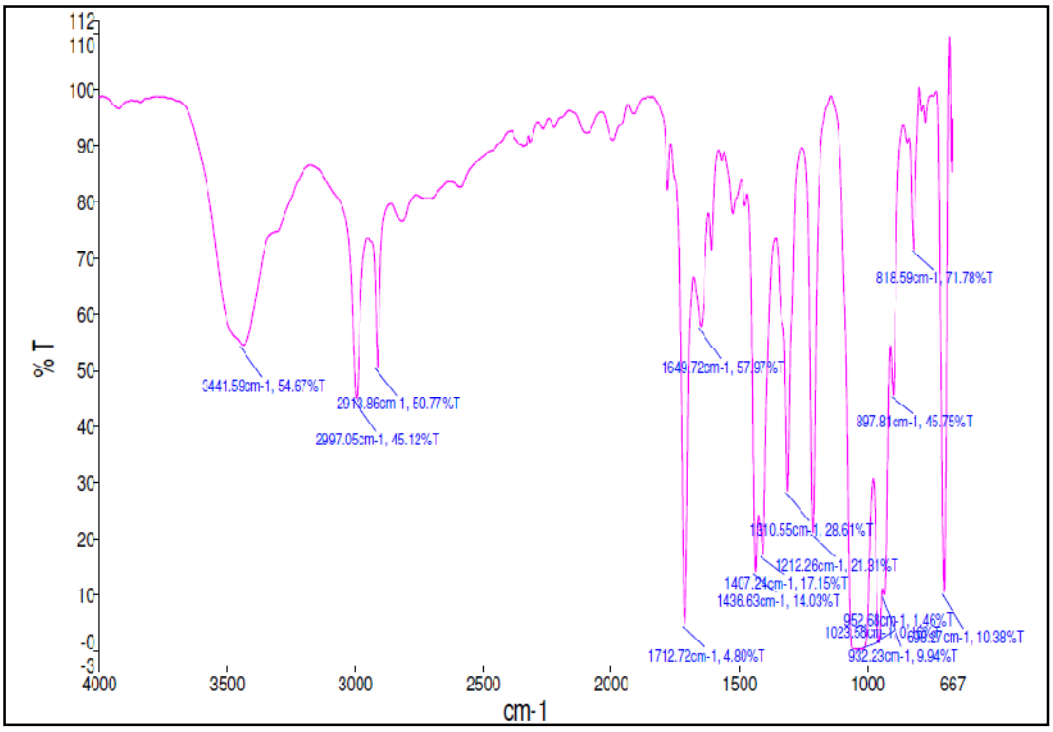

Fig. 7D. FTIR spectra of folate conjugated fatty acid (f-PEG-ALA)

4.4.2. ^{1}H-NMR characterization

^{1}H-NMR of folate attached nanoemulsion was performed and characteristic peaks were indentified and appropriately marked that confirmed the conjugation of folate to ALA. The peaks observed for ALA-PEG-NH_2 was 1 (3.66, 2H, d, broad peak of protonated NH_2 protons), 2 (3.31-3.46, 2H, dd, two adjacent peaks for PEG); 3 (7.85, 1H, m, CONH), 4 (2.14, 2H, t, methylene), 5 (1.18-1.46, 12H, m, methylene); 6 (5.28, 6H, m, ethene); 7 (2.66, 4H, s, methylene); 8 (2.13-2.19, 2H, m, methylene); 9 (0.78-0.80, 3H, t, methyl) **(Fig. 8a)**. Important peaks of folate decorated ALA (ALA-PEG-folate) was 1 (8.35, 1H, s, dihydropteridin NH); 2 (3.76, 2H, d, broad peak of protonated NH_2 protons); 3 (8.58, 1H, s, dihydropteridine CH); 4 (2.42, 2H, s, methylene); 5 (3.44, 3H, m, aliphatic NH); 6 (6.58 & 7.54, 4H, dd, aromatic CH); 7,11,13 (6.83, 3H, m, CONH); 8 (1.18, 1H, s, aliphatic CH); 9 (2.27, 4H, s, methylene); 10, 14 (2.14, 4H, t, methylene); 12 (3.35-3.46, 2H, dd, two adjacent peaks for PEG); 15 (1.18-1.53, 12H, m, methylene); 16 (5.27, 6H, m, ethene); 17 (2.66, 4H, s, methylene); 18 (2.10-2.18, 2H, m, methylene); 19 (0.70-0.80, 3H, t, methyl). **(Fig. 8b)**.

4.4.3. Estimation of Folate Content attached to the surface

The amount of folate attached to the Dox-NE surface was measured through UV-Vis absorption method. The content of folate attached to the NE surface was found to be 10.33 µmol.g^{-1} of NE formulation.

4.4.4. Physicochemical characterization of f-Dox-NE

Folic acid was anchored to the Dox nanoemulsion surface with the help of the NHS and DCC. Surface modification through attachment of the folate over the NE droplets increased the globule size of Dox-NE to 55.2±3.3 nm from 52.7±2.8 nm; however, the surface charge was not changed (zeta potential -31±2 mV) due to involvement of covalent bond (amide) formation rather than ionic linkage or surface adsorption. The percent entrapment efficiency and percent drug loading of f-Dox-NE were found to be 92.51 ± 3.62% and be 0.47±.03%, respectively.

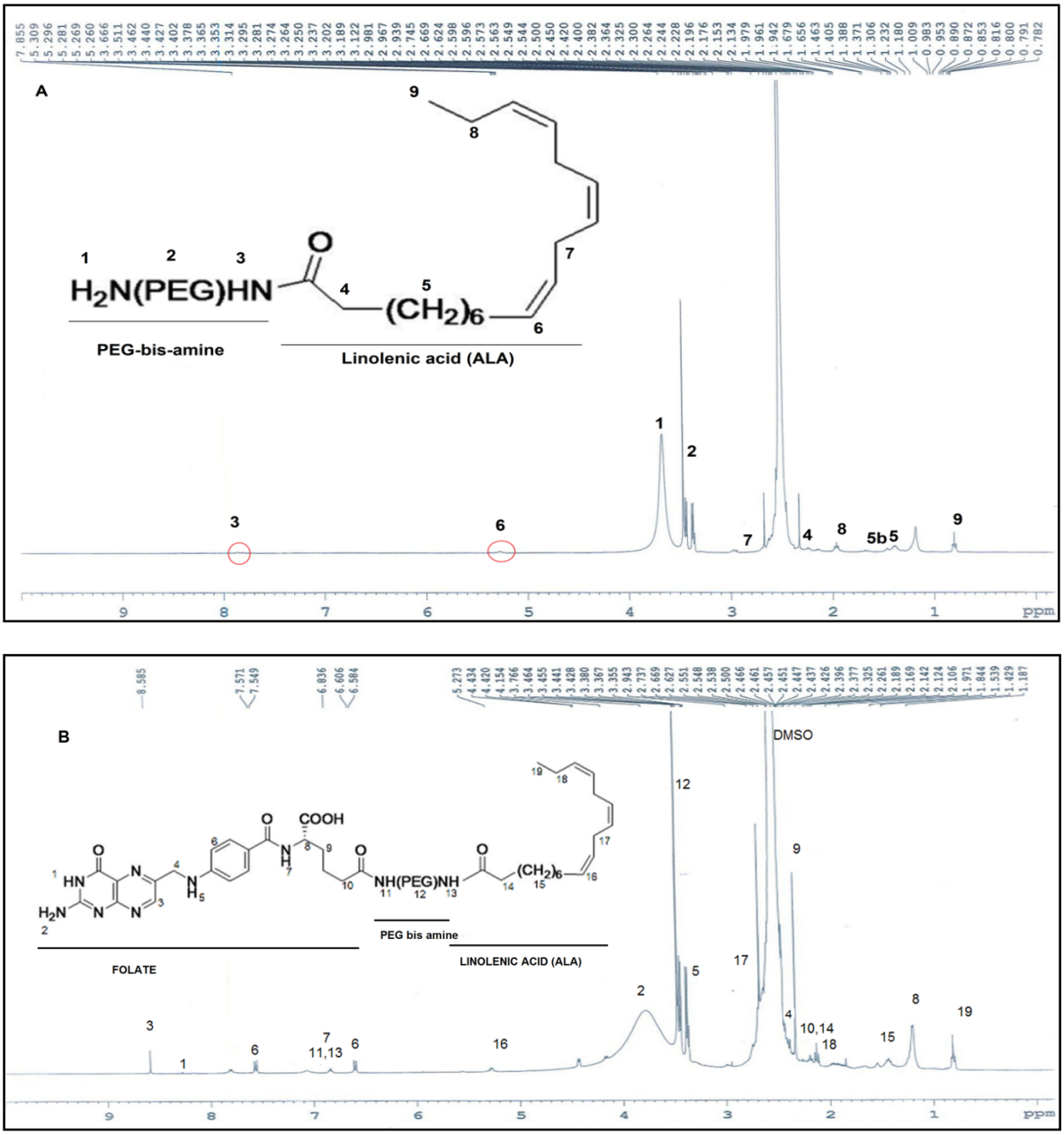

Fig. 8. ^{1}H-NMR spectrum of (a) PEG-NH_2 attached ALA (ALA-PEG-NH_2) (b) folate modified nanoemulsion (f-Dox-NE)

4.4.5. Comparative study of *In vitro* drug diffusion

There was significant improvement in Dox diffusion from nanoemulsion compared to the standard drug solution and marketed formulation. The cumulative drug diffused from standard and marketed formulation was 82.00±2.30% and 101.71±3.10% in 2 h, respectively. However, drug diffused from f-Dox-NE was only about 20% in the same

time period. The optimized NE (f-Dox-NE) showed cumulative Dox diffusion of 55.47±3.40%, 70.22±5.02%, 86.97±3.50%, and 94.86±1.87% in 12, 24, 36, and 72 h, respectively **(Fig. 9)**. f-Dox-NE presented sustained release pattern extended till 72 h. No significant changes were observed in the Dox diffusion profiles from NE before (Dox-NE) and after (f-Dox-NE) the surface decoration of the NE with folate ($p>0.05$).

4.4.6. Robustness to dilution

To access the robustness of f-Dox-NE, it was diluted 100, 500 and 1000 times with PBS 7.4, respectively. The f-Dox-NE exhibited robustness on dilution of the nanoemulsion with the PBS pH 7.4. Further, no sign of precipitation and cloudiness was evident even after 24 h.

4.4.7. Thermodynamic studies of f-Dox-NE

To ensure the stability of the formulation against different stresses, a NE must pass through the thermodynamic stability studies. The optimum formulation (f-Dox-NE) was found to be stable as there was no cracking, creaming, phase separation or drug precipitation after centrifugation and freeze-thaw cycles indicating stability of the nanoemulsion system.

4.4.8. Transmission electron microscopy studies of f-Dox-NE

All the globules of the optimized formulation (f-Dox-NE) displayed smooth surface and spherical shape with a size range of 20.80-65.99 nm as evident from TEM images **(Fig. 10)**.

4.4.9. Stability of formulations in plasma and intravenous infusion solutions

The stability of the optimized nanoemulsion (f-Dox-NE) was accessed visually for globule aggregation and by diluting the sample in plasma and infusion solutions. Observations were made for changes in globule size, if any, over 24 h at 37 °C. No particle aggregation and change in globule size was observed demonstrating that the formulation was non-aggregated and showed no sign of disruption even in presence of plasma proteins and electrolytes.

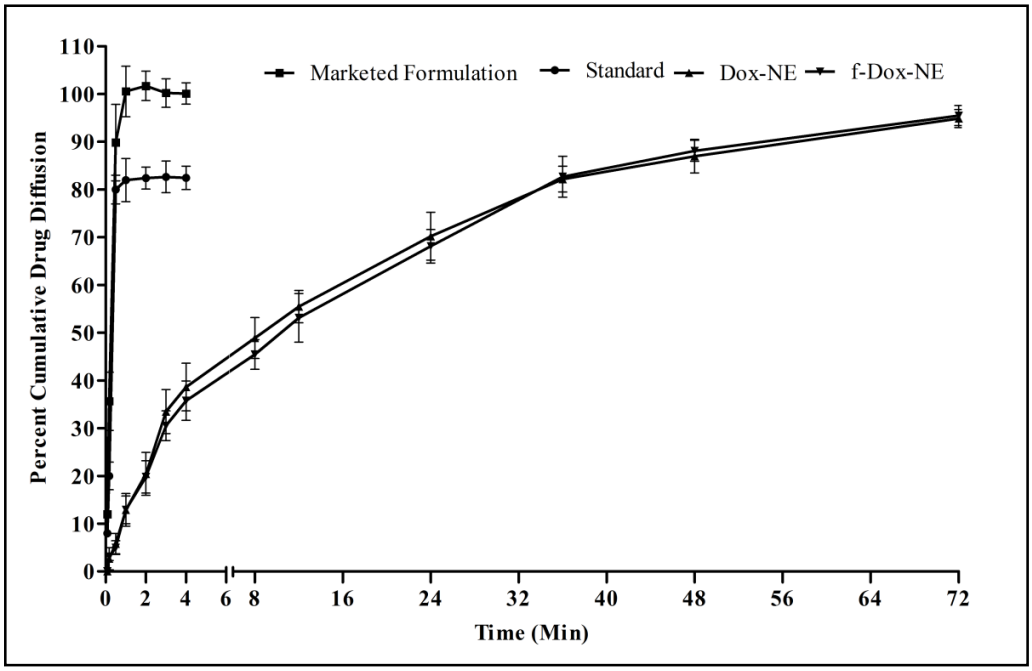

Fig. 9. Drug diffusion comparisons of standard drug, marketed formulation with Dox-NE and f-Dox-NE. [Data is presented as mean±SD (n=3)]

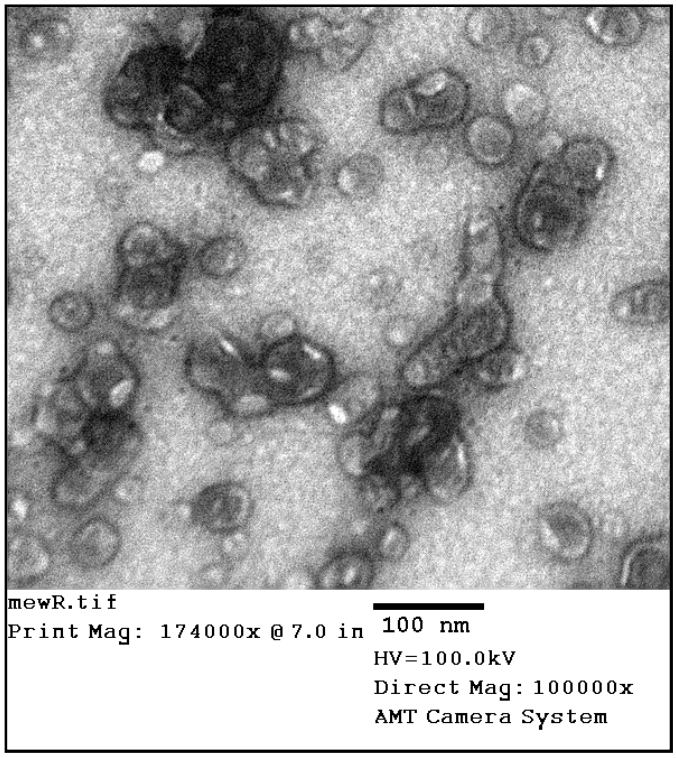

Fig. 10. TEM image of f-Dox-NE depicting nanoemulsion globules

4.4.10. Stability studies

The stability studies of f-Dox-NE confirmed the robust nature of the system under the specified stability conditions without any significant change in globule size, F2 values and drug content **(Table 8)**.

Table 8. Effect on the parameters of formulation during the stability studies

Time (months)	40±2 °C/75%±5% RH			25±2 °C/60±5% RH			5±3 °C		
	Drug Content (mg/g of formulation)	Globule Size (nm)	f_2 value (%)	Drug Content (mg/g of formulation)	Globule Size (nm)	f_2 value (%)	Drug Content (mg/g of formulation)	Globule Size (nm)	f_2 value (%)
0	5.08±0.12	55.2±3.3	95.6	5.08±0.12	55.2±3.3	97.4	5.08±0.12	55.2±2.4	95.1
1	5.11±0.18	51.9±3.6	94.1	5.01±0.09	57.2±2.5	95.2	4.97±0.19	58.1±2.1	96.8
3	4.98±0.14	54.1±2.8	95.6	4.89±0.21	52.2±3.4	96.6	4.98±0.13	55.1±3.2	95.2
6	5.06±0.09	56.7±2.7	95.6	4.96±0.11	56.9±2.4	97.2	5.02±0.12	54.8±2.9	95.9

4.5. *In vitro* studies

4.5.1. Cell Cytotoxicity study (MTT assay)

The percent cell viability against the drug treatment for different formulation viz., Dox solution (control), Dox-NE, f-Dox-NE and ALA-NE are presented in **Fig. 11**. IC50 values of the Dox-NE, f-Dox-NE against MCF-7 cell line were calculated and recorded as 2.11 ± 0.21 $\mu g.mL^{-1}$ and 1.49 ± 0.16 $\mu g.mL^{-1}$, respectively. As a control, the IC50 value of Dox was 3.31±0.20 $\mu g.mL^{-1}$. For the placebo optimized nanoemulsion that contains ALA nanoemulsion without Dox (ALA-NE), the IC_{50} value observed was 4865±448 $\mu g.mL^{-1}$ (data not shown).

4.5.2. Cell Cycle Analysis through FACS Analysis

The distribution of MCF-7 cells when treated with varios formulation and drug were evaluated through fluorescence activated cell sorting (FACS) analysis and the percentage in various stages of the cell cycle are presented in **Fig. 12**. The cellular distribution in different phases of cell cycle for the control cells (no treatment) was 67.52% in S phase, 7.70% in G1 phase and 24.78% in G2/M phase **(Fig. 12A)**. However, in f-Dox-NE treated cells the cell distribution was 38.29% in G1 phase, 19.82% in S phase and 41.90% in G2/M phase. Upon incubation with standard drug (**Fig. 12B)** highest percentage of

cells were observed in the G1 phase (53.34%) followed by S phase (27.24%) and G2/M phase (25.00%), while the ALA-NE incubated group showed highest percentage of cells in G2/M phase (88.38%) of the cell cycle (**Fig. 12C)**. Apoptotic cell population as visualized in ALA-NE and f-Dox-NE treated cell groups suggested that these formulations forced the cells to enter in the process of programmed cell death **(Fig. 12 C&D)** (Musa et al. 2015).

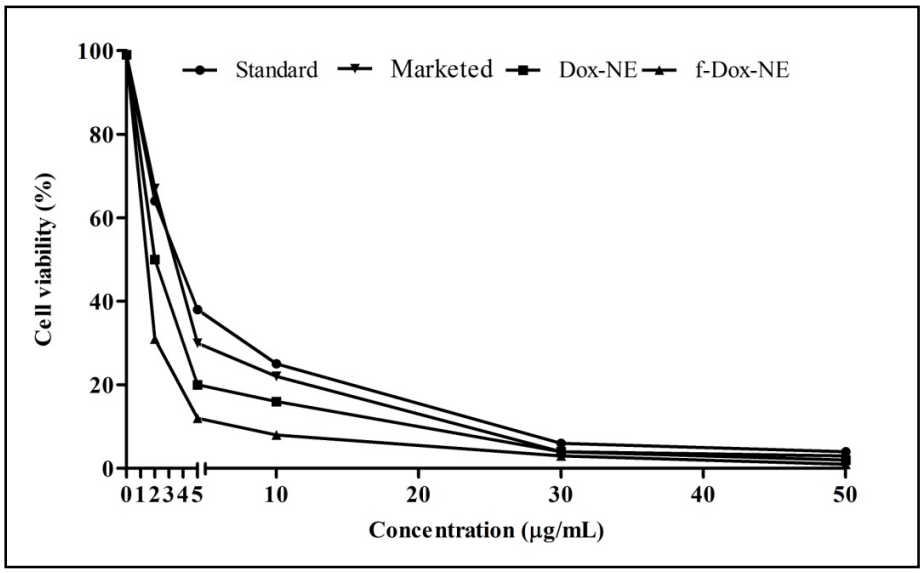

Fig. 11. Cell viability through MTT assay of the differently treated cells groups, Standard, marketed formulation, Dox-NE and f-Dox-NE (n=3).

4.5.3. Cell proliferation studies

The percent inhibition in the cell proliferation data revealed highest percent inhibition of the cellular proliferation for the f-Dox-NE (89.12±2.55%) and Dox-NE (71.40±2.43%) of the MCF-7 cells compared to the control cells ($p<0.001$) measured by the change in fluorescence intensity of reduced form of the Alamar Blue® **(Fig 13A)**. The Dox-NE and f-Dox-NE showed significant cellular proliferation inhibition as compared to the standard drug (48.98±3.77%) and the marketed (53.34±4.02%) formulations ($p<0.05$) as well. The placebo formulation having ALA only (ALA-NE) showed 21.89±4.56% of the cell growth inhibition in comparison to the control treated group. The data of ALA-NE suggested that ALA has substantial anticancer and antiproliferative potential which is in corroboration with previously publish reports (Iyengar et al. 2013, Roy et al. 2017). Similar results could be inferred from the data of Alamar Blue® reduction **(Fig. 13B).** The

f-Dox-NE group showed least dye reduction indicating least cell viability and therefore caused the highest cellular mortality of the MCF-7 cell lines (O'Brien et al. 2000, Wang et al. 2018). The Alamar Blue® reduction data suggested that order of cellular mortality in the different groups was ALA-NE > Standard > marketed > Dox-NE > f-Dox-NE.

4.5.4. Evaluation of reactive oxygen species (ROS)

To investigate the cytotoxic effects of the ALA-NE, standard, marketed formulation, Dox-NE, f-Dox-NE, intracellular production of the ROS, was evaluated through measurement of DCFDA fluorescence. DCFDA, a fluorogenic dye is one of the most widely used techniques for directly measuring the oxidation-reduction state of the cell (Figueroa et al. 2018, Ottonello et al. 2001). After diffusion into the cell, the DCFDA is deacetylated by cellular esterases into a non-fluorescence form DCF. This form is again oxidized by ROS to fluorogenic DCF form which can be measured fluorometrically.

The results of DCFDA fluorescence showed that the f-Dox-NE and Dox-NE caused significant ($p<0.01$) cellular mortality and hence lower fluorescence in comparison with standard and the marketed formulation was observed (**Fig. 13C)**. Owing to the lower cell death and increased cellular proliferation in case standard and marketed formulation treated groups more dye is reduced as evidenced by higher fluorescence intensity.

4.5.5. Mitochondrial membrane potential (MMP)

Rhodamine-123 (Rh-123) dye displayed MMP-dependent uptake and selective accumulation into the mitochondria of the living cells accompanied by the red spectral shifts followed by the quenching of fluorescence, which makes it a suitable agent to monitor the mitochondrial membrane potential of the cells undergoing apoptosis. The effect of the formulations on the MMP change was elucidated using Rh-123 efflux, because apoptosis in the cells triggers a collapse of the MMP. This results in the lower uptake and retention of the Rh-123 in the mitochondria. The data of the MMP studies revealed that treatment with the various formulations, the f-Dox-NE and Dox-NE induced significant decrease of the MMP compared to the standard and the marketed formulation. The MMP data indicated that significant ($p<0.01$) mitochondrial dysfunction in the MCF-7 cell lines was induced by the f-Dox-NE and Dox-NE **(Fig. 13D)** (Al-Qubaisi et al. 2013, Musa et al. 2015).

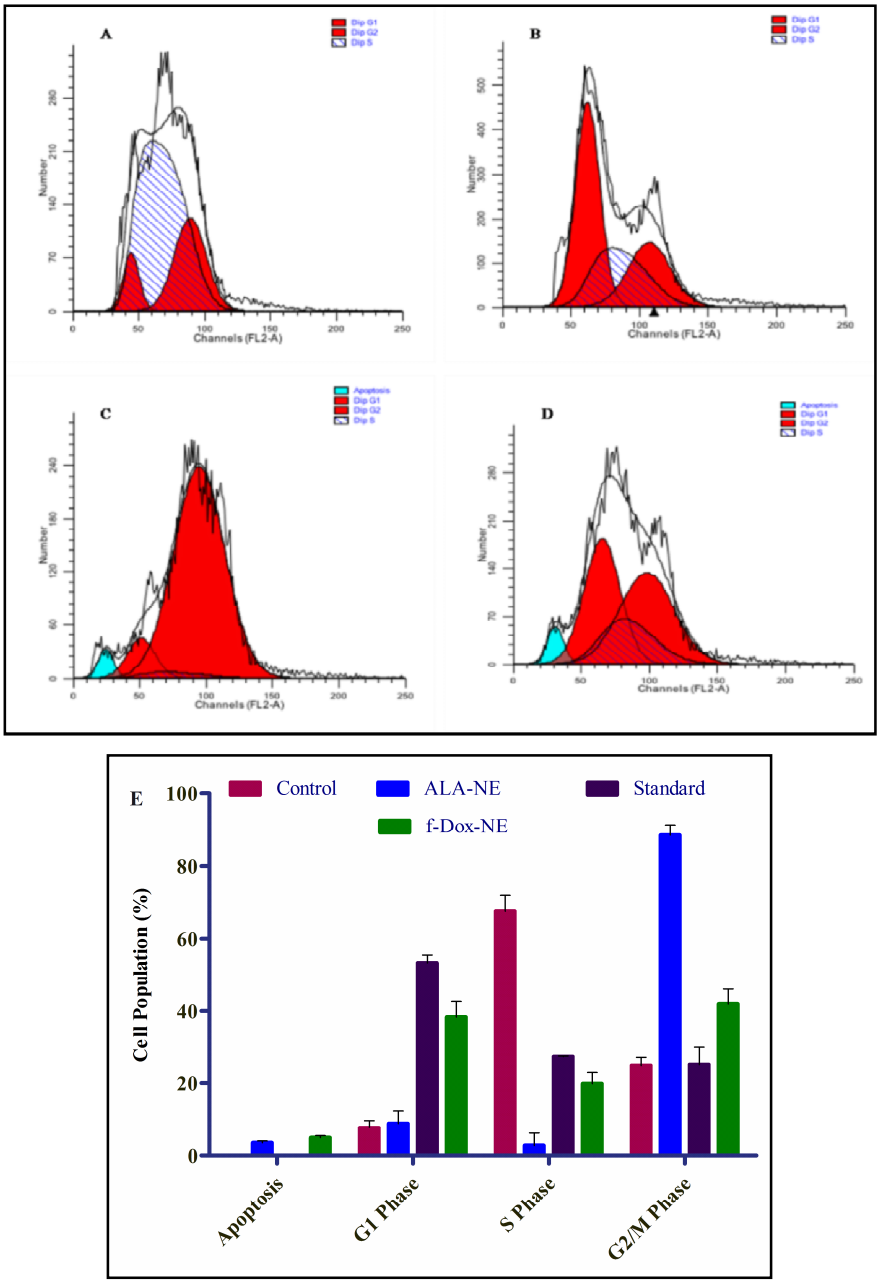

Fig. 12. FACS analysis of the cell cycle phase distribution for the differently treated cells; (A) Control (no treatment), (B) Standard (Pure Dox), (C) ALA-NE (blank NE formulation with ALA) (D) f-Dox-NE; (E) Graph depicting the comparative account of the cells present in the different phases for treatment groups (A-D).

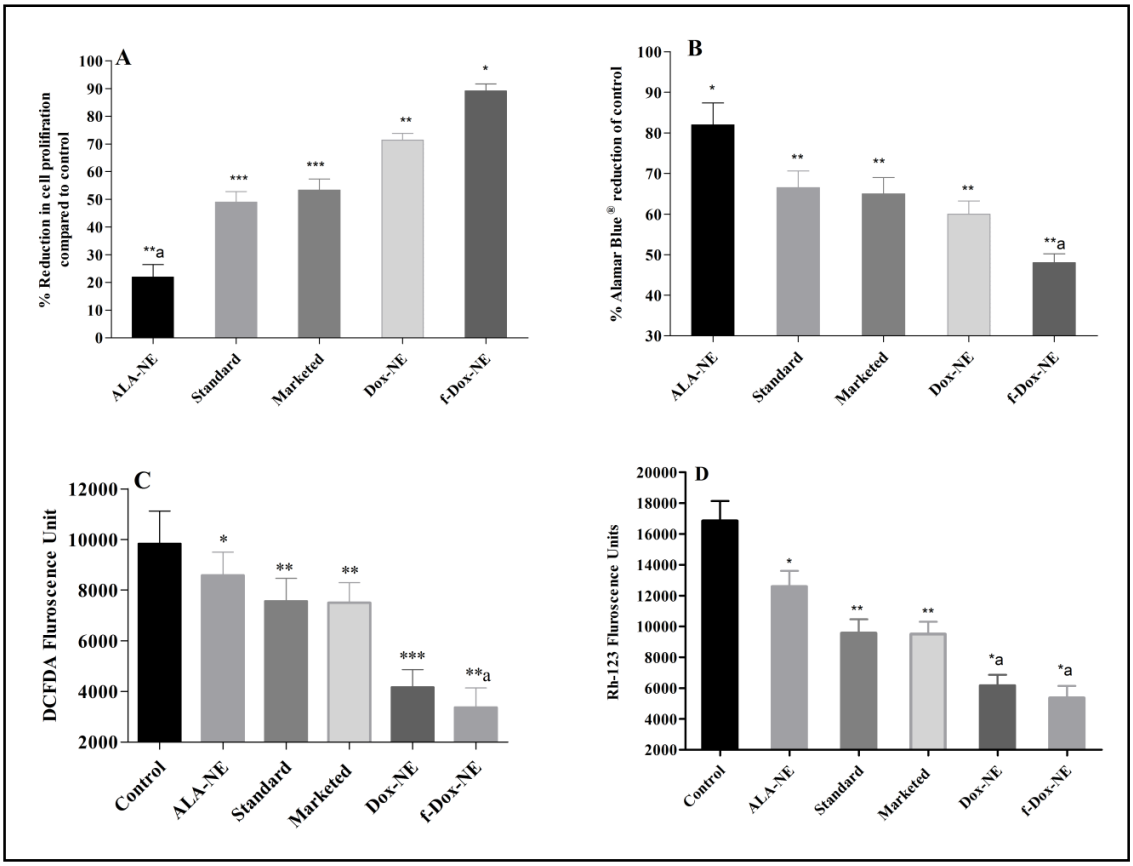

Fig. 13. *In vitro* studies on MCF-7 cell line of differently treated cells groups, *i.e.*, control (no treatment), ALA-NE (blank NE with ALA only), Standard (Dox solution), f-Dox-NE (folate decorated Dox loaded NE). (A) % reduction in cell proliferation, (B) %Alamar Blue® reduction as compared to the control (no treatment), (C) DCFDA fluorescence units presenting the ROS levels, and (D) Rh-123 fluorescence unit depicting variation in the MMP. [Data presented as the Mean±SD, n=3. *** $p<0.001$, ** $p<0.01$, * $p<0.05$ with respect to control, **a $p<0.01$ with respect to the marketed and the standard groups]

4.6. *In vivo* studies

The results of the *in vitro* cell lines studies encouraged the authors to further validate the efficacy of the folate decorated nanoemulsion through the *in vivo* experiments. This was performed through DMBA induced mammary gland carcinoma in female wistar rats. The DMBA induced mammary gland carcinoma model was already established in our laboratory and also reported in several pieces of literatures (Alessandra-Perini et al. 2018, Haque and Pattanayak 2018, Kwon et al. 2018, Roy et al. 2017). DMBA i.e., 7,12-

Dimethylbenz[a]anthracene is a highly lipophilic molecule. It requires metabolic activation before it can act as a carcinogen. It is activated in several tissues including mammary glands. In the mammary gland tissues, DMBA is converted to its epoxide form which is an active metabolite of DMBA. It has a capacity to damage the DNA molecule. This is the main event that induces carcinogenesis in mammary gland tissue. Due to the higher cellular proliferation index in types 1 and 2 lobules, higher metabolic activity is present in these lobules and therefore more epoxides are formed.

4.6.1. Tumor Incidence and tumor burden

Tumor incidence and total tumor burden are well-established methods to monitor the tumor progression in cancer-induced animal models. The tumor incidence observations revealed that 8 animals out of 10 developed cancer in the toxic group, while two animals died before the development of any physical signs of cancer. In case of ALA-NE treated group 7 animals displayed tumor after 12 weeks of study, while in standard and marketed treated groups 5 animals displayed cancer development. However, in case of Dox-NE and f-Dox-NE treated groups, the tumor incidence was markedly lower with 4 and 3 animals, respectively.

Similarly, total tumor burden data depicted that toxic control group showed highest tumor volume followed by ALA-NE, standard, marketed and Dox-NE, while f-Dox-NE showed the least progression in tumor indicating highest efficacy against tumors **(Table 9)**.

Table 9. Tumor incidence and tumor burden of mammary gland carcinoma in DMBA induced female albino wistar rats

Treatment Groups	No. of rats with tumors/total rats	Total tumor burden (cm^3)
Control	0/10	-
Toxic	8/10	412.67±43.22
ALA-NE	7/10	250.39±20.72
Standard Drug	5/10	185.48±21.31
Marketed Formulation	5/10	180.89±18.15
Dox-NE	4/10	127.81±12.44
f-Dox-NE	3/10	95.61±11.23

4.6.2. Weight variation

Changes in weight of individual groups during course of study are recorded in **Fig. 14**. The plots for the test groups (group IV-VII) during study period showed significantly less

weight reduction from initial mean weight in animals as compared to the DMBA only administered group (Group II, toxic control) ($p<0.05$) Dox-NE and f-Dox-NE showed least weight reduction as compared to other groups.

4.6.3. Animal survival studies

The survival plot illustrated lowest animal deaths and highest percent animal survival for f-Dox-NE among treated groups at the end of the study with 80% animal survival after DMBA administration **(Fig. 15)**. The f-Dox-NE revealed a marked reduction in animal mortality when compared with standard and marketed ($p<0.01$) formulation. When the effects of ALA-NE **(Fig. 15)** were compared to the toxic group a correlation of the anticancer potential of ALA was observed which is corroborated by the results of previous study [10]. The marginal advantage for the folate anchored NLCs (f-Dox-NE) over unmodified NLCs (Dox-NE) is clearly evident from the data which suggests targeted delivery of folate guided f-Dox-NE to the FR overexpressed in tumor cells.

4.6.4. Biochemical estimation of antioxidant marker

As illustrated in **Tables 10**, the mean levels for TBARs, protein carbonyl, glutathione GSH, SOD, and catalase were significantly disturbed in the DMBA treated groups as compared to the control group. A pronounced increase in the values of TBARs and protein carbonyl in the toxic control group as compared to the control group postulates the significant protein and lipid peroxidation after the DMBA treatment **(Table 10)**. The f-Dox-NE and standard drug treatment successfully decreased the level of protein carbonyl (32.95±0.9 nmol/mL unit) and TBARs levels as compared to the toxic control.

The level of GSH, SOD and catalase in the DMBA treated group (0.99±0.09 mg%, 0.043±0.005 units of SOD/mg of protein and 12.78±0.31 nm of H_2O_2/min/mg of protein, respectively) were significantly ($p<0.05$) restored after treatment with the standard drug, marketed formulation and f-Dox-NE. Corresponding to the levels of GSH, SOD and catalase in the standard drug and the marketed formulation treated group; the f-Dox-NE treated group significantly restored the same (i.e., 1.22±0.05 mg %, 0.031±0.005 units of SOD/mg of protein, and 21.66±0.32 nm of H_2O_2/ min/mg of protein, respectively) which was comparable to the normal control. A notable restoration of the antioxidant defense system was observed in the ALA-NE treated group.

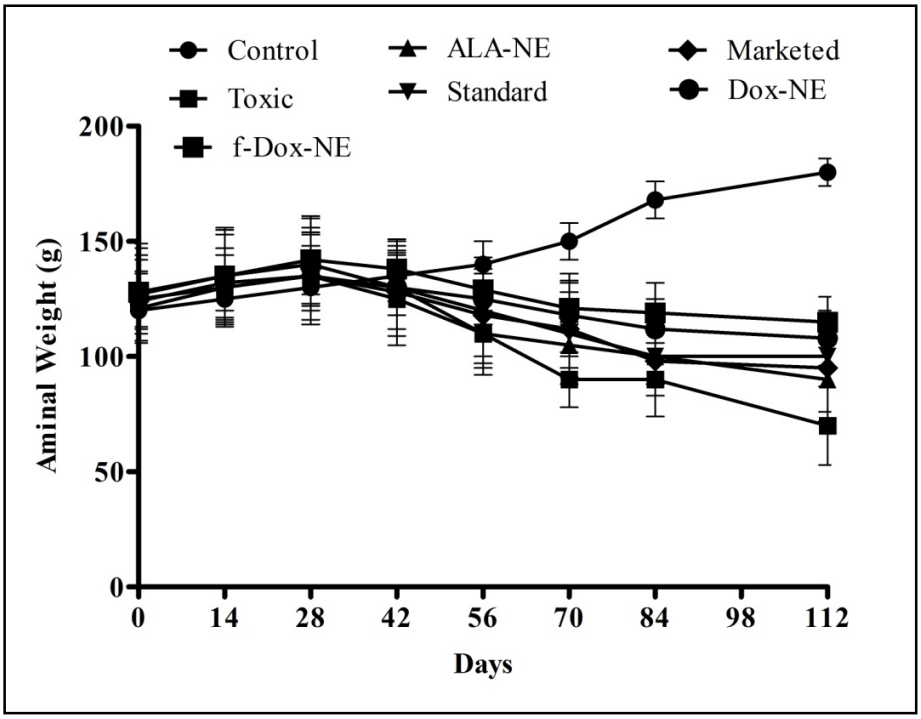

Fig. 14. Weight variation in animals treated with Control (normal saline), toxic control, ALA-NE, standard drug solution, Marketed formulation, Dox-NE, f-Dox-NE. [Data is presented as mean of group, n=10]

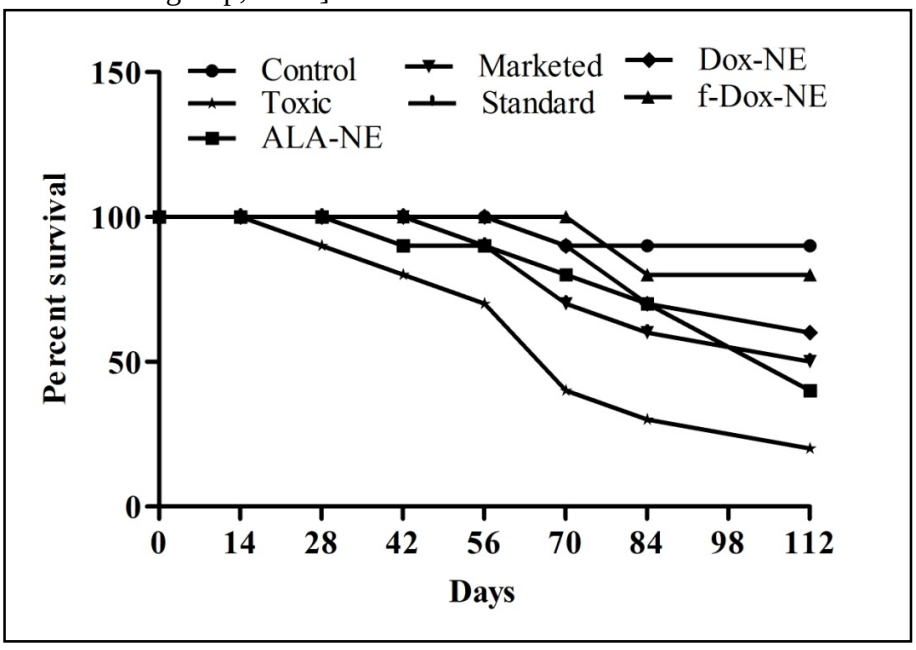

Fig. 15. Survival graph with percent animal survived treated with Control (normal saline), toxic control, ALA-NE, standard drug solution, Marketed formulation, Dox-NE, f-Dox-NE. [Data is presented as mean of group, n=10]

Table 10. Effect of treatment groups on oxidative stress markers in DMBA induced rat mammary gland carcinoma

Groups	TBARs (nm of MDA/µg of protein	Protein carbonyl nmol/mg of protein	GSH (Mg %)	SOD (units of SOD/mg of protein)	Catalase (nmol of H_2O_2/ min/mg of protein)
Control	0.20±0.02	40.35±1.08	1.20±0.08	0.034±0.003	22.03±0.81
Toxic	0.49±0.14	55.56±6.75	0.99±0.09	0.043±0.005	12.78±0.31
ALA-NE	0.39±0.12	49.04±3.80	1.10±0.08	0.035±0.002	16.52±0.22
Standard Drug	0.30±0.13	41.51±2.33	1.15±0.10	0.030±0.002	18.55±0.33
Marketed Formulation	0.31±0.15	40.51±2.85	1.15±0.12	0.028±0.004	17.67±0.45
Dox-NE	0.25±0.06	44.64±1.37	1.18±0.07	0.025±0.003	20.44±0.57
f-Dox-NE	0.22±0.06	42.05±1.80	1.22±0.05	0.031±0.005	21.66±0.32

4.6.5. Western blotting

To quantify the changes in the protein expression, the mammary gland samples of different groups were investigated by western blot analysis. The expression of anti-apoptotic proteins (bcl2, MMP-9) was increased after the DMBA administration to rats. The opposite effect, *i.e*., downregulation of pro-apoptotic markers like bax and caspase-9 was observed on the DMBA treated animals. The treatment of DMBA induced mice with different formulations i.e., Dox and f-Dox-NE offered the reinstatement of the anti-apoptotic and pro-apoptotic markers **(Fig. 16a)**. The densitometric data suggested that the treated groups restored the markers as compared to the toxic group favorably signifying apoptosis **(Fig. 16b)**. Among the different treatment group, the f-Dox-NE showed the highest restoration of anti-apoptotic and pro-apoptotic markers in comparison to the standard drug group ($p<0.05$). Further, it has been reported earlier that the MMP-9 and members of the bcl-2 family protein, including bcl-2, bax, bad, bcl-X_L *etc*. are critical for breast cancer cell migration, invasion, and cancer metastasis (Karroum et al. 2012, Ogretmen and Safa 1996, Vimala et al. 2014). The results obtained through western

blotting confirmed that the folate-decorated NE efficiently regulated breast cancer cell migration and invasion in cancer induced mice.

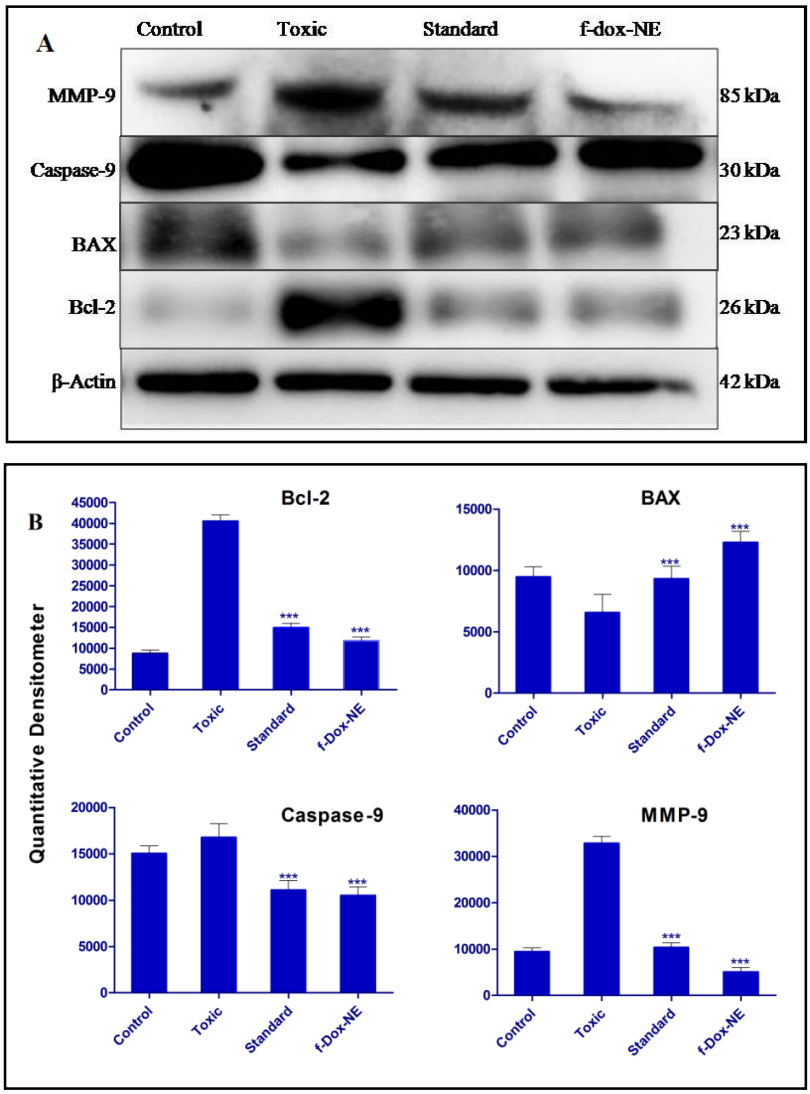

Fig. 16. Regulation of mitochondrial associated protein signaling in mammary gland cells. (A) Protein extracted from individual groups [control, DMBA administered toxic, Standard and f-Dox-NE]. (B) Desitometric data for expression of individual protein in different groups. [Values are presented as Mean ± SD (n=3). The test groups were compared to the DMBA treated (Toxic) group (*p<0.05, **p<0.01, ***p<0.001)]

4.6.6. Microscopy of whole mounts of mammary glands through carmine staining

Angiogenesis and cellular proliferation are distinctive characteristics for the cancer growth and progression. The carmine staining represented that in the DMBA treated

group, there was marked increase in number of AB/TEB, demonstrating cellular proliferation in mammary gland. The AB/TEBs represents the largest bulbous structures present at the terminal ends of the mammalian epithelial tree. The analogous structures in case of human breast are the terminal ductal lobular units. The treated groups afforded a significant defense against cellular proliferation. As evident in the histogram, the effect of Dox-NE and f-Dox-NE was more efficient in diminishing the count of AB/TEBs as compared to the toxic ($p<0.001$), the standard and the marketed groups ($p<0.05$), respectively **(Fig. 17)** (Moraes et al. 2009, Moraes et al. 2007, Roy et al. 2017).

4.6.7. Cardiotoxicity studies

Cardiotoxic effect of Dox was evident with the profound elevation of MDA levels and the lowering of GSH levels in heart tissue as compared to the control. However, significant favorable improvement in the MDA and GSH levels were evident with the ALA-NE, f-Dox-NE treatment in respective groups **(Fig. 18 A&B)**.

4.6.8. Biodistribution of Doxorubicin

Higher targeting efficiency of the delivery system is often anticipated for the successful outcome of anticancer therapy. A comparative account of the Dox concentration in the different organs is presented in **Fig. 19**. The Dox levels attained in the mammary carcinoma was highest in the case of the f-Dox-NE (45.23±2.51 µg/g organ in 4 h) followed by the Dox-NE (35.43±2.91 µg/g organ in 4 h) indicating the specific accumulation of the folate decorated NE in FR over-expressed mammary tumor cells **(Fig. 19 C&D)**. The Dox levels in case of pure Dox and the marketed formulation were nearly similar **(Fig. 19 A&B)** and were significantly lower in comparison to f-Dox-NE ($p<0.001$) treated group. The Dox level was significantly higher at 4 h post injection and was barely detectable after 48 h (except for f-Dox-NE group), owing to the short half-life of the drug in the blood. Further, significant higher Dox levels were maintained in the mammary cancer cells for a period of upto 48 h (25.78±1.42 µg/g organ) in the f-Dox-NE ($p<0.001$); upto 12 h (25.55±2.22 µg/g organ) in the Dox-NE ($p<0.001$) treated groups *vis-à-vis* the pure Dox (15.55±2.25 µg/g in 12 h, 1.78±0.42 µg/g in 48 h) and the marketed formulation (14.54±2.21 µg/g in 12 h, 1.79±0.38 µg/g in 48 h) treated groups.

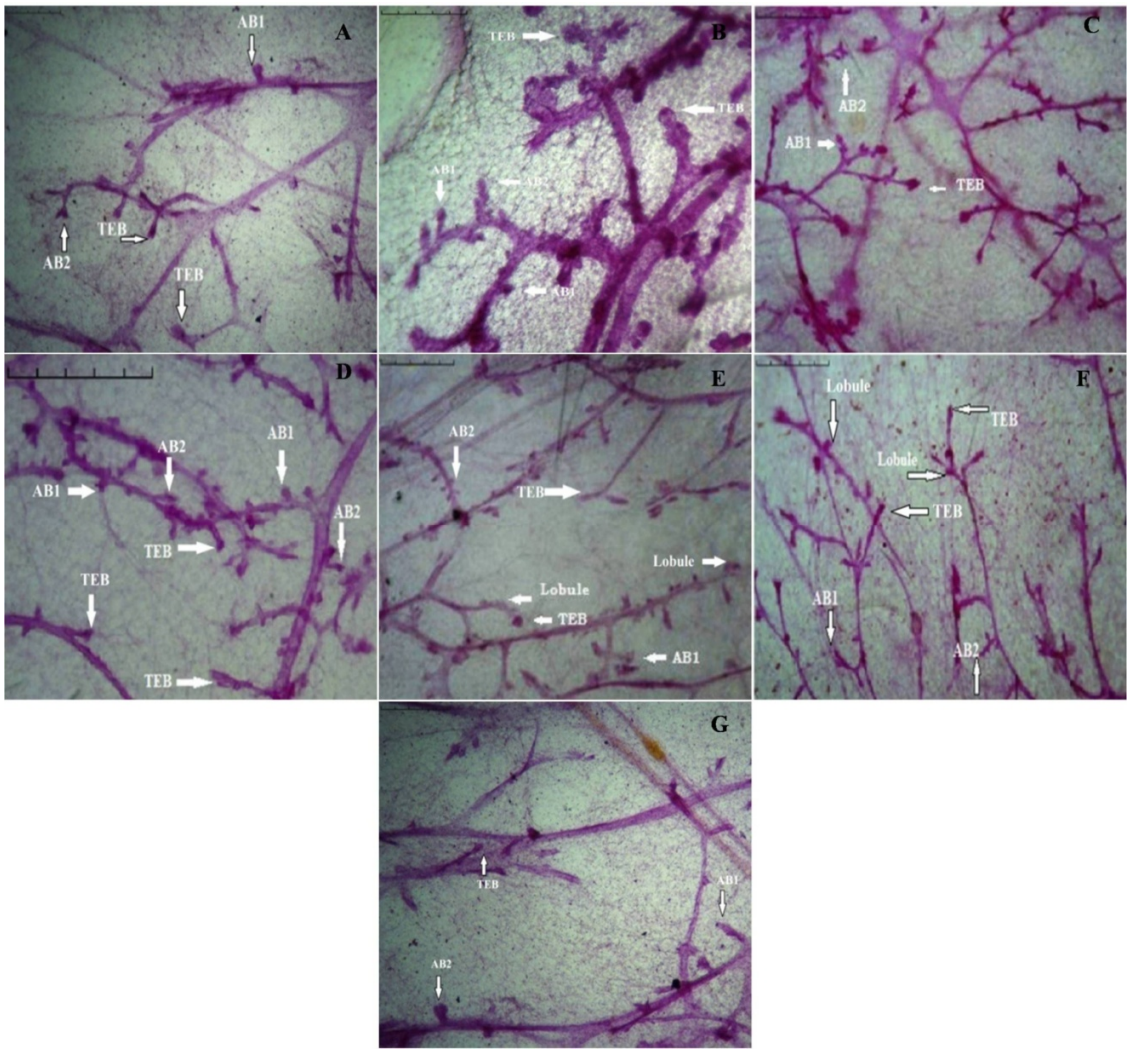

Fig. 17. Whole mount of the mammary gland tissue of the animal groups (A) control (normal saline), (B) toxic control, (C) ALA-NE, (D) standard drug solution, (E) marketed formulation , (F) Dox-NE, (G) f-Dox-NE. [TEB: Terminal end bud; AB: Alveolar bud]

Similar inference can be drawn for other time points as well. Among different organs, highest Dox concentration was observed in the liver followed by the spleen, the heart and the kidneys **(Fig. 19 A-D)**. The Dox level in the heart tissue in f-Dox-NE treated group was lesser when compared to the other groups ($p<0.05$) **(Fig. 19 A-D)**. The results are in corroboration with the cardiotoxicity results as described earlier. Overall, the Dox levels in different organs of the f–Dox-NE treated group were relatively lower than that of other animal groups, which was in accordance with the earlier published literature (Bae et al. 2013, Liu et al. 2011).

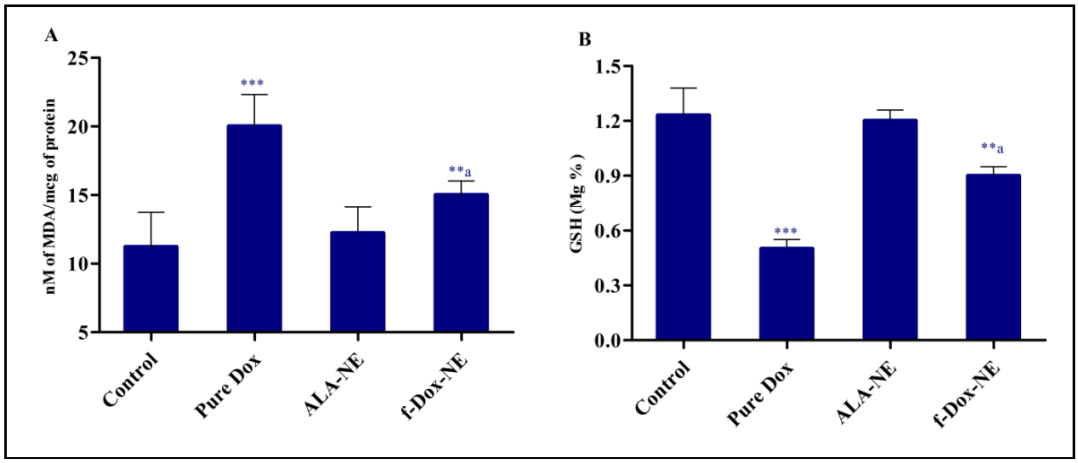

Fig. 18. Effect of Dox treatment on (A) MDA levels and (B) GSH levels in rat heart tissue. Control, pure Dox, ALA-NE and f-Dox-NE. [Values are Mean ± SD, (n = 6); *** P<0.001 versus control and **a p<0.01 versus Dox treatment.]

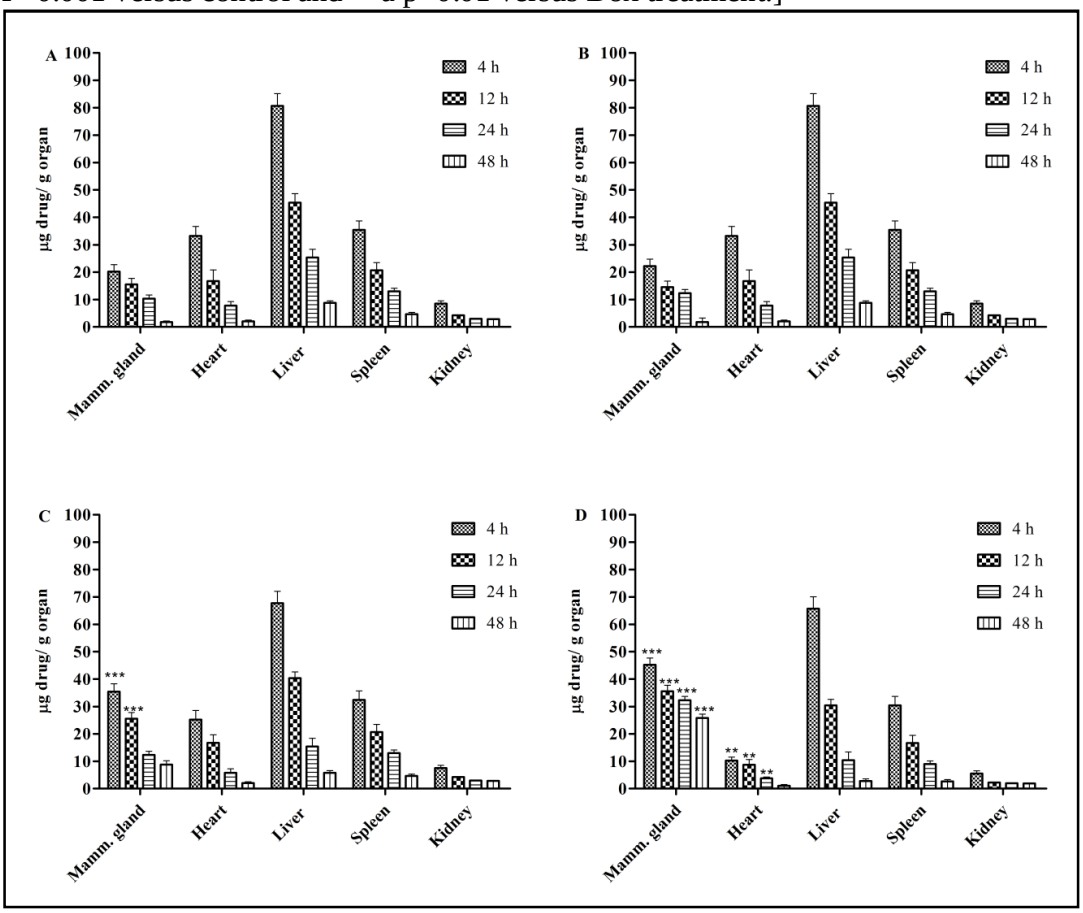

Fig. 19. Amount of Dox in different organs after i.v. administration through tail vein (10 mg/kg Dox equivalent dose) of (A) Standard (B) Marketed formulation (C) Dox-NE (D) f-Dox-NE. [Values are presented as Mean ± SD (n=6); *** p<0.001 as compared to standard and marketed; ** p<0.05 as compared to other groups]

5. Discussion

In the era of nanomedicine therapies, advancement in the targeted therapies, antibody therapies, small molecules drug conjugates *etc.* have attracted much interest of the formulation scientist. Targeted nanomedicine can also be best designated as a 'molecularly designed' delivery system capable of carrying multiple drugs, identifying a particular site of action through through relevant receptors overexpressed on the target cell and specifically accumulating at the site (Jiang et al. 2013, Kandadi et al. 2012, Kouchakzadeh et al. 2017, Lammers et al. 2008, Liu et al. 2011, Mizushima 1996). Here, the aim was to develop a folate decorated ALA based nanoemulsion of doxorubicin for therapy of mammary gland carcinoma.

For an ideal delivery system, the drug should remain in a solubilized form in the system during the course of storage as well as in the systemic circulation after administration into the human body. Lower drug solubility may lead to the supersaturation resulting in precipitation of the drug (Tripathi et al. 2016). Ternary phase diagram facilitated the finding of the compositions of the lipid and the emulgents leading to the formation of the nanoemulsion. The systematic and scientific tools like QbD and DoE are often invaluable in the development and optimization of the drug delivery system. Box-Behnken design served the objective of the optimization of delivery system and selection of the best possible composition scientifically as well as economically (Singh et al. 2011, Tripathi et al. 2016). Considering the delivery system, route of administration, safety, nature of excipients, solubility of the drug and TPD, ALA (as lipid phase), lecithin and Tween 80 in equal weight ratio (as emulgent), cholesterol (as co-emulgent) were selected as CMAs (critical material attributes) for the nanoemulsion system. Quadratic mathematical model best explained the influence of the CMAs on the CQAs, *i.e.*, globule size, entrapment efficiency, drug loading and drug release. The selected CMAs significantly influenced the performance of the final product. Cholesterol, selected as co-emulgent, has been shown to improve stability of the lipid nanocarriers and to control the drug release from the delivery system (Liu et al. 2017). The cholesterol and lecithin are nontoxic, biocompatible and natural components which can safely be used in the systemic delivery system. Non-ionic emulgents like Tween 80 are considered safer than their ionic counterparts and are frequently accepted for systemic administration (Singh et al. 2017a,

Singh et al. 2017b). The globule size of a nanoemulsion is a vital factor for the *in vitro* and *in vivo* performance because it modulates the rate and extent of the drug release, the solubility of the drug into the system and passage of oil globules through the biological membranes and blood capillaries. The TEM and globule size analysis results illustrated the successful formation of the nanoemulsion. The drug release studies depicted that the standard drug and the marketed formulation possess an immediate type of drug release profiles. In contrast, the Dox-NE and f-Dox-NE showed sustained release behavior owing to the slower diffusion of the drug from the lipidic environment thereby providing a therapeutic concentration for a longer time period, *i.e.,* upto 48-72 h (Choudhury et al. 2014, Singh et al. 2017a, Singh et al. 2017b). The developed nanoemulsions were thermodynamically stable and robust to the dilutions. During the formulation of NE, both ALA as well as ALA-PEG-NH_2 were taken in 20:1 w/w ratio. Since ALA-PEG-NH_2 accounts for only 0.95% w/w of the formulation and ALA accounts for 30.50% w/w, its inherent qualities would nonetheless be displayed. ALA-PEG-NH_2 would naturally align itself on the surface because of its hydrophilic linker (PEG) on which ligand (folate) would attach, while unmodified ALA being hydrophobic in nature, would naturally position itself within the core of oil droplets. The folate targeting ligand decoration was successfully performed and conjugation was affirmed by FTIR, ^{1}H-NMR spectrum and folate content assay which was in corroboration with previous studies (Bae et al. 2013, Liu et al. 2011, Liu et al. 2017, Stella et al. 2000). Upon systemic administration, the physical stability of the nanoemulsion is susceptible to globule aggregation and physical disruption, leading to rapid clearance, abrupt drug release and dose dumping from the formulation. Whereas, a stable delivery system leads to longer systemic circulation and residence time, thereby increasing the possibility of higher tumor accumulation through enhanced permeability and retention (EPR) effect (Ganta et al. 2016, Kanoujia et al. 2016, Singh et al. 2017a).

In vitro studies like the cell cytotoxicity studies revealed 54.98% increment in the cell mortality after the DOX was encapsulated into the nanoemulsion as observed by the IC50 values. Compared with the DOX and dox-NE, the f-dox-NE treatment exhibited significantly higher cellular mortality in the MCF-7 cells, *i.e.,* 29.38% and 54.98% ($p<0.01$), which was probably related to folate mediated cellular interaction with the lipid cell membrane leading to the higher internalization of the drug delivery system into the

MCF-7 cells**.** The cell cycle analysis revealed marked cellular arrest of the MCF-7 cell lines in the G1 and G2/M phase in the f-Dox-NE treated cells while Dox only arrested most of the cells in the G1 phase. The incorporation of ALA and Dox in nanoemulsion system shifted the cellular population from G1 phase and increased the cell population in the G2 and S phase. This can be explained by the fact that ALA is known to arrest the cells, particularly in the G2/M phase. The combined effect of the DOX and ALA treatment was much stronger on cell cycle phase arrest than that of either the DOX or ALA. The cell proliferation study established that the folate decorated nanoemulsion permeated to a larger extent in the MCF-7 cells due to the overexpressed folate receptors. Further, better integration of the lipid-based carrier to the cellular membrane of the MCF-7 cell lines were demonstrated by the higher cancer cell growth inhibition or cancer cell mortality (Huan et al. 2009, Weitman et al. 1992). The above statement was further supported by the lowest reduction of Alamar Blue® dye by f-dox-NE treated MCF-7 cells. Further, different formulation treated group caused the higher cellular growth inhibition and cancer cell apoptosis in comparison to control cell population. Increased production and accumulation of reactive oxygen system in the MCF-7 cells resulted in damage of different cellular components like proteins, phospholipids, DNA *etc.* This damage to cellular components caused an increase in mitochondrial membrane permeability which ultimately leads the cancer cells to programmed cell death. It has been established that loss of MMP is often results into the initiation of the intrinsic apoptotic pathways in the mitochondria. The agents demonstrating anticancer activity are known to depolarize the mitochondrial potential in the cultured MCF-7 cell line (Al-Qubaisi et al. 2013, Roy et al. 2017)s. These finding suggest the role of the mitochondria in apoptosis of the cancer cells. Recently, it has been demonstrated in that ALA posses strong anticancer potential that promotes the mitochondrial apoptosis in the DMBA induced mammary gland carcinoma (Roy et al. 2017).

In vivo evaluation of the anticancer efficacy of the optimized nanoemulsion system was performed in mammary gland tumor induced in rats using DMBA as a cancer-inducing agent. The rat model was established and validated in our laboratory earlier (Roy et al. 2017). The animal weight changes, animal survival and total tumor volume indicated mammary gland tumor induction and progression in DMBA administered animals. The reactive oxygen species are constantly generated during metabolic activity in aerobic

cells and are counterbalanced by antioxidant enzymatic bio-machineries. However, under stress conditions as in tumor, the ROS countering effects of these enzymatic bio-machineries are suppressed. Marked damage to the cellular proteins and lipids was observed in DMBA administered animals when monitored for TBARS and protein carbonyl which are a peroxidative marker of the lipid and protein peroxidation marker, respectively. Similarly, increased ROS generation also compromised the antioxidant bio-machineries of SOD, GSH and catalase as these work in coordination to neutralize the oxidative species through series of peroxidation, dismutation and oxidation reactions (Al-Qubaisi et al. 2013, Roy et al. 2017).

Several anti-apoptotic and pro-apoptotic protein expressions have been shown to be modulated in breast cancer. Among different proteins overexpressed, expression of Bcl-2 and MMP-9 as anti-apoptotic proteins, and Caspase-9 and BAX as pro-apoptotic proteins were monitored in the present study. Also, Bcl-2 and MMP-9 are established as pro-migratory proteins and are shown to be overexpressed in the mammary gland carcinoma which in turn promotes the cancer cell proliferation and metastasis (Ogretmen and Safa 1996, Vimala et al. 2014). The results of western blotting assay indicated that Bcl-2 and MMP-9 are over-expressed in DMBA administered groups which were successfully restored by f-Dox-NE treatment which indicates the higher anticancer potential of the modified nanoemulsion. The MMP-9 regulates PKC and ERK1/2 signaling pathways (Karroum et al. 2012) and the Bcl-2 family proteins act through COX-Va, myosin Va and Twist1 (Ogretmen and Safa 1996, Um 2016, Vimala et al. 2014). The roles of these proteins are critical for the regulation of mammary cancer cell migration, invasion, and cancer metastasis (Karroum et al. 2012, Ogretmen and Safa 1996, Vimala et al. 2014).

For examination of cellular proliferation and angiogenesis, the whole mount preparation was performed and cellular proliferation and angiogenesis was presented through an increase in the AB/TEBs and lobules count. The undifferentiated structures and higher AB/TEBs counts are considered as the point of the angiogenesis and malignant transformations. The treatment with the f-Dox-NE resulted in shrinking of the AB/TEB count to sizable amount indicating a positive modulatory effect on carcinoma and malignant transformation achieved by the targeted delivery of Dox and the ameliorative and cancer inhibitory potential of the ALA against cellular proliferation.

Doxorubicin is considered to be among first-line therapy drugs for benign as well as metastatic breast carcinoma. However, in recent decade the use of Dox is declining due to development of cardiotoxicity and drug resistance. It has been found that cardiotoxicity related to doxorubicin originates from the lipid and protein peroxidation in cardiac tissue (Trivedi et al. 2011). The f-Dox-NE treated group showed no significant alteration of markers of cardiotoxicity supporting the cardioprotective potential of ALA for cardiac cells and the targeted delivery reducing the inappropriate disposition of doxorubicin. There have been several reports regarding the involvement of numerous complex mechanisms that exert beneficial effects of ALA in cardiovascular diseases. These mechanisms involved anti-inflammation, regulation of cardiac ion channels, modulatation of membrane micro-domains and cell signaling pathways, reduction of triglyceride synthesis, and anti-thrombotic and anti-arrhythmic effects. ALA inhibits nuclear factor-κ B activity, downregulate sterol regulatory element binding protein-1c gene expression involve in inflammation and fatty acid synthesis (Adkins and Kelley 2010, Maehre et al. 2015). The biodistribution studies further affirmed the cardiotoxicity data by indicating selective accumulation of the folate decorated nanoemulsion owing to folate receptor over-expression in mammary gland carcinoma. However, a significant fraction of the Dox in case of Dox-NE and f-Dox-NE was found to be selectively accumulated in the liver and spleen, indicating the involvement of mononuclear phagocytic system. However, the folate decoration showed no significant change in concentration of doxorubicin in the liver which may be explained by a higher uptake of the folate anchored nanoemulsion by the liver cells as it is a major storage organ of folate (Hu et al. 2014, Shinoda et al. 1998).

As discussed above, folate-mediated doxorubicin delivery was found to be safe and effective in controlling the cellular proliferation, invasion and metastasis in case of mammary gland carcinoma. The relative selectivity of folate anchored nanoemulsions for mammary cancer might be explained on the basis of high folate requirement for rapid cellular proliferation which happens in most of the cancerous cells. Therefore, folate receptors are highly upregulated in several cancers like lung, mammary gland, colon, kidney and brain. But obvious, the folate has high affinity (Kd~10-10M) for folate receptors. These receptors facilitated the selected binding and endocytosis of the delivery systems into the tumor cells. Attachment of folate to longer PEG chain (MW 3.4 kDa)

resulted in effective folate receptor-mediated association and internalization of folate decorated nanoemulsion in cancerous cells. Further, the superiority of f-Dox-NE and Dox-NE is better explained through the presence of ALA that ALA has an anticancer effect of its own towards highly proliferating cancer cells and being a polyunsaturated fatty acid it acts to counterbalance the ROS (*i.e.,* pro-oxidants) for normal cells. Also, superior interaction of the lipid based carrier to the cellular membrane, leading to a higher internalization and better anticancer effect of the drug delivery system.

6. Conclusion

QbD based concept was successfully employed for development of a stable nanoemulsion as revealed by physicochemical characterization. FTIR and 1H NMR data established the anchoring of folate onto the surface of the nanoemulsion. ALA showed strong antioxidant, anticancer, cardioprotective activity and enhanced the anticancer potential of Dox. *In vitro* studies in breast cancer cell lines, MCF-7, demonstrated antiproliferative, cytotoxic effects and apoptotic potential of the developed formulation through reactive oxygen species and mitochondrial membrane mediated cell death. Western blotting successfully demonstrated that the modulation of the pro/anti-apoptotic and pro/anti-migratory proteins expression by the folate decorated nanoemulsion. Percent animal survival, animal weight reduction, tumor volume and cardiotoxicity data elucidated higher safety and efficacy of the nanoemulsion vis-à-vis marketed formulation. The folate attachment to the surface preferentially delivered the drug to the target site which was affirmed through biodistribution analysis. From the above pieces of evidences, we can conclude that the proliferative and metastatic actions are induced by DMBA and are curtailed by f-Dox-NE through activation of the mitochondria-mediated apoptotic pathway and downregulation of anti-apoptotic and pro-migratory proteins. Apart from being safe, ALA behaves like anti-inflammatory, antioxidant and anticancer agent. In light of the above studies, it can be concluded that a safe lipid like ALA, which has multiple health benefits due to the presence of ω-3 fatty acid can be can be a superior alternative to metallic, ceramic or polymeric nanoparticles. for anticancer therapy. Nanoformulations are already being used commercially and such translations could prove to be beneficial in the long run.

7. Reference

Adkins Y, Kelley DS (2010) Mechanisms underlying the cardioprotective effects of omega-3 polyunsaturated fatty acids. J Nutr Biochem. 21(9):781-92.

Al-Qubaisi MS, Rasedee A, Flaifel MH, Ahmad SH, Hussein-Al-Ali S, Hussein MZ, Zainal Z, Alhassan FH, Taufiq-Yap YH, Eid EE, Arbab IA, Al-Asbahi BA, Webster TJ, El Zowalaty ME (2013) Induction of apoptosis in cancer cells by NiZn ferrite nanoparticles through mitochondrial cytochrome C release. Int J Nanomedicine. 8(0):4115-29.

Alessandra-Perini J, Perini JA, Rodrigues-Baptista KC, de Moura RS, Junior AP, Dos Santos TA, Souza PJC, Nasciutti LE, Machado DE (2018) Euterpe oleracea extract inhibits tumorigenesis effect of the chemical carcinogen DMBA in breast experimental cancer. BMC Complement Altern Med. 18(1):116.

Alkhatib MH, AlBishi HM (2013) In vitro evaluation of antitumor activity of doxorubicin-loaded nanoemulsion in MCF-7 human breast cancer cells. J Nanopart Res. 15(1489

Alshabanah OA, Hafez MM, Al-Harbi MM, Hassan ZK, Al Rejaie SS, Asiri YA, Sayed-Ahmed MM (2010) Doxorubicin toxicity can be ameliorated during antioxidant L-carnitine supplementation. Oxid Med Cell Longev. 3(6):428-33.

Arya M, Tiwari P, Tripathi CB, Parashar P, Singh M, Sinha P, Yadav NP, Kaithwas G, Gupta KP, Saraf SA (2017) Colloidal Vesicular System of Inositol Hexaphosphate to Counteract DMBA Induced Dysregulation of Markers Pertaining to Cellular Proliferation/Differentiation and Inflammation of Epidermal Layer in Mouse Model. Mol Pharm. 14(3):928-39.

Bae PK, Jung J, Lim SJ, Kim D, Kim SK, Chung BH (2013) Bimodal perfluorocarbon nanoemulsions for nasopharyngeal carcinoma targeting. Mol Imaging Biol. 15(4):401-10.

Cai C, Lothstein L, Morrison RR, Hofmann PA (2010) Protection from doxorubicin-induced cardiomyopathy using the modified anthracycline N-benzyladriamycin-14-valerate (AD 198). J Pharmacol Exp Ther. 335(1):223-30.

Calder PC (2012) The role of marine omega-3 (n-3) fatty acids in inflammatory processes, atherosclerosis and plaque stability. Mol Nutr Food Res. 56(7):1073-80.

Choudhury H, Gorain B, Karmakar S, Biswas E, Dey G, Barik R, Mandal M, Pal TK (2014) Improvement of cellular uptake, in vitro antitumor activity and sustained release profile with increased bioavailability from a nanoemulsion platform. Int J Pharm. 460(1-2):131-43.

Dharmalingam SR, Ramamurthy S, Chidambaram K, Nadaraju S (2014) A simple HPLC bioanalytical method for the determination of doxorubicin hydrochloride in rat plasma: application to pharmacokinetic studies. Trop J Pharm Res. 13(3):409-15.

Doroshow JH (1986) Prevention of doxorubicin-induced killing of MCF-7 human breast cancer cells by oxygen radical scavengers and iron chelating agents. Biochem Biophys Res Commun. 135(1):330-5.

Figueroa D, Asaduzzaman M, Young F (2018) Real time monitoring and quantification of reactive oxygen species in breast cancer cell line MCF-7 by 2',7'-dichlorofluorescin diacetate (DCFDA) assay. J Pharmacol Toxicol Methods. 94(Pt 1):26-33.

Ganta S, Singh A, Rawal Y, Cacaccio J, Patel NR, Kulkarni P, Ferris CF, Amiji MM, Coleman TP (2016) Formulation development of a novel targeted theranostic nanoemulsion of docetaxel to overcome multidrug resistance in ovarian cancer. Drug Deliv. 23(3):968-80.

Haque MW, Pattanayak SP (2018) Taxifolin Inhibits 7,12-Dimethylbenz(a)anthracene-induced Breast Carcinogenesis by Regulating AhR/CYP1A1 Signaling Pathway. Pharmacogn Mag. 13(4):S749-S55.

Hu D, Sheng Z, Fang S, Wang Y, Gao D, Zhang P, Gong P, Ma Y, Cai L (2014) Folate receptor-targeting gold nanoclusters as fluorescence enzyme mimetic nanoprobes for tumor molecular colocalization diagnosis. Theranostics. 4(2):142-53.

Huan ML, Zhou SY, Teng ZH, Zhang BL, Liu XY, Wang JP, Mei QB (2009) Conjugation with alpha-linolenic acid improves cancer cell uptake and cytotoxicity of doxorubicin. Bioorg Med Chem Lett. 19(9):2579-84

Iyengar NM, Hudis CA, Gucalp A (2013) Omega-3 fatty acids for the prevention of breast cancer: an update and state of the science. Curr Breast Cancer Rep. 5(3):247-54.

Jiang SP, He SN, Li YL, Feng DL, Lu XY, Du YZ, Yu HY, Hu FQ, Yuan H (2013) Preparation and characteristics of lipid nanoemulsion formulations loaded with doxorubicin. Int J Nanomedicine. 8(0):3141-50.

Kaithwas G, Majumdar DK (2012) In vitro antioxidant and in vivo antidiabetic, antihyperlipidemic activity of linseed oil against streptozotocin-induced toxicity in albino rats. Eur J Lipid Sci Technol. 114(11):1237–45.

Kandadi P, Syed MA, Goparaboina S, Veerabrahma K (2012) Albumin coupled lipid nanoemulsions of diclofenac for targeted delivery to inflammation. Nanomedicine. 8(7):1162-71.

Kanoujia J, Singh M, Singh P, Saraf SA (2016) Novel genipin crosslinked atorvastatin loaded sericin nanoparticles for their enhanced antihyperlipidemic activity. Mater Sci Eng C Mater Biol Appl. 69(0):967-76.

Karroum A, Mirshahi P, Faussat AM, Therwath A, Mirshahi M, Hatmi M (2012) Tubular network formation by adriamycin-resistant MCF-7 breast cancer cells is closely linked to MMP-9 and VEGFR-2/VEGFR-3 over-expressions. Eur J Pharmacol. 685(1-3):1-7.

Kouchakzadeh H, Soudi T, Aghda NH, Shojaosadati SA (2017) Ligand-modified Biopolymeric Nanoparticles as Efficient Tools for Targeted Cancer Therapy. Curr Pharm Des. 23(35):5336-48.

Kwon YJ, Ye DJ, Baek HS, Chun YJ (2018) 7,12-Dimethylbenz[alpha]anthracene increases cell proliferation and invasion through induction of Wnt/beta-catenin signaling and EMT process. Environ Toxicol

Lammers T, Hennink WE, Storm G (2008) Tumour-targeted nanomedicines: principles and practice. Br J Cancer. 99(3):392-7.

Lee ES, Na K, Bae YH (2005) Doxorubicin loaded pH-sensitive polymeric micelles for reversal of resistant MCF-7 tumor. J Control Release. 103(2):405-18.

Lee RJ, Low PS (1994) Delivery of liposomes into cultured KB cells via folate receptor-mediated endocytosis. J Biol Chem. 269(5):3198-31204.

Liu D, Liu F, Liu Z, Wang L, Zhang N (2011) Tumor specific delivery and therapy by double-targeted nanostructured lipid carriers with anti-VEGFR-2 antibody. Mol Pharm. 8(6):2291-301.

Liu Y, Yu XM, Sun RJ, Pan XL (2017) Folate-Functionalized Lipid Nanoemulsion to Deliver Chemo-Radiotherapeutics Together for the Effective Treatment of Nasopharyngeal Carcinoma. AAPS PharmSciTech. 18(4):1374-81.

Maehre HK, Jensen IJ, Elvevoll EO, Eilertsen KE (2015) omega-3 Fatty Acids and Cardiovascular Diseases: Effects, Mechanisms and Dietary Relevance. Int J Mol Sci. 16(9):22636-61.

Mizushima Y (1996) Lipid microspheres (lipid emulsions) as a drug carrier — An overview. Adv Drug Deliv Rev. 20(2–3):113-15.

Moraes RC, Chang H, Harrington N, Landua JD, Prigge JT, Lane TF, Wainwright BJ, Hamel PA, Lewis MT (2009) Ptch1 is required locally for mammary gland morphogenesis and systemically for ductal elongation. Development. 136(9):1423-32.

Moraes RC, Zhang X, Harrington N, Fung JY, Wu MF, Hilsenbeck SG, Allred DC, Lewis MT (2007) Constitutive activation of smoothened (SMO) in mammary glands of transgenic mice leads to increased proliferation, altered differentiation and ductal dysplasia. Development. 134(6):1231-42.

Musa MA, Latinwo LM, Virgile C, Badisa VL, Gbadebo AJ (2015) Synthesis and in vitro evaluation of 3-(4-nitrophenyl)coumarin derivatives in tumor cell lines. Bioorg Chem. 58(0):96-103.

O'Brien J, Wilson I, Orton T, Pognan F (2000) Investigation of the Alamar Blue (resazurin) fluorescent dye for the assessment of mammalian cell cytotoxicity. Eur J Biochem. 267(17):5421-26.

Ogretmen B, Safa AR (1996) Down-regulation of apoptosis-related bcl-2 but not bcl-xL or bax proteins in multidrug-resistant MCF-7/Adr human breast cancer cells. Int J Cancer. 67(5):608-14.

Ottonello L, Frumento G, Arduino N, Dapino P, Tortolina G, Dallegri F (2001) Immune complex stimulation of neutrophil apoptosis: investigating the involvement of oxidative and nonoxidative pathways. Free Radic Biol Med. 30(2):161-69.

Park SJ, Wu CH, Safa AR (2004) A P-glycoprotein- and MRP1-independent doxorubicin-resistant variant of the MCF-7 breast cancer cell line with defects in caspase-6, -7, -8, -9 and -10 activation pathways. Anticancer Res. 24(1):123-31.

Riccardi C, Nicoletti I (2006) Analysis of apoptosis by propidium iodide staining and flow cytometry. Nat Protoc. 1(3):1458-61.

Roy S, Rawat AK, Sammi SR, Devi U, Singh M, Gautam S, Yadav RK, Rawat JK, Singh L, Ansari MN, Saeedan AS, Pandey R, Kumar D, Kaithwas G (2017) Alpha-linolenic acid stabilizes HIF-1 alpha and downregulates FASN to promote mitochondrial apoptosis for mammary gland chemoprevention. Oncotarget. 8(41):70049-71.

Shinoda T, Takagi A, Maeda A, Kagatani S, Konno Y, Hashida M (1998) In vivo fate of folate-BSA in non-tumor- and tumor-bearing mice. J Pharm Sci. 87(12):1521-6.

Siegel RL, Miller KD, Jemal A (2017) Cancer Statistics, 2017. CA Cancer J Clin. 67(1):7-30.

Singh B, Kapil R, Nandi M, Ahuja N (2011) Developing oral drug delivery systems using formulation by design: vital precepts, retrospect and prospects. Expert Opin Drug Deliv. 8(10):1341-60.

Singh M, Kanoujia J, Parashar P, Arya M, Tripathi CB, Sinha VR, Saraf SK, Saraf SA (2018) Augmented bioavailability of felodipine through an alpha-linolenic acid-based microemulsion. Drug Deliv Transl Res. 8(1):204-25.

Singh M, Kanoujia J, Singh P, Tripathi CB, Arya M, Parashar P, Sinha VR, Saraf SA (2016a) Development of an α-linolenic acid containing soft nanocarrier for oral delivery: in vitro and in vivo evaluation. RSC Adv. 6(81):77590-602.

Singh N, Parashar P, Tripathi CB, Kanoujia J, Kaithwas G, Saraf SA (2017a) Oral delivery of allopurinol niosomes in treatment of gout in animal model. J Liposome Res. 27(2):130-38.

Singh S, Singh M, Tripathi CB, Arya M, Saraf SA (2016b) Development and evaluation of ultra-small nanostructured lipid carriers: novel topical delivery system for athlete's foot. Drug Deliv Transl Res. 6(1):38-47.

Singh Y, Meher JG, Raval K, Khan FA, Chaurasia M, Jain NK, Chourasia MK (2017b) Nanoemulsion: Concepts, development and applications in drug delivery. J Control Release. 252(0):28-49.

Stella B, Arpicco S, Peracchia MT, Desmaele D, Hoebeke J, Renoir M, D'Angelo J, Cattel L, Couvreur P (2000) Design of folic acid-conjugated nanoparticles for drug targeting. J Pharm Sci. 89(11):1452-64.

Tripathi CB, Beg S, Kaur R, Shukla G, Bandopadhyay S, Singh B (2016) Systematic development of optimized SNEDDS of artemether with improved biopharmaceutical and antimalarial potential. Drug Deliv. 23(9):3209-23.

Tripathi CB, Gupta N, Kumar P, Singh AK, Raj V, Parashar P, Singh M, Kanoujia J, Arya M, Saraf SA, Saha S (2017) Omega-3 Fatty Acid Synergized Novel Nanoemulsifying System for Rosuvastatin Delivery: In Vitro and In Vivo Evaluation. AAPS PharmSciTech: doi: 10.1208/s12249-017-0933-8.

Trivedi PP, Kushwaha S, Tripathi DN, Jena GB (2011) Cardioprotective effects of hesperetin against doxorubicin-induced oxidative stress and DNA damage in rat. Cardiovasc Toxicol. 11(3):215-25.

Um HD (2016) Bcl-2 family proteins as regulators of cancer cell invasion and metastasis: a review focusing on mitochondrial respiration and reactive oxygen species. Oncotarget. 7(5):5193-203.

Vimala K, Sundarraj S, Paulpandi M, Vengatesan S, Kannan S (2014) Green synthesized doxorubicin loaded zinc oxide nanoparticles regulates the Bax and Bcl-2 expression in breast and colon carcinoma. Process Biochem. 49(1):160-72.

Wang W, Xu B, Li Q, Jiang D, Yan S (2018) Anticancer effects of a novel PanRAF inhibitor in a hepatocellular carcinoma cell line. Mol Med Rep. 17(4):6185-93.

Wang X, Teng Z, Wang H, Wang C, Liu Y, Tang Y, Wu J, Sun J, Wang H, Wang J, Lu G (2014) Increasing the cytotoxicity of doxorubicin in breast cancer MCF-7 cells with multidrug resistance using a mesoporous silica nanoparticle drug delivery system. Int J Clin Exp Pathol. 7(4):1337-47.

Weitman SD, Weinberg AG, Coney LR, Zurawski VR, Jennings DS, Kamen BA (1992) Cellular localization of the folate receptor: potential role in drug toxicity and folate homeostasis. Cancer Res. 52(23):6708-11.

1. Introduction

Lipid nanoparticles are generally made up of a solid matrix. In the case of solid lipid nanoparticles the liquid lipid of the conventional of o/w emulsions are replaced by a solid lipid. The particle so formed remains in its solid state at room temperature and during storage. The first generation of such particles, *i.e.*, solid lipid nanoparticles (SLN) were developed two decades earlier. However, in the case of the second generation technology of SLNs, the particles are prepared by using a blend of two lipids, *i.e.*, a solid lipid and a liquid lipid. The resulting blend is termed as nanostructured lipid carriers (NLCs). Generally SLNs and NLCs remained in their solid form at physiological temperature. The blend of the solid lipid and the liquid lipid tends to have a disorderly structure which results in several spaces in between the solid lipid and the liquid lipid. The solubility of the drug is normally higher in the case of liquid lipid (Fernandes et al. 2017, Singh et al. 2016b, Singh et al. 2016d). NLCs have been utilized as the newer generation of novel drug delivery systems for systemic drug delivery. NLCs improve selective accumulation of drug inside cancer and have shown enhanced safety for normal tissue (Cho et al. 2008, Kouchakzadeh et al. 2017, Oliveira et al. 2017).

Tumor is one of the leading causes of mortality, worldwide (Siegel et al. 2017). Even though several advancements have been made in cancer therapy, the primary hurdle for clinical application of such drugs or delivery systems is their undesired side effects on normal tissue due to inappropriate drug disposition. Targeted drug delivery systems are superior because they overcome the problem of delivering a drug to a site where it not required. This in-turn also reduces the side effects of the drug which are a major disadvantage of chemotherapy. Recent findings suggest that biotin or biotin-conjugates can be constructively targeted to the tumor cells with the help of overexpressed biotin-selective transporters (Ren et al. 2015). Biotin play a critical role in cellular signaling mechanism, gene regulation and chromatin structure (Zempleni et al. 2009). Human cells are incapable of biotin synthesis, therefore, depend on external sources for supply. The mammalian cells uptake these molecules through biotin selective transporters and SMVT. The biotin receptors are overexpressed in several aggressive tumors such as leukemia, ovarian, colon, lung, renal and breast tumor (Ren et al. 2015, Wu et al. 2016b, Zempleni et al. 2009)

Nature has always offered several agents which are used for their therapeutic effect since times immemorial. *Perilla frutescens* seed oil contains good quantities of ω3-fatty acids (54-69%) and has been known to play significant role in altering the cell membrane fluidity, genetic expressions and cell signaling mechanisms. Further, ω3-FA has shown the potential to inhibit tumorigenesis (D'Eliseo and Velotti 2016, Iyengar et al. 2013, Narisawa et al. 1994, Roy et al. 2017, Tripathi et al. 2017)

In the current study, *Perilla frutescens* oil based NLCs were envisaged for the site-specific delivery of doxorubicin in the DMBA induced mammary gland tumor. We envisaged employing *Perilla frutescens* oil as the liquid lipid to develop Dox loaded NLCs. Further, NLCs were biotinylated and characterized for various physicochemical properties, *in vitro* efficacy on MCF-7 cell line and *in vivo* efficacy in DMBA induced mammary gland carcinoma in female albino wistar rats.

2. Materials

S. No.	Materials	Source
1.	Doxorubicin	Miracalus Pharma, India
2.	Methanol	ThermoFischer Scientific (Qualigens)
3.	Hydrochloric acid	S.D. Fine chemicals Ltd., Mumbai, India
4.	Ethanol	S.D. Fine chemicals Ltd., Mumbai, India
5.	Methanol	ThermoFischer Scientific (Qualigens)
6.	Acetone	ThermoFischer Scientific (Qualigens)
7.	Isopropyl alcohol	ThermoFischer Scientific (Qualigens)
8.	Acetonitrile HPLC grade	ThermoFischer Scientific (Qualigens)
9.	Methanol HPLC grade	ThermoFisher Scientific (Qualigens)
10.	Seasame oil	Sugandhco Pvt. Ltd, India
11.	Rice brian oil	Sugandhco Pvt. Ltd, India
12.	Soya bean oil	Sugandhco Pvt. Ltd, India
13.	Perilla oil	Sugandhco Pvt. Ltd, India
14.	Oleic acid	Fisher Scientific Pvt. Ltd., Mumbai, India
15.	Tween 20	HiMedia Laboratories (Mumbai)
16.	Tween 80	HiMedia Laboratories (Mumbai)
17.	Span 80	HiMedia Laboratories (Mumbai)
18.	Lecithin	HiMedia Laboratories (Mumbai)
19.	PEG 200	HiMedia Laboratories (Mumbai)
20.	PEG 400	HiMedia Laboratories (Mumbai)
21.	PEG 600	HiMedia Laboratories (Mumbai)
22.	Sodium hydroxide	SDFCL Pvt. Ltd., Mumbai, India
23.	N-hydroxysuccinimide (NHS)	Sigma Aldrich, USA
24.	N,N'-Dicyclohexylcarbodiimide (DCC)	Sigma Aldrich, USA
25.	Poly(ethylene glycol) bis(amine) (PEG-bis-amine	Sigma Aldrich, USA
26.	2-mercaptoethanol	Sigma Aldrich, USA
27.	Propidium Iodide	Sigma Aldrich, USA
28.	RNase A	Sigma Aldrich, USA
29.	Eagle's Minimum Essential Medium (EMEM)	Sigma Aldrich, USA
30.	Fetal Bovine Serum	Sigma Aldrich, USA
31.	Hank's Balanced Salt Solution (HBSS)	Sigma Aldrich, USA
32.	MTT (3-(4,5-Dimethylthiazol-2-yl)-2,5-diphenyl tetrazolium bromide)	Sigma Aldrich, USA

33.	2, 7-dichlorofluorescin diacetate (DCFDA)	Thermo Fisher Scientific, USA
34.	Alamar blue® reagent	Thermo Fisher Scientific, USA
35.	Rhodamine 123 (Rh-123)	Thermo Fisher Scientific, USA
36.	Radio Immuno Precipitation Assay (RIPA) lysis buffer	Thermo Fisher Scientific, USA
37.	Antibodies	Santa Cruz, USA

3. Methods

3.1. Preformulation Studies

3.1.1. Selection of Solid Lipid

Various Solid lipid were screened and a suitable solid lipid selected on the basis of stability and particle size of prepared NLCs. NLCs were prepared using melt-emulsification followed by sonication method using glyceryl monostearate and stearic acid as solid lipid and perilla oil as liquid lipid (total lipid 2%) and lecithin (3%) as a surfactant (Singh et al. 2016b, Singh et al. 2016c, Singh et al. 2016d).

3.1.2. Selection of liquid lipid

Liquid lipid was selected on the basis of solubility of the drug. Different lipids screened for use as liquid lipid was perilla oil, rice bran oil, soyabean oil, oleic acid and sesame oil. The procedure followed is described in section 3.3.1.1 of chapter III.

3.1.3. Selection of Surfactant

The surfactant was selected on the basis of water absorption capacities of a fixed amount of total lipid (50 mg) and surfactant (50 mg) (Singh et al. 2016b, Singh et al. 2016c, Singh et al. 2016d). Different surfactants studied were lecithin, sodium deoxycholate and sodium cholate.

3.1.4. Optimization of liquid and solid lipid ratio

The ratio of liquid lipids and solid lipid were optimized by formulating the NLCs with different ratio of solid and liquid lipids, *i.e.*, 50:50, 60:40, 70:30 and 80:20, and characterized for stability for a week and particle size recorded (Singh et al. 2016b, Singh et al. 2016c, Singh et al. 2016d).

3.1.5. Selection of formulation technique

Two different methods for preparation of NLCs were tried for the preparation of Dox loaded NLCs.

3.1.5.1. Solvent evaporation technique

Solid lipid (stearic acid) was melted and liquid lipid (*Perilla frutescens* oil) was added to it under continuous stirring in a water bath maintained at 70±2°C. To the above mixture doxorubicin (10 mg) triethanolamine (20 mg) and surfactant (lecithin, 5%) was added. Prepared lipid phase was dissolved in 10 ml of chloroform. Subsequently,

the above organic solution was immediately poured into aqueous phase maintained at (70±2°C) under mechanical stirring at 1000 rpm to form a primary emulsion. The above mixture was subjected immediately to sonication to form a microemulsion. Finally, the dispersion was cooled at room temperature under continuous stirring to form NLC.

3.1.5.2. Melt-emulsification followed by sonication method

The Dox-loaded NLCs were prepared by melt-emulsification followed by sonication method (Singh et al. 2016b). Briefly, lipid phase consisting of solid lipid (stearic acid) and liquid lipid (*Perilla frutescens* oil), Dox (10 mg), triethanolamine (20 mg) and surfactant (lecithin) were melted at 60±5 °C to form a homogenous lipid phase. Meanwhile, the aqueous phase consisting of EDTA (8 mg) dispersed in distilled water was maintained at 70 °C. The aqueous phase was then added dropwise to the lipid phase to obtain coarse primary emulsion which was immediately subjected to sonication to form a microemulsion through a probe-type sonicator (Labsonic® M, Sartorius, Germany, at 80% amplitude and 6 cycles) for 20 min. Afterward, the dispersion was cooled in an ice water bath for quick congealing and stored at 4°C till further use (Singh et al. 2016b, Singh et al. 2016c, Singh et al. 2016d).

3.2. Formulation development through Experimental design

On the basis of above studies, critical factors (CMAs) affecting the formation of NLCs viz., lipid amount (solid and liquid lipids), surfactant amount (lecithin) and sonication time were selected for optimization of NLCs. The most suitable ranges of factors, like lipid quantity, amount of surfactant and sonication time (10-30 min) were identified based on the previous experiments performed in our laboratories and literature (Singh et al. 2017, Singh et al. 2016b, Singh et al. 2016c, Singh et al. 2016d). Response surface methodology was employed for systematic development of formulation. Among different RSM design, the central composite design (CCD) with α=1 was selected for optimization purpose of NLCs as it enables the quantification of factor effects and interaction among factors. The selected design is capable of detecting the extent of nonlinearity through quadratic mathematical models. From CCD the composition of 17 experimental batches emerged **(Table 1)**. These were prepared in the laboratory and subsequently evaluated. Various batches were characterized for CQAs of product, *viz.*, drug content, particle size, entrapment

efficiency and drug release. The characterization data obtained for different batches was fitted with second-order polynomial equations using multiple linear regression analysis to establish a correlation between factors and responses through Design Expert 8.0 software (trial version, M/s Stat-Ease, USA) (Singh et al. 2011, Tripathi et al. 2016).

Table 1. Layout of DoE plan and physicochemical parameters for Dox loaded NLCs prepared as per the CCD.

Factor	Factors	Unit	Levels		
			low	intermediate	high
X_1	Total lipid concentration	%	1	2	3
X_2	Surfactant concentration	%	1	3	5
X_3	Sonication time	min	10	20	30

Code	Drug (mg)	Lipid (mg) (X_1)	S_{mix} (mg) (X_2)	Cholesterol (mg) (X_2)
NLC 1	10	1	1	10
NLC 2	10	3	1	10
NLC 3	10	1	5	10
NLC 4	10	3	5	10
NLC 5	10	1	1	30
NLC 6	10	3	1	30
NLC 7	10	1	5	30
NLC 8	10	3	5	30
NLC 9	10	1	3	20
NLC 10	10	3	3	20
NLC 11	10	2	1	20
NLC 12	10	2	5	20
NLC 13	10	2	3	10
NLC 14	10	2	3	30
NLC 15	10	2	3	20
NLC 16	10	2	3	20
NLC 17	10	2	3	20

3.3. Determination particle size

The particle size of NLCs was analyzed employing NanoPlus zeta/nano particle analyzer (M/s Micromeritics Instrument Corporation, USA). The instrument contains

a 4mW He-Ne laser light source operating at a wavelength of 633 nm and works on the principle of non-invasive backscatter optics (NIBS) (Singh et al. 2011, Tripathi et al. 2016, Tripathi et al. 2017).

The measurements were made at detection angle of 90° and the measurement position within the cuvette was automatically determined by the software. The instrument recorded the intensity of fluctuation of laser beam and correlated it with the particle size distribution of NLCs.

3.4. Entrapment efficiency and drug content

The drug content and entrapment efficiency of Dox in NLCs were determined using reported procedure with some modifications (Mussi et al. 2014). The entrapment efficiency was measured by keeping NLCs (1 mL) in dialysis bag for 2 h. The amount of drug dialyzed was estimated using UV-Vis spectrophotometer (M/s Labtronics-LT 2910) at 485 nm. The Doxorubicin entrapment and drug content was calculated using equation 1 and 2, respectively.

$$\text{Entarpment Efficiency (\%)} = \frac{Wt - Waq}{Wt} x100 \qquad \textbf{...Eq. (1)}$$

$$\text{Drug content (mg/g)} = \frac{WL}{Wnp} \qquad \textbf{...Eq. (2)}$$

where, W_t was the total amount of doxorubicin in NLCs, W_{aq} was Dox in aqueous phase, W_L was amount of drug loaded in nanoparticles, W_{np} was total weight of nanoparticles.

3.5. Drug diffusion study from NLCs

Method followed has been previously mentioned in **section 3.3.7 of chapter III.**

3.6. Preparation of biotinylated NLCs

3.6.1. Formation of NHS ester of biotin:

Activation of biotin was performed as per method described earlier (Lee and Low 1994, Wu et al. 2016a). Biotin (16.13 mg), N,N'-Dicyclohexylcarbodiimide (DCC-13.63 mg) and N-hydroxysuccinimide (NHS-7.6 mg) (1:1:1 molar ratio) in dimethylsulfoxide. The above solution was stirred for 2 h. Then solution was kept in dark place and reaction was allowed to complete overnight at room temperature. After completion of reaction the Biotin-NHS was precipitated by using acetone (**Fig. 1, Scheme 1)**. The precipitate was separated and dried under vacuum.

3.6.2. Activation of fatty acid:

The fatty acid was activated by attachment of PEG-bis-amine to form fatty acid with primary amine terminal. Stearic acid PEG-NH_2 (ST-PEG-NH_2) was prepared by dissolving stearic acid (18.79 mg) and DCC (13.63 mg) in DMSO and allowed to react overnight under stirring in dark (**Fig. 1, Scheme 2)**. Then PEG-bis-amine (231.21 mg) was accurately weighed, added to the above reaction mixture and kept under stirred for 3 h to obtain activated form of stearic acid (ST-PEG-NH_2). The dicyclohexylurea precipitate obtained as byproduct was separated and the filtrate was dried under vacuum to obtain ST-PEG-NH_2 (Lee and Low 1994, Wu et al. 2016a).

3.6.3. Attachment of Biotin to activated Stearic acid

To form biotin decorated NLCs, biotin–NHS (35.95 mg) was dissolved in DMF added in excess molar amount in comparison to ST-PEG-NH_2 (2:1) and added to the aqueous dispersion of NLC prepared with mixture of activated stearic acid (127.27 mg) and stearic acid (1272.73 mg) in 1:10 w/w ratio. The reaction was allowed to react overnight under continuous stirring (**Fig. 1, Scheme 3)**. Reaction was completed by adding 2-mercaptoethanol (10 mmol) to above reaction mixture (Lee and Low 1994, Wu et al. 2016a). Subsequently, the reaction mixture was kept in a dialysis bag and dialyzed against distilled water for 2 h. After dialysis the product was lyophilized and stored at 4 °C for further use.

3.7. Characterization of biotinylated NLCs

3.7.1. FTIR characterization

Method followed has been previously mentioned in **section 3.10.1 of chapter III.**

3.7.2. ^{1}H-NMR characterization

Method followed has been previously mentioned in **section 3.10.2 of chapter III.**

3.7.3. Biotin content assay

The biotin content of biotinylated NLCs (b-Dox-NLCs) was determined by HABA-avidin competitive binding assay (Wu et al. 2016a). HABA was dissolved in 5 mL 0.1 M aqueous NaOH solution to produce 0.1 mmol solution. Side by side solution of avidin was prepared by adding 5 mg of avidin in 9.7 mL Of PBS pH 7.2. 300 µL of HABA solution was then added to avidin solution to obtain HABA-avidin complex. Now, 50 µL of biotin anchored NLCs (1 $mg.mL^{-1}$) were added to HABA-avidin

solution and mixed gently. The change in UV-Vis absorption before and after addition of biotin anchored NLCs to HABA-avidin solution was recorded through UV-Vis microplate reader at 500 nm and amount of biotin was calculated per mg of NLCs.

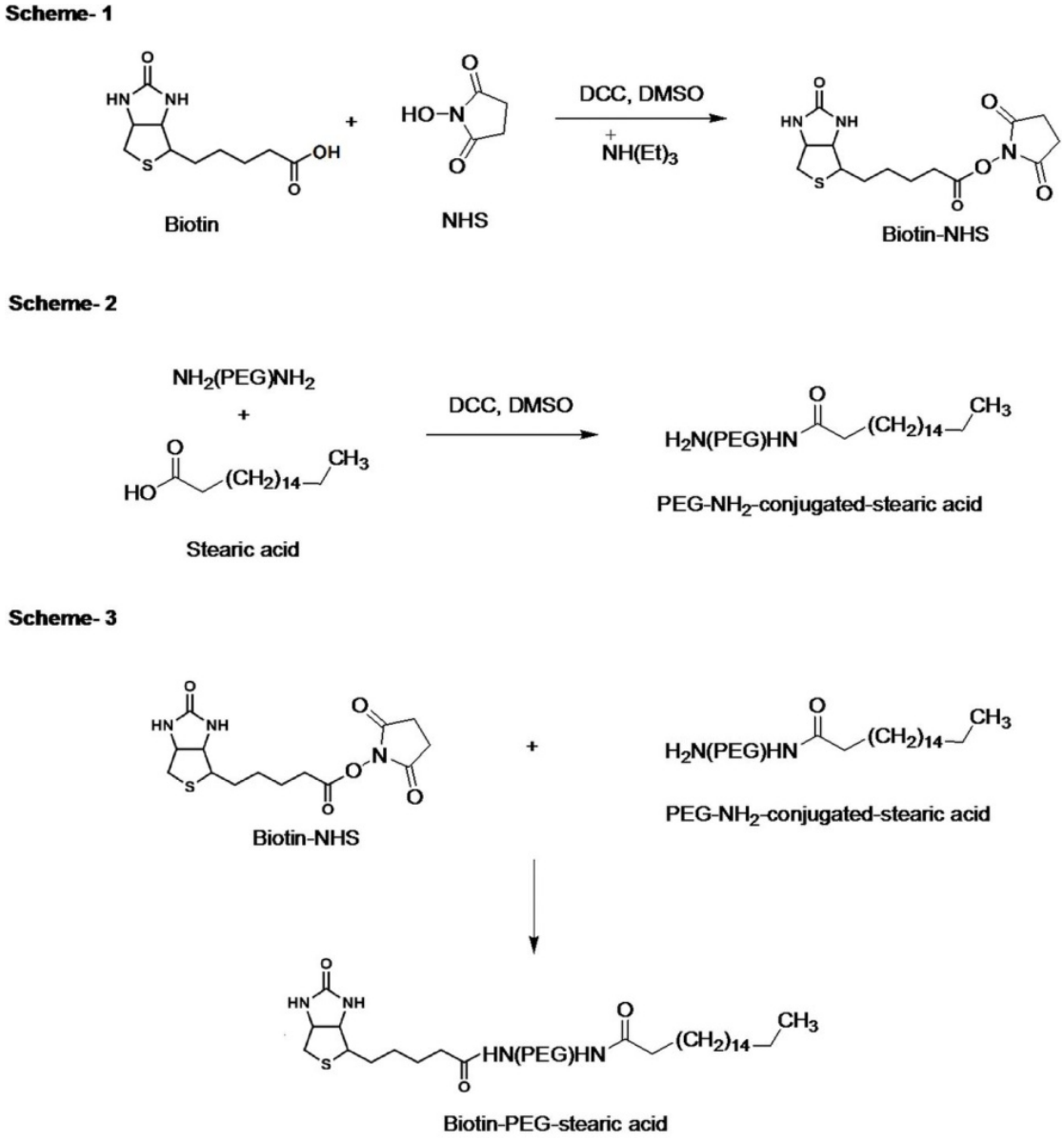

Fig. 1. Schematic representation of modification of fatty acid; **Scheme 1:** synthesis of biotin-NHS ester, **Scheme 2:** synthesis of PEG-NH_2 conjugated stearic acid (ST-PEG-NH2) and **Scheme 3:** attachment of biotin to PEG-NH_2 conjugated stearic acid to prepare biotinylated NLCs.

3.7.4. Physicochemical characterization

Particle size, Entrapment efficiency, drug content and drug release of biotin decorated NLCs were done as per method previously stated.

3.7.5. Transmission electron microscopy studies of f-Dox-NE

Method followed has been previously mentioned in **section 3.10.7 of chapter III.**

3.7.5. Stability in plasma and intravenous infusion solutions

Method followed has been previously mentioned in **section 3.10.8 of chapter III.**

3.7.6. Stability studies

Method followed has been previously mentioned in **section 3.10.9 of chapter III.**

3.8. *In vitro* studies

3.8.1. Cell culture conditions

Method followed has been previously mentioned in **section 3.11.1 of chapter III.**

3.8.2. Cell cytotoxicity study

Method followed has been previously mentioned in **section 3.11.2 of chapter III.**

3.8.3. Cell Cycle Analysis through FACS Analysis

Method followed has been previously mentioned in **section 3.11.3 of chapter III.**

3.8.4. Cell proliferation studies

Method followed has been previously mentioned in **section 3.11.4 of chapter III.**

3.8.5. Determination of reactive oxygen species

Method followed has been previously mentioned in **section 3.11.5 of chapter III.**

3.8.6. Determination of mitochondrial membrane potential

Method followed has been previously mentioned in **section 3.11.6 of chapter III.**

3.8.7. Cellular uptake through FACS analysis

The MCF-7 cells were seeded into 96-well plates (3x103 cells per well) and incubated for 24 h and treated with Dox-NLCs, b-Dox-NLCs and Dox and Dox for 4 h, washed with PBS thrice, trypsinized, centrifuged, and re-suspended in PBS and analyzed through FACS analysis at 490/585 nm (M/s BD Biosciences, Franklin Lakes, NJ). Dead cells and debris were removed using forward scatter versus side scatter technique (Mussi et al. 2014).

3.9. *In vivo* study

In vivo studies were performed according to the CPCSEA guidelines for laboratory animals and ethics, Department of Animal Welfare, Government of India, after getting approval from Institutional Animal Ethical Committee (SDCOPVS/AH/CPCSEA/01/0078). Albino wistar female rats weighing 120-150 g were housed in standard condition, fed with standard pellet diet and water *ad libitum.*

3.9.1. Treatment schedule for different animal groups

Animals were randomized and divided into six groups of 10 animals each. Group I (control) received normal saline, Group II (toxic control) received DMBA only, Group III (p-NLCs formulation) recived NLCs of ω3-FA, Group IV (standard drug) received Dox solution, Group V received marketed formulation, Group VI received Dox-NLCs and Group VII received b-Dox-NLCs **(Table 2)**. Carcinoma was induced by single tail vein injection of DMBA (8 mg/kg) on 'Day 1' in each group (except Group I). The drug/formulations were administered (10 mg/kg e.q. Dox) thrice/weeks in last six weeks of total 16 weeks (or 112 days) of *in vivo* studies. A lag time of 10 weeks or 70 days was provided to develop the tumor in animals. Tumor occurrence and size of tumor was verified by diameter of mammary glands of rats; changes in animal weight and duration of survival of animals throughout the study. The blood samples were collected through retro orbital puncture under mild chloroform anesthesia; serum was isolated and stored at -20 °C till further use. Animals were sacrificed humanely on completion of the study (112^{th} day) after DMBA treatment and mammary gland tissues were removed and stored at -80 °C till further evaluation (Roy et al. 2017).

Table 2. Treatment groups selected for *in vivo* anticancer studies

Sr. No.	Groups	Treatment
1.	Group I (negative control)	received normal saline
2.	Group II (toxic control)	received normal saline and DMBA
3.	Group III (p-NLCs or plaebo formulation)	NLCs with perilla oil + DMBA
4.	Group IV (standard drug)	Dox solution + DMBA
5.	Group V (marketed formulation)	Marketed formulation + DMBA
6.	Group VI (test 1)	Dox-NLCs+DMBA
7.	Group VII (test 2)	b-Dox-NLCs+ DMBA

3.9.2. Biochemical Estimation

Method followed has been previously mentioned in **section 3.12.2 of chapter III.**

3.9.3. Western blotting for different apoptotic markers

Western blotting was performed for different apoptotic markers viz., Bcl-2, p16, BAX, MMP-9, caspase-9 using appropriate antibodies *viz.*, bcl-2 (sc-7382), p16 (sc-1207), BAX (sc-23959), caspase-9 (sc-56073) (all are mouse monoclonal) and MMP-9 (sc-6840, goat polyclonal). Method followed has been previously mentioned in **section 3.12.3 of chapter III.**

3.9.4. Microscopy of whole mounts of mammary glands through carmine staining

Method followed has been previously mentioned in **section 3.12.4 of chapter III.**

3.9.5. Hematoxyline & Eosin staining of mammary gland tissue

A small piece of mammary gland tissue excised from different groups after completion of study was fixed in formalin solution and embedded in the wax. Sections (5μm) were prepared using microtome followed by staining with hematoxyline and eosin (H&E). The sections were visualized and photographed at 40X using digital microscope for pathological changes, if any (Roy et al. 2017).

3.9.6. Cardiotoxicity

Method followed has been previously mentioned in **section 3.12.5 of chapter III.**

3.9.7. Biodistribution Studies

Method followed has been previously mentioned in **section 3.12.6 of chapter III.**

3.10. Statistical analysis

Method followed has been previously mentioned in **section 3.13 of chapter III.**

4. RESULTS

4.1. Preformulation Studies

4.1.1. Selection of Solid Lipid

Glyceryl monostearate and stearic acid was studied as solid lipid because both are naturally occurring and generally regarded as safe. Based on stability and particle size stearic acid was selected as solid lipid for development of NLCs. Between the studied solid lipids, the NLCs prepared with stearic acid were found in lower size range as compared to GMS, i.e., 331.69nm and 421.77 nm, respectively.

4.1.2. Selection of liquid lipid

The liquid lipid screened for the current study was *Perilla frutescens* oil, rice bran oil, soyabean oil, oleic acid and sesame oil. These oils are well known for their high ω3-FA content along with strong antioxidant, anti-inflammatory, cardioprotective and tumor-inhibitory potential. On the basis of equilibrium solubility *Perilla frutescens* oil was selected as liquid lipid **(Table 3)**.

4.1.3. Selection of Surfactant

Among different biological surfactants, lecithin demonstrated highest waster absoption capacity (21.54 % w/w) followed by sodium deoxycholate (16.67 % w/w) and sodium cholate (9.52 % w/w).

Table 3. Solubility of drug in various liquid lipids

Sr. No.	Name of Excepient	Solubility (mg/ml)
1	Rice bran oil	21.3±3.1
2	Perilla oil	22.6±2.2
3	Soyabean oil	15.4±3.5
4	Oleic acid	20.5±3.3
5	Sesame oil	12.1±3.6

4.1.4. Optimization of liquid and solid lipid ratio

The particle size and stability of NLCs prepared with different ratio of solid and liquid lipid is given in **Table 4**. The data suggested that ratio of solid and liquid lipid in 70:30 yielded NLCs that showed lowest particle size and was stable upto one week. Hence, ratio of solid and liquid lipid in 70:30 was selected for further development.

Table 4. Parameters of NLCs prepared with different ratio of solid and liquid lipid

Sr. No.	Ratio of liquid and solid lipid	Particle Size (nm)	Stability
1	50:50	181.32	Unstable
2	60:40	241.51	Unstable
3	70:30	327.93	Stable
4	80:20	391.24	Stable

4.1.5. Selection of formulation technique

Melt-emulsification followed by sonication method was selected for the preparation of NLCs as this method yielded stable NLCs with particle size (359.51 nm). While, solvent diffusion method yielded NLCs with particle size 447.39 nm and size of

4.2. Preparation and optimization of NLCs as per experimental design

MLRA method was employed to analyze the observed data **(Table 5)** for experimental trials suggested as per experimental design and second-order quadratic models were found to be the best fit for the current set of data. This model appropriately defined the relationship between factors and responses of the formulated NLCs (Singh et al. 2011, Tripathi et al. 2016, Tripathi et al. 2017). The response surface plots **(Fig. 2 A-D)** and ANOVA tables **(Table 6A-D)** explicitly described the effects of lipid concentration, surfactant and sonication time on various responses of NLCs.

Table 5. Physicochemical parameters for Dox loaded NLCs prepared as per the CCD.

Code	Drug (mg)	X_1	X_2	X_3	Particle Size (Y_1)	Entrapment Efficiency (Y_2)	Drug Release (Y_3)	Drug Content (Y_4)
NLC1	10	1	1	10	202.3±4.2	90.51±2.41	81.76±4.54	20.33±2.43
NLC2	10	3	1	10	260.1±3.8	96.32±3.12	69.21±5.22	17.42±2.12
NLC3	10	1	5	10	182.6±4.5	92.12±3.22	87.22±6.41	08.45±3.47
NLC4	10	3	5	10	222.5±5.1	93.33±1.98	81.99±4.95	10.67±3.12
NLC5	10	1	1	30	153.2±2.8	92.98±1.02	95.76±3.22	21.38±2.36
NLC6	10	3	1	30	227.1±3.7	99.25±1.21	75.76±4.69	19.74±1.89
NLC7	10	1	5	30	82.3±5.1	95.21±2.12	98.95±2.01	11.64±1.62
NLC8	10	3	5	30	140.1±5.3	99.64±1.12	89.59±3.33	11.01±2.67
NLC9	10	1	3	20	98.5±2.2	94.33±3.41	95.55±4.35	16.67±3.12
NLC10	10	3	3	20	149.1±3.2	98.99±2.11	84.69±6.67	15.12±3.41
NLC11	10	2	1	20	157.4±4.2	98.48±1.81	88.52±4.96	23.76±3.51

NLC12	10	2	5	20	89.2±3.3	99.12±11.01	87.34±2.33	13.33±4.44
NLC13	10	2	3	10	170.1±2.5	95.89±2.18	90.79±3.32	16.67±4.22
NLC14	10	2	3	30	91.3±1.9	99.53±1.11	98.33±1.99	19.21±3.50
NLC15	10	2	3	20	102.2±1.9	99.36±1.02	97.34±1.83	18.78±4.12
NLC16	10	2	3	20	98.1±2.5	99.22±1.21	95.47±2.51	19.11±1.21
NLC17	10	2	3	20	96.4±1.7	98.78±2.01	98.67±2.11	18.94±2.45

[Data presented as mean±SD, n=3]

As displayed in **Fig. 2A** and **Table 6A**, a nonlinear relationship was observed between particle size and selected factors. All three factors selected showed a significant effect on particle size of NLCs. Also, a significant interaction between lipid and surfactant; and lipid and sonication time was observed. Increase in surfactant concentration and sonication time resulted in a nonlinear decrease in particle size. While an increase in lipid concentration resulted in increase in particle size. Effect of selected factors on drug release is portrayed in **Fig 2B** and **Table 6B.** A significant effect of lipid, surfactant and sonication time on drug release was observed. The increment in lipid concentration resulted in a sharp nonlinear decrease in the release as revealed in **Fig 2B**. However, opposite effect on drug release can be observed in case of increase in surfactant concentration. The sonication time revealed a positive effect on drug release. Also, a significant interaction between lipid and surfactant was observed as revealed in ANOVA **Table 6B**.

As revealed in **Fig. 2C,** concentration of surfactant showed the most significant effect on drug content (calculated based on the data obtained for entrapment). With an increase in surfactant concentration, the drug content was found to decrease linearly. An increase in lipid concentration resulted in the increase in drug content up to middle levels, but further increments in lipid concentration resulted in a decrease in drug content of NLCs. Sonication time was found to increase the drug content of NLCs. Also, significant interaction between lipid and surfactant was observed **(Table 6C)**. In case of entrapment efficiency, significant effect of total lipid and sonication time was observed **(Fig. 2D)**. There was no significant effect of surfactant on entrapment efficiency **(Table 6D)**.

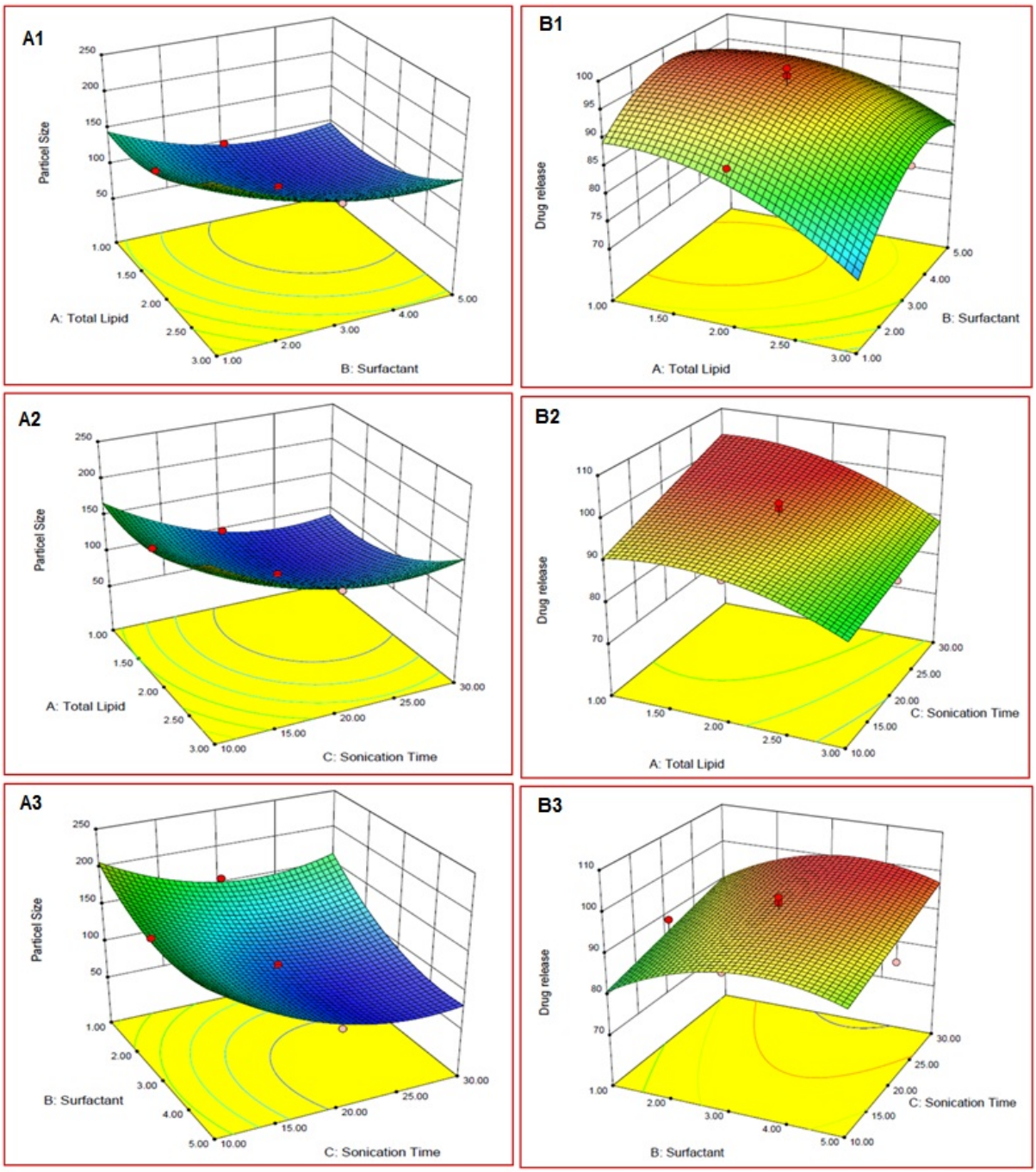

Fig. 2 (A&B). Response surface plots showing the influence of total lipid (%), surfactant (%) and sonication time (min) on (A, 1-3) Particle size (nm) (B, 1-3) drug release (%) of the NLCs.

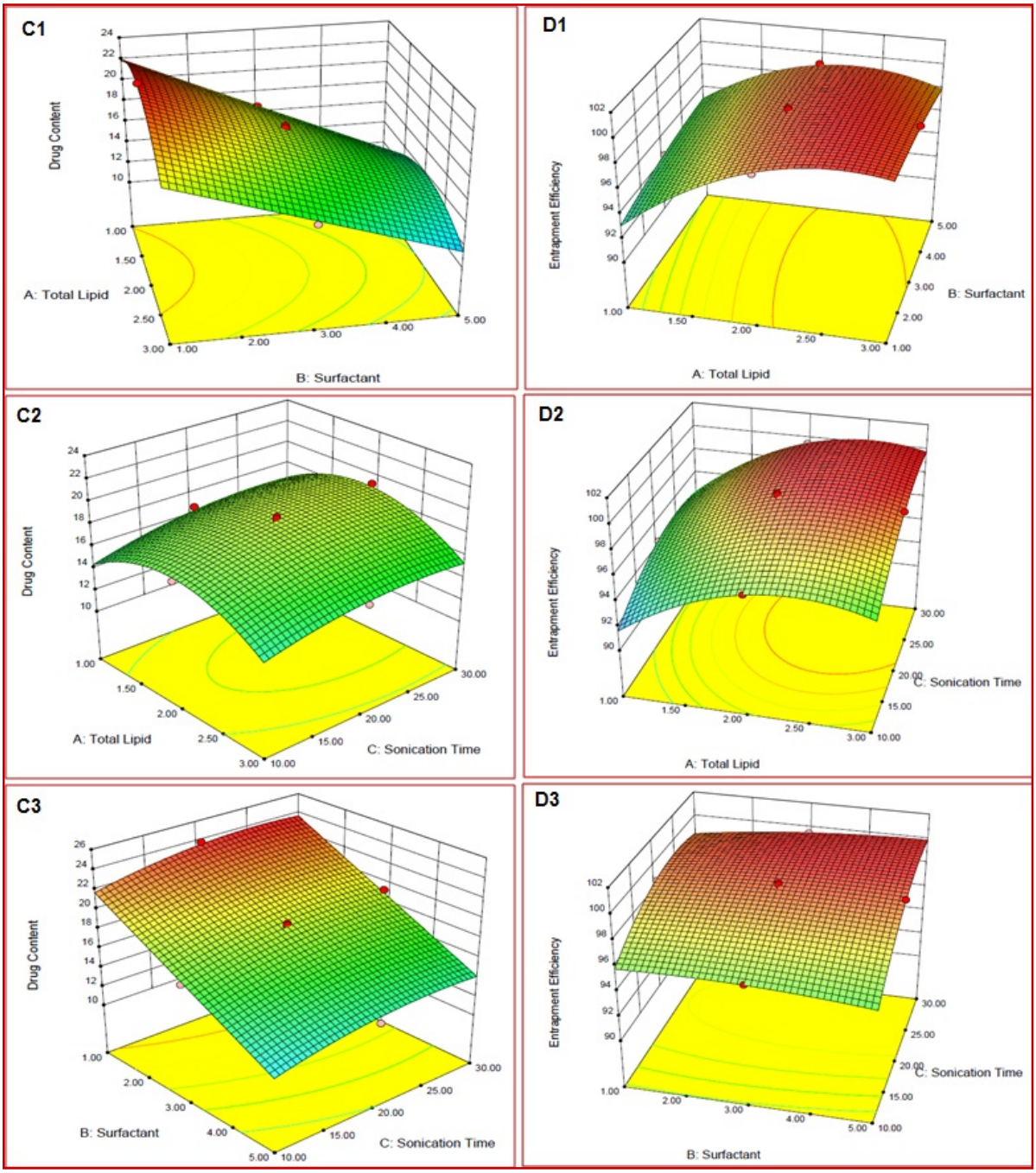

Fig. 2(C&D). Response surface plots showing the influence of total lipid (%), surfactant (%) and sonication time (min) on (C, 1-3) Drug content (mg/g of NLCs) (D, 1-3) entrapment efficiency (%) of the NLCs.

Table 6A. ANOVA table for quadratic model fitting of particle size

Source	Sum of Squares	df	Mean Square	F Value	p-value Prob > F	
Model	49706.73	9	5522.97	206.70	< 0.0001	Significant
A-Total Lipid	7896.10	1	7896.10	295.52	< 0.0001	Significant
B-Surfactant	8065.60	1	8065.60	301.87	< 0.0001	Significant
C-Sonication Time	11764.90	1	11764.90	440.32	< 0.0001	Significant
AB	144.50	1	144.50	5.41	0.0530	Significant
AC	144.50	1	144.50	5.41	0.0530	Significant
BC	1250.00	1	1250.00	46.78	0.0002	Not significant
A^2	1859.56	1	1859.56	69.60	< 0.0001	Significant
B^2	1789.64	1	1789.65	66.98	< 0.0001	Significant
C^2	2979.04	1	2979.04	111.49	< 0.0001	Significant
Residual	187.034	7	26.72			
Lack of Fit	168.37	5	33.67	3.61	0.2311	Not significant
Pure Error	18.67	2	9.33			
Corr. Total	49893.76	16				

P<0.05 was considered as significant.

Table 6B. ANOVA table for modified quadratic model fitting of Drug release

Source	Sum of Squares	df	Mean Square	F Value	p-value Prob > F	
Model	1111.07	7	158.72	22.05	< 0.0001	Significant
A-Total Lipid	336.52	1	336.52	46.75	< 0.0001	Significant
B-Surfactant	116.21	1	116.21	16.15	0.0030	Significant
C-Sonication Time	224.96	1	224.96	31.26	0.0003	Significant
AB	40.37	1	40.37	5.61	0.0420	Significant
AC	16.73	1	16.73	2.32	0.1617	Not significant
A^2	57.65	1	57.65	8.01	0.0197	Significant
B^2	130.05	1	130.05	18.07	0.0021	Significant
Residual	64.78	9	7.20			Significant
Lack of Fit	59.61	7	8.52	3.30	0.2525	Not significant
Pure Error	5.17	2	2.58			
Corr. Total	1175.85	16				

P<0.05 was considered as significant.

Table 6C. ANOVA table for linear model fitting of drug content

Source	Sum of Squares	df	Mean Square	F Value	p-value Prob > F	
Model	288.80	7	41.26	108.18	< 0.0001	Significant
A-Total Lipid	2.03	1	2.03	5.33	0.0463	Significant
B-Surfactant	225.91	1	225.91	592.38	< 0.0001	Significant
C-Sonication Time	8.91	1	8.91	23.37	0.0009	Significant
AB	4.71	1	4.71	12.36	0.0066	Significant
AC	0.31	1	0.31	0.82	0.3893	Not significant
A^2	25.01	1	25.01	65.58	< 0.0001	Significant
C^2	2.08	1	2.08	5.45	0.0444	Significant
Residual	3.43	9	0.38			
Lack of Fit	3.38	7	0.48	17.72	0.0544	Not significant
Pure Error	0.05	2	0.03			
Corr. Total	292.23	16				

P<0.05 was considered as significant.

Table 6D. ANOVA table for quadratic model fitting of entrapment efficiency, P<0.05 was considered as significant.

Source	Sum of Squares	df	Mean Square	F Value	p-value Prob > F	
Model	147.20	9	16.36	95.92	< 0.0001	Significant
A-Total Lipid	50.04	1	50.04	293.47	< 0.0001	Significant
B-Surfactant	0.36	1	0.36	2.14	0.1870	Not significant
C-Sonication Time	34.11	1	34.11	200.06	< 0.0001	Significant
AB	5.17	1	5.17	30.31	0.0009	Significant
AC	1.70	1	1.70	9.98	0.0159	Significant
BC	1.97	1	1.97	11.55	0.0115	Significant
A^2	16.29	1	16.29	95.50	< 0.0001	Significant
B^2	0.28	1	0.28	1.66	0.2380	Not significant
C^2	5.37	1	5.37	31.48	0.0008	Significant
Residual	1.19	7	0.17			
Lack of Fit	1.01	5	0.20	2.21	0.3407	Not significant
Pure Error	0.18	2	0.09			
Corr. Total	148.40	16				

P<0.05 was considered as significant.

4.3. Optimization of NLCs and overlay plots

Graphical optimization method utilizing overlay plot was employed wherein certain constraints were applied on different responses for defining the design space and identifying the optimum formulation. The constraints for optimization of the NLCs were applied like, particle size should be lower than 150 nm, drug release should be more than 90%, EE more than 95% and drug content should be more than 15 mg/g of NLCs (Singh et al. 2011, Tripathi et al. 2016, Tripathi et al. 2017). The optimized NLCs formulation (Dox-NLCs) optimized by the software contained lipid-2% w/w (composed of 7:3 ratio of stearic acid to perilla oil), surfactant-3% w/w along with optimum duration for sonication 20 min **(Fig. 2E)**. The predicted values for optimized NEs are presented in **Table 7** which suggests a good agreement between predicted and observed values.

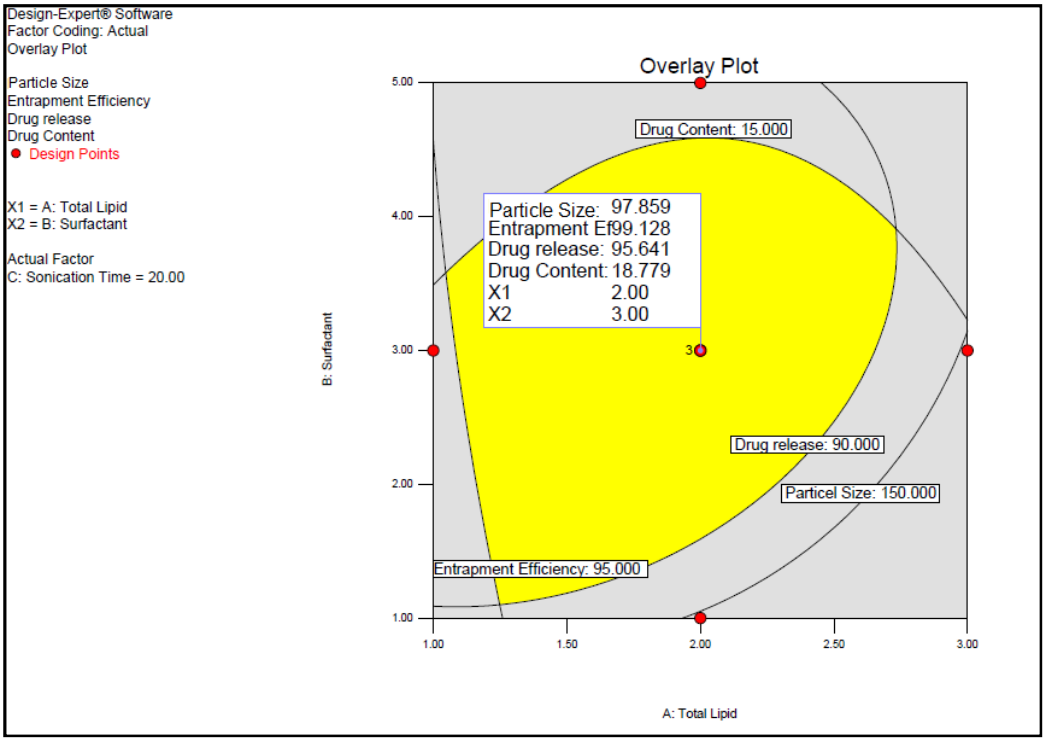

Fig. 2E. Overlay plot depicting the desirable region (design space) as highlighted area for the NLCs. Inset flag presents the composition of optimized nanoemulsion [total lipid (X_1) 2%, Surfactant (X_2) 3% and Sonication time (X_3) 20 min] and predicted values of CQAs.

Table 7. Predicted and observed values of responses for optimized NLCs (Dox-NLCs)

S. No.	Parameters	Predicted value	Observed Value
1.	Particle size (nm)	97.86	100.5±2.3
2.	Drug release in 72 h (%)	95.64	96.67±1.87
3.	Entrapment efficiency (%)	99.12	99.31±1.27
4.	drug content (mg/g of NLCs)	18.77	19.84±2.8

4.2. Preparation of biotinylated NLCs

Here, biotin was used as a targeting ligand to decorate *Perilla frutescens* oil based nanostructured lipid carrier for doxorubicin targeted delivery mammary gland carcinoma in rat model.

4.3. Characterization of biotinylated NLCs

4.3.1. FTIR Characterization

The attachment of biotin to NLCs was successfully affirmed by characteristic FTIR peaks of biotin, NHS ester of biotin and modified stearic acid. The synthesis of NHS ester of biotin was assessed through IR spectroscopy **(Fig. 3A & Fig. 6, chapter II)** with important peaks obtained at 3,4440 cm^{-1} imidazole band that overlaps with the (N–H) absorptions, $–CH_2$ groups stretching at 2995 cm^{-1} and deformations at 2,921.7 cm^{-1}, C=O stretch at 1644.5 cm^{-1}, N-H bending 1550 cm^{-1}, $–CH_2$ group bending at 1435 cm^{-1} and (C–O) stretching of ester at 1026.9 cm^{-1} (strong two bands, overlapped). The spectra of biotinylated-PEG-stearic acid were characterized by bands at 3,440 cm^{-1} imidazole band overlapped with (N–H) stretch of secondary amide group, (C=O) stretch at 1712.84 cm-1, (C–O) stretching of PEG chain at 1210 cm^{-1} and 1,042.95 cm^{-1}, –CH2 group stretching at 2911.3 cm^{-1} and $–CH_2$ group bending at 1435.76 cm^{-1} **(Fig. 3B)**.

4.3.2. ^{1}H-NMR characterization

^{1}H-NMR of biotin anchored NLCs were performed and characteristic peaks were appropriately marked **(Fig. 4)** which established the conjugation of biotin to stearic acid. Important peaks can be described as, oxohexahydrothienoimidazol ring of biotin shows 1H-NMR peaks at: **a** (6.30, s, 1H); **b** (6.38, s, 1H); **c** (4.11, t, 1H); **d** (4.28, q, 1H); **e** (2.78, dd, 2H); **f** (3.06, q, 1H). Pentanoic chain of biotin shows proton signals

at: **g, h, i** (3.35-3.38, m, 6H, methylene); **j** (2.1, q, 2H). Two adjacent peaks for PEG were observed at: **k** (3.35-3.46, dd, 2H); Stearic acid shows proton signals at: **l** (2.1, q, 2H); **m** (1.41-1.49, 28H, m, C_{3-16} methylene); **n** (1.24-1.32, m, 2H, C_{17} methylene); **o** (0.78-0.82, m, 3H, C_{18} methyl) **(Fig 4.)**.

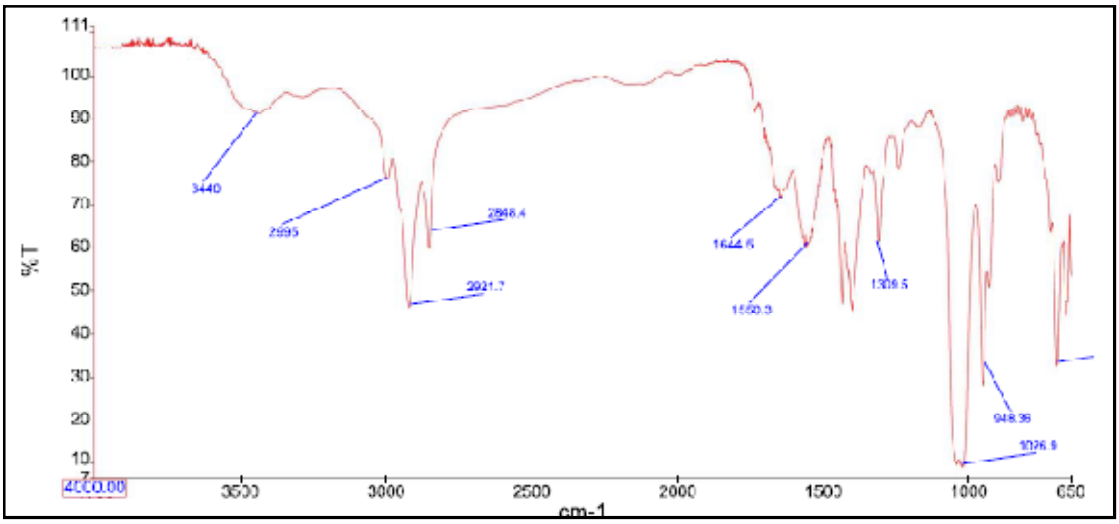

Fig. 3A. FTIR spectra of NHS-Biotin

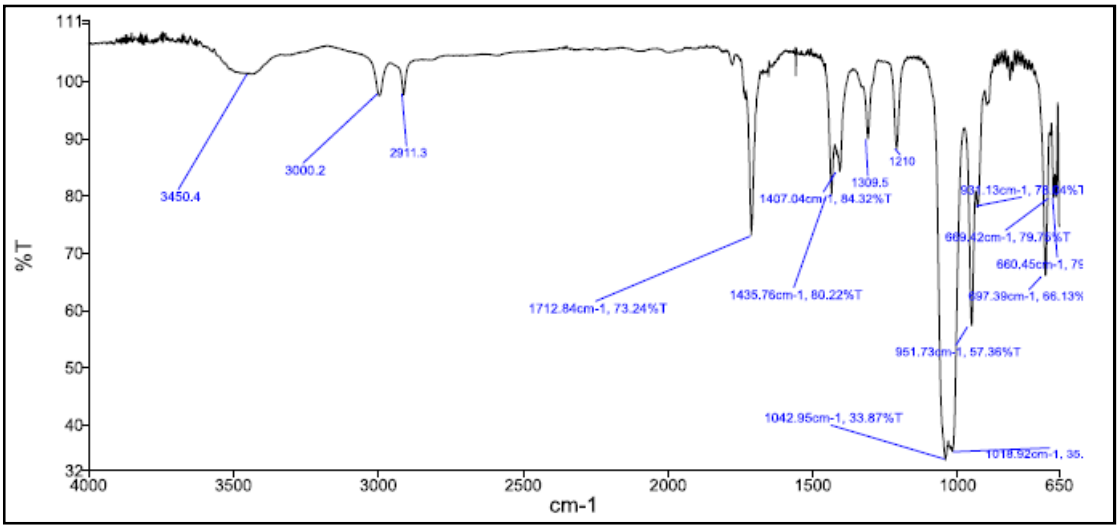

Fig. 3B. FTIR spectra of biotin-PEG-stearic acid

4.3.3. Biotin content assay

The biotin content anchored to NLCs (b-Dox-NLCs) surface was observed to be 5.85±0.64 µg.g-1of NLCs (Wu et al. 2016a).

4.3.4. Physicochemical characterization

Particle size of b-Dox-NLCs was found to be 105.2±3.5 nm. Biotinylation increased the size of NLCs from 100.5±2.3 nm to 105.2±3.5 nm. The surface charge of NLCs

did not changes as observed through zeta potential values, i.e., -35±2 mV. The anchoring of biotin to the NLCs surface was effected through formation of amide bond among –COOH group NH_2 group of SA-PEG-NH_2. Hence, zeta potential of the particles remained unaltered as it does not involve ionic interactions or surface adsorption phenomena. The drug entrapment efficiency for b-Dox-NLCs was observed to be 99.15±1.71% and drug content of b-Dox-NLCs were found to be 19.67±2.6 $mg.g^{-1}$ of NLCs.

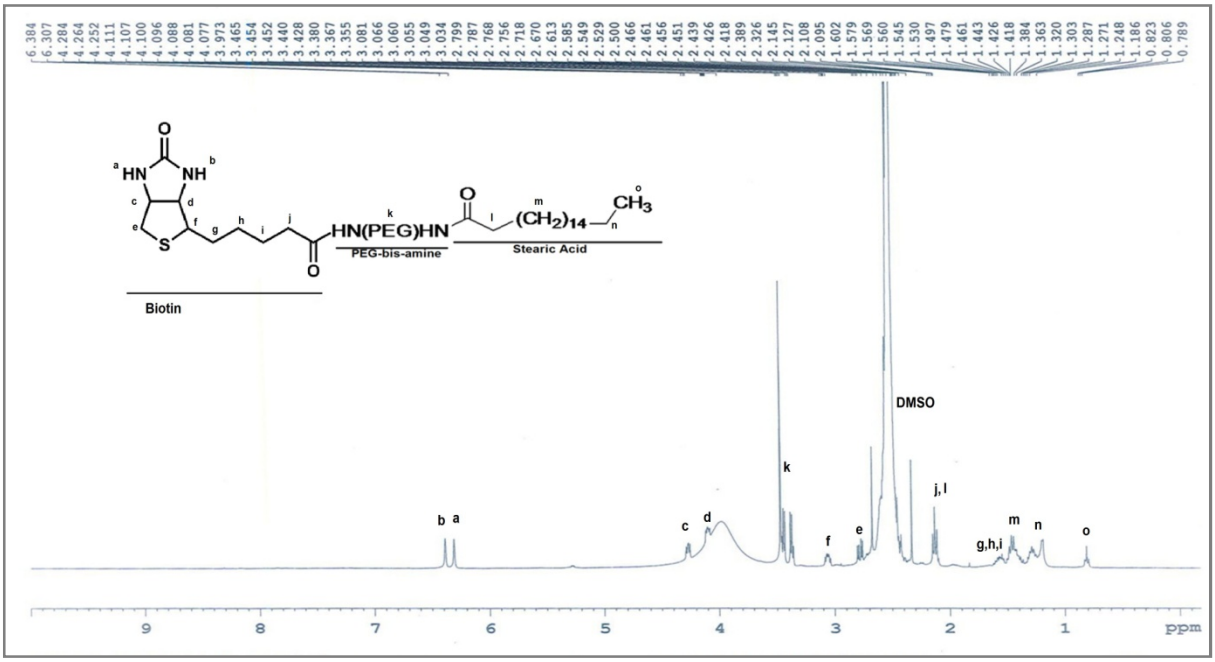

Fig. 4. NMR spectra of biotinylated stearic acid (b-PEG-SA)

4.3.5. *In vitro* drug release comparison

Drug release comparisons of the different formulation, *i.e.,* biotinylated Dox-NLCs (b-Dox-NLCs) and Dox-NLCs with standard drug and the marketed formulation showed sustained and pH dependent drug release from the NLCs **(Table 8 and Fig. 5)**. The cumulative drug release for the standard drug solution and the marketed formulations was 82.41±2.40% and 101.52±3.11%, respectively, in 2 h indicating pH independent drug release from both the formulations. An immediate type of drug release was observed from standard and marketed formulations. However, b-Dox-NLCs showed sustained and incomplete drug release which attained a plateau phase of 55.39±3.27% after 72 h. At lower pH of release media higher drug release i.e., 81.63±4.5% at pH 6.8, 98.66±3.43% at pH 5.4 was observed. A sustained release behavior was demonstrated by the NLCs with an initial burst release (34.42±4.50% in

2 h). As expected, lower pH (*i.e.*, pH 5.4) resulted in acceleration of the drug release with more than 70% of the drug release from NLCs in first 24 h. The drug (98.67±2.43%) releases was found to be nearly complete from f-Dox-NLCs at pH 5.4 in 72 h. No change in drug release between biotinylated and non-biotinylated NLCs as observed at physiological pH of pH 7.4.

Table 8. Release parameters of standard, marketed formulation, Dox-NLCs and b-Dox-NLCs at different pH

Time (h)	Standard (pH 7.4)	Standard (pH 6.8)	Marketed (pH 7.4)	Marketed (pH 6.8)	b-Dox-NLCs (pH 7.4)	b-Dox-NLCs (pH 6.8)	b-dox-NLCs (pH 5.4)	Dox-NLCs (pH 7.4)
1	81.97±4.5	85.97±4.5	101.54±5.3	101.54±5.3	20.91±2.4	26.89±3.4	33.91±2.9	23.91±2.4
2	82.41±2.4	86.41±2.3	101.52±3.1	102.71±3.1	27.24±3.5	34.42±4.5	42.78±3.4	28.24±3.5
3	82.65±3.33	85.65±3.33	100.22±2.99	101.22±2.99	35.59±4.6	41.49±4.6	50.54±3.1	33.59±4.6
4	82.45±2.45	85.45±2.45	100.11±2.23	101.11±2.23	40.14±4.02	49.61±5	58.77±4.1	41.14±4.02
8					42.82±4.3	55.88±4.3	64.43±3.1	41.28±4.3
12					43.47±3.4	63.47±3.4	72.12±5.1	43.74±3.4
24					49.22±5	72.22±5	83.11±3.5	48.22±5
36					51.21±2.7	79.18±2.7	92.67±4.3	51.98±2.7
48					55.79±3.5	80.79±3.5	97.11±2.2	56.29±3.5
60					55.26±4.21	81.97±4.03	98.62±3.21	56.6±4.21
72					55.39±3.27	81.63±4.05	98.66±3.43	56.59±3.27

[All the data is presented as mean±SD, n=3]

4.3.6. Transmission Electron Microscopy studies

All the particles of the formulation (b-Dox-NLCs) displayed uniform and spherical shape within the size range of 25.0-90.92 nm **(Fig. 6)**.

4.3.7. Stability of formulations in plasma and intravenous infusion solutions

A physically stable formulation is often expected for a drug delivery system for storage as well as longer circulation time and tumor accumulation through EPR effect. No particle aggregation and no significant change in particle size distribution of NLCs after storage with different formulations were observed, suggesting that the formulation was non-aggregated. There was no sign of disruption of b-Dox-NLCs in the presence of plasma proteins and electrolytes, either.

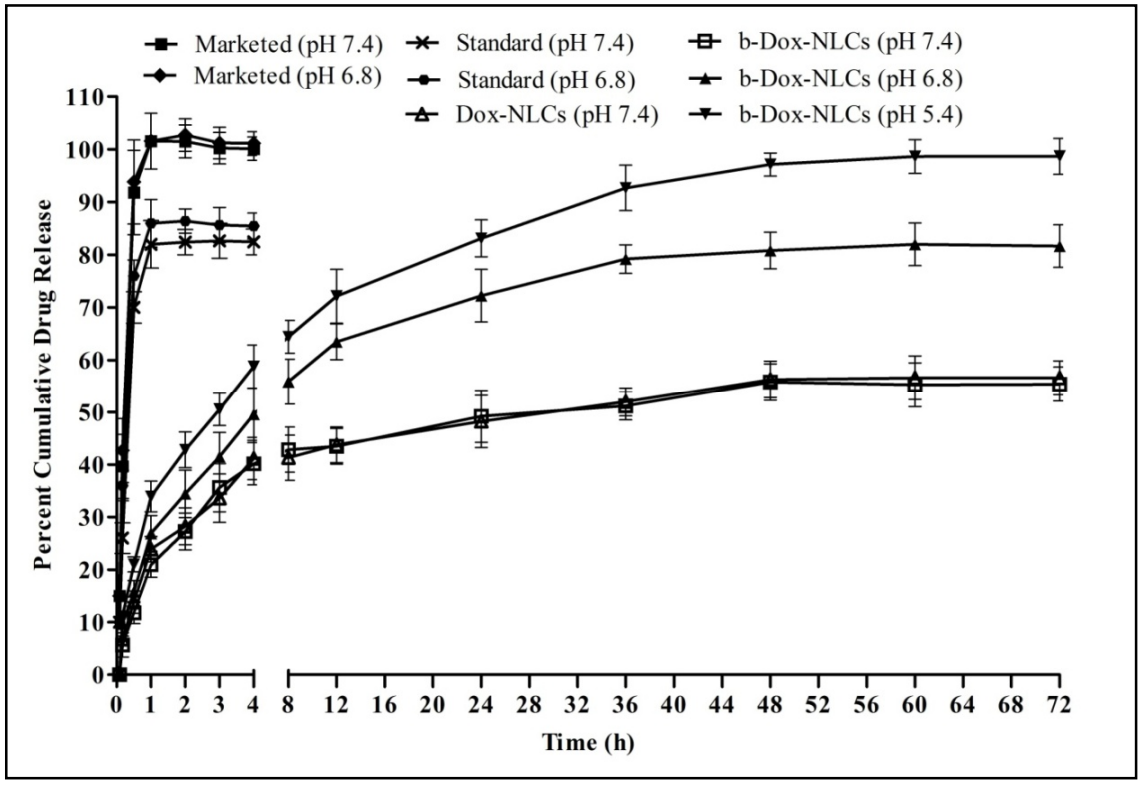

Fig. 5. Cumulative drug released for standard drug, marketed formulation, Dox-NLCs and b-Dox-NLCs. [Data is presented as mean±SD (n=6)]

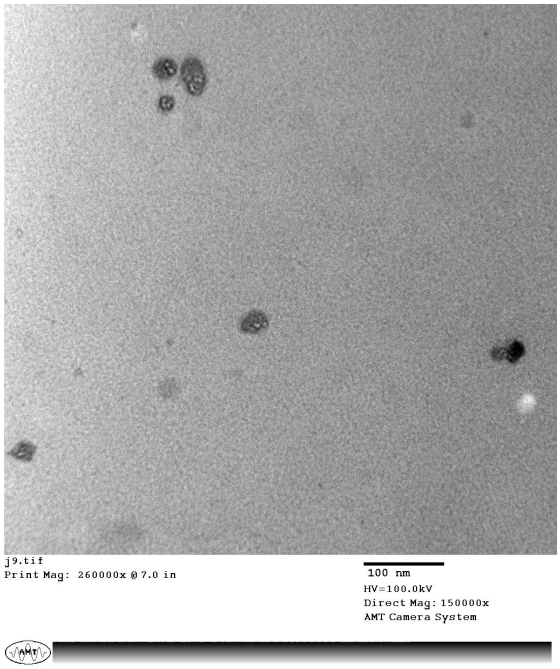

Fig. 6. TEM image of final formulation of b-Dox-NLCs depicting NLCs particles of uniform and spherical particles

4.3.8. Stability studies

The stability study data for the b-Dox-NLCs after storage for six months under different conditions assured that the optimized formulation was robust and stable under the specified stability conditions as significant change was not evident in particle size, F_2-values and drug content **(Table 9)** indicating formation of stable formulation (Singh et al. 2016d, Tripathi et al. 2016).

Table 9. Effect on the parameters of formulation during the stability studies

Time (months)	40±2 °C/75%±5% RH			25±2 °C/60±5% RH			5±3 °C		
	Drug Content (mg/g of formulation)	Particle Size (nm)	f_2 value (%)	Drug Content (mg/g of formulation)	Particle Size (nm)	f_2 value (%)	Drug Content (mg/g of formulation)	Particle Size (nm)	f_2 value (%)
0	19.67±2.6	105.2±3.5	91.6	19.67±2.6	105.2±3.5	91.6	19.67±2.6	105.2±3.5	91.6
1	20.11±2.3	107.1±3.1	89.7	19.71±2.8	104.6±2.8	93.4	19.41±2.9	104.8±2.9	81.5
3	20.33±2.5	106.6±2.5	93.6	20.22±1.9	106.7±2.3	89.9	18.99±1.9	106.6±2.4	92.6
6	18.97±1.6	109.2±3.7	85.2	19.57±2.1	106.9±3.6	88.6	19.47±2.4	104.5±3.1	89.9

4.4. *In vitro* studies

4.4.1. Cell Cytotoxicity study

MTT assay was performed to establish the cytotoxicity of different formulations, i.e., standard, marketed, Dox-NLCs and b-Dox-NLCs towards MCF-7 cell lines. IC_{50} values for b-Dox-NLCs, Dox-NLCs, Dox and marketed formulation against MCF-7 cell lines were observed as 1.02±0.18, 1.80±0.32, 2.96±0.33 and 2.806±0.21 $\mu g.mL^{-1}$, respectively **(Fig. 7)**. The cytotoxicity of f-Dox-NLCs and Dox-NLCs was significantly higher as compared to marketed and standard formulations. For NLCs loaded with ω3-FA only (p-NLCs), the IC_{50} value was found to be 4465±267 $\mu g.mL^{-1}$(data not shown). The IC_{50} value for p-NLCs indicated that *Perilla frutescens* oil has cytotoxicity potential for MCF-7 cells.

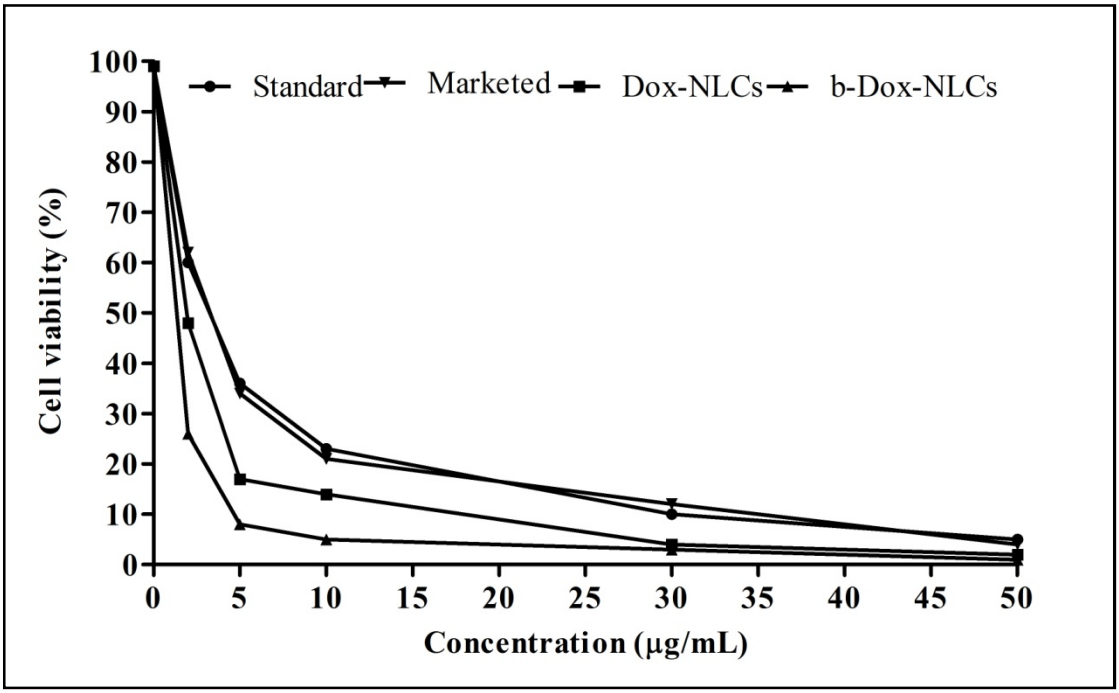

Fig. 7. Percent cell viability accessed through MTT assay for different cells groups treated with Standard (Pure Dox solution), marketed formulation, Dox-NLCs and b-Dox-NLCs.

4.4.2. Cell Cycle Analysis through FACS Technique

FACS analysis was performed to signify the phases of MCF-7 cellular arrest in various treated groups **(Fig. 8 A-E)**. Cellular arrest in different phases of the cell cycle showed that control group receiving no drug treatments, the cells were arrested 7.70% in G1 phase, 67.52% in S phase and 24.78% in G2/M phase (**Fig. 8A**). For the standard treatment group receiving doxorubicin solution the cells were arrested at G1 phase (46.56%), S phase (28.46%) and G2/M phase (25.00%) (**Fig. 8B**). For p-NLCs treated group cell distribution was found to be G1 phase (51.79%), G2 phase (16.47%) and S phase (31.74%) (**Fig. 8C**). The distribution of cells in b-Dox-NLCs treated cells were found to be 53.34% in G1 phase, 27.24% in S phase and 19.42% in G2/M phase (**Fig. 8D**). Apoptotic cell population was visualized in p-NLCs (9.02%) group suggesting that ω3-FA loaded NLCs were capable of inducing the apoptosis in the MCF-7 cell lines **(Fig. 8C)**.

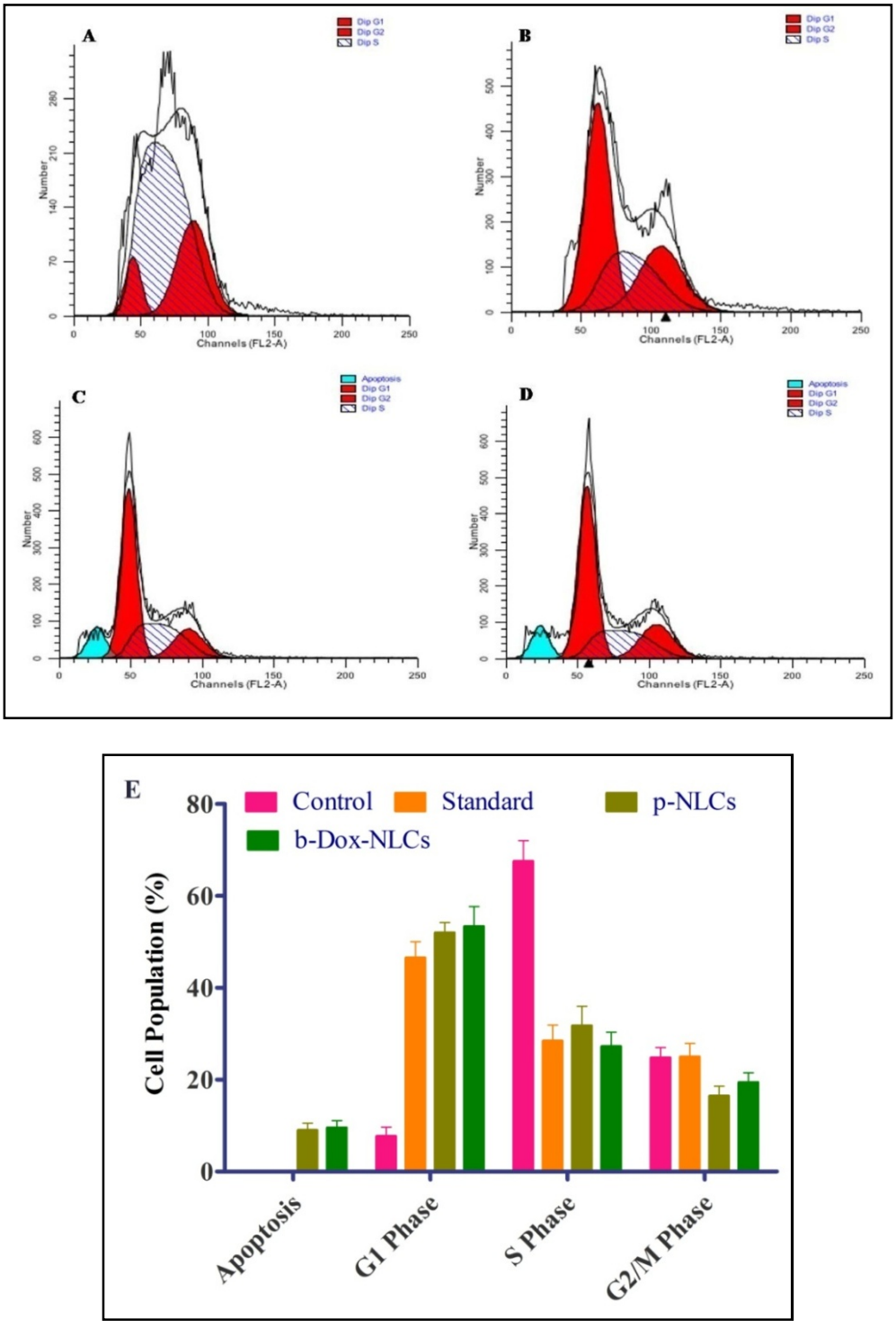

Fig. 8. FACS analysis of the cell treated with (A) Control (no treatment), (B) Standard (Dox solution), (C) p-NLCs (blank NLCs formulation with *Perilla frutescens* oil, no Dox), (D) b-Dox-NLCs representing cell distribution in different phase of cell cycle. (E) Percent population of cell in different phases.

4.4.3. Cell proliferation studies

Chemical reduction of Alamar Blue® from its oxidised, non-fluorescent blue form to its reduced fluorescent red form owing to the natural metabolic activity in highly proliferating MCF-7 cell lines provided a tool to examine the actual state of cellular proliferation. Cellular metabolic activity was indicated by the reduction of the blue dye to its fluorescent red form (O'Brien et al. 2000, Wang et al. 2018). The inhibition of cellular proliferation and Alamar Blue® reduction data depicted highest percent of cell proliferation inhibition for b-Dox-NLCs and Dox-NLCs *viz-à-viz* control cells ($p<0.001$) **(Fig. 9A&B)**. The b-Dox-NLCs and Dox-NLCs showed significant cell proliferation inhibition ($p<0.001$, $p<0.01$, respectively) as compared to standard and marketed formulations. The blank formulation having ω3-FA only (p-NLCs) showed 18.88±2.66% of the cell growth inhibition in contrast to the control group (Iyengar et al. 2013, Roy et al. 2017). The order for inhibition of cellular proliferation data was found to be in following order, b-Dox-NLCs> Dox-NLCs>marketed>standard>p-NLCs. Since, dead cells lack the metabolic activity therefore no change in color was observed and they also lack florescence suggesting that biotinylated NLCs were much more efficient to inhibit the MCF-7 cells.

4.4.4. Determination of mitochondrial membrane potential

MMP-dependent Rh-123 uptake and preferential accumulation into the mitochondria of the living cells followed by red spectral shifts and the quenching of fluorescence was employed to measure the changes of MMP of the MCF-7 cells undergoing apoptosis. The apoptosis in the cells results in the collapse of the MMP thereby lowering Rh-123 uptake and increased retention in the mitochondria (Al-Qubaisi et al. 2013, Musa et al. 2015). The results MMP showed that the b-Dox-NLCs and Dox-NLCs resulted in significantly ($p<0.01$) lower levels of Rh-123 fluorescence due to the higher cellular mortality in MCF-7 cells as compared to standard and the marketed formulation as shown in the **Fig. 10**. Further, b-Dox-NLCs were most effective in terms of reducing the number of MCF-7 cells as compared to non-biotinylated NLCs, standard, marketed and p-NLCs ($p<0.05$).

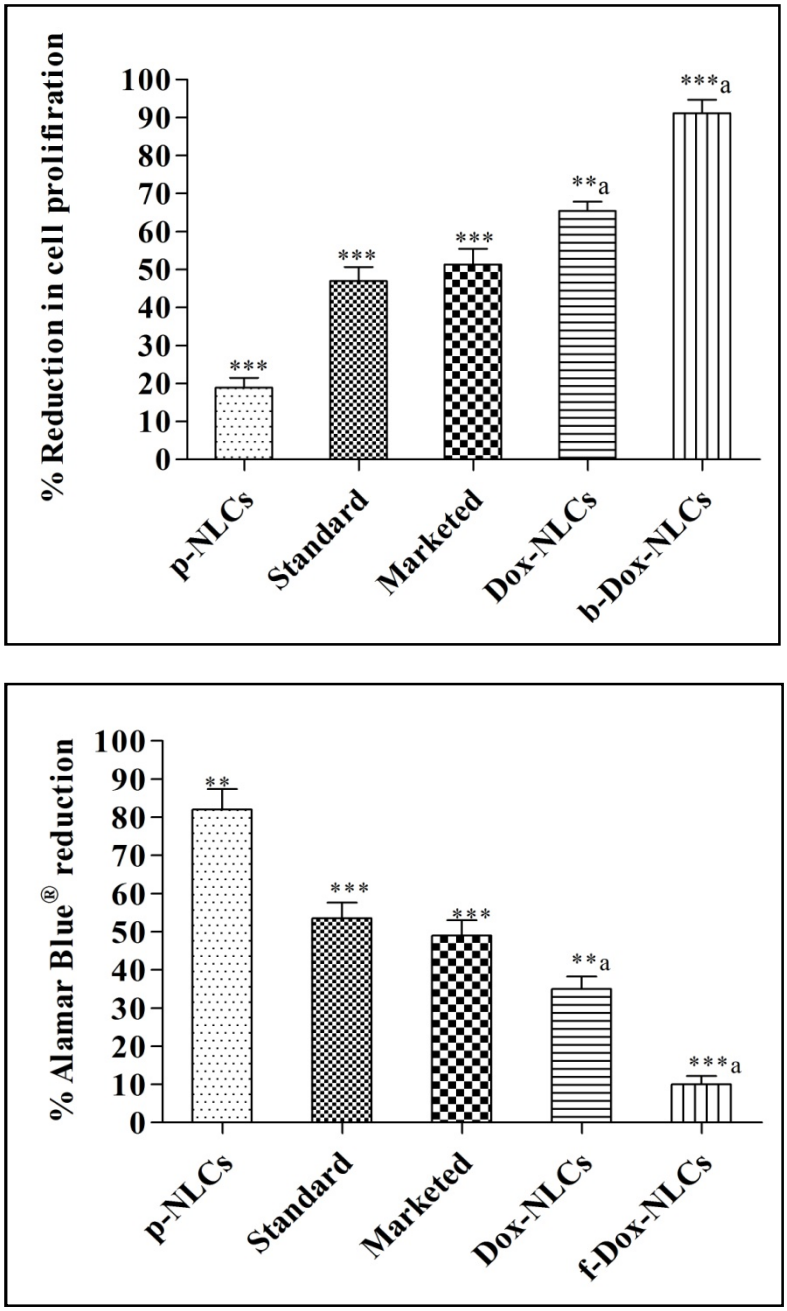

Fig. 9. Comparative presentation of *in vitro* data of formulations treated MCF-7 cell groups, *i.e.*, control, p-NLCs, Standard, marketed, Dox-NLCs b-Dox-NLCs. (A) % reduction in cell proliferation, and (B) %Almar Blue® reduction, compared to control group. [Data presented as the Mean±SD, n=3. *** $p<0.001$, ** $p<0.01$ with respect to control, **a $p<0.01$ w.r.t. marketed]

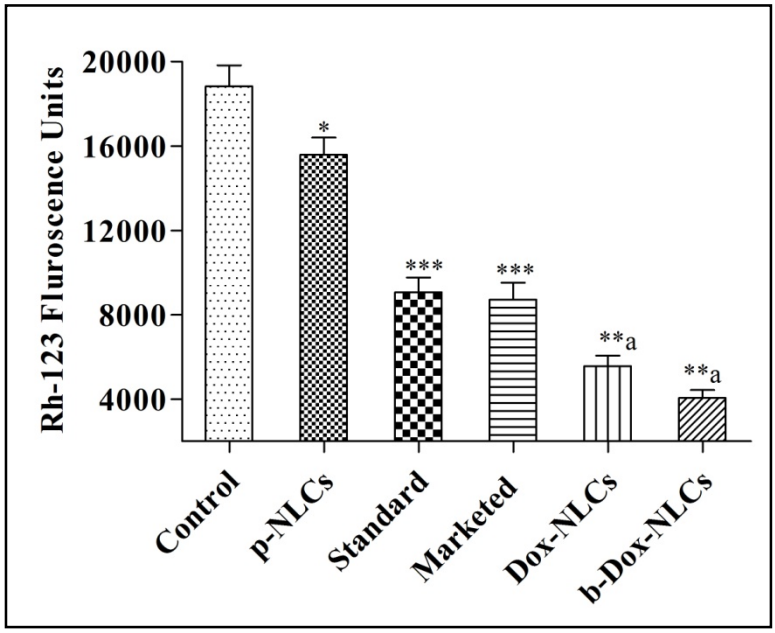

Fig. 10. Comparative presentation of Rh-123 fluorescence unit depicting MMP of cell groups, *i.e.,* control, p-NLCs, Standard, b-Dox-NLCs. [Data presented as the Mean±SD, n=3. *** p<0.001, * p<0.05 with respect to control, **a p<0.01 w.r.t. marketed]

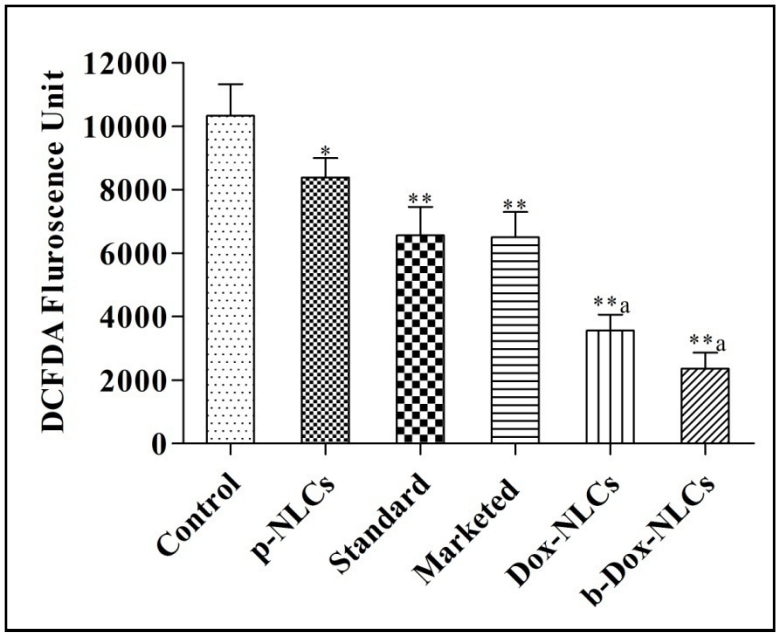

Fig. 11. Comparative presentation of DCF-DA fluorescence units presenting the ROS levels of cell groups, *i.e.,* control, p-NLCs, Standard, b-Dox-NLCs. [Data presented as the Mean±SD, n=3. ** p<0.01, * p<0.05 with respect to control, **a p<0.01 w.r.t. marketed]

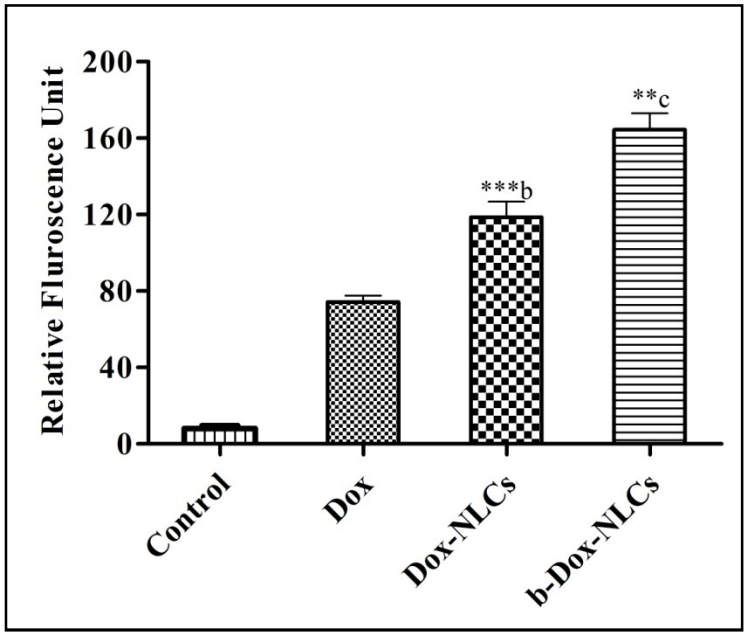

Fig. 12. Comparative presentation of relative fluorescence of FITC for cellular uptake determination of cell groups, *i.e.,* control, p-NLCs, Standard, b-Dox-NLCs. [Data presented as the Mean±SD, n=3. ***b $p<0.001$ w.r.t. Dox and ***c $p<0.001$ w.r.t. Dox-NLCs]

4.4.5. Determination of reactive oxygen species and mitochondrial membrane potential

DCF-DA is a reduced form of dye which is a cell-permeant and non-fluorescent in nature which upon entering into the cell gets converted into its fluorescent form DCF, after cleavage of acetate groups by intracellular esterase followed by oxidation (Figueroa et al. 2018, Ottonello et al. 2001).

The results of ROS estimation showed that the b-Dox-NLCs and Dox-NLCs resulted in significantly higher cellular mortality ($p<0.01$) indicated by lower levels of fluorescence as compared to standard and the marketed formulation as shown in the **Fig. 11**. Further, biotinylated NLCs were significantly more effective in terms of reducing the number of living cells as compared to non-biotinylated NLCs ($p<0.05$).

4.4.6. Cellular uptake through FACS analysis

The relative fluorescence of FITC for Dox, Dox-NLCs and b-Dox-NLCs treated groups **(Fig. 12)** demonstrated significant ($p<0.001$) cellular uptake of NLCs in comparison with doxorubicin solution. Biotin-anchored NLCs (b-Dox-NLCs) significantly increased the cellular internalization of Dox-loaded NLCs ($p<0.01$) when

compared with non-modified NLCs (Dox-NLCs) indicating biotin-mediated cellular uptake into MCF-7 cells.

4.5. *In vivo* studies

The positive outcomes of the *in vitro* studies prompted further investigation of *in vivo* anticancer efficacy of the developed carrier system in tumor-induced animal model. DMBA as a mammary gland carcinogen in rat has previously been established and validated in our laboratory. Mammary carcinoma induced with DMBA has been established to be morphologically and histopathologically similar to the human breast carcinoma (Alessandra-Perini et al. 2018, Haque and Pattanayak 2018, Kwon et al. 2018, Roy et al. 2017).

4.5.1. Tumor progression monitoring

Tumor progression was monitored through total tumor volume, animal weight changes and animal survival studies in the cancer-induced animal models. Animal weight, percentage survival and total tumor burden demonstrated mammary gland cancer development and progression in DMBA treated animal groups.

Significant weight reduction in mean weight of groups from day '0' was observed in toxic control (~45%) and p-NLCs (~36%) treated groups as compared to the treated groups, *i.e.,* b-Dox-NLCs (~5%), marketed (~15%) etc. from initial mean weights, respectively **(Fig. 13A)**. This indicates the lower rates of tumor incidences in groups treated with b-Dox-NLCs and Dox-NLCs.

Data of percentage animal survival throughout the study period suggested that highest animal survival was observed in the case of b-Dox-NLCs treated group followed by Dox-NLCs, standard and marketed drug treated groups. Results of the percent survival plot showed highest and lowest mortality in toxic and b-Dox-NLCs treated group, respectively **(Fig.13B)**. Total tumor volume measured in the various groups is presented in **Table 10.** Data revealed that toxic group possessed highest tumor volume while b-Dox-NLCs treated group resulted in lowest tumor volume among different groups studied.

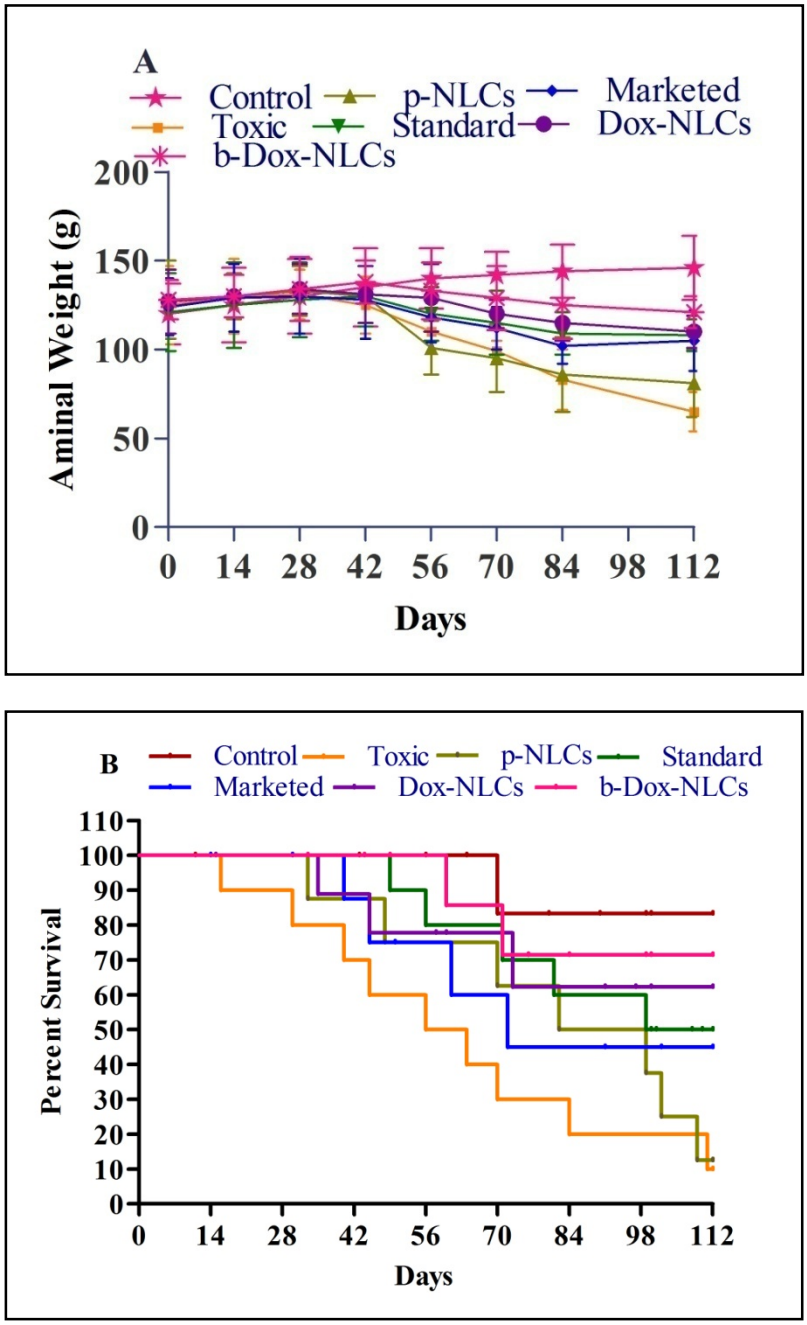

Fig. 13. (A) Mean body weight variation in animals groups (B) Kaplan-Meier plot representing percent animal survived throughout study [Data presented as mean±SD of group, n=10].

The effect of perilla oil (p-NLCs treated group), when correlated to the toxic group, the potential of ω3-FA content of *Perilla frutescens* oil in cancer prevention was clearly evident which was in corroboration with previous reports (D'Eliseo and Velotti 2016, Iyengar et al. 2013, Narisawa et al. 1994, Roy et al. 2017).

4.5.2. Biochemical estimation

It has been shown in different reports that treatment of animals with DMBA resulted in a significant disturbance in the biochemical machinery of cells. A Marked rise in the levels of biochemical markers in the toxic control group showed that significant lipid (TBARs) and protein (protein carbonyl) peroxidation occurs after DMBA administration. Treatment with different formulations successfully restored the levels of these biomarkers **(Table 10)**.

The DMBA treatment also resulted in significant changes in the equilibrium of antioxidant biochmicals like SOD, GSH, and catalase at a cellular level. The treatment of animals with formulations restored the levels of these biochemical's indicating the efficacy of the formulations. The effect of different formulations on the restoration of the biochemical markers was observed in the following order, b-Dox-NLCs>Dox-NLCs>marketed~standard>p-NLCs.

Table 10. Effect of treatment groups on tumor burden and oxidative stress markers in DMBA induced rat mammary gland carcinoma

Groups	**Tumor burden (cm^3)**	**TBARs (nm of MDA/µg of protein**	**Protein carbonyl nmol/mg of protein**	**GSH (Mg %)**	**SOD (units of SOD/mg of protein)**	**Catalase (nmol of H_2O_2/ min/mg of protein)**
Control	-	0.21± 0.03	41.99±1.02	1.31±0.08	0.028±0.002	23.44±1.42
Toxic Control	472.71±53.42	0.52±0.04	62.63±6.65	0.73±0.09	0.048±0.006	10.07±1.53
p-NLCs	393.91±40.23 **	0.43±0.05	58.12±3.81	0.81±0.08	0.045±0.003	13.25±1.12
Standard Drug	217.66±39.44 ***	0.34±0.04 *	49.11±2.23*	1.04±0.07 **	0.037±0.003*	18.52±2.02**
Marketed	220.77±28.53 ***	0.30±0.03 **	48.51±1.51*	1.07±0.08 **	0.036±0.003*	17.70±1.01**
Dox-NLCs**	164.95±22.48 ***a	0.24±0.03 *a	43.04±1.01**a	1.18±0.07	0.029±0.002* a	20.66±1.54*a
b-Dox-NLCs***	90.91±21.23* **a	0.21±0.02 **a	42.09±1.70**a	1.29±0.05 *a	0.028±0.001* *a	21.96±1.21**a

* p<0.05, ** p<0.01, *** p<0.001 w.r.t. toxic group; *a p<0.05, **a p<0.01, ***a p<0.001 w.r.t. marketed formulation treated group; data presented as mean±SD, n=10

4.5.3. Western blot analysis

Western blot analysis of the tissues separated from different animal groups was performed to evaluate the level of expression of different apoptosis modulating markers. The expression of anti-apoptotic markers i.e., bcl-2 (Ogretmen and Safa 1996, Vimala et al. 2014), MMP-9 (Karroum et al. 2012) and pro-apoptotic markers, i.e., BAX (Vimala et al. 2014), caspase-9 (Park et al. 2004) and p16 (Elmore et al. 2002, Hu et al. 2002) was estimated. It was found that levels of anti-apoptotic markers were upregulated while pro-apoptotic markers were downregulated after the DMBA administration to animals. Treatment with different formulations i.e., standard and b-Dox-NLCs offered significant restoration of these markers to the extent of the efficacy as compared to the toxic group favorably indicated apoptosis **(Fig. 14A)**. Densitometry data revealed the superiority of b-Dox-NLCs over Dox treatment in modulating the levels of different proteins **(Fig. 14B)**. Further, the MMP-9, p16 and members of the bcl-2 family protein, including bcl-2, BAX *etc*. exhibited an important role in breast cancer migration and invasion (Elmore et al. 2002, Hu et al. 2002, Karroum et al. 2012, Vimala et al. 2014). The result demonstrated that the biotin decorated NLCs can effectively reduce the mammary tumor cell metastasis in the disease induced rats.

4.5.4. Microscopy of whole mounts and H&E stain of mammary glands

The DMBA administration resulted in a significant increase in the number of AB/TEB in mammary gland tissue was as observed under a microscope, demonstrating the cellular proliferation in the mammary glands as depicted by carmine staining of tissue of toxic group. The treated groups presented significant defense against cell proliferation on DMBA treatment depicted by a lower number of AB/TEB count in treated groups. The effect of Dox-NLCs and b-Dox-NLCs was more prominent in lowering the AB/TEBs count as compared to standard and marketed formulation treatment **(Fig. 15)**. Similar results were observed after H&E staining of mammary gland tissues of the different groups represented through ducts, adipocytes, LCT, DCT and tissue architecture. Treatment with NLC based formulations showed significant restoration of cellular architecture closer to normal tissues (Kaithwas and Majumdar 2012, Moraes et al. 2009, Moraes et al. 2007, Roy et al. 2017).

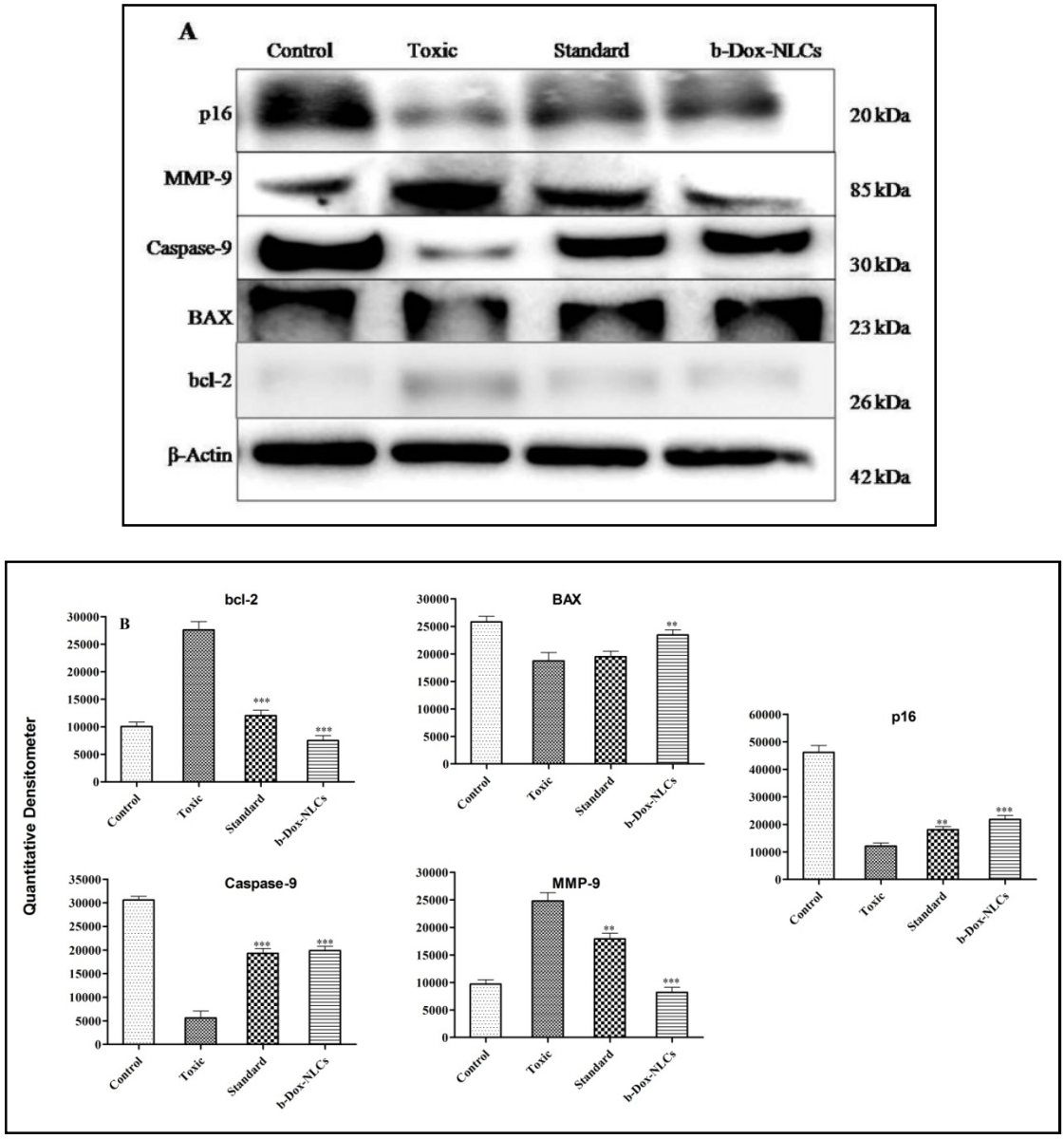

Fig. 14. (A) Immunoblot representing the regulation of mitochondria associated apoptosis modulating proteins isolated from mammary gland tissue of individual groups. (B) Level of proteins *viz.* BAX, caspase-9, bcl-2, MMP-9 and p16, extracted for individual groups *i.e.*, control, toxic control, Standard and b-Dox-NLCs. β-Actin was used as loading control. [Values are presented as Mean ± SD (n=3). The test groups were compared to the toxic group (*p<0.05, **p<0.01, ***p<0.001).]

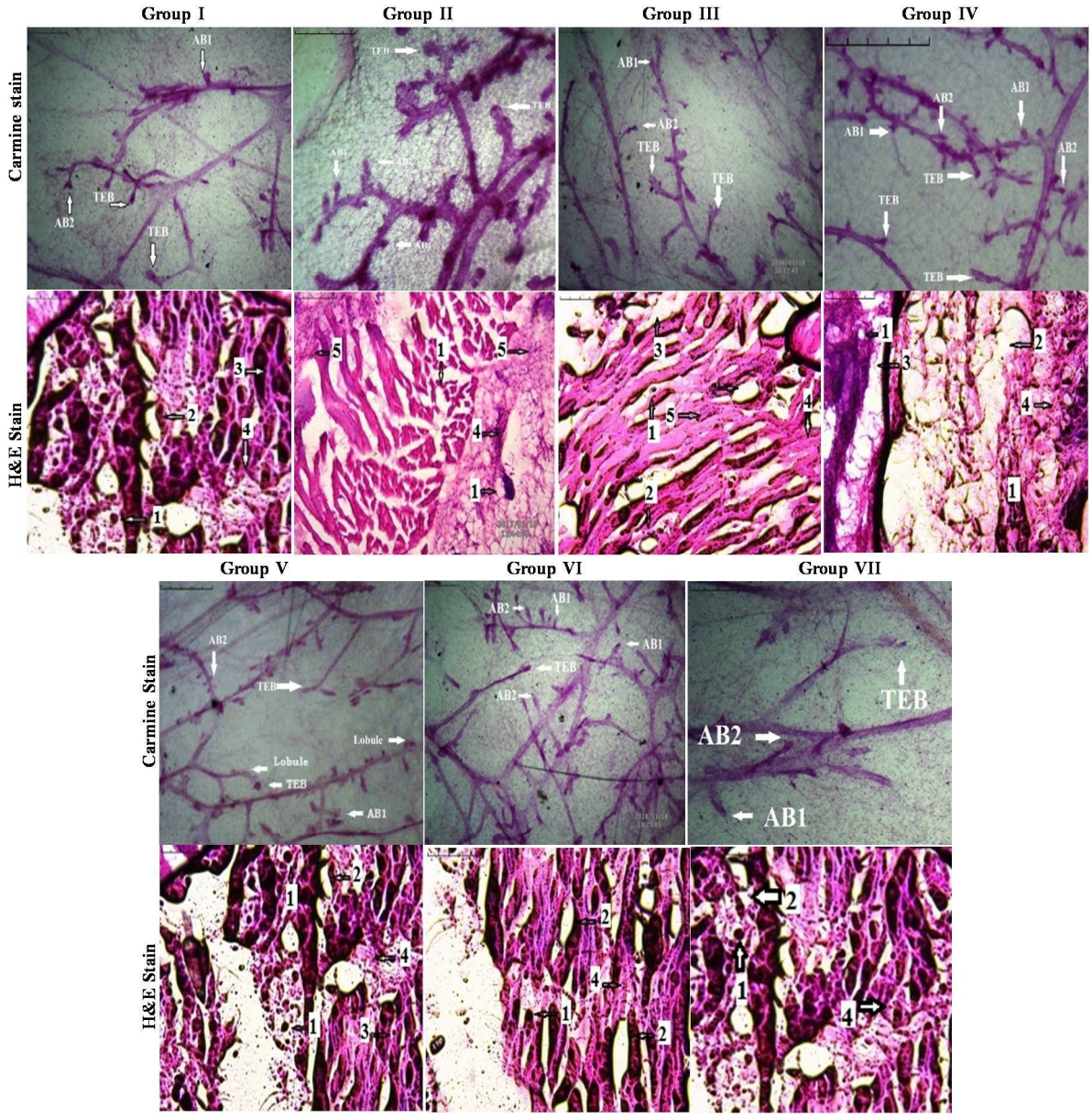

Fig. 15. Whole mount of the mammary gland tissue and histograms of H&E stain of the animal groups (A) Group I (Control), (B) Group II (toxic control), (C) Group III (p-NLCs, blank NLCs, no Dox), (D) Group IV (standard drug solution or Dox solution), (E) Group V (Marketed formulation), (F) Group VI (Dox-NLCs), (G) Group VII (b-Dox-NLCs). [TEB-Terminal end bud, AB-Alveolar buds; 1-ducts, 2-adepocytes, 3-LCT, 4-MCT, 5-lyphocytes].

4.5.5. Cardiotoxicity studies

Doxorubicin is known to induce cardiotoxicity due to dose-related lipid and protein peroxidation resulting in tissue necrosis in cardiac tissues. Dox administrations in experimental animals caused the significant changes in MDA and GSH levels in

cardiac tissues (Cai et al. 2010, Trivedi et al. 2011). However, b-Dox-NLCs treated group showed no significant changes in the levels of these markers indicating lack of any lipid or protein peroxidation in cardiac tissues **(Fig. 16A&B)**. Also, p-NLCs that contain perilla oil, only, showed no change level of these markers and the MDA and GSH levels were unaltered.

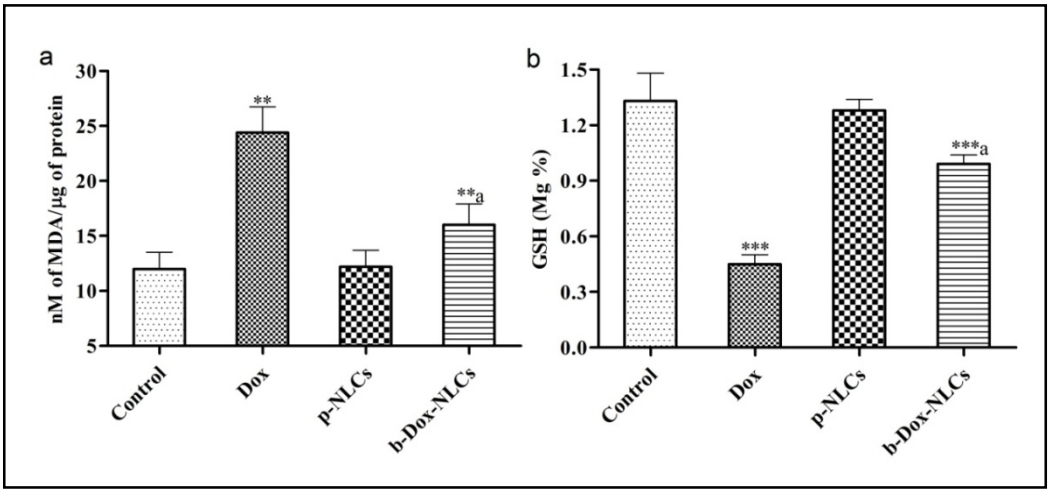

Fig. 16. Plot showing (A) MDA levels and (B) GSH levels in rat heart tissue after treatment with Control, p-NLCs, Dox and b-Dox-NLCs. All treatments were given as once a week for 5 weeks with equivalent Dox 4 $mg.kg^{-1}$. [All the values are expressed as mean ± SD, (n = 6); ** $p<0.01$, *** $p<0.001$ versus control and **a $p<0.01$, ***a $p<0.001$ versus Dox treatment.]

4.5.6. Biodistribution studies

Higher targeting efficiency of the delivery system is often required for the successful outcome of anticancer drug therapy without affecting normal tissues. A comparative account of the Dox concentration in the different tissue/organs is presented in **Fig. 17**. The Dox levels attained in the mammary carcinoma was highest in the case of the b-Dox-NLCs (55.03±2.55 µg/g organ in 4 h) followed by the Dox-NLCs (45.81±3.22 µg/g organ in 4 h) indicating the specific accumulation of the biotin decorated NLCs in mammary tumor cells **(Fig. 17 C&D)**. The Dox levels in case of pure Dox and the marketed formulation were nearly similar **(Fig. 17 A&B)** and were significantly lower in comparison to b-Dox-NLCs ($p<0.001$) treated group. The Dox level was significantly higher at 4 h post injection and was barely detectable after 48 h (except for b-Dox-NLCs group), owing to the short half-life of the drug in blood. Further, significantly higher Dox levels were maintained in the mammary cancer cells for a period of upto 48 h (20.77±1.33 µg/g organ) in the b-Dox-NLCs ($p<0.001$); upto 12 h

(20.15±2.56 µg/g organ) in the Dox-NLCs ($p<0.001$) treated groups *vis-à-vis* the pure Dox (14.53±2.22 µg/g in 12 h, 1.67±1.42 µg/g in 48 h) and the marketed formulation (17.55±2.01 µg/g in 12 h, 1.57±1.33 µg/g in 48 h) treated groups. Similar inference can be drawn for other time points as well. Among different organs, highest Dox concentration was observed in the liver followed by the spleen, the heart and the kidney. The Dox level in the heart tissue in b-Dox-NLCs treated group was lesser when compared to the other groups ($p<0.05$). The results are in corroboration with the cardiotoxicity results as described earlier. Overall, the Dox levels in different organs of the biotin decorated NLCs were relatively lower than that of other animal groups, which was in accordance with the published literature (Dharmalingam et al. 2014, Lee et al. 2005).

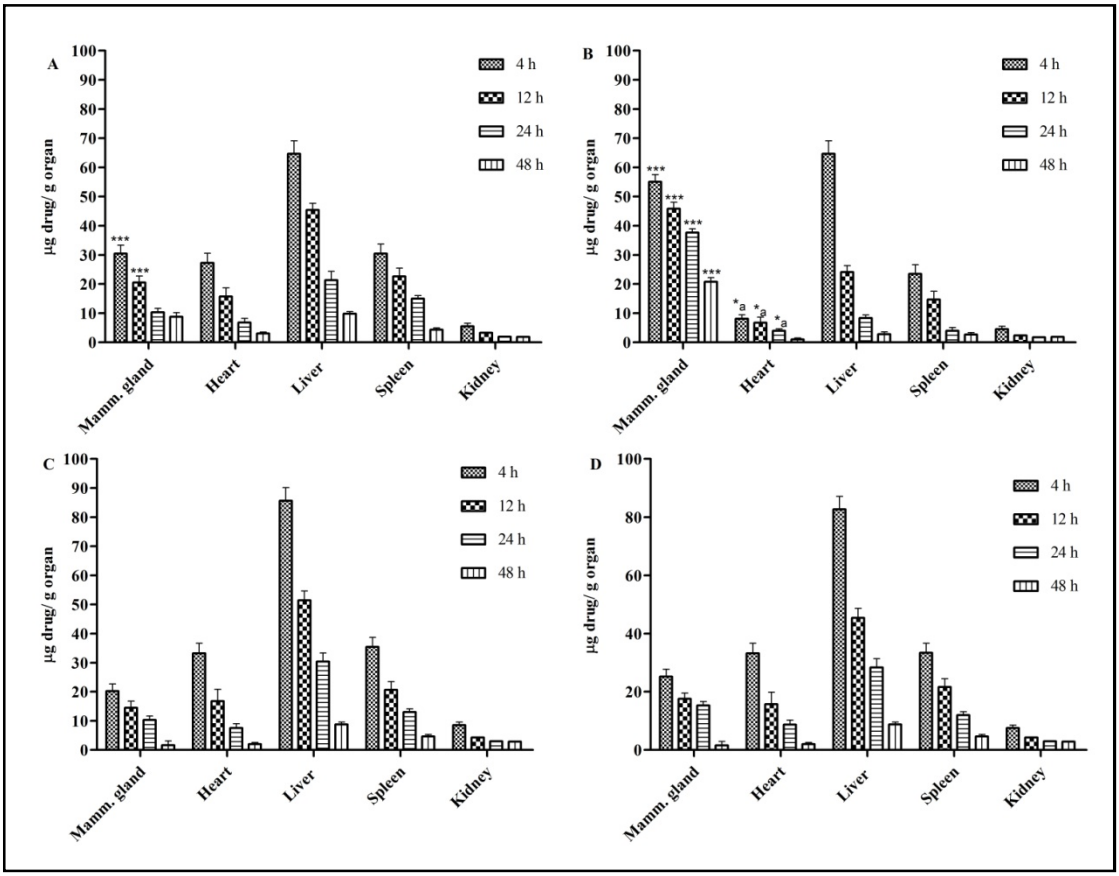

Fig. 17. Level of Dox in different organs (mammary gland, heart, liver, spleen, and kidney) after i.v. administration through tail vein (10 mg/kg Dox equivalent dose) of (A) Dox-NE (B) b-Dox-NLCs, (C) Standard (Pure Dox solution), and (D) Marketed formulation, in DMBA (8 mg/kg) induced rats. [Values are presented as Mean ± SD (n=6); *** $p<0.001$ as compared to standard and marketed; *a $p<0.05$ as compared to other groups].

5. Discussion

In the era of nanomedicine therapies, advancement in targeted therapies, antibody therapies, small molecules drug conjugates etc. have earned more and more interest of formulation scientists in the current period. Targeted drug delivery systems modified with molecular ligand are capable of selective delivery and accumulation of one or multiple drugs loaded or encapsulated into the system to the targeted disease or site through relevant receptors overexpressed on the target cells or tissue (Jiang et al. 2013, Kandadi et al. 2012, Kouchakzadeh et al. 2017, Lammers et al. 2008, Liu et al. 2011, Mizushima 1996). In the present study, biotin was exploited as a targeting molecule to surface modify *Perilla frutescence* oil based nanostructured lipid carriers for doxorubicin targeted delivery to mammary gland carcinoma using in rat animal model.

For the preparation of NLCs melt emulsification followed by sonication was selected that produced the stable and smaller nanoparticles. Between the solid lipids, stearic acid yielded lowest particle size ranges. Particle size and stability data suggested that solid lipid and liquid lipid in range ratio of 70:30 produced stable and narrower particles and hence selected for further studies (Singh et al. 2016b, Singh et al. 2016c, Singh et al. 2016d). QbD concept was successfully employed for development and optimization of NLCs. Central composite design was employed, 17 experimental trials were performed and optimized formulation was identified using overlay plot. The optimized formulation contained 2% w/w of total lipid, 3% w/w surfactant, triethanolamine 20 mg and along with 20 min of sonication time (Singh et al. 2011, Tripathi et al. 2016, Tripathi et al. 2017).

The attachment of biotin to NLCs was successfully affirmed by characteristic FTIR peaks and NMR spectrum of modified stearic acid and HABA/avidin assay. HABA is a dye that shows UV maxima (λ_{max}) at 350 nm. It can bind to avidin to form HABA avidin complex, in the same binding site that is used by biotin to form an avidin-biotin complex. HABA after formation of a complex with avidin gives maximum UV absorption maxima at 500 nm. The affinity of HABA is much weaker ($K_{d,}$ 10^{-6} M)) as compared to the affinity of biotin to avidin (K_d, 10^{-15} M). Therefore, addition of biotinylated NLCs to the solution of avidin/HABA complex, HABA is competitively and quantitatively replaced by biotin from avidin/HABA complex, and this

replacement was quantitatively observed by a decrease in absorbance maxima at 500 nm (Bae et al. 2013, Lee and Low 1994, Wu et al. 2016a).

SA-PEG-NH_2, a hydrophilic moiety, would naturally align itself on the surface of NLCs with PEG-NH_2 chain protruding out on which biotin was attached. Since SA-PEG-NH_2 accounts for approximately 2.5% w/w of the formulation, the inherent qualities of stearic acid would nonetheless be displayed.

Incorporation of liquid lipid enabled a higher drug loading and controlled release of the drug. Higher liquid lipid content was able to dissolve drug in the matrix as well as prevented expulsion of drug from nanoparticles. Addition of triethanolamine resulted in the formation of Dox free base from doxorubicin hydrochloride, thereby improving the lipophilicity and solubility of Dox in the lipid phase. Further, an addition of anionic polyunsaturated fatty acid (ω3-FA content of *Perilla frutescence* oil) has shown to increase the entrapment of drug to lipid matrix via the formation of hydrophobic ion pairing (HIP) with amphiphilic Dox as described below.

$DOX\text{-}NH_3^+ + N(CH_2CH_2OH)_3 \leftrightarrow DOX\text{-}NH_2 + NH^+(CH_2CH_2OH)_3Cl$

$DOX\text{-}NH_2 + R\text{-}COOH \leftrightarrow DOX\text{-}NH_3^+R\text{-}COO$

$R\text{-}COOH + N(CH_2CH_2OH)_3 \leftrightarrow R\text{-}COO \quad + NH^+(CH_2CH_2OH)_3$

The HIP strategy involves modification of the lipophilicity of the drugs of amphiphilic or ionizable nature by shielding their charge with a lipophilic counter-ion without involving chemical modification. Further, the interaction between the lipophilic tails of ion pairs and the solid lipid matrix may lead to disorderly arrangement of the lipid crystalline structure. Also, the charges of both the ions are masked or shielded through long hydrocarbon moieties attached to the ionic groups, consequently, hydrophobicity higher than that of both the respective molecules separately, occurs (Mussi et al. 2013, Oliveira et al. 2017).

Dox released from NLCs at physiological conditions was found to be slower and incomplete in comparison to release at relatively lower pH, *i.e.,* pH 6.8 and pH 5.4**.** The acidic environment causes the dissociation of Dox and ω3-fatty acids ion-pairs and erosion of lipid matrix resulting into faster release of Dox from lipid matrix. Faster release at lower pH is a desirable characteristic for drug delivery to the tumor as relatively acidic microenvironment has been observed inside tumors which might

facilitate site specific delivery (Cai et al. 2010, Lee et al. 2005, Tannock and Rotin 1989). The TEM and particle size analysis results showed the successful formation of nanostructured lipid carriers. There was no particle aggregation and no significant change in particle size distribution which confirmed the formation of a physically stable formulation. Accelerated stability studies demonstrated the formation of a robust and stable formulation which would retain its characteristics even after storage for a longer period of time.

Cellular cytotoxicity studies through MTT assay revealed higher mortality as reflected through IC_{50} values of biotinylated NLCs followed by Dox-NLCs, Dox and marketed formulations. FACS analysis of the cells treated with different formulation showed that Dox treatment arrested most of the cells in G1 phase followed by S phase and G2 phase. The NLCs containing *Perilla frutescens* oil, only, arrested the cells in G2/M phase while b-Dox-NLCs arrested cells in G1 as well as G2 phase of cell cycle. Cellular proliferation, ROS and MMP studies demonstrated the superiority of biotin anchored NLCs in promoting cellular apoptosis and thereby resulting in higher cellular mortalities in comparison to formulations. Anticancer agents have been shown to depolarize the mitochondrial associated potential which leads to the initiation of the mitochondria mediated apoptotic pathway in tumor cells. The cellular uptake studies further supported the above results for higher cellular mortality and cytotoxicity of b-Dox-NLCs when compared to Dox. The above inferences can better be explained through positive interaction of lipidic nanoparticles with lipid cell membrane in case of both Dox-NLCs and b-Dox-NLCs. The relatively higher cytotoxicity in case of b-Dox-NLCs can be best justified through receptor ligand interaction of biotin overexpressed receptor followed by cellular internalization. Several studies have reported the anti-tumorigenic potential of ω3-fatty acids that can induce the mitochondrial apoptosis in mammary gland carcinoma which may provide another possible explanation for higher cellular mortality after b-Dox-NLCs treatment (Figueroa et al. 2018, Huan et al. 2009, Lee et al. 2005, Musa et al. 2015, O'Brien et al. 2000, Ottonello et al. 2001, Riccardi and Nicoletti 2006, Roy et al. 2017, Singh et al. 2016a, Vimala et al. 2014, Wang et al. 2014, Weitman et al. 1992).

The positive outcomes observed through *in vitro* studies provided strong evidences to further explore the delivery system for *in vivo* anticancer efficacy of biotin decorated NLCs systems in DMBA induced breast tumor in rat as animal model. A reduction

(48%) in mean animal weights was observed in case of toxic group. In case of other groups p-NLCs treated group showed 36.71% reduction, standard group 10.74% reduction, marketed formulation 15.32% reduction, Dox-NE 13.38% reduction, while b-Dox-NLCs showed least reduction in weight of animal from day '0' of the study. In line with above data, highest number of animals survived after completion of study in case of f-Dox-NLCs treated groups. The lowest percentage survival was observed in case of toxic group. Further, total tumor burden demonstrated the induction and progression of mammary gland cancer in DMBA treated animal groups was found to be highest in case toxic group. While b-Dox-NLCs treated group demonstrated lowest toxicity. Aerobic cells constantly produce reactive oxygen species which are counter balanced by antioxidant enzymatic biochemicals like, GSH, SOD and catalase. However, under the stress conditions like tumor, these enzymatic biochemicals are suppressed (Kaithwas and Majumdar 2012, Roy et al. 2017). Pronounced damage of the cellular proteins and lipids was observed in DMBA administered animals as depicted through TBARS, a peroxidative marker of the lipid and protein carbonyl, the protein peroxidation marker. Similarly, increased ROS generation also compromised the antioxidant bio-machineries as indicated through SOD, GSH and catalase levels, as these biochemical's act in close coordination to neutralize the oxidative species through series of peroxidation, dismutation and oxidation reactions (Al-Qubaisi et al. 2013, Kaithwas and Majumdar 2012). The b-Dox-NE treatment significantly restored these biomarkers viz-à-viz marketed and standard formulation.

The results of western blotting assay demonstrated the overexpression of anti-apoptotic and pro-metastatic markers like bcl-2 and MMP-9; and downregulation of pro-apoptotic and anti-metastatic proteins such as Caspase-9, p16 and BAX on DMBA administration to the rats. Treatment with b-Dox-NLCs and Dox leads to restoration of these proteins to a level closer to the control group. The effect was far more pronounced in the former group (b-Dox-NLCs). Role of bcl-2, MMP-9, p16 and BAX are critical for metastasis of mammary cancer cells (Elmore et al. 2002, Hu et al. 2002, Karroum et al. 2012, Lee et al. 2005, Singh et al. 2016a, Vimala et al. 2014, Wang et al. 2014). MMP-9 act through PKC and ERK1/2 signaling pathways (Karroum et al. 2012) and bcl-2 family proteins viz., bcl-2 and BAX act through COX Va, myosin Va and Twist1 (Ogretmen and Safa 1996, Um 2016, Vimala et al. 2014). Upregulation of p16 have been shown to inhibit cdks (accelerate cellular

proliferation), through deregulation of cyclin D1, which in turn dephosphorylates RB. This result in the deactivation of the transcription factors E2F, involved in DNA synthesis and cell cycle progression (Elmore et al. 2002, Hu et al. 2002). ω3-FA stabilizes HIF-1 α and down-regulates FASN that initiate mitochondrial apoptosis in mammary gland carcinoma (Roy et al. 2017). The treatment with b-Dox-NLCs resulted in lowering of AB/TEB count, restoration of cellular architecture and morphology manifested through decrease in micro-vessel formation and absence of enlarged capillaries. These observations suggested a tumor modulatory effect mediated by the targeted delivery of Dox and the ameliorative activity of the ω3-FA content of *Perilla frutescens* oil (Kaithwas and Majumdar 2012, Moraes et al. 2009, Moraes et al. 2007, Roy et al. 2017). The biodistribution and cardiotoxicity data further confirmed the selective accumulation of the biotin guided NLCs to biotin receptors which are overexpressed in mammary gland carcinoma. Higher uptake of NLCs by liver and spleen may possibly be explained through the involvement of mononuclear phagocytic systems as well as higher capture by liver cells as it acts as a major storage organ for biotin.

As evident from previous discussion, biotin attached delivery system effectively regulated the cancer proliferation, invasion and migration in mammary gland carcinoma. The mammalian cells are incapable of themselves synthesizing the biotin; therefore it is taken up through transport systems like high-affinity biotin transporter or sodium-dependent multivitamin transporter (SMVT). The overexpression of SMVT as well as increased biotin uptake capacity in the cancer cells may be a possible explanation for selective uptake of biotin decorated NLCs for mammary cancer. Attachment of biotin through a relatively long PEG chain linker resulted in effective ligand-receptor association and internalization of the complex in cancer cells. The above findings would further be described by the facts; firstly that ω3-FA of *Perilla frutescens* oil has cancer ameliorative and inhibitory effect. Also, these act as antioxidants for normal cells, thereby preventing the drug induced toxicities. Secondly, biotinylation of NLCs directed the system specifically to mammary gland cancer cells and facilitated endocytosis of the delivery systems to the cancer cells. Finally, the acidic microenvironment of the tumor cells facilitated drug release from NLCs would further enhance site specific drug delivery. The combined effects of the above should effectively address mammary gland carcinoma.

6. Conclusion

Systematic development and exhaustive evaluation of *Perilla frutescens* oil based NLCs was attempted for site specific delivery of doxorubicin to DMBA induced mammary gland cancer. Biotin anchored NLCs were successfully developed and investigated for different physicochemical parameters that confirm the formation of NLCs with drug extended release. Quaternary ammonium compound (triethylamine) helped in improvement of entrapment of amphiphilic molecule, *i.e.,* doxorubicin in lipidic matrix of NLCs through hydrophobic ion pairing with fatty acids. CCD helped in successful development of NLCs as revealed by physicochemical evaluations. ω3-FA as well as other content of *Perilla frutescence* oil showed strong antioxidant activity for normal cells as well as enhanced the anticancer potential of Dox in cancer cells. The anti-proliferative and apoptotic potential of the NLCs formulation were confirmed through the activity against MCF-7 cell lines. The developed NLCs revealed higher cytotoxicity towards MCF-7 tumor cells as shown through ROS and MMP data suggesting mitochondria mediated apoptosis. Western blotting studies revealed an upregulation of pro-apoptotic and anti-migratory proteins by NLCs treatment. *In vivo* anticancer studies in DMBA induced rat mammary gland model suggested higher safety and efficacy of NLCs *viz-à-viz* marketed formulation. Biodistribution studies affirmed that the biotinylated NLCs selectively accumulate in the tumor. Therefore, we can conclude that the NLCs can act as a potential alternative to the conventional formulations in mammary gland carcinoma therapy.

7. References

Al-Qubaisi MS, Rasedee A, Flaifel MH, Ahmad SH, Hussein-Al-Ali S, Hussein MZ, Zainal Z, Alhassan FH, Taufiq-Yap YH, Eid EE, Arbab IA, Al-Asbahi BA, Webster TJ, El Zowalaty ME (2013) Induction of apoptosis in cancer cells by NiZn ferrite nanoparticles through mitochondrial cytochrome C release. Int J Nanomedicine. 8(0):4115-29.

Alessandra-Perini J, Perini JA, Rodrigues-Baptista KC, de Moura RS, Junior AP, Dos Santos TA, Souza PJC, Nasciutti LE, Machado DE (2018) Euterpe oleracea extract inhibits tumorigenesis effect of the chemical carcinogen DMBA in breast experimental cancer. BMC Complement Altern Med. 18(1):116.

Bae PK, Jung J, Lim SJ, Kim D, Kim SK, Chung BH (2013) Bimodal perfluorocarbon nanoemulsions for nasopharyngeal carcinoma targeting. Mol Imaging Biol. 15(4):401-10.

Cai C, Lothstein L, Morrison RR, Hofmann PA (2010) Protection from doxorubicin-induced cardiomyopathy using the modified anthracycline N-benzyladriamycin-14-valerate (AD 198). J Pharmacol Exp Ther. 335(1):223-30.

Cho K, Wang X, Nie S, Chen ZG, Shin DM (2008) Therapeutic nanoparticles for drug delivery in cancer. Clin Cancer Res. 14(5):1310-16.

D'Eliseo D, Velotti F (2016) Omega-3 Fatty Acids and Cancer Cell Cytotoxicity: Implications for Multi-Targeted Cancer Therapy. J Clin Med. 5(2):pii: E15.

Dharmalingam SR, Ramamurthy S, Chidambaram K, Nadaraju S (2014) A simple HPLC bioanalytical method for the determination of doxorubicin hydrochloride in rat plasma: application to pharmacokinetic studies. Trop J Pharm Res. 13(3):409-15.

Elmore LW, Rehder CW, Di X, McChesney PA, Jackson-Cook CK, Gewirtz DA, Holt SE (2002) Adriamycin-induced senescence in breast tumor cells involves functional p53 and telomere dysfunction. J Biol Chem. 277(38):35509-15.

Fernandes RS, Silva JO, Mussi SV, Lopes SCA, Leite EA, Cassali GD, Cardoso VN, Townsend DM, Colletti PM, Ferreira LAM, Rubello D, de Barros ALB (2017) Nanostructured Lipid Carrier Co-loaded with Doxorubicin and Docosahexaenoic Acid as a Theranostic Agent: Evaluation of Biodistribution and Antitumor Activity in Experimental Model. Mol Imaging Biol: doi: 10.1007/s11307-017-1133-3.

Figueroa D, Asaduzzaman M, Young F (2018) Real time monitoring and quantification of reactive oxygen species in breast cancer cell line MCF-7 by 2',7'-dichlorofluorescin diacetate (DCFDA) assay. J Pharmacol Toxicol Methods. 94(Pt 1):26-33.

Haque MW, Pattanayak SP (2018) Taxifolin Inhibits 7,12-Dimethylbenz(a)anthracene-induced Breast Carcinogenesis by Regulating AhR/CYP1A1 Signaling Pathway. Pharmacogn Mag. 13(4):S749-S55.

Hu H, Ahn NS, Yang X, Lee YS, Kang KS (2002) Ganoderma lucidum extract induces cell cycle arrest and apoptosis in MCF-7 human breast cancer cell. Int J Cancer. 102(3):250-53.

Huan ML, Zhou SY, Teng ZH, Zhang BL, Liu XY, Wang JP, Mei QB (2009) Conjugation with alpha-linolenic acid improves cancer cell uptake and cytotoxicity of doxorubicin. Bioorg Med Chem Lett. 19(9):2579-84

Iyengar NM, Hudis CA, Gucalp A (2013) Omega-3 fatty acids for the prevention of breast cancer: an update and state of the science. Curr Breast Cancer Rep. 5(3):247-54.

Jiang SP, He SN, Li YL, Feng DL, Lu XY, Du YZ, Yu HY, Hu FQ, Yuan H (2013) Preparation and characteristics of lipid nanoemulsion formulations loaded with doxorubicin. Int J Nanomedicine. 8(0):3141-50.

Kaithwas G, Majumdar DK (2012) In vitro antioxidant and in vivo antidiabetic, antihyperlipidemic activity of linseed oil against streptozotocin-induced toxicity in albino rats. Eur J Lipid Sci Technol. 114(11):1237–45.

Kandadi P, Syed MA, Goparaboina S, Veerabrahma K (2012) Albumin coupled lipid nanoemulsions of diclofenac for targeted delivery to inflammation. Nanomedicine. 8(7):1162-71.

Karroum A, Mirshahi P, Faussat AM, Therwath A, Mirshahi M, Hatmi M (2012) Tubular network formation by adriamycin-resistant MCF-7 breast cancer cells is closely linked to MMP-9 and VEGFR-2/VEGFR-3 over-expressions. Eur J Pharmacol. 685(1-3):1-7.

Kouchakzadeh H, Soudi T, Aghda NH, Shojaosadati SA (2017) Ligand-modified Biopolymeric Nanoparticles as Efficient Tools for Targeted Cancer Therapy. Curr Pharm Des. 23(35):5336-48.

Kwon YJ, Ye DJ, Baek HS, Chun YJ (2018) 7,12-Dimethylbenz[alpha]anthracene increases cell proliferation and invasion through induction of Wnt/beta-catenin signaling and EMT process. Environ Toxicol

Lammers T, Hennink WE, Storm G (2008) Tumour-targeted nanomedicines: principles and practice. Br J Cancer. 99(3):392-7.

Lee ES, Na K, Bae YH (2005) Doxorubicin loaded pH-sensitive polymeric micelles for reversal of resistant MCF-7 tumor. J Control Release. 103(2):405-18.

Lee RJ, Low PS (1994) Delivery of liposomes into cultured KB cells via folate receptor-mediated endocytosis. J Biol Chem. 269(5):3198-31204.

Liu D, Liu F, Liu Z, Wang L, Zhang N (2011) Tumor specific delivery and therapy by double-targeted nanostructured lipid carriers with anti-VEGFR-2 antibody. Mol Pharm. 8(6):2291-301.

Mizushima Y (1996) Lipid microspheres (lipid emulsions) as a drug carrier — An overview. Adv Drug Deliv Rev. 20(2–3):113-15.

Moraes RC, Chang H, Harrington N, Landua JD, Prigge JT, Lane TF, Wainwright BJ, Hamel PA, Lewis MT (2009) Ptch1 is required locally for mammary gland morphogenesis and systemically for ductal elongation. Development. 136(9):1423-32.

Moraes RC, Zhang X, Harrington N, Fung JY, Wu MF, Hilsenbeck SG, Allred DC, Lewis MT (2007) Constitutive activation of smoothened (SMO) in mammary glands of transgenic mice leads to increased proliferation, altered differentiation and ductal dysplasia. Development. 134(6):1231-42.

Musa MA, Latinwo LM, Virgile C, Badisa VL, Gbadebo AJ (2015) Synthesis and in vitro evaluation of 3-(4-nitrophenyl)coumarin derivatives in tumor cell lines. Bioorg Chem. 58(0):96-103.

Mussi SV, Sawant R, Perche F, Oliveira MC, Azevedo RB, Ferreira LA, Torchilin VP (2014) Novel nanostructured lipid carrier co-loaded with doxorubicin and

docosahexaenoic acid demonstrates enhanced in vitro activity and overcomes drug resistance in MCF-7/Adr cells. Pharm Res. 31(8):1882-92.

Mussi SV, Silva RC, Oliveira MC, Lucci CM, Azevedo RB, Ferreira LA (2013) New approach to improve encapsulation and antitumor activity of doxorubicin loaded in solid lipid nanoparticles. Eur J Pharm Sci. 48(1-2):282-90.

Narisawa T, Fukaura Y, Yazawa K, Ishikawa C, Isoda Y, Nishizawa Y (1994) Colon cancer prevention with a small amount of dietary perilla oil high in alpha-linolenic acid in an animal model. Cancer. 73(8):2069-75.

O'Brien J, Wilson I, Orton T, Pognan F (2000) Investigation of the Alamar Blue (resazurin) fluorescent dye for the assessment of mammalian cell cytotoxicity. Eur J Biochem. 267(17):5421-26.

Ogretmen B, Safa AR (1996) Down-regulation of apoptosis-related bcl-2 but not bcl-xL or bax proteins in multidrug-resistant MCF-7/Adr human breast cancer cells. Int J Cancer. 67(5):608-14.

Oliveira MS, Goulart GCA, Ferreira LAM, Carneiro G (2017) Hydrophobic ion pairing as a strategy to improve drug encapsulation into lipid nanocarriers for the cancer treatment. Expert Opin Drug Deliv. 14(8):983-95.

Ottonello L, Frumento G, Arduino N, Dapino P, Tortolina G, Dallegri F (2001) Immune complex stimulation of neutrophil apoptosis: investigating the involvement of oxidative and nonoxidative pathways. Free Radic Biol Med. 30(2):161-69.

Park SJ, Wu CH, Safa AR (2004) A P-glycoprotein- and MRP1-independent doxorubicin-resistant variant of the MCF-7 breast cancer cell line with defects in caspase-6, -7, -8, -9 and -10 activation pathways. Anticancer Res. 24(1):123-31.

Ren WX, Han J, Uhm S, Jang YJ, Kang C, Kim JH, Kim JS (2015) Recent development of biotin conjugation in biological imaging, sensing, and target delivery. Chem Commun (Camb). 51(52):10403-18.

Riccardi C, Nicoletti I (2006) Analysis of apoptosis by propidium iodide staining and flow cytometry. Nat Protoc. 1(3):1458-61.

Roy S, Rawat AK, Sammi SR, Devi U, Singh M, Gautam S, Yadav RK, Rawat JK, Singh L, Ansari MN, Saeedan AS, Pandey R, Kumar D, Kaithwas G (2017) Alpha-

linolenic acid stabilizes HIF-1 alpha and downregulates FASN to promote mitochondrial apoptosis for mammary gland chemoprevention. Oncotarget. 8(41):70049-71.

Siegel RL, Miller KD, Jemal A (2017) Cancer Statistics, 2017. CA Cancer J Clin. 67(1):7-30.

Singh B, Kapil R, Nandi M, Ahuja N (2011) Developing oral drug delivery systems using formulation by design: vital precepts, retrospect and prospects. Expert Opin Drug Deliv. 8(10):1341-60.

Singh M, Kanoujia J, Singh P, Tripathi CB, Arya M, Parashar P, Sinha VR, Saraf SA (2016a) Development of an α-linolenic acid containing soft nanocarrier for oral delivery: in vitro and in vivo evaluation. RSC Adv. 6(81):77590-602.

Singh N, Parashar P, Tripathi CB, Kanoujia J, Kaithwas G, Saraf SA (2017) Oral delivery of allopurinol niosomes in treatment of gout in animal model. J Liposome Res. 27(2):130-38.

Singh P, Arya M, Kanoujia J, Singh M, Gupta KP, Saraf SA (2016b) Design of topical nanostructured lipid carrier of silymarin and its effect on 7, 12-dimethylbenz [a] anthracene (DMBA) induced cellular differentiation in mouse skin. RSC Adv. 6(88):84965-77.

Singh P, Singh M, Kanoujia J, Arya M, Saraf SK, Saraf SA (2016c) Process optimization and photostability of silymarin nanostructured lipid carriers: effect on UV-irradiated rat skin and SK-MEL 2 cell line. Drug Deliv Transl Res. 6(5):597-609.

Singh S, Singh M, Tripathi CB, Arya M, Saraf SA (2016d) Development and evaluation of ultra-small nanostructured lipid carriers: novel topical delivery system for athlete's foot. Drug Deliv Transl Res. 6(1):38-47.

Tannock IF, Rotin D (1989) Acid pH in tumors and its potential for therapeutic exploitation. Cancer Res. 49(16):4373-84.

Tripathi CB, Beg S, Kaur R, Shukla G, Bandopadhyay S, Singh B (2016) Systematic development of optimized SNEDDS of artemether with improved biopharmaceutical and antimalarial potential. Drug Deliv. 23(9):3209-23.

Tripathi CB, Gupta N, Kumar P, Singh AK, Raj V, Parashar P, Singh M, Kanoujia J, Arya M, Saraf SA, Saha S (2017) Omega-3 Fatty Acid Synergized Novel Nanoemulsifying System for Rosuvastatin Delivery: In Vitro and In Vivo Evaluation. AAPS PharmSciTech: doi: 10.1208/s12249-017-0933-8.

Trivedi PP, Kushwaha S, Tripathi DN, Jena GB (2011) Cardioprotective effects of hesperetin against doxorubicin-induced oxidative stress and DNA damage in rat. Cardiovasc Toxicol. 11(3):215-25.

Um HD (2016) Bcl-2 family proteins as regulators of cancer cell invasion and metastasis: a review focusing on mitochondrial respiration and reactive oxygen species. Oncotarget. 7(5):5193-203.

Vimala K, Sundarraj S, Paulpandi M, Vengatesan S, Kannan S (2014) Green synthesized doxorubicin loaded zinc oxide nanoparticles regulates the Bax and Bcl-2 expression in breast and colon carcinoma. Process Biochem. 49(1):160-72.

Wang W, Xu B, Li Q, Jiang D, Yan S (2018) Anticancer effects of a novel PanRAF inhibitor in a hepatocellular carcinoma cell line. Mol Med Rep. 17(4):6185-93.

Wang X, Teng Z, Wang H, Wang C, Liu Y, Tang Y, Wu J, Sun J, Wang H, Wang J, Lu G (2014) Increasing the cytotoxicity of doxorubicin in breast cancer MCF-7 cells with multidrug resistance using a mesoporous silica nanoparticle drug delivery system. Int J Clin Exp Pathol. 7(4):1337-47.

Weitman SD, Weinberg AG, Coney LR, Zurawski VR, Jennings DS, Kamen BA (1992) Cellular localization of the folate receptor: potential role in drug toxicity and folate homeostasis. Cancer Res. 52(23):6708-11.

Wu J-L, He X-Y, Jiang P-Y, Gong M-Q, Zhuo R-X, Cheng S-X (2016a) Biotinylated carboxymethyl chitosan/CaCO3 hybrid nanoparticles for targeted drug delivery to overcome tumor drug resistance. RSC Adv. 6(69083–93

Wu J-L, He X-Y, Jiang P-Y, Gong M-Q, Zhuo R-X, Cheng S-X (2016b) Biotinylated carboxymethyl chitosan/CaCO 3 hybrid nanoparticles for targeted drug delivery to overcome tumor drug resistance. RSC Adv. 6(73):69083-93.

Zempleni J, Wijeratne SS, Hassan YI (2009) Biotin. Biofactors. 35(1):36-46.

Summary and Conclusion

The current study aims at development and characterization of lipidic nanocarrier system for targeted drug delivery to breast cancer. The targeted delivery approach was employed for improvement of the potency of such systems to deliver the drug molecules specifically to the cancer cells thereby avoiding dose related toxicity. Naturally occurring agents with antioxidant and tumor inhibitory potential (α-linolenic acid (ALA) and *Perilla frutescence* oil in current study) was incorporated in lipidic systems potentiated the effect of anticancer molecules extensively utilized in breast cancer chemotherapy, *i.e.*, doxorubicin. Also, antioxidant property of these lipids helped in reducing the drug induced toxic effects. This approach maximized the therapeutic benefits of anticancer agents in comparison to conventional formulations.

The anticancer drug selected for current study was doxorubicin as it is utilized as first line therapy of benign as well as metastatic breast carcinoma. Further, doxorubicin therapy is restricted due to the development of cardiotoxicity and drug resistance. Doxorubicin was characterized for identification and purity by FTIR, NMR and UV spectroscopy.

Drug solubility of the drug was performed in various lipids, emulgents and co-emulgents. The excipients with highest solubility for drug were selected for development of nanoemulsion system. For NLCs, solid lipid, liquid lipids and surfactant was selected on the basis of stability, particle size, solubility and water absorption capacities.

Based upon solubility, stability and water absorption capacities, the α-linolenic acid, lecithin, Tween 80, and cholesterol were selected for the development of nanoemulsion. Similarly for development of NLCs, stearic acid, perilla oil, and lecithin were selected based on stability and water absorption capacities.

Pseudo-ternary phase diagram was constructed for selection of ratio of emulgents, i.e., by titrating different ratios of emulgents with aqueous phase. Lecithin and Tween 80 in 1:1 ratio showed highest nanoemulsion region with ALA as lipid phase. Water absorption capacity suggested that cholesterol among different co-emulgents produces nanoemulsion with highest stability and lowest globule sizes. For NLCs, solid lipid and liquid lipid in ratio of 70:30 yielded NLCs with lowest particle size and stability.

For the optimization purpose of nanoemulsion various factors selected include α-linolenic acid as lipid phase, lecithin and Tween 80 (1:1) as surfactant mixture and cholesterol as co-emulgent. 3-factor 3-level Box Behnken design (BBD) was selected for optimization of nanoemulsion which suggested 17 experimental trails with different combination of factors. Similarly, stearic acid and perilla oil (70:30) as lipid phase, lecithin as surfactant and sonication time were selected as factors for optimization using central composite design (CCD) (α=1) with 15 experimental trials. All the trials for nanoemulsion and NLCs were separately formulated and characterized for response variables like, particle size, dug release, entrapment efficiency and drug loading/drug content.

The observed data for both the systems were analyzed mathematically for model development to fit the data using quadratic equations that generated best fitted equations. Response surface methodology (RSM) best demonstrated the relationships among selected factors and responses along with interactions among factors, if any and was therefore selected. The RSM suggested significant effect of lipids surfactants and co-surfactant on different responses i.e., particle size, dug release, entrapment efficiency and drug loading/drug content of nanoemulsion and NLCs. Triethanolamine was added to NLCs that enhanced the entrapment of amphiphilic doxorubicin to the system by hydrophobic ion interactions best known as hydrophobic ion pairing (HIP) phenomenon.

Further, the design space was created and optimized formulation was identified by putting some criteria for different response factors. The criteria applied for the nanoemulsion optimization were globule size less than 100 nm, entrapment efficiency more that 90%, drug release more that 80% and drug loading more that 10% fixed. The criteria for optimization of the NLCs were applied like, particle size should be lower than 150 nm, drug release should be more than 90%, EE more than 95% and drug content should be more than 15 mg/g of NLCs.

The formulation composition optimized for nanoemulsion (Dox-NE) was ALA-400 mg), Lecithin-350 mg, Tween 80 (350 mg) and cholesterol-150 mg), where as the composition of NLCs (Dox-NLCs) was lipid-2% w/w (composed of 7:3 ratio of stearic acid to perilla oil), surfactant-3% w/w (lecithin) along with optimum

concentration of sonication time as 20 min. Good correlation was observed between observed values and predicted values of response variables of both the systems.

The folate was successfully anchored on the surface of nanoemulsions with help of NHS (N-hydroxysuccinimide) and DCC (N,N'-Dicyclohexylcarbodiimide) as observed by characteristic peaks for different groups and structural compositions in FTIR and NMR spectrum. Folate content analysis supported the anchoring of folate to the surface and the amount of folate attached was found to be 10.33 $\mu mol.g^{-1}$ of NE formulation (f-Dox-NE). The physicochemical characterization of f-Dox-NE revealed the globule size of 55.2±3.3 nm, zeta potential -31±2 mV, entrapment efficiency of 92.51 ± 3.62% and percent drug loading of 0.47±.03%, respectively.

The biotin was successfully attached on the surface of NLCs with help of NHS and DCC as represented by characteristic peaks in FTIR and NMR spectrum. Biotin content analysis supported the anchoring of biotin to the surface of NLCs and folate content was found to be 5.85±0.64 $\mu g.g^{-1}$of NLCs (b-Dox-NLCs). The physicochemical characterization of b-Dox-NLCs revealed the globule size of 105.2±3.5 nm, zeta potential -35±2 mV, entrapment efficiency of 99.15±1.71% and drug content of 19.67±2.6 $mg.g^{-1}$ of NLCs, respectively.

There was significant improvement in doxorubicin release from the optimized nanoemulsion when compared with the standard drug and marketed formulation. f-Dox-NE exhibited sustained release behaviour with 94.86±1.87% drug release in 72 h. b-Dox-NLCs showed sustained and pH dependent drug release with faster drug release as the pH was lowered, *i.e.*, 55.39±3.27% at pH 7.4, 81.63±4.5% at pH 6.8 and 98.66±3.43% at pH 5.4 in 72 h. No significant change in the doxorubicin release profiles was observed before and after surface decoration in both the formulations.

The f-Dox-NE and b-Dox-NLCs were found to be stable and robust as observed from different stability indicating studies like, dilution stability, thermodynamic stability as well as stability in plasma and intravenous infusion solutions. The accelerated stability studies as per ICH guidelines also exhibited stable formulations.

In vitro cell lines studies performed in the MCF-7 cell lines showed superiority of f-Dox-NE and b-Dox-NLCs as observed from cell cytotoxicity assay, cell cycle

analysis, cellular proliferation studies, mitochondrial membrane potential and reactive oxygen species studies.

MTT assay showed that cell cytotoxicity potential for f-Dox-NE and b-Dox-NLCs were 54.98% and 63.64%, respectively, higher as compared to marketed formulation. Also, the placebo formulation without having drug showed significant cell cytotoxicity potential as exhibited by IC_{50} values for ALA-NE and p-NLCs, i.e., 4865±448 and 4465±267 $\mu g.mL^{-1}$, respectively.

Cell cycle studies through Fluorescence-activated cell sorting (FACS) demonstrated that ALA-NE, Dox solution and f-Dox-NE arrested the MCF-7 cells in G2 phase, G1phase and G1&G2/M phase respectively. While, p-NLCs, Dox solution and b-Dox-NLCs arrested the MCF-7 cells preferentially in G1-phase, G1-phase and G1&G2/M phase, respectively.

Cell proliferation studies exhibited the inhibition of cellular proliferation for nanoemulsion was in order of ALA-NE < Standard < marketed < Dox-NE < f-Dox-NE. While, the order for inhibition of cellular proliferation of different NLCs was found as p-NLCs < Standard < marketed < Dox-NLCs < b-Dox-NLCs. The data suggested that modified formulations exhibited highest cellular mortality as compared to marketed and standard formulations. Similarly, reactive oxygen species (ROS) and mitochondrial membrane potential (MMP) data suggested the superiority of the biotinylated NLCs and folate anchored nanoemulsions as compared to marketed and standard formulations. Cellular uptake studies demonstrated higher uptake of modified formulation in comparison to marketed formulation.

The superiority of modified formulations as revealed through *in vitro* cell lines data indicated that surface modifications helped these formulations in better cellular internalization through overexpressed receptors and better interaction between lipidic formulations and lipidic cell membrane leading to higher concentration of cytotoxic drug inside cell and hence higher cell mortality. Also, the tumor inhibitory potential of incorporated lipid phase (ALA and perilla oil) further potentiated the effects of anticancer agent resulting in better efficacy of such formulations.

In vivo studies were performed in female albino wistar rats, weighing 120-150 g. The experiment was performed according to the CPCSEA guidelines for laboratory

animals and ethics, Department of animal welfare, Government of India Animals were randomized and divided into seven groups of 10 animals each. Mammary gland carcinoma in each group (except control group) was induced by single tail vein injection of 7,12-Dimethylbenz[a]anthracene (DMBA) (8 mg/kg i.v.) on day 1. The drug/formulations were administered (10 mg/kg e.q. Dox) thrice/weeks in last six weeks of total 16 weeks of *in vivo* studies. A gap of 10 weeks was provided to develop the cancer in animals. Tumor incidence and size were monitored by measuring the diameter of mammary glands of rats, weight and survival of animals during the study.

Toxic group evidenced highest tumor volume, tumor incidence, reduction in animal weight and mortality in animals followed by standard group, marketed group, Dox-NE and f-Dox-NE. In case of nanoemulsion formulation reduction in animal weight reduction was found to be 44% for toxic group, 29.68% reduction for ALA-NE, 17.35% for standard group, 23.38% for marketed formulation, 14.96% for Dox-NE and 10.15% for b-Dox-NE group. Similarly for NLCs formulation, toxic group showed mean reduction in animal weight of 48%, p-NLCs treated group showed 36.71% reduction, standard group 10.74% reduction, marketed formulation 15.32% reduction, Dox-NE 13.38% reduction and b-Dox-NE group showed 5.47% reduction.

In case of animal survival highest animal survived the study for f-Dox-NE groups followed by Dox-NE, marketed and standard treated groups. Toxic group showed lowest animal survival. Similar results were also observed in case of NLC formulation. Parallel trends were observed for tumor incidence and tumor volumes in both the formulations.

Treatment of animals with DMBA resulted in significant disturbance in biochemical machineries of cells indicated by marked rise in the levels of biochemical markers like Thiobarbituric acid reactive substances (TBARS), protein carbonyl, glutathione (GSH), Superoxide dismutase (SOD) and catalase. Treatment with different formulation curtailed the levels of these markers and order of activity observed was f-Dox-NE>Dox-NE> marketed~ standard>ALA-NE. Likewise, surface modified NLCs showed highest efficacy in reinstatement of the levels of these biomarkers.

Western blotting data suggested that DMBA administration to the animals caused the elevation of antiapoptotic proteins like bcl-2, and MMP-9 and down-regulation of

pro-apoptotic markers such as bax and caspase-9. The treatment of animal with Dox and f-Dox-NE restored the level of these proteins towards normal but the effect was more profound in case of f-Dox-NE. Bcl-2 and MMP-9 have been shown to promote the breast tumor migration, invasion and metastasis. The level of these proteins were restored by treatment of animal with f-Dox-NE indicating that the formulation was able to inhibit tumor metastasis in DMBA administered animals. Treatment of DMBA treated group with b-Dox-NLCs resulted in downregulation of anti-apoptotic proteins bcl-2 and MMP-9 while upregulated the level of expression of pro-apoptotic proteins like BAX, caspase-9 and p16 indicating tumor inhibitory potential of the formulation. Further, the MMP-9, p16 and members of the bcl-2 family protein, including bcl-2, BAX *etc*. exhibited an important role in breast cancer migration, invasion and metastasis. The results demonstrated that the biotin decorated NLCs can effectively reduce the mammary tumor cell metastasis in the disease induced rats.

Angiogenesis and cellular proliferation are distinctive characteristics for the cancer growth and progression represented through Alveolar buds/terminal end buds (AB/TEB) count and cellular architecture of mammary gland tissue. The DMBA administration resulted in significant increase in the number of AB/TEB and significant changes in ducts, adipocytes, Loose connective tissue, Dense connective tissue and tissue architecture in mammary gland tissues as depicted by carmine staining and H&E stain. Dox-NE and f-Dox-NE was more efficient in diminishing the count of AB/TEBs as compared to the standard and the marketed groups. Similarly, b-Dox-NLCs treatment resulted in restoration of cellular architecture and lowering in the AB/TEBs count.

Doxorubicin is known to exhibit cardiotoxicity due to dose related cardiac tissue damage and necrosis. Doxorubicin treatment resulted in significantly alterations in levels of MDA and GSH in cardiac tissue. Surface modified drug delivery treated groups showed no significant changes in the MDA and GSH levels of cardiac tissues. The results suggested preferential delivery by molecularly guided systems through the overexpressed receptor cancer site.

The Dox levels attained in the mammary carcinoma was highest in the case of the f-Dox-NE (45.23±2.51 µg/g organ in 4 h) followed by the Dox-NE (35.43±2.91 µg/g organ in 4 h) indicating the specific accumulation of the folate decorated

nanoemulsion in FR over-expressed mammary tumor cells. Further, significant higher Dox levels were maintained in the mammary cancer cells for a period of upto 48 h (25.78±1.42 µg/g organ) in the f-Dox-NE ($p<0.001$); upto 12 h (25.55±2.22 µg/g organ) in the Dox-NE ($p<0.001$) treated groups *vis-à-vis* the pure Dox (15.55±2.25 µg/g in 12 h, 1.78±0.42 µg/g in 48 h) and the marketed formulation (14.54±2.21 µg/g in 12 h, 1.79±0.38 µg/g in 48 h) treated groups. Among different organs, highest Dox concentration was observed in the liver followed by the spleen, the heart and the kidney. Overall, the Dox levels in different organs of the folate decorated NE were relatively lower than that of other animal groups. Similar, results were observed in case biotinylated NLCs with highest concentration was maintained by b-Dox-NLCs in cancer tissue followed by Dox-NE, standard and marketed drug. The biodistribution data further affirmed the selective accumulation of the biotinylated NLCs to the biotin receptor which is over-expressed in the condition of mammary gland carcinoma.

As summarized above, ligand guided drug delivery system was safe and effective in regulating the cancer proliferation, invasion and migration in mammary gland carcinoma. The mammalian cells are incapable of themselves synthesizing the some of the biomolecules and therefore it is taken up through some transport systems like high-affinity biotin transporter or sodium-dependent multivitamin transporter (SMVT) in case of biotin and high affinity folate receptor for folate uptake. The overexpression of these receptors and selective uptake capacity for these molecules in the cancer cells may be a possible explanation for selective uptake of molecularly decorated NLCs for mammary cancer. Attachment of targeting ligands through a relatively long PEG chain linker resulted in effective ligand-receptor association and internalization of the complex in cancer cells. Further, it has been demonstrated that ALA and perilla oil has cancer ameliorative and inhibitory effect, also, act as antioxidants for normal cells, thereby preventing the drug induced toxicities. Further prolonged drug release maintained higher concentration of anticancer molecules that resulted in higher cell cytotoxicity. The combined effects of the above would effectively address mammary gland carcinoma. Therefore, it can be concluded that being safe and effective, these formulations can be used as a better alternative to the conventional formulations in management of mammary gland carcinoma. Further, the translational potential of this drug delivery system could prove to be beneficial for patients after suitable clinical evaluations, as future scope.

Publications

1. **Tripathi CB,** Parashar P, Arya M, Singh M, Kanoujia J, Kiathwas G, Saraf SA. QbD based Development of α-Linolenic Acid Potentiated Nanoemulsion for Targeted Delivery of Doxorubicin in DMBA Induced Mammary Gland Carcinoma: in vitro and in vivo Evaluation. Drug Deliv Transl Res. 2018. (Accepted, Manuscript ID: DDTR-D-17-00322) **(Impact Factor: 3.094)**

2. **Tripathi CB,** Gupta N, Kumar P, Singh AK, Raj V, Parashar P, Singh M, Kanoujia J, Arya M, Saraf SA, Saha S. Omega-3 Fatty Acid synergised Novel Nanoemulsifyng System for Rosuvastatin Delivery: *In vitro* and *In vivo* Evaluation. AAPS PharmSciTech. 2018;19(3):1205-1218. **(Impact Factor: 2.45)**

3. **Tripathi CB,** Parashar P, Arya M, Singh M, Kanoujia J, Kiathwas G, Saraf SA. Apoptotic Cell Death in MCF-7 cells and Mammary Carcinoma through Regulation of bcl-2, BAX, MMP-9, caspase-9 and p16 by Biotin Anchored Perilla frutescence Oil based Nanostructured Lipid Carrier of Doxorubicin. Chemico-biological interactions. 2018 (communicated). **(Impact Factor: 3.14)**

4. **Tripathi CB**, Beg S, Kaur R, Shukla G, Bandopadhyay S, Singh B. Systematic development of optimized SNEDDS of artemether with improved biopharmaceutical and antimalarial potential. Drug Deliv. 2016;23(9):3209-3223. **(Impact Factor: 6.402)**

5. Singh M, Kanoujia J, Parashar P, Arya M, **Tripathi CB**, Sinha VR, Saraf SK, Saraf SA. Augmented bioavailability of felodipine through a α-linolenic acid based microemulsion. Drug Deliv Transl Res. 2018;8(1):204-225. **(Impact Factor: 3.094)**

6. Singh M, Kanoujia J, Singh P, **Tripathi CB**, Arya M, Parashar P, Sinha VR, Saraf SA, Development of α-linolenic acid containing soft nanocarrier for oral delivery: in vitro and in vivo evaluation. RSC Adv. 2016;6, 77590–77602. **(Impact Factor: 3.289)**

7. Singh M, Kanoujia J, Parashar P, Arya M, **Tripathi CB**, Sinha VR, Saraf SK, Saraf SA. Assessment of improved buccal permeation and bioavailability of

felodipine microemulsion-based cross-linked polycarbophil gel. Drug Deliv Transl Res. 2018. doi: 10.1007/s13346-018-0489-5. **(Impact Factor: 3.094)**

8. Arya M, Tiwari P, **Tripathi CB**, Parashar P, Singh M, Sinha P, Yadav NP, Kaithwas G, Gupta KP, Saraf SA. Novel niosomal lotion of Inositol hexaphosphate against inflammation/ hyperplasia in epidermal layer of Swiss albino mice. 2016. Mol. Pharmaceutics, 2016, 14 (3), 928–939. **(Impact Factor:4.342)**

9. Singh N, Parashar P, **Tripathi CB**, Kanoujia J, Kaithwas G, Saraf SA. Oral delivery of allopurinol niosomes in treatment of gout in animal model. J Liposome Res. 2017;27(2):130-138. **(Impact Factor: 1.797)**

10. Verma J, Kanoujia J, Parashar P**, Tripathi CB**, Saraf SA. Wound healing applications of sericin/chitosan-capped silver nanoparticles incorporated hydrogel. Drug Deliv Transl Res. 2017;7(1):77-88. **(Impact Factor: 3.094)**

11. Singh M, Kanoujia J, Singh P, Parashar P, Arya M, Tripathi CB, Sinha V, Saraf SA. Development of an α-linolenic acid containing soft nanocarrier for oral delivery part II: buccoadhesive gel. RSC Adv. 2016 6,101602-12. **(Impact Factor:3.289)**

12. Kanoujia J, Singh M, Singh P, Parashar P, **Tripathi CB**, Arya M, Saraf S. Genipin crosslinked soy-whey based bioactive material for atorvastatin loaded nanoparticles: preparation, characterization and in vivo antihyperlipidemic study. 2016; RSC Advances, 96 **(Impact Factor: 3.289)**

13. Singh S, Singh M, **Tripathi CB**, Arya M, Saraf SA. Development and Evaluation of Ultra-Small Nanostructured Lipid Carriers: Novel Topical Delivery System for Athlete's Foot. Drug Deliv Transl Res. 2016; 6(1): 38-47. **(Impact Factor: 3.094)**

14. Ganggwar N, Singh M, Parashar P, **Tripathi CB**, Arya M, Saraf SA, Saha S. Topical Delivery of Fluconazole via Microemulsion Incorporated Hydrogel for the Management of Fungal Dermatophytosis. Current Drug Therapy, 2016,11(2): 129 - 141.

15. Bhardwaj A, Dwivedi H, Kymonil KM, Pareek A, Upadhyay SA, **Tripathi CB**, Saraf SA. Self dispersible lipidic formulation of poorly water soluble

Boswellic acids: An anti-inflammatory agent of natural origin. Indian Journal of natural product and resources, 2016; 7(1): 9-18.

16. Rawat D, **Tripathi CB**, Parashar P, Singh M, Kaithwas G, Saraf SA. Development and Characterization of Nanostructured Lipid Carriers of *Vetiveria Zizanoides* oil for Therapeutic Potential in Prickly Heat Treatment. Journal of Pharmacy and Pharmaceutical Sciences, 2015; 2: 162–171.

17. Haider FM, Kanoujia J, **Tripathi CB**, Arya M, Kaithwas G, Saraf SA. Pioglitazone loaded niosomes as vesicular carriers for anti-diabetic activity: Optimization by central composite design. Journal of Pharmaceutical Sciences and Pharmacology, 2015; 2; 11–20.

18. Singh B, Bhatowa R, **Tripathi CB**, Kapil R. Developing Micro-/Nano-particulate Drug Delivery Systems using "Design of Experiments (DoE)", International Journal of Pharmaceutical Investigation. 2011;1(2): 75-87.

Conferences

- Oral presentation in National science Day celebration and Seminar on 'fostering scientific temper for welfare of society and surroundings' at BBAU, Lucknow. 27-28 Feb. 2018
- Presented poster in 'A national conference on tourists and green spaces: healthier lifestyles approaches from nature' dated 15-16 July 2017.
- Presented Poster in International Conference on Updates in Cancer Prevention and Research (ICUCPR-2017) & Satellite Conference on Translational Research: Trends and Implications (IPCBBAU-2017) dated 14^{th}-16^{th} & 20^{th} February 2017.
- Attended and participated in oral presentation in 3^{rd} Lucknow Science Congress LUSCON-2015 on "Hope for Society through Drug Research", Lucknow. October 31^{st} - November 2^{nd}, 2015.
- Attended and presented poster in 2^{nd} National Seminar on "Profession of Pharmacy: Challenges & Opportunities", Lucknow. 18^{th} October, 2015

- Attended and presented poster in International Pharmaceutical Conference-2015 on "Nanoformulations and Translational Research: Small Getting Bigger", Lucknow. February 2-3, 2015.
- Attended 15th Indo-US Flow Cytometry Workshop on Application of Flow Cytometry in Biomedical Research, Lucknow, October 29-31, 2014.
- Attended and presented poster in International Pharmaceutical Conference-2015 on patents, BBAU, Lucknow, March 18, 2013.
- Attended and presented poster in International Pharmaceutical Conference-2015 on "Nanoformulations and Translational Research: Small Getting Bigger", Lucknow. February 2-3, 2015.
- Attended 15th Indo-US Flow Cytometry Workshop on Application of Flow Cytometry in Biomedical Research, Lucknow, October 29-31, 2014.
- Attended International Symposium on advances in Material Characterization, Lucknow. July 14, 2014.
- Attended and presented poster in 2nd Lucknow Science Congress, Lucknow. March 27-28, 2014.
- Attended and presented poster in IHPA Golden Jubilee Conference-2014, Lucknow. March 1-2, 2014.

Plagiarism report of thesis

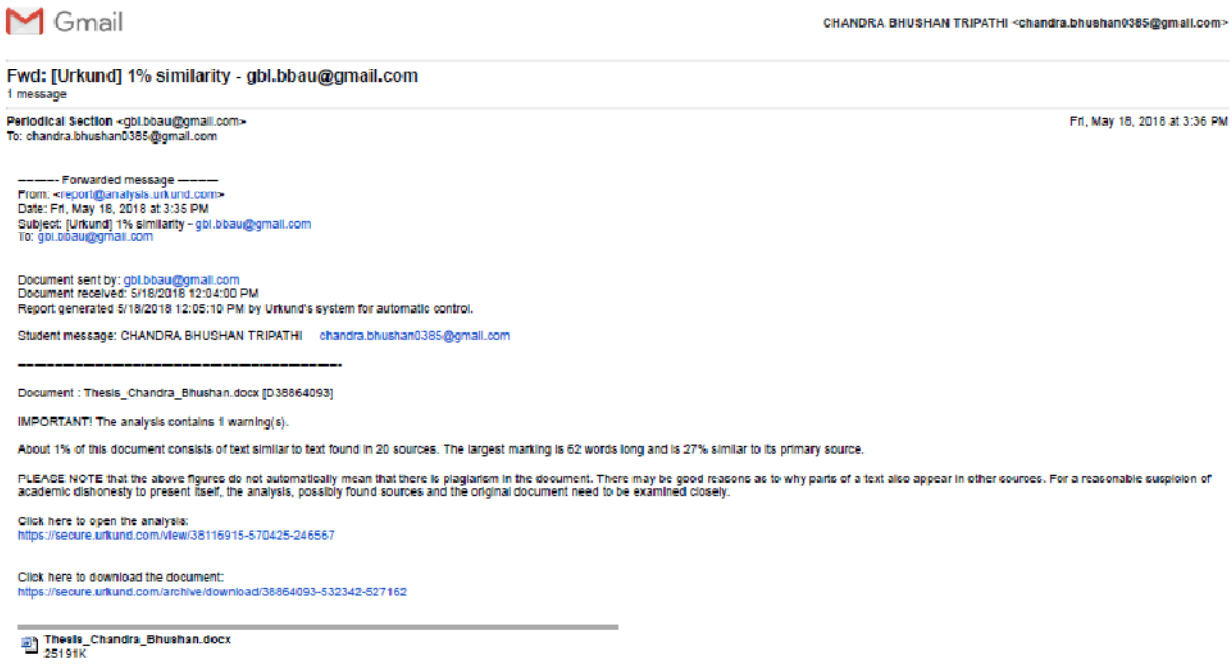

Gmail CHANDRA BHUSHAN TRIPATHI <chandra.bhushan0385@gmail.com>

Fwd: [Urkund] 1% similarity - gbl.bbau@gmail.com
1 message

Periodical Section <gbl.bbau@gmail.com> Fri, May 18, 2018 at 3:36 PM
To: chandra.bhushan0385@gmail.com

---------- Forwarded message ----------
From: <report@analysis.urkund.com>
Date: Fri, May 18, 2018 at 3:35 PM
Subject: [Urkund] 1% similarity - gbl.bbau@gmail.com
To: gbl.bbau@gmail.com

Document sent by: gbl.bbau@gmail.com
Document received: 5/18/2018 12:04:00 PM
Report generated 5/18/2018 12:05:10 PM by Urkund's system for automatic control.

Student message: CHANDRA BHUSHAN TRIPATHI chandra.bhushan0385@gmail.com

---

Document : Thesis_Chandra_Bhushan.docx [D38864093]

IMPORTANT! The analysis contains 1 warning(s).

About 1% of this document consists of text similar to text found in 20 sources. The largest marking is 62 words long and is 27% similar to its primary source.

PLEASE NOTE that the above figures do not automatically mean that there is plagiarism in the document. There may be good reasons as to why parts of a text also appear in other sources. For a reasonable suspicion of academic dishonesty to present itself, the analysis, possibly found sources and the original document need to be examined closely.

Click here to open the analysis:
https://secure.urkund.com/view/38116915-570425-246567

Click here to download the document:
https://secure.urkund.com/archive/download/38864093-532342-527162

Thesis_Chandra_Bhushan.docx
25191K

Institutional Animal Ethical Committee Approval

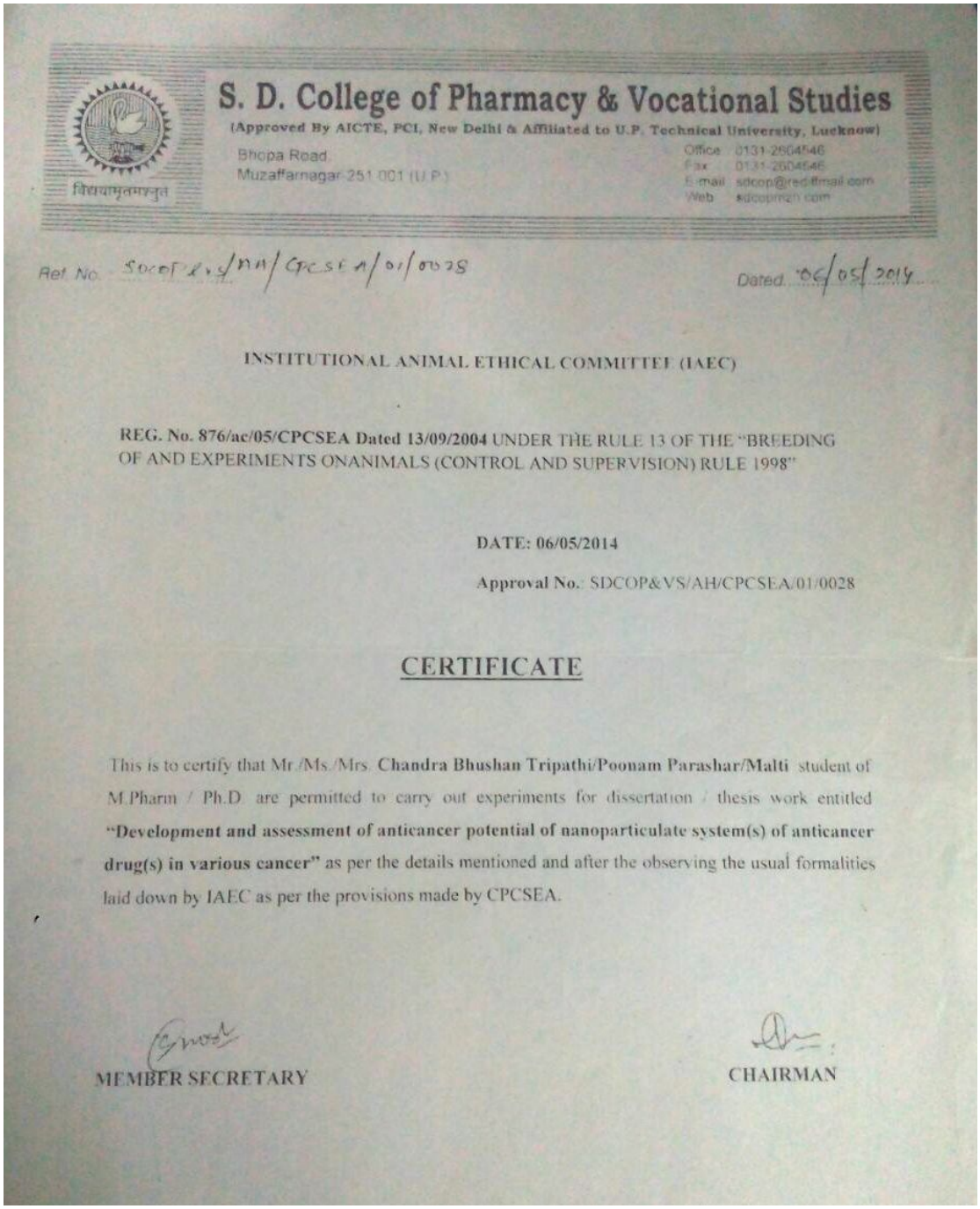

S. D. College of Pharmacy & Vocational Studies

(Approved By AICTE, PCI, New Delhi & Affiliated to U.P. Technical University, Lucknow)

Bhopa Road,
Muzaffarnagar-251 001 (U.P.)

Office : 0131-2604546
Fax : 0131-2604546
E-mail : sdcop@rediffmail.com
Web : sdcoprizn.com

विद्यामृतमश्नुते

Ref. No. SDCOP&VS/AH/CPCSEA/01/0028 Dated 06/05/2014

INSTITUTIONAL ANIMAL ETHICAL COMMITTEE (IAEC)

REG. No. 876/ac/05/CPCSEA Dated 13/09/2004 UNDER THE RULE 13 OF THE "BREEDING OF AND EXPERIMENTS ONANIMALS (CONTROL AND SUPERVISION) RULE 1998"

DATE: 06/05/2014

Approval No. SDCOP&VS/AH/CPCSEA/01/0028

CERTIFICATE

This is to certify that Mr./Ms./Mrs. **Chandra Bhushan Tripathi/Poonam Parashar/Malti** student of M.Pharm / Ph.D are permitted to carry out experiments for dissertation / thesis work entitled **"Development and assessment of anticancer potential of nanoparticulate system(s) of anticancer drug(s) in various cancer"** as per the details mentioned and after the observing the usual formalities laid down by IAEC as per the provisions made by CPCSEA.

MEMBER SECRETARY

CHAIRMAN

Brief Curriculum Vitae

Name: Chandra Bhushan Tripathi

Date of birth: 06-03-1985

Education: B.Pharm (2009) from Dr. K.N. Modi Institute of Pharmaceutical Education and Research, Ghaziabad, U.P. and M.Pharm (Pharmaceutics, 2011) from University Institute of Pharmaceutical Sciences, Panjab University, Chandigarh.

M.Pharm project: Formulation Optimization Studies on Self-Nanoemulsifying Drug Delivery Systems (SNEDDS) of Artemether with Enhanced Bioavailability Potential at "Panjab University", Chandigarh**.** (An Industrial Project July-2010 to June 2011), under the guidance of Prof V R Sinha

PhD project: Development and Characterization of Targeted Nanoparticulate System for Tumor Metastasis Inhibition under the guidance of Prof. Shubhini A saraf (Head and Dean) at Dept. of Pharmaceutical Sciences, Babasaheb Bhimrao Ambedkar University, Lucknow.

Research Publications:

1. Ten (18) international/national research/review articles
2. Eight (13) oral/poster presentation in national/international seminars/conferences

Research expertise: Lipidic and polymeric nanoparticulate system, tablets, capsules, and colloidal nanocarrires such as microemulsion and nanoemulsion

Permanent Address

S/o R. N. Tripathi
Village- Pratappur, Post-
Jaswal, Dist.-Sant Kabir
Nagar, U.P. 272271

(Chandra Bhushan Tripathi)

Drug Delivery and Translational Research
https://doi.org/10.1007/s13346-018-0525-5

ORIGINAL ARTICLE

QbD-based development of α-linolenic acid potentiated nanoemulsion for targeted delivery of doxorubicin in DMBA-induced mammary gland carcinoma: in vitro and in vivo evaluation

Chandra Bhushan Tripathi[1] · Poonam Parashar[1] · Malti Arya[1] · Mahendra Singh[1] · Jovita Kanoujia[1] · Gaurav Kaithwas[1] · Shubhini A. Saraf[1]

Abstract

Breast cancer is the most common cancer of occurrence in women and has the highest mortality incidence rate therein. The present study envisaged to develop doxorubicin (Dox) loaded folate functionalized nanoemulsion (NE) for profound therapeutic activity against mammary gland cancer. NE was prepared using pseudo-ternary phase diagrams utilizing α-linolenic acid (ALA) as lipid phase, to further enhance the anticancer potential of Dox. Box-Behnken design was employed to systematically develop the NE. Optimized NE (f-Dox-NE) was evaluated for in vitro and in vivo performance. f-Dox-NE, with globule size 55.2 ± 3.3 nm, zeta potential −31 ± 2 mV, entrapment 92.51 ± 3.62%, drug loading 0.42 ± 0.08% and percent drug release 94.86 ± 1.87% in 72 h, was capable of reducing cell viability in MCF-7 cell lines *vis-à-vis* pure and marketed drug. Further, mechanistic studies in MCF-7 cell lines demonstrated that f-Dox-NE induces cellular apoptosis by reactive oxygen species generated and mitochondrial membrane mediated apoptosis. The antitumor effect was evaluated in 7,12-dimethylbenz[a]anthracene (DMBA) induced mammary gland tumor in female Albino Wistar rats. f-Dox-NE exhibited enhanced antitumor targeting potential, therapeutic safety and efficacy *vis-à-vis* pure and marketed drug, as revealed by tumor volume, animal survival, weight variation, cardiotoxicity and biodistribution studies. f-Dox-NE restored the biochemical parameters viz., SOD, catalase, TBARS and protein carbonyl, towards normal levels in comparison to DMBA induced animal group. f-Dox-NE displayed downregulation of anti-apoptotic (Bcl-2 and MMP-9) proteins and upregulation of pro-apoptotic proteins (caspase-9 and BAX). The experimental results suggest that ALA augmented folate functionalized NE are able to overcome the challenges of developing safe and effective delivery system with enhanced potential for mammary gland carcinoma therapy.

Keywords Doxorubicin · α-linolenic acid · Nanoemulsion · MCF-7 cell lines · Western blot · Anticancer

Introduction

Nowadays, tumor is one of the most prominent causes of death in developing as well as developed countries. The burden is expected to amplify owing to the environmental pollution, presence of carcinogen in environment, radiation, obesity, hormonal imbalance, development of drug resistance, lack of specific targeted therapies etc. among other factors. Lifestyle habits such as physical inactivity, smoking, poor diet, and reproductive changes have further enhanced the tumor burden [1, 2]. Lung cancer has surpassed the incidences of breast cancer; however, mammary gland carcinoma remains the leading factor for cancer deaths in females [1–4].

Doxorubicin (Dox) is an anthracycline anticancer drug obtained from the fungus *Streptococcus peuceticus var. caesius*. It is one of the most potent chemotherapeutic agent among modern day breast anticancer therapies. Anticancer activity of Dox is due to its activity against topoisomerase II which plays a vital role in the negative supercoiling of DNA. Dox intercalates into the DNA causing the alteration in stereochemical conformation of the double-helical structure.

Electronic supplementary material The online version of this article (https://doi.org/10.1007/s13346-018-0525-5) contains supplementary material, which is available to authorized users.

✉ Shubhini A. Saraf
shubhini.saraf@gmail.com

[1] Department of Pharmaceutical Sciences, School of Biosciences & Biotechnology, Babasaheb Bhimrao Ambedkar University (A Central University), Vidya Vihar, Rae Bareli Road, Lucknow 226025, India

Published online: 10 May 2018

AAPS PharmSciTech (© 2017)
DOI: 10.1208/s12249-017-0933-8

Research Article

ω-3 Fatty Acid Synergized Novel Nanoemulsifying System for Rosuvastatin Delivery: *In Vitro* and *In Vivo* Evaluation

Chandra Bhushan Tripathi,[1] Neha Gupta,[1] Pranesh Kumar,[1] Ashok Kumar Singh,[1] Vinit Raj,[1] Poonam Parashar,[1] Mahendra Singh,[1] Jovita Kanoujia,[1] Malti Arya,[1] Shubhini A. Saraf,[1,2] and Sudipta Saha[1,2]

Received 22 August 2017; accepted 27 November 2017

Abstract. The present study was undertaken to improve rosuvastatin (RSV) bioavailability and pharmacological response through formation of SNES using *Perilla frutescens* oil as lipid carrier. The composition of oil was estimated by fatty acid methyl ester (FAME) analysis using gas chromatography. Solubility of RSV in *Perilla frutescens* oil and Cremophor EL was 25.0 ± 3.0 and 60.0 ± 5.0 mg/mL, respectively. Later, nanophasic maps and a central composite design were employed to determine the maximum nanoemulsion region and further optimize SNES in this study. Finally, the optimized formulation was evaluated *in vitro* and *in vivo*. FAME analysis revealed that PUFA content was 70.3% of total fatty acid. Optimized SNES formulation demonstrated particle size of 17.90 nm, dissolution 98.80%, cloud point 45°C, emulsification time 2 min, and viscosity 241.41 ± 5.52 cP. The hypolipidemic property of SNES was further explored using Triton X-100-induced hyperlipidemic rat model, and there were reductions of serum cholesterol, triglyceride, and LDL and VLDL levels in the SNES-treated group as compared to the toxic control. Pharmacokinetic study of SNES revealed significantly higher C_{max} (60.13 ± 25.43 ng/mL) and $AUC_{0-\infty}$ (6195 ± 42.38 ng h/mL) *vis-à-vis* marketed tablet (284.80 ± 13.44 ng/mL, 3131.72 ± 51.93 ng h/mL, respectively). RSV was successfully incorporated into ω-3 fatty acid-based SNES with improved pharmacokinetic parameters (~ 2-fold improved bioavailability) and better hypolipidemic properties, owing to the synergistic effects of hepatic lipid regulation itself. The results clearly explicated that ω-3 fatty acid-based SNES effectively enhanced bioavailability and pharmacological responses of RSV, suggesting that these formulations may be useful as alternative for hyperlipidemia treatment in future drug design perspective.

KEY WORDS: rosuvastatin; self-nanoemulsifying system; ω-3 fatty acid; hypolipidemic action; *Perilla frutescens* oil.

INTRODUCTION

In recent years, nanosized drug delivery systems especially the lipidic ones have emerged as a promising tool to enhance the bioavailability of many poorly water-soluble hydrophobic drugs classified under BCS class II (1). In fact, the most popular approach is the incorporation of the active lipophilic component into inert lipid vehicles such as oils, surfactant, solid dispersions, nanolipid carriers, nanoemulsifying formulations, liposomes, *etc.* (2). Nanoemulsifying systems have shown great promise for enhancing bioavailability of poorly soluble compounds by increasing the membrane fluidity to facilitate transcellular absorption. The mechanisms for the same would be loosening tight junctions to allow paracellular transport, inhibiting P-gp and/or CYP450 to increase intracellular concentration, and stimulating lipoprotein/chylomicron production by lipid and absorption through lymphatic systems (3). Self-nanoemulsifying system (SNES), also known as nanoemulsion liquid preconcentrate, is thermodynamically stable and optically isotropic transparent colloidal system consisting of natural or synthetic oil and surfactant usually in combination with a co-surfactant that spontaneously emulsifies when exposed to an aqueous environment or fluid of the gastrointestinal tract to form oil-in-water nanoemulsion with droplet size 300 nm or less. These systems may directly absorb into the lymphatic system, thereby avoiding the hepatic first-pass metabolism (4).

There are several factors which influence the potential of SNES for enhancement of oral bioavailability. The most

Chandra Bhushan Tripathi and Neha Gupta contributed equally to this work.

Electronic supplementary material The online version of this article (https://doi.org/10.1208/s12249-017-0933-8) contains supplementary material, which is available to authorized users.

[1] Department of Pharmaceutical Sciences, Babasaheb Bhimrao Ambedkar University, Vidya Vihar, Rae Bareli Road, Lucknow, 226025, India.

[2] To whom correspondence should be addressed. (e-mail: shubhini.saraf@gmail.com; sudiptapharm@gmail.com)

Published online: 19 December 2017

Drug Delivery

http://informahealthcare.com/drd
ISSN: 1071-7544 (print), 1521-0464 (electronic)

Drug Deliv, 2016; 23(9): 3209–3223
 DOI: 10.3109/10717544.2016.1162876

Taylor & Francis
Taylor & Francis Group

RESEARCH ARTICLE

Systematic development of optimized SNEDDS of artemether with improved biopharmaceutical and antimalarial potential

Chandra Bhushan Tripathi[1], Sarwar Beg[1], Ripandeep Kaur[2], Geeta Shukla[3], Shantanu Bandopadhyay[4], and Bhupinder Singh[1,2]

[1]UGC Centre of Advanced Studies, University Institute of Pharmaceutical Sciences, Panjab University, Chandigarh, India, [2]UGC- Centre of Excellence in Applications of Nanomaterials, Nanoparticles and Nanocomposites (Biomedical Sciences), Panjab University, Chandigarh, India, [3]Department of Microbiology, Panjab University, Chandigarh, India, and [4]Division of Pharmaceutics, PDM College of Pharmacy, Sarai Aurangabad, Bahadurgarh, Haryana, India

Abstract

The current studies entail systematic development of self-nanoemulsifying drug delivery systems (SNEDDS) containing medium-chain triglycerides (MCTs) and long-chain triglycerides (LCTs) for augmenting the biopharmaceutical performance of artemether. Equilibrium solubility and pseudoternary phase diagram studies facilitated selection of Captex 355 and Ethyl oleate as MCTs and LCTs, and Cremophor RH 40 and Tween 80 as surfactants, while Transcutol HP as cosolvent for formulating the SNEDDS. Systematic optimization was performed employing the Box–Behnken design taking concentrations of lipid, surfactant and cosolvent as the critical material attributes (CMAs), while evaluating for globule size, emulsification time, dissolution efficiency and permeation as the critical quality attributes (CQAs). *In situ* single pass intestinal perfusion (SPIP) studies in Wistar rats substantiated significant augmentation in the absorption (5- to 6-fold) and permeation (4- to 5-fold) parameters from the optimized MCT and LCT-SNEDDS vis-à-vis the pure drug. *In vivo* pharmacodynamic studies in *Plasmodium berghi* infected laca mice exhibited superior reduction in the levels of percent parasitemia, SGOT, SGPT and bilirubin, followed by higher survival rate of the animals by optimized MCT-SNEDDS followed by LCT-SNEDDS vis-à-vis the pure drug, which was subsequently ratified through histopathological examination of liver tissues. Overall, the studies construed successful development of the optimized SNEDDS of artemether with distinctly improved biopharmaceutical and antimalarial potential.

Keywords

Absorption, parasitemia, nanoemulsion, quality by design, solubility

History

Received 17 January 2016
Revised 1 March 2016
Accepted 3 March 2016

Introduction

Artemether, a semi-synthetic derivative of artemisinin extracted from the plant *Artemisia annua* is primarily used for the treatment and management of malarial infections. Pharmacologically, it is a gametocidal agent found to be highly effective against malaria caused by multidrug-resistant *Plasmodium falciparum* (Tran et al., 1996; Van Hensbroek et al., 1996; Makanga, 2014). Being a BCS class II drug, it exhibits poor solubility and high lipophilicity (log *p* of 3.8), and undergoes extensive hepatic first-pass effect and metabolism by CYP3A4 isozymes, leading eventually to its low oral bioavailability (i.e., <45%) (Van Hensbroek et al., 1996; Grace et al., 1999). Multiple drug delivery systems like, micronization, solid dispersions (Shah & Mashru, 2008), inclusion complexes (Yang et al., 2009), complexation with hydrophilic polymers (Jain & Gupta, 2008) and supersaturable systems (Mandawgade et al., 2008) have been explored for enhancing the oral bioavailability of artemether, yet none of these formulations are considered to be highly satisfactory for enhancing the oral bioavailability ostensibly owing to their dissolution rate enhancement characteristics only.

Of late, the lipid-based self-nanoemulsifying drug delivery systems (SNEDDS) have proved their worth as one of the highly promising systems for ameliorating the oral bioavailability of drugs, especially belonging to the BCS class II and IV categories (Singh et al., 2011b; Beg et al., 2015a, 2015b). These primarily constitute the isotropic mixtures of lipids, surfactants, cosurfactants and/or cosolvents, which upon spontaneous emulsification in presence of gastrointestinal fluid produce ultrafine oil-in-water nanoemulsion with particle size less than 100 nm (Singh et al., 2009). Many literature reports have vouched the merits of SNEDDS in addressing the issues of low oral bioavailability of drugs, owing to its holistic approach for enhancing the solubility, circumventing the hepatic first-pass effect, increasing the

Address for correspondence: Dr Bhupinder Singh Bhoop, M Pharm, PhD, D St, Professor (Pharmaceutics & Biopharmaceutics), UGC Centre of Advanced Studies, Coordinator, UGC Centre for Excellence in Nanoscience and Nanotechnology, University Institute of Pharmaceutical Sciences, Panjab University, Chandigarh 160 014, India. Tel: +91 172 2534103. Fax: +91 172 2543101. Email: bsbhoop@yahoo.com; bsbhoop@gmail.com

Drug Delivery and Translational Research (2018) 8:204–225
https://doi.org/10.1007/s13346-017-0453-9

ORIGINAL ARTICLE

Augmented bioavailability of felodipine through an α-linolenic acid-based microemulsion

Mahendra Singh[1] · Jovita Kanoujia[1] · Poonam Parashar[1] · Malti Arya[1] · Chandra B. Tripathi[1] · V. R. Sinha[2] · Shailendra K. Saraf[3] · Shubhini A. Saraf[1]

Published online: 4 December 2017

Abstract

The oral bioavailability of felodipine, a dihydropyridine calcium channel antagonist, is about 15%. This may be due to poor water solubility, and a lower intestinal permeability than a BCS class I drug, and hepatic first-pass metabolism of the drug. Many drugs are unpopular due to solubility issues. The goal of this study was to develop and optimize a felodipine-containing microemulsion to improve the intestinal permeability and bioavailability of the drug. The felodipine microemulsions were developed with the selected components, i.e., α-linolenic acid as the oil phase, Tween 80 as a surfactant, and isopropyl alcohol as co-surfactant using Box-Behnken design and characterized for in vitro release and particle size. The optimized felodipine-loaded microemulsion was investigated for physicochemical interaction, surface morphology, intestinal permeability, rheology, cytotoxicity, cellular uptake, pharmacodynamic (electrocardiogram and heart rate variability), and pharmacokinetic studies to explore its suitability as a promising oral drug delivery system for the treatment of hypertension. The optimized felodipine-loaded microemulsion showed significantly higher ($P < 0.05$) apparent permeability coefficients (Papp) at 7.918×10^{-5} cm/s after 1 h, when compared with conventional formulations that are marketed tablet, drug oily solution, and drug emulsion, which showed a maximum Papp of 3.013, 4.428, and 5.335×10^{-5} cm/s, respectively. The optimized felodipine-loaded microemulsion showed biocompatibility and no cytotoxicity. Cellular uptake studies confirmed payload delivery to a cellular site on the J774.A1 cell line. The rheology study of the optimized felodipine-loaded microemulsion revealed Newtonian-type flow behavior and discontinuous microemulsion formation. In pharmacodynamic studies, significant differences in parameters were observed between the optimized felodipine-loaded microemulsion and marketed formulation. The optimized felodipine-loaded microemulsion showed significantly higher ($p < 0.01$) C_{max} (7.12 ± 1.04 μg/ml) than marketed tablets (2.44 ± 1.03 μg/ml). It was found that AUC_{last} obtained from the optimized felodipine-loaded microemulsion (84.53 ± 10.73 μg h/ml) was significantly higher ($p < 0.01$) than the marketed tablet (27.41 ± 5.54 μg h/ml). The relative bioavailability (Fr) of the optimized felodipine-loaded microemulsion was about 308.3% higher than that of the marketed formulation. The results demonstrate that the prepared microemulsion is an advanced and efficient oral delivery system of felodipine for the management of hypertension.

Keywords Microemulsion · α-Linolenic acid · Cytotoxicity · Cellular uptake · Electrocardiogram · Heart rate variability

Introduction

Felodipine (FEL) is a dihydropyridine calcium antagonist widely used as a selective vasodilator in cardiovascular disorders, primarily in arterial hypertension [1]. It is a crystalline drug and practically insoluble in water [2].

It is a biopharmaceutical classification system (BCS) class-II drug, lipophilic in nature, highly photosensitive and exhibits poor aqueous solubility, undergoes extensive first-pass metabolism, and exhibits poor bioavailability [3]. Even though FEL is rapidly absorbed after oral administration, it is important to enhance the

Electronic supplementary material The online version of this article (https://doi.org/10.1007/s13346-017-0453-9) contains supplementary material, which is available to authorized users.

✉ Shubhini A. Saraf
shubhini.saraf@gmail.com

[1] Department of Pharmaceutical Sciences, Babasaheb Bhimrao Ambedkar University (A Central University), Vidya Vihar, Raebareli Road, Lucknow, UP 226025, India

[2] University Institute of Pharmaceutical Sciences, Sector-14, Panjab University, Chandigarh, UT 160014, India

[3] Faculty of Pharmacy, B.B.D.N.I.I.T, Lucknow, India

View Article Online
DOI: 10.1039/C6RA15166C

Development of α-linolenic acid containing soft nanocarrier for oral delivery: *In vitro* and *in vivo* evaluation

Mahendra Singh[1], Jovita Kanoujia[1], Pooja Singh[1], Chandra B Tripathi, Malti Arya[1], Poonam Parashar[1], Vivek R Sinha[2], Shubhini A Saraf[1*]

[*]Corresponding author

[1]Department of Pharmaceutical Sciences, Babasaheb Bhimrao Ambedkar University (A Central University) Vidya Vihar, Raebareli Road, Lucknow-226025, U.P., India.

[2]University Institute of Pharmaceutical Sciences, Sector-14, Panjab University, Chandigarh-160014 (UT), India

Graphical abstract